

**Cell-seeded scaffolds based on poly(ethylene oxide) and  
poly(butylene terephthalate) block copolymers for  
bone tissue engineering**

**M.B. Claase**

Members of the committee:

Chairman/secretary:	prof. dr. A. Blik	University of Twente
Promotor:	prof. dr. J. Feijen	University of Twente
Assistant promotor:	dr. D.W. Grijpma	University of Twente
Expert:	dr. J.D. de Bruijn	IsoTis OrthoBiologics
Members:	prof. dr. C.A. van Blitterswijk prof. dr. ir. J.F.J. Engbersen prof. dr. J.A. Jansen prof. dr. I. Vermes dr. S.K. Bulstra	University of Twente University of Twente University of Nijmegen University of Twente Academic Hospital Maastricht

The research described in this thesis was financially supported by the European Community Brite-Euram project BE97-4612.

This publication was sponsored by IsoTis OrthoBiologics (Bilthoven, The Netherlands), Ssens BV (Hengelo, The Netherlands), Scanco Medical AG (Bassersdorf, Switzerland) and the Nederlandse Vereniging voor Biomaterialen en Tissue Engineering (NBTE).



**SCANCOMEDICAL**

Cell-seeded scaffolds based on poly(ethylene oxide) and poly(butylene terephthalate) block copolymers for bone tissue engineering

By M.B. Claase

Ph.D. Thesis, University of Twente, Enschede, The Netherlands, 2004.  
With references – With summary in English and Dutch  
ISBN 90-365-2000-2

Copyright © M.B. Claase 2004  
All rights reserved.

Cover design by Dorien Bellaar.  
Printed by PrintPartners Ipskamp, Enschede, The Netherlands, 2004.



**CELL-SEEDED SCAFFOLDS BASED ON POLY(ETHYLENE OXIDE) AND  
POLY(BUTYLENE TEREPHTHALATE) BLOCK COPOLYMERS FOR  
BONE TISSUE ENGINEERING**

**PROEFSCHRIFT**

ter verkrijging van  
de graad van doctor aan de Universiteit Twente,  
op gezag van de rector magnificus,  
prof. dr. F.A. van Vught,  
volgens besluit van het College voor Promoties  
in het openbaar te verdedigen  
op vrijdag 13 februari 2004 om 13.15 uur

door

Menno Bernard Claase

geboren op 17 januari 1973

te Nijmegen

Dit proefschrift is goedgekeurd door:

Promotor: prof. dr. J. Feijen

Assistent-promotor: dr. D.W. Grijpma

*She is trapped inside a month of grey  
And they take a little every day  
She is a victim of her own responses  
Shackled to a heart that wants to settle  
And then runs away  
It's a sin to be fading endlessly  
Yeah, but she is alright with me*

*She is leaving on a walkaway  
She is leaving me in disarray  
In the absence of a place to be  
She stands there looking back at me  
Hesitates, and then turns away  
She'll change so suddenly  
She's just like mercury  
Yeah, but she's alright with me*

*Keep some sorrow in your hearts and minds  
For the things that die before their time  
For the restlessly abandoned homes  
The tired and weary rambler's bones  
And stay beside me where I lie  
She's entwined in me  
Crazy as can be  
Yeah, but she's alright with me*

*Mercury - Counting Crows*

Voor mijn moeder en  
voor diegenen die hier zo graag  
bij hadden willen zijn, maar dat  
helaas niet meer kunnen



# Voorwoord

*Think where man's glory most begins and ends,  
And say my glory was I had such friends.*

W.B. Yeats (1865-1939)

Vijf jaar voorbij. Vijf jaar afwisselend werk, dat beschreven staat in zo'n 190 pagina's. Eigenlijk zouden er even zo veel pagina's beschikbaar moeten zijn voor alle dingen die naast dat onderzoek gebeurd zijn. En vooral ook om al die mensen te bedanken die bijgedragen hebben aan dit werk en die het tot zo'n leuke tijd gemaakt hebben. Ik heb het bijzondere voorrecht gehad om veel van mijn collega's ook vrienden te mogen noemen.

Allereerst wil ik graag professor Feijen bedanken voor de gelegenheid die hij mij geboden heeft om te kunnen promoveren. Uw kennis en oog voor detail zijn bijzonder waardevol geweest bij het tot stand komen van dit proefschrift. Daarnaast wil ik u ook bedanken voor de wetenschappelijke vrijheid, die mij gegeven is, om zoveel verschillende dingen te mogen doen. Ik heb de afgelopen jaren enorm veel geleerd.

Dirk Grijpma, je was bijna bij iedere stap, die ik in deze afgelopen jaren gezet heb, aanwezig. Dit proefschrift is dan ook mede tot stand gekomen door je niet aflatende inzet. Ik wil je hartelijk bedanken voor alle correcties en wijze lessen, op polymeergebied, maar vooral op het gebied van onderzoek in het algemeen. Het feit dat je deur altijd letterlijk en figuurlijk openstond heb ik zeer gewaardeerd. Ook wil ik nog zeggen dat je bekende, of moet ik zeggen beruchte, activeringsenergiecurve me nog lang zal heugen.

Aangezien ik veel van mijn werk bij IsoTis heb mogen doen, was het onontbeerlijk om ook daar een begeleider te hebben. Joost de Bruijn heeft me dan ook ingewijd in de wondere wereld van de biologie. Joost, bedankt voor alle vrijheid die me geboden is bij IsoTis om al die experimenten te doen, die ik zo graag wilde doen. Immers zonder cellen zou er in dit proefschrift weinig overblijven van tissue engineering.

The research described in this thesis was done as part of a European Brite-Euram project. Therefore I would like to thank all the project partners: professor Fernando Monteiro, professor Bevis (and his wife), dr. Rui Reis, dr. Francesco Degli-Innocenti and Brian Brookshaw for their interest in my work and the very pleasant meetings we have had.

En dan zijn er al die mensen die kleine of grote bijdrages hebben geleverd aan het 'daadwerkelijke' onderzoek (het praktisch werk) en dat waren er velen. Voor dat ik begin wil ik er graag nog even op wijzen dat aan de genoemde volgorde op geen enkele wijze 'rechten' ontleend kunnen worden.

Allereerst wil ik mijn studenten bedanken. Martijn, helaas is je werk een appendix geworden, maar ik realiseer me heel goed dat netjes hard werken helaas niet altijd het gewenste resultaat oplevert.

Claudia, it was a pleasure to work with you. Like Ana and Sandra, you managed to show me why those ‘tripeiros’ are so proud of their city and rightly so. I wish you both all the best in the future.

Karin, je bent ‘het cement’ van de afdeling. En ja, dat is een compliment, want zonder jou zouden vele dingen niet gebeuren, of in ieder geval veel te laat. Hoe druk je ook bent, je maakt altijd tijd als er iets geregeld moet worden. Hetzelfde geldt overigens ook voor Gerda en Geneviève. Dames bedankt.

In het lab vervullen een aantal mensen een zelfde rol. Zlata en John, bedankt voor de hulp en Jan voor de nuttige adviezen. Clemens, zonder jou zou een groot deel van de apparatuur niet werken (maar dat heeft helaas niet iedereen door) en zou er erg weinig onderzoek gedaan kunnen worden. Bedankt voor alle hulp bij het opzetten van de GPC.

Ook heb ik vele uren mogen doorbrengen in het donkere hok waar Mark Smithers zijn SEM ‘bestuurt’. Mark, jij bent echt ‘multitasking’, als geen ander kun je mooie foto’s maken en tegelijk de laatste roddels op de UT vertellen.

Andres Laib at Scanco Medical I would like to thank for the CT scans. At the end of my Ph.D. research that data was really the icing on the cake.

Tja, en dan het dagelijks leven op het lab. Hoewel er soms gedacht wordt dat de ‘moderne’ AIO hier (te) weinig tijd doorbrengt, zijn hier toch vele uren doorgebracht. Ana, Audrey, Miechel, Monica, Luuk, MOR, Martijn, Qingpu, Zheng, Boon Hua, Martijn, bedankt voor alle gezelligheid. En sorry, dat ik jullie zo nu en dan een beetje geterroriseerd heb met mijn muziek, maar het is nu eenmaal wetenschappelijk bewezen (zie hoofdstuk 3) dat een polycondensatie beter loopt met Limp Bizkit als achtergrondmuziek. Ook wil ik graag de ‘plasma-boys’, MOR, Luuk en Ype bedanken. Zonder plasmabehandelingen zou dit proefschrift bij hoofdstuk 3 ophouden.

Zoals al eerder vermeld is een groot deel van de tijd doorgebracht bij IsoTis. Hoewel iets minder luidruchtig was het daar niet minder gezellig. Allereerst wil ik Sandra, Sanne, Marjan, Mirella en Patrick bedanken voor het geduld (nou ja, in ieder geval bij vier van de vijf) dat jullie met me hadden om mij celkweek-, implantatie- en histologietechnieken te leren. En verder Aart, Jeroen B., Monica, Riemke, Tim, Jos, Tahir, Florence, Hongjun, Joost de Wijn, Jeroen P., Peter en Fabienne voor de gezellige babbeltjes en de hulp tussendoor.

Naast het werk op het lab, zit de ‘moderne’ AIO ook veel op zijn kantoor, achter zijn computer. Om het ook daar naar je zin te hebben zijn leuke kamergenoten onontbeerlijk. Daarom: Jeroen, Marcel en Boon Hua, bedankt.

But of all the roommates there is of course one who deserves a few extra lines. Zhiyuan, I really admire the way how you approach work and life in general. And I am very grateful that two people with such different characters and from two very different countries were able to become such good friends.

Naast werk bestaat er ook nog iets zoals een sociaal leven en zoals bij vele mensen bestond dat van mij ook uit eten, sporten, film kijken en nog vele andere zaken. En hoewel dit vaak met de zelfde mensen gebeurde heb ik toch een kleine verdeling gemaakt. Mijn mensmaatjes (en nee, het eten is niet zo geweldig, maar het gezelschap des te meer): Louis, Geert, Montse, Léon, Léon, Albi en mijn tennismaatjes: Ana, Laura, Priscilla, Miechel, Zhiyuan, Ype.

En natuurlijk zijn er dan nog vele andere die ik niet genoemd heb: Pedro, Kathrin, Fenghua, Judith, Francesca R., Francesca S., Kinsuk, Pratip, Vipin, Barbara, Bas, Joost, Ingrid, Mark, Christine, Marianne, dr. Ankone, Dries, Wilco, Debby, Edwin, Tom, Raymond en Marcos. Bedankt voor alle gezelligheid.

Toch wil ik twee mensen nog even apart vermelden.

Louis, hoewel we op dezelfde datum begonnen, eindig ik exact 364 dagen later. Toch hebben we beiden veel dezelfde dingen op bijna hetzelfde moment meegemaakt. Ik ben dan ook blij dat ik zoveel met jou heb kunnen delen.

Audrey, if there is a person in the world who can be more stubborn than I am, than it is surely you. Like true musketeers, it always was a pleasure to cross (s)words with you. Nevertheless together with the third musketeer it always was and hopefully will be: one for all and all for one.

En dan natuurlijk mijn paranimfen.

Ana, who would ever think that a big Dutch guy and a small Portuguese lady would ever become such close friends. It has been a great time, unfortunately we will see each other much less in the future. But with a bit of effort I am sure that this will be a friendship for life, so I am thankful to have met you.

Oskar, ik ken je al zolang als ik me kan herinneren, misschien zou de kwalificatie 'broer' je dan ook wel beter passen, maar goed, we zijn geen familie. Ik weet dat ik je met die 60 minuten op het podium geen plezier doe, maar ik ben er trots op dat je ook hier weer naast me staat.

Tot slot wil ik, wie anders dan, mijn moeder bedanken. Ma, zonder al je steun en hulp was nog niet de helft van dit werk tot stand gekomen. Bedankt voor alles.

Bedankt allemaal, ik zal jullie missen !

*Menno*





# Table of contents

<b>Chapter 1</b>	General introduction	1
<b>Chapter 2</b>	Porous structures for bone tissue engineering: a literature review	7
<b>Chapter 3</b>	Synthesis, processing and characterization of poly(ethylene oxide)/poly(butylene terephthalate) block copolymers	37
<b>Chapter 4</b>	Enhanced bone marrow stromal cell adhesion and growth on segmented poly(ether ester)s based on poly(ethylene oxide) and poly(butylene terephthalate)	53
<b>Chapter 5</b>	Porous PEOT/PBT scaffolds for bone tissue engineering: preparation, characterization and in vitro bone marrow stromal cell culturing	65
<b>Chapter 6</b>	Ectopic bone formation in cell-seeded poly(ethylene oxide)/poly(butylene terephthalate) copolymer scaffolds: I. Effects of pore structure	81
<b>Chapter 7</b>	Ectopic bone formation in cell-seeded poly(ethylene oxide)/poly(butylene terephthalate) copolymer scaffolds: II. Effects of porosity	103
<b>Chapter 8</b>	General discussion and conclusions	123
<b>Appendix A</b>	Synthesis of PEG-RGD conjugates	131
<b>Appendix B</b>	Grafting of poly(ethylene oxide)/poly(butylene terephthalate) block copolymers onto hydroxyapatite particles	139
<b>Summary</b>		155
<b>Samenvatting</b>		159
<b>Curriculum vitae</b>		163
<b>List of publications</b>		165
<b>Color figures</b>		167



# Chapter 1

## General introduction

*These are the voyages of the Starship Enterprise. Its five year mission...  
to boldly go where no man has gone before.*

Gene Roddenberry (1921-1991)

### Tissue engineering

Tissue engineering is a rapidly developing technology that is directed to the design and development of constructs that can be used to maintain or improve the function of human tissues or organs. The application of tissue engineering differs from standard therapies by the fact that the engineered products become integrated within the patient, affording a potentially permanent and specific cure for the disease, injury or impairment. It is an interdisciplinary field that applies the principles of biology and engineering to medicine.<sup>[1,2]</sup>

As an indication of the scope of the problem that tissue engineering addresses, worldwide organ replacement therapies utilizing standard metallic or polymeric devices consume 8 percent of medical spending, or approximately €300 billion per year.<sup>[3]</sup> The potential market world-wide for tissue-engineered products is estimated at nearly €100 billion per year.<sup>[4]</sup>

A more general definition can be found in The Williams Dictionary for Biomaterials<sup>[5]</sup>: 'Tissue engineering is the persuasion of the body to heal itself through the delivery to appropriate sites, of molecular signals, cells and supporting structures.' Although very short, this definition addresses the three main components of tissue engineering:

1. molecular signals, such as growth factors, that stimulate the proliferation and differentiation of cells in vitro and/or in vivo, the infiltration by surrounding tissue and the vascularization of the tissue-engineered construct
2. cells, to regenerate the lost or damaged tissue
3. scaffolds, i.e. gels or (porous) supporting structures that allow cell attachment and tissue ingrowth

The technology of tissue engineering is being applied to (re)generate several human organs and tissues. Examples are skin, cartilage, tendon, liver, esophagus, trachea, urothelial tissue, cardiovascular structures, intestine and bone.<sup>[2,6,7]</sup>

The cell-based nature of tissue engineering distinguishes it from 'guided tissue regeneration' in which a scaffold is designed to encourage regeneration solely by the action of cells residing at the site of transplantation.<sup>[8]</sup> In tissue engineering differentiated cells, like osteoblasts, chondrocytes and fibroblasts and also so-called progenitors (or stem) cells have been used for the reconstruction of bone, cartilage or skin.<sup>[2,6]</sup>

Table 1.1 gives an overview of different cell-based tissue engineering approaches. Examples of stem cells are the totipotent zygote, the much debated embryonic stem cells, hemapoietic stem cells and mesenchymal stem cells. During human development mesenchymal stem cells are present in a variety of tissues, in adults they are prevalent in bone marrow. These mesenchymal stem cells can be isolated, expanded in culture and stimulated to differentiate into bone, cartilage, muscle, marrow stroma, tendon, fat and a variety of other connective tissues.<sup>[9]</sup>

Table 1.1 - Current cell-based approaches to tissue engineering.<sup>[8]</sup>

Stem cell-based tissue engineering		Non stem cell-based tissue engineering	
Blood vessels	Liver	Bladder	Meniscus
Bone*	Pancreas	Cartilage (ear, nose and joints)*	Oral mucosa
Cartilage	Nervous tissue*	Heart valves	Salivary gland
Cornea*	Skeletal muscle	Intestine	Trachea
Dentin	Skin*	Kidney	Ureter
Heart muscle			Urethra

\*: In clinical studies

Many cell types are anchorage dependent and require the presence of a substrate to retain their ability to proliferate and perform their specific or differentiated function.<sup>[10]</sup> The primary role of a scaffold is to provide a temporary substrate to which transplanted cells can adhere. Cell attachment (influenced by the surface characteristics of the scaffold) is an important factor, but the function of many organs is also dependent on cell morphology and the three-dimensional spatial relationship of cells and extracellular matrix. It has been shown that porous scaffolds with well defined interconnected pore networks are capable of performing such an organizational role.<sup>[10]</sup>

## Bone replacement

Bone is a complex material consisting of many components.<sup>[11,12]</sup> Cortical bone, for instance, consists of an extracellular organic matrix, spatially arranged and highly organized, with a basic calcium phosphate called hydroxyapatite, that is defective and poorly crystallized.<sup>[11,13,14]</sup> The organization gives bone its unique structural and biomechanical properties. Mature bone exists as compact bone (cortical bone) or as trabecular bone (cancellous or spongy bone). Trabecular bone is less dense than compact bone and forms an open-celled structure. Bone is made up of 69 % inorganic material and 9 % water. The remaining organic material is made up of 90 % insoluble collagen and 10 % non-collagenous protein.<sup>[13]</sup> Bone is a dynamic tissue, which is constantly being remodelled, i.e. being resorbed and (re)formed. The respective cells that are responsible for these processes are osteoclasts<sup>[15]</sup> and osteoblasts.<sup>[16]</sup>

When bone is injured, it does not heal with a fibrous scar as do virtually all other tissues. The response of bone to injury is to regenerate bone tissue and then remodel that newly formed bone in the direction of local stresses.<sup>[17]</sup> The mechanical function of bone, once lost by injury or other means, can only be regained by restoring skeletal continuity at the location of interest. The first record of the use of a bone graft was in 1668 by Job Janszoon van Meek'ren. Van Meek'ren stated that he read a report of it in a letter to Rev. Engebert Sloot of Slooterdijk from

John Kraanwinkel, a missionary in Russia, where the operation had been performed. It consisted of the transplantation of a piece of bone from a dog's skull into a cranial defect of a soldier. Although healing was observed, the Church ordered the removal of the graft.<sup>[18]</sup>

Nowadays the clinical 'gold standard' in bone transplantation is the transplantation of an autogenous trabecular graft. The open porous structure of trabecular bone permits the deposition of new bone directly on the trabeculae. Trabecular transplants are revascularized much more rapidly than compact bone transplants. Revascularization of the trabecular graft occurs through the open marrow spaces.<sup>[17]</sup>

The inherent drawback of the use of autologous trabecular grafts, however, is that the grafts have to be removed from another place in the human body, resulting in donor-site morbidity.

A possible alternative is the use of allogeneic bone. This, however, shows a lower osteogenic capacity, a higher resorption rate, a larger immunogenic response and less extensive revascularization of the graft. Currently, the use of allogeneic bone has declined due to recent concerns over the possibility of viral contamination of the graft material and possible transmission of live virus to the recipient.<sup>[19]</sup> Xenogeneic bone is generally not considered for use as a bone graft substitute, as it elicits an acute antigenic response resulting in failure in the majority of cases.<sup>[19]</sup>

Tissue engineering can circumvent existing problems in bone replacement<sup>[20-24]</sup>, with several systems already in the stage of clinical trials.<sup>[25]</sup>

## PEOT/PBT copolymers

In this thesis the materials of interest for the preparation of scaffolds for bone tissue engineering are copolymers of poly(ethylene oxide) and poly(butylene terephthalate), PEOT/PBT. The general chemical structure is indicated in Figure 1.1.

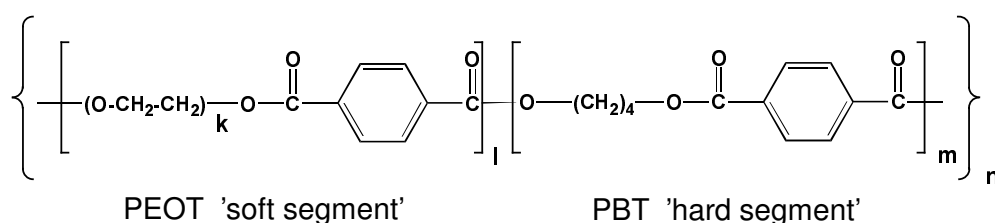


Figure 1.1 - Structure of PEOT/PBT block copolymers.

The composition of these segmented block copolymers is indicated as  $a\text{PEOT}b\text{PBT}c$ , with  $a$  the molecular weight of the poly(ethylene glycol) starting compound,  $b$  the weight percentage of the PEOT soft segments and  $c$  the weight percentage of the PBT hard segments. The mechanical and physical properties of these materials can be tuned by varying the PBT (hard segment) content and PEOT (soft segment) content and PEO molecular weight.<sup>[26,27]</sup> Several subcutaneous and intra-bone (tibia) implantations of dense and porous blocks and porous films in rats and goats showed bone bonding, calcification and degradation for PEOT/PBT copolymers with high PEO content (1000PEOT70PBT30 and 1000PEOT60PBT40).<sup>[28-31]</sup> Biocompatibility and degradation have also been observed for PEOT/PBT microspheres, representing a much larger surface to volume ratio (as is the case for porous structures) than solid implants.<sup>[32]</sup> These results suggest that PEOT/PBT copolymers and especially those with a high PEO content are most appropriate as scaffold materials for bone tissue engineering.

Implantation of the polymeric material in the form of porous blocks into critical size defects in goat<sup>[33]</sup> and human<sup>[34]</sup> ilia, however, did not result in healing of the defects. In vitro culture in an osteogenic medium of bone marrow stromal cell (BMSC)-seeded hydroxyapatite scaffolds resulted in the generation of bone-like tissue. Subcutaneous implantation of these in vitro cell-seeded and cultured tissue/cell ceramic constructs in rats, resulted in the formation of higher amounts of bone when compared to cell-seeded scaffolds not cultured in vitro prior to implantation.<sup>[35]</sup> Porous PEOT/PBT structures seeded and cultured with BMSCs are likely to have an osteoinductive effect and therefore more suited for bone tissue engineering than porous PEOT/PBT structures without BMSCs.

## Objective

The objective of this study is to develop polymeric scaffolds containing BMSCs, cultured in an osteogenic medium, that can be used for the formation of functional bone tissue upon implantation. The proposed polymer/cell constructs comprise *bone marrow stromal cells* that are *seeded* and *cultured* in three-dimensional porous biodegradable polymer scaffolds, based on PEOT/PBT (polyethylene oxide/polybutylene terephthalate) copolymers. To study the osteogenic potential of the cultured polymer/cell constructs, rat BMSCs were seeded and cultured on PEOT/PBT scaffolds and subsequently subcutaneously implanted in immunodeficient nude mice. These PEOT/PBT copolymers should be able to attach bone marrow stromal cells for in vitro culturing to produce bone-like tissue in vitro. Techniques for the preparation of porous structures that allow good control over porosity and pore size need to be developed to obtain an optimal pore morphology suitable for nutrient exchange and tissue formation in vitro and in vivo.

Therefore the research is directed towards:

- Optimizing the properties of the more hydrophilic PEOT/PBT copolymer compositions and properties for BMSC attachment.
- Developing techniques for the preparation of porous structures that allow good control over porosity and pore size.
- Characterizing the scaffolds and studying the effects of different scaffold morphologies on in vitro BMSC culturing.
- Studying the effect of scaffold material and morphology of BMSC-seeded and cultured constructs on ectopic bone formation.

## Outline of this thesis

In this thesis the synthesis of PEOT/PBT copolymers, the preparation of porous structures and the in vitro and in vivo evaluation of rat bone marrow stromal cell-seeded and cultured PEOT/PBT scaffolds are described.

**Chapter 2** gives an overview of bone tissue engineering approaches, with emphasis on preparation methods and properties of porous scaffolds. Different approaches to prepare scaffolds with desired morphologies are discussed.

**Chapter 3** deals with the 50-100 g and 1 kg scale synthesis of PEOT/PBT copolymers and their subsequent analysis with <sup>1</sup>H-NMR and GPC. Several chemical characteristics and mechanical properties of these polymers are discussed. In contrast to our expectations BMSC attachment onto hydrophilic PEOT/PBT copolymers was poor. Cell attachment could be considerably improved by CO<sub>2</sub> gas plasma treatments as described in **Chapter 4**. Gas plasma treatments were shown to be an essential step to enable rat bone marrow stromal cells to

attach to the more hydrophilic PEOT/PBT copolymers. An attempt to improve cell attachment by use of PEO-RGD conjugates is described in **Appendix A**. Blending of hydroxyapatite (HA) also improved the cell attachment of bone marrow stromal cells. The grafting of PEOT/PBT onto HA particles to improve the composite properties is described in **Appendix B**.

**Chapter 5** deals with the gas plasma treatments of porous PEOT/PBT structures and the in vitro rat bone marrow stromal cell culture in these scaffolds. It was shown that pore surface modification also took place within the scaffold, enabling cell attachment throughout the scaffold.

The ectopic bone formation in cell-seeded and cultured porous PEOT/PBT structures after subcutaneous implantation in nude mice is investigated in **Chapters 6 and 7**. **Chapter 6** describes the preparation of scaffolds with different pore structures at a constant porosity of approximately 80 %. The obtained scaffolds were characterized in terms of porosity, pore size distribution, average pore size, accessible pore volume and accessible pore surface area using micro computed tomography ( $\mu$ -CT). The effects of scaffold pore structure, cell seeding and in vitro culture on ectopic bone formation were studied. Similar studies as described in **Chapter 6** were conducted using scaffolds of different porosities with comparable pore structures and are described in **Chapter 7**. Besides bone formation, scaffolds of low porosity showed cartilage formation. This phenomenon is explained in terms of limited pore accessibility leading to an oxygen-poor environment that favors cartilage formation.

**Chapter 8** ends this thesis with general conclusions and suggestions for further research.

## References

1. R. Langer, J.P. Vacanti *Tissue engineering Science* **1993**, 260, 920-926.
2. R. Langer, J.P. Vacanti, C.A. Vacanti, A. Atala, L.E. Freed, G. Vunjak-Novakovic *Tissue Engineering: Biomedical Applications* Tissue Eng. **1995**, 1, 151-161.
3. L.V. McIntire "WTEC Panel Report on Tissue Engineering Research," International Technology Research Institute, World Technology (WTEC) Division **2002**.
4. European Commission Enterprise Directorate-General *Need for a legislative framework for human tissue engineering and tissue-engineered products* 'Consultation document' **June 2002**.
5. D.F. Williams *The Williams Dictionary of Biomaterials* Liverpool University Press, Liverpool, United Kingdom **1999**.
6. J.J. Marler, J. Upton, R. Langer, J.P. Vacanti *Transplantation of cells in matrices for tissue regeneration* Adv. Drug Deliv. Rev. **1998**, 33, 165-182.
7. J.R. Fuchs, B.A. Nasser, J.P. Vacanti *Tissue engineering: A 21st century solution to surgical reconstruction* Ann. Thorac. Surg. **2001**, 72, 577-591.
8. P. Bianco, P.G. Robey *Stem cells in tissue engineering* Nature **2001**, 414, 118-121.
9. A.I. Caplan, S.P. Bruder *Mesenchymal stem cells: building blocks for molecular medicine in the 21st century* Trends Mol. Med **2001**, 7, 259-264.
10. R.C. Thomson, M.C. Wake, M.J. Yaszemski, A.G. Mikos *Biodegradable polymer scaffolds to regenerate organs* Adv. Polym.Sci. **1995**, 122, 245-274.
11. S.C. Marks Jr., D.C. Hermey *The structure and development of bone* J.P. Bilezikian, L.G. Raisz and G.A. Rodan, Ed.; Academic Press: San Diego, U.S.A. **1996**.
12. G. Karsenty *The complexities of skeletal biology* Nature **2003**, 423, 316-318.
13. E.M. Raif, M.-F. Harmand *Molecular interface characterization in human bone matrix* Biomaterials **1993**, 14, 978-984.
14. T.A. Taton *Nanotechnology - Boning up on biology* Nature **2001**, 412, 491-492.
15. S.L. Teitelbaum *Bone resorption by osteoclasts* Science **2000**, 289, 1504-1508.
16. P. Ducy, T. Schinke, G. Karsenty *The osteoblast: A sophisticated fibroblast under central surveillance* Science **2000**, 289, 1501-1504.
17. M.J. Yaszemski, R.G. Payne, W.C. Hayes, R. Langer, A. Mikos, G. *Evolution of bone transplantation: molecular, cellular and tissue strategies to engineer human bone* Biomaterials **1996**, 17, 175-185.

18. J.J. van Meekren *Heel- en Genees-konstige Aanmerkkingen* Caspar Commelijn: Amsterdam, The Netherlands **1668**.
19. C.J. Damien, J.R. Parsons *Bone-graft and bone-graft substitutes - a review of current technology and applications* J. Appl. Biomater. **1991**, 2, 187-208.
20. S.P. Bruder, B.S. Fox *Tissue engineering of bone - Cell based strategies* Clin. Orthop. Rel. Res. **1999**, S68-S83.
21. M. Braddock, P. Houston, C. Campbell, P. Ashcroft *Born again bone: Tissue engineering for bone repair* News Physiol. Sci. **2001**, 16, 208-213.
22. F. Rose, R.O.C. Oreffo *Bone tissue engineering: Hope vs hype* Biochem. Biophys. Res. Commun. **2002**, 292, 1-7.
23. S.P. Bruder, N. Jaiswal, N.S. Ricalton, J.D. Mosca, K.H. Kraus, S. Kadiyala *Mesenchymal stem cells in osteobiology and applied bone regeneration* Clin. Orthop. Rel. Res. **1998**, S247-S256.
24. R. Cancedda, B. Dozin, P. Giannoni, R. Quarto *Tissue engineering and cell therapy of cartilage and bone* Matrix Biol. **2003**, 22, 81-91.
25. R.F. Service *Tissue engineers build new bone* Science **2000**, 289, 1498-1500.
26. A.A. Deschamps, D.W. Grijpma, J. Feijen *Poly(ethylene oxide)/poly(butylene terephthalate) segmented block copolymers: the effect of copolymer composition on physical properties and degradation* Polymer **2001**, 42, 9335-9345.
27. R.J.B. Sakkers, J.R. de Wijn, R.A.J. Dalmeyer, R. Brand, C.A. van Blitterswijk *Evaluation of copolymers of polyethylene oxide and polybutylene terephthalate (polyactive): mechanical behaviour* J. Mater. Sci.-Mater. Med. **1998**, 9, 375-379.
28. C.A. van Blitterswijk, J. van der Brink, H. Leenders, D. Bakker *The effect of PEO ratio on degradation, calcification and bone bonding of PEO/PBT copolymer (Polyactive)* Cells and Materials **1993**, 3, 23-36.
29. C.A. van Blitterswijk, D. Bakker, S.C. Hesseling, H.K. Koerten *Reactions of cells at implant surfaces* Biomaterials **1991**, 12, 187-193.
30. A.M. Radder, H. Leenders, C.A. van Blitterswijk *Bone-bonding behavior of poly(ethylene oxide)-polybutylene terephthalate copolymer coatings and bulk implants - a comparative-study* Biomaterials **1995**, 16, 507-513.
31. A.M. Radder, H. Leenders, C.A. van Blitterswijk *Application of porous PEO/PBT copolymers for bone replacement* J. Biomed. Mater. Res. **1996**, 30, 341-351.
32. R. van Dijkhuizen-Radersma, S.C. Hesseling, P.E. Kaim, K. de Groot, J.M. Bezemer *Biocompatibility and degradation of poly(ether-ester) microspheres: in vitro and in vivo evaluation* Biomaterials **2002**, 23, 4719-4729.
33. M.L.C. Anderson, W.J.A. Dhert, J.D. de Bruijn, R.A.J. Dalmeijer, H. Leenders, C.A. van Blitterswijk, A.J. Verbout *Critical size defect in the goat's os ilium - A model to evaluate bone grafts and substitutes* Clin. Orthop. Rel. Res. **1999**, 231-239.
34. M. Roessler, A. Wilke, P. Griss, H. Kienapfel *Missing osteoconductive effect of a resorbable PEO/PBT copolymer in human bone defects: A clinically relevant pilot study with contrary results to previous animal studies* J. Biomed. Mater. Res. **2000**, 53, 167-173.
35. S.C. Mendes, M. Sleijster, A. van den Muysenberg, J.D. de Bruijn, C.A. van Blitterswijk *A cultured living bone equivalent enhances bone formation when compared to a cell seeding approach* J. Mater. Sci.-Mater. Med. **2002**, 13, 575-581.



# Chapter 2

## Porous structures for bone tissue engineering: a literature review

*If you steal from one author, it's plagiarism; if you steal from many, it's research.*

Wilson Mizner (1876-1933)

### Approaches to bone tissue engineering

In analogy to three main components of tissue engineering as mentioned in Chapter 1 the main research subjects in bone tissue engineering are: a) osteoinductive agents (molecular signals), b) (osteogenic) cells and c) scaffolds, i.e. gels or (porous) supporting structures.<sup>[1]</sup> In order to obtain functional tissue in vivo it is important that the tissue engineered construct becomes well vascularized and embedded in the host tissue.<sup>[2]</sup>

Osteoinduction is defined as the ability to induce pluripotent cells, from a non-osseous environment to differentiate into chondrocytes and osteoblasts, which culminates in bone formation. An osteoinductive material allows bone tissue repair in a location that would normally not heal if left untreated. Osteoconduction also supports the ingrowth of capillaries and cells from the host into the three-dimensional support structure to form bone. An osteoconductive material guides repair in a location where normal healing would occur if left untreated.<sup>[2]</sup>

Biomaterials seeded with the appropriate cells and/or containing suitable growth factors can be osteoinductive, where the material by itself is at best only osteoconductive.

### Osteoinductive agents in bone tissue engineering

For bone induction, osteoconductive biodegradable materials stimulate repair of bone defects by allowing ingrowth of osteoblasts from the border of the defect. Osteoinduction for healing of defects, that otherwise do not unify, can be achieved in various manners such as pre-seeding osteoblasts and/or incorporating bioactive molecules into the polymer scaffold. Specific growth factors, released from such scaffolds aid in the induction of host parenchymal cell migration, proliferation and differentiation or improve engraftment of seeded cells, on or in the polymer scaffold, resulting in more efficient tissue regeneration. The three-dimensional polymer scaffold defines the volume of the newly formed tissue.<sup>[3]</sup>

Transforming growth factor  $\beta$ 1 (TGF- $\beta$ 1), bone morphogenetic protein-2 (BMP-2), and osteogenic protein (OP-1 or BMP-7) are the most frequently employed osteogenic factors. They are members of the transforming growth factor- $\beta$  (TGF- $\beta$ ) superfamily.<sup>[3]</sup>

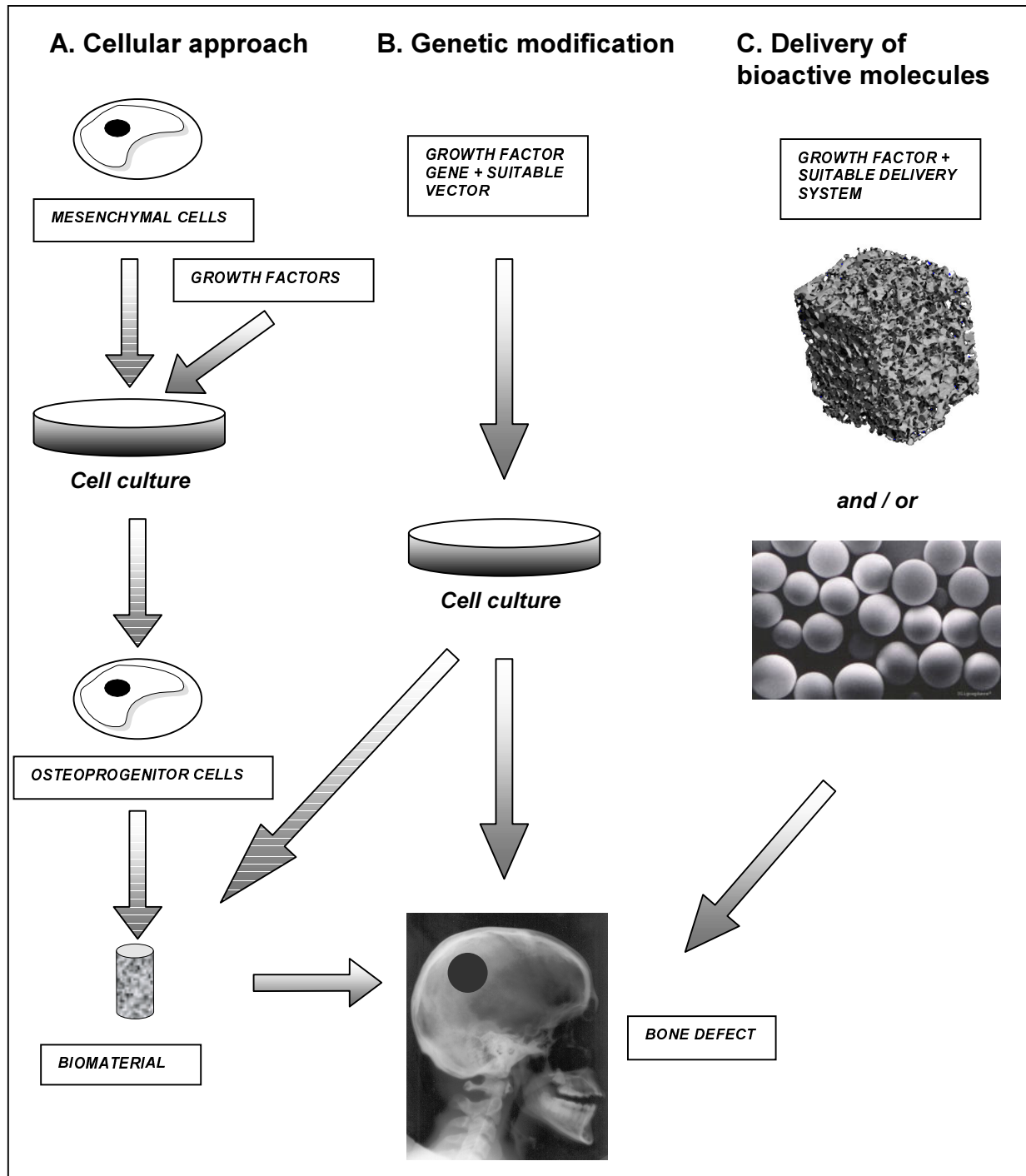


Figure 2.1 - Schematic representation of the use of bioactive molecules such as growth factors in bone tissue engineering after reference.[8] A: by inducing suitable cell differentiation in in vitro cell culture. B: by genetically modifying cells with a growth factor gene, in vitro or directly in vivo. C: by controlled release at the site of the bone defect by a suitable carrier material like porous scaffolds and/or microspheres.

Growth factors belonging to the TGF- $\beta$  superfamily have a wide range of activity in animal growth and development. This family is composed of at least 25 different molecules which retain the seven-cysteine residues within the mature region of the protein. Among these growth factors, the subfamily of bone morphogenetic proteins (BMPs) is composed of at least 15 molecules. These molecules are present in many organisms ranging from lower organisms

such as yeast to higher organisms such as mammals, with high homology among various species.<sup>[4]</sup>

BMPs are sequestered primarily in bone and are liberated following fracture or damage, recruiting pluripotent cells to the defect site to differentiate into osteogenic cells.<sup>[5]</sup> These factors were originally discovered by Urist et al.<sup>[6,7]</sup> from extracts of demineralised bone and were found to induce new bone formation in ectopic sites.

Three approaches in the use of bioactive molecules for instance growth factors like BMPs in bone tissue engineering can be identified and are represented in Figure 2.1. BMPs can play a role in approaches involving cells, genetic modification and the (controlled) delivery bioactive molecules. The cellular approach involves the transplantation of cultured osteogenic cells derived from host bone marrow.<sup>[8]</sup>

Although the in vitro cell culture takes time (up to several weeks), using patient-own cells appears a very promising method, which will be discussed in more detail in the next section. Addition of BMPs or other growth factors to the cell culture medium makes efficient differentiation and proliferation possible. Other bioactive molecules, such as certain types of fibroblast growth factor (FGF) or dexamethasone can also be used in this technique.

Gene therapy involves the transduction of genes encoding for BMPs to cells delivered to the repair site.<sup>[8]</sup> Cells can be transfected both in vitro and in vivo using a suitable vector (virus, liposome, polymer etc.). Gene therapy appears to be more effective than cell or cytokine therapy, because it develops a cellular vehicle that can provide a sustained local release of BMP, which may enable the host to respond to this osteoinductive stimulus in an effective manner.<sup>[8]</sup> The selection of the vector, however, (both in vitro and in vivo) remains a concern, since the patient's safety is of primary importance. The development of an appropriate vector should render gene therapy into a major improvement in bone tissue engineering.

The delivery of bioactive molecules involves the implantation of appropriate delivery systems containing bioactive molecules like growth factors, like BMPs.<sup>[8]</sup> Some of the proteins are available in relatively large quantities due to recombinant DNA techniques (rhBMPs), many others are only available in small amounts. The major obstacle for clinical application, however, is the selection of the most appropriate carrier material for the drug delivery system.<sup>[8]</sup> An important fact is that BMPs act locally and therefore must be delivered in a controlled manner directly at the site of regeneration. These osteoinductive proteins must be applied within a therapeutic concentration range if they are to be consistently effective in generating healthy bone. Too low a concentration of morphogen may lead to a mosaic of unhealthy bone and fat, with inadequate mechanical characteristics. Too high a concentration of morphogen may actually inhibit osteogenesis or induce excessive bone outside prescribed graft boundaries.<sup>[5]</sup> Recombinant human bone morphogenetic protein-2 (rhBMP-2) induced pluripotent mesenchymal stem cell differentiation depending on the concentration applied in vitro: low concentrations favored adipocytes and high concentrations chondrocytes and osteoblasts.<sup>[3]</sup>

Table 2.1 presents an overview of polymeric carrier systems studied for the release of growth factors for bone tissue engineering.

## Osteogenic cells in bone tissue engineering

Osteoblast-like cells are excellent candidates for bone tissue engineering, but compared to stem cells they have a reduced ability to proliferate as they are fully differentiated. An adult stem cell is an undifferentiated (unspecialized) cell present in a differentiated tissue, which renews itself and becomes specialized to yield all of the cell types of the tissue from which it was originated. Adult stem cells self-renew in vivo.

Table 2.1 - In vivo and in vitro bone tissue engineering combining the release of growth factors with polymeric or composite carriers. (after reference [9]).

Growth factor	Carrier material	Carrier type	Animal model	Reference
In vivo:				
FGF-2	Collagen	Porous matrix	Rat mandibular	[10]
BFGF	Hyaff <sup>®</sup>	Fibre mesh	Rat radius	[11]
PDGF-BB	Chitosan and chitosan/PLLA	Porous matrix	Rat cranium	[12,13]
PDGF-BB	PLLA/TCP	Porous membrane	Rabbit cranium	[14]
IGF-I/TGF-β1	PDLLA	Coating	Minipig tibiae	[15]
IGF-I/TGF-β1	PDLLA	Coating	Rat tibiae / fibula	[16,17]
TGF-β1	PPF	Porous matrix	Rabbit cranium	[18]
BMP-2	Collagen	Porous matrix	Rabbit tibiae	[19]
BMP-2	Collagen	Porous matrix	Rat ectopic	[20,21]
BMP-2	NiPAM based	Hydrogel	Rat ectopic	[22]
BMP-2	Collagen	Porous matrix	Dog femur	[23,24]
BMP-2	Collagen/HA	Non-porous matrix	Dog radius / ulna	[25]
BMP-2	Collagen/BCP	Porous matrix	Rabbit spine	[26]
OP-1 (BMP-7)	Collagen	Injectable paste	Rat femur	[27]
OP-1 (BMP-7)	Collagen/allograft	Impaction in a Ti implant	Dog humerus	[28]
BMP-2, 4 and 6 (alone)	Helistat <sup>®</sup>	Porous matrix	Rat ectopic	[29]
BMP-2, 4 and 6 (alone)	Dexon <sup>®</sup>	Fibre mesh	Rat ectopic	[29]
BP	Chitosan	Injectable gel	Rat dorsal	[30]
In vitro:				
IL-2	Dextran based	Hydrogel	CTTL-2	[31]
TGF-β1	Dextran derivatives	Hydrogel	MLEC C3H10T1/2	[32]
BMP-2	PLGA + gelatin	Porous matrix	MC3T3-E1 ROB	[33]
BFGF	Hyaff <sup>®</sup>	Porous matrix	BMSC	[34]
BFGF	PLGA	Porous matrix	Fibroblast	[35]
VEGF	PLG	Porous matrix	HMVEC(nd) and HMVEC	[36,37]

Abbreviations: bFGF, basic fibroblast growth factor; BMP, bone morphogenetic protein; BMSC, rat bone marrow stromal cells; BP, bone protein; C3H10T1/2, pluripotent cell line isolated from early mouse embryos; CTTL-2, rhlL-2 dependent murine tumor-specific cytotoxic T-cell line; Dexon<sup>®</sup>, poly(glycolic acid) mesh; IGF, insuline-like growth factor; IL, interleukin; FGF, fibroblast growth factor; HA, hydroxyapatite; Helistat<sup>®</sup>, chemically crosslinked collagen sponge; HMVEC, human dermal microvascular endothelial cells; HMVEC(nd), human dermal microvascular endothelial cells isolated from neonatal dermis; Hyaff<sup>®</sup>, non-woven hyaluronic acid-based polymer scaffold; MC3T3-E1, osteoblastic cell line established from calvaria of late mouse embryos; MLEC, mink lung epithelial cells; NiPAM, *N*-isopropylacrylamide; PDGF, platelet derived growth factor; PDLLA, poly(DL-lactide); PLG, poly(lactide-co-glycolide); PLGA, poly(DL-lactide-co-glycolide); PLLA, poly(L-lactide); PPF, poly(propylene fumarate); ROB, rat primary osteoblastic cells; TCP, tricalcium phosphate; TGF-β, transforming growth factor-β; VEGF, vascular endothelial growth factor.

Their progeny includes both new stem cells and committed progenitors with a more restricted differentiation potential. These progenitors in turn give rise to differentiated cell types. Bone marrow stromal cells (BMSCs) are responsible for the maintenance of bone turnover throughout life and can be regarded as a mesenchymal progenitor/precursor cell population derived from adult stem cells.

Cultured BMSCs can be stimulated to differentiate into bone, cartilage, muscle, marrow stroma, tendon, fat and a variety of other connective tissues.<sup>[38]</sup> BMSCs remain, at the

moment, the most interesting and widely studied cells used in (pre)clinical bone tissue engineering studies.<sup>[39]</sup> Implanting BMSCs seeded ceramic scaffolds subcutaneously into immunodeficient mice can be used to evaluate bone formation. For this BMSCs from different animal species (rat, quail, mice, dog and human) have been used. It is worth mentioning that although differing with respect to the test animal (dog, sheep), implantation site (femur, tibia), origin of the ceramic scaffold (synthetic, natural), chemical composition, geometry and resorbability of the biomaterial, many studies indicate a significant advantage in the healing of the segmental bone defect when BMSCs seeded bioceramic scaffolds are used.<sup>[39]</sup> Bone regeneration in clinically significant large segmental defects was observed upon implantation of bioceramic scaffolds, seeded with BMSCs that were previously in vitro expanded to increase the number of osteoprogenitor cells. Implantation of bioceramic scaffolds, that were only seeded with fresh bone marrow not previously expanded in culture, did not result in healing of the segmental defects.<sup>[40]</sup> Because a very low percentage of mesenchymal stem cells is present in marrow (1 per 100,000 nucleated cells), expansion in vitro is necessary to obtain a significant number of stem cells for (re)implantation at the surgical site to form bone tissue.<sup>[40]</sup> The non-immunogenic nature of autologous mesenchymal stem cells has opened up the potential of these cells in cartilage and bone repair.<sup>[41]</sup>

As mentioned previously, bone marrow contains a small population of progenitor cells that are capable of differentiating into bone, cartilage, muscle, tendon and other connective tissues.<sup>[38]</sup> The in vitro culture of rat BMSCs in an osteogenic medium containing dexamethasone,  $\beta$ -glycerophosphate and L-ascorbic acid greatly increases the amount of cells with an osteoblastic phenotype.<sup>[42-46]</sup> Dexamethasone also has shown a favorable effect on the in vivo osteogenic potential of human BMSCs.<sup>[47]</sup>

The implantation of ceramics<sup>[40,48,49]</sup>, that were seeded with BMSCs expanded in culture to increase the number of osteogenic cells, into critical size defects led to healing of these defects. Implantation of porous PLGA scaffolds seeded with previously expanded rat BMSCs and further cultured has led to ectopic bone formation in the rat mesentery.<sup>[50]</sup> In many systems seeding followed by a period of in vitro cell culture of BMSCs on a porous scaffold, resulted in improved bone formation in vivo compared to scaffolds that were seeded and implanted immediately.<sup>[50-52]</sup>

A schematic overview of the process of isolation, in vitro expansion and differentiation in an osteogenic medium, seeding, further in vitro expansion and differentiation in an osteogenic medium and subsequent reimplantation, as is also applied in this research, is shown in Figure 2.2. As a model system for bone tissue engineering the cell-seeded and cultured scaffolds were subcutaneously implanted in immunodeficient mice to study ectopic bone formation.

## Scaffolds in bone tissue engineering

### *Scaffold requirements*

The primary role of a scaffold is to provide a temporary substrate to which transplanted cells can adhere. Many cell types are anchorage dependent and require the presence of a substrate to retain their ability to proliferate and perform their specific or differentiated function.<sup>[53]</sup>

The effectiveness of a given material in achieving these goals is dependent mainly on its surface chemistry, which determines the interaction between cell and substrate. The function of many organs is dependent not only on cell morphology but also on the three-dimensional spatial relationship between cells and extracellular matrix.

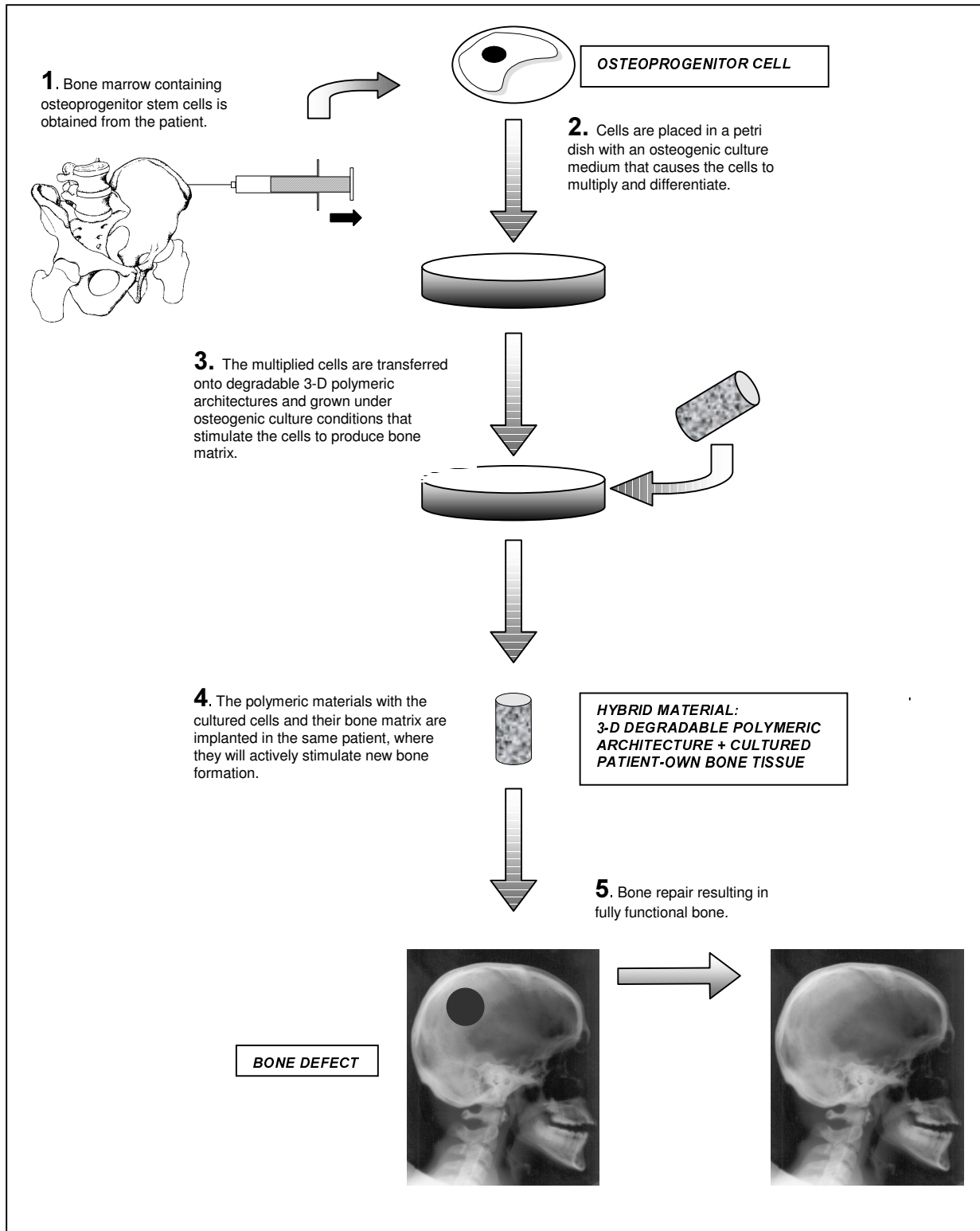


Figure 2.2 - Schematic representation of a cell-based tissue engineering approach for the (re)generation of bone. The use of patient-own cells limits possible immune responses upon implantation of the polymer-cell hybrid. Porous ceramics and polymers (without further reinforcement) are unsuitable for load-bearing applications.

Porous scaffolds with well-defined interconnected pore networks allow the organization of cells to form a tissue.<sup>[53]</sup> Highly porous scaffolds are desirable in this respect, since they provide a large void volume into which transplanted cells may be seeded. The major

advantage of utilizing biodegradable materials for tissue regeneration is that they act only as temporary substrates that are eventually removed from the body leaving only natural tissue.<sup>[53]</sup> Ideally, a scaffold material for tissue regeneration should possess the following key characteristics: (1) possess surface properties that promote cell adhesion, proliferation and differentiation; (2) degrade with a controlled degradation rate; (3) be biocompatible and degrade with degradation products that can be excreted via metabolic pathways; (4) possess a large surface area for cell attachment; (5) be easily processable into three-dimensional shapes; (6) the tissue engineered construct should have mechanical properties sufficient to withstand in vivo stresses at the site of implantation.<sup>[53,54]</sup>

Based on the available literature from 1991 to 1996 Brekke and Toth gathered a more extensive list of requirements essential for osteoinductive bone substitutes.<sup>[55]</sup> An overview of the relevant characteristics is shown in Table 2.2.

The required mechanical properties of the scaffold depend on the strategy that is followed to engineer the desired tissue. In one strategy, the scaffold supports the polymer/cell/tissue construct from the time of cell seeding up to the point where the hard tissue transplant is remodelled by the host tissue.

When used in the generation of load-bearing tissues such as articular cartilage and bone, the scaffold must then serve an additional function; it must provide sufficient temporary mechanical support to withstand in vivo stresses and loading, immediately after implantation. In another strategy, the mechanical properties of the scaffold only need to allow for cell proliferation, cell differentiation and tissue formation in vitro (in a bioreactor). The physical support by the 3-D scaffold should be maintained until the engineered tissue has sufficient mechanical integrity to support itself; this functional tissue is then implanted.<sup>[56]</sup> Clearly the second strategy demands much less of the scaffold with respect to the required mechanical strength and stiffness.

Another point that has to be focused on is the diffusion of nutrients into and metabolic/waste products out of the 3-D scaffold.

Although, an interconnected macropore-structure of 300-500  $\mu\text{m}$  enhances the diffusion rates to and from the center of a scaffold compared to scaffolds with smaller pores, transportation of the nutrients and by-products may not be sufficient for large scaffold volumes, i.e scaffolds with large distances from the center to the outside.<sup>[56-58]</sup>

A uniformly distributed and interconnected pore structures is important, so that an organized network of tissue constituents can be formed. In the reconstruction of structural tissues like cartilage and bone, scaffolds must be processable into devices of varying thickness and shape with well interconnected pores.<sup>[59]</sup>

### *Mechanical properties considerations*

Two types of bone can be distinguished: a dense solid (compact bone) and a porous network of connecting rods and plates (cancellous or trabecular bone). The most obvious difference between the two types of bone is their relative density. Bone with a porosity over 30 % is classified as cancellous, that with a porosity less than 30 % as compact. In most bones in the skeleton both types are present, the dense compact bone forming an outer shell surrounding a core of trabecular bone. The mechanical characteristics of this bone sandwich depend on the properties of its components and on their geometry. Bone grows, in response to the loads applied to it (Wolff's law). The density of bone in a particular location depends on the magnitude of the applied loads, the anisotropy of the structure depends upon the direction of the applied loads.<sup>[60]</sup> The architecture of trabecular bone, i.e. the shape, size and connectivity of individual trabeculae, varies widely with anatomic site.

Table 2.2 - Selected characteristics required for osteoinductive bone substitutes based on reference [55] and references therein.

General category	Specific device characteristic	
I. Biocompatibility	<p>Must be biocompatible</p> <p>Low tissue reactivity and resist host rejection</p> <p>Must not elicit a chronic foreign body giant cell reaction</p> <p>Non toxic</p> <p>Must be nonimmunogenic and non-antigenic</p> <p>Must be free of transmittable disease</p>	<p>Must be biodegradable, bioresorbable, bioerodable and bioadsorbable</p> <p>Must be broken down by the living system</p> <p>Asymptomatic biodegradation to biocompatible products</p> <p>Degradation products must be removed via metabolic means</p> <p>Must be completely degraded and completely replaced by de novo bone</p> <p>Must resorb in register with new bone formation</p>
II. Gross architecture qualities	<p>Readily cut, carved or sculpted to provide precise contour (cannot be brittle)</p> <p>Must resist crumbling during insertion (implantation)</p> <p>Rigid enough to provide immediate soft tissue support and prevent immediate soft tissue collapse (possess certain minimum mechanical characteristics)</p> <p>Must be porous, allowing tissue ingrowth and stabilization</p> <p>Maximum pore density to optimize cell ingrowth and formation of bone</p> <p>Must possess a minimum pore density of 75 %</p>	<p>Must possess appropriate special dimensions (geometry) to optimize cell ingrowth</p> <p>Flexibility of formulation for different degrees of solidity (support)</p> <p>Gross architectural pattern should be similar to that of cancellous bone (random pore structure, architecturally specific for tissue being treated)</p> <p>Pores must have interconnectivity (interconnecting fenestrations)</p> <p>Must possess a large surface area (substratum for cell attachment)</p> <p>Average pore size of 200-400 <math>\mu\text{m}</math></p>
III. Osteoconduction	<p>Must be osteoconductive</p> <p>Promote bone ingrowth from host bone margins</p> <p>Possess surface characteristics that optimize bone ingrowth</p>	<p>Provide scaffold allowing ingrowth of bone</p> <p>Pore size optimized for osteoconduction</p>
IV. Chemotaxis	<p>Afford chemotaxis for mesenchymal cells</p> <p>Provide means for cell attachment</p>	<p>Provide surface charge that encourages cell attachment and general electric ambiance attractive to mesenchymal cells</p> <p>Bind with endogeneous chemotactic ground substances</p>
V. Angiogenesis and vascularization	<p>Promote rapid angiogenesis and vascularization of the device</p> <p>Consistently provide solid vascularized bone to host bone</p>	<p>Must be hydrophilic, absorb fluid blood rapidly, and reinforce initial blood clot</p>
VI. Delivery and control of osteoinductive protein	<p>Promote proliferation of osteoprogenitor cells</p> <p>Should be biochemically inert with respect to the osteoinductive protein</p>	<p>Promote differentiation of bone and marrow (osteoinductive)</p>
VII. Administrative issues	<p>Must be fabricated of materials already approved by FDA for human use</p> <p>Must be cost effective over autograft</p>	<p>Constituent materials must be in abundant supply</p> <p>Verifiable sterilization of complete device</p>



Even so, trabecular bone is generally characterized as a porous material consisting of an interconnected network of rod- and plate-like trabeculae. The density of the solid component of human trabecular bone is fairly constant and is in the approximate range of 1.6-2.0 g/cm<sup>3</sup>. Both modulus and strength are strongly related to the density. The bone volume fraction typically ranges from 0.05 for highly porous trabecular bone to 0.60 for dense trabecular bone. The density of trabecular bone varies substantially and is typically in the range of 0.05-0.10 g/cm<sup>3</sup>.<sup>[61]</sup> It appears that for trabecular bone, the modulus and strength change with the square of the density.<sup>[61]</sup> At higher densities (higher than approximately 0.035 g/cm<sup>3</sup>) the modulus varies with the cube of density.<sup>[60]</sup> Moduli of trabecular tissue have been reported in the range of 1 to 13 GPa.

The properties of porous materials are largely determined by fundamental morphological parameters like size, shape and number of pores, cellular structure anisotropy, pore size distribution, surface area etc.<sup>[62-64]</sup> In practice most porous materials, due to the diversity of pore types, cannot be defined by only one single geometrical structural parameter as for other types of solids (type and volume of an elementary cell, interplanar or interatomic distances, etc.). Not only the size and shape of the pore itself, but also the size and configuration of the space between the pores filled with the matrix material, i.e. the walls and struts of the pores, determine the properties of porous materials.

Much work has been done on porous polymers. The main factor determining the mechanical properties of porous polymer scaffolds is the relative density or porosity. Like with bone, there is an exponential decrease in the Young's and compression modulus with increasing porosity.<sup>[65,66]</sup>

All other conditions being the same (chemical composition, volumetric weight, closeness of pores), the pore size can considerably affect the properties of porous polymers.<sup>[63,64]</sup> An increase of the pore size causes a rise in Young's modulus of both flexible and rigid porous polymers. It has been found that for many flexible porous polymers the tensile strength and ultimate elongation are higher when the pore size decreases. When the pore size is increased, the compressive strength of porous polymers decreases. Based on theoretical calculations, it was found that the disorder of the pore structure significantly determines the mechanical properties of the scaffold (an increase in stiffness with increasing disorder was observed).<sup>[67]</sup>

If the biodegradable polymer matrices need to simultaneously function as a temporary mechanical support in vivo, mechanical properties comparable to the mid-range values for trabecular bone strength and modulus are desired: 5-10 MPa strength and 50-100 MPa modulus (the exact values are dependent on the density of the trabecular bone, in humans 0.1–1.0 g/cm<sup>3</sup>)<sup>[68]</sup>. One must, however, realize that, if one uses these scaffolds in a bioreactor (in vitro) to create a functional tissue (that is to be implanted later), the mechanical requirements can be much less stringent since in a bioreactor the scaffold is exposed to different forces than in vivo. Although the final tissue engineered construct should preferably have a modulus comparable to bone, the modulus of the scaffold for in vitro culture does not necessarily need to be equal to that of bone.

## Scaffold materials in bone tissue engineering

### *Polymers and composites*

Bone regeneration requires four components: a morphogenetic signal, responsive host cells that will respond to the signal, a suitable carrier of this signal that can deliver it to specific sites (and then serve as a scaffold for the growth of the responsive host cells), and a viable well vascularized host bed.<sup>[2]</sup> Bone tissue engineering involves the use of a scaffolding material to either induce formation of bone from the surrounding tissue or to act as a carrier or

template for implanted bone cells or other agents. Materials used as bone tissue-engineered scaffolds may be injectable or rigid, the latter requiring a surgical implantation procedure. The materials commonly used are ceramics, polymers or composites. The ceramics and polymers can be either absorbable or non-absorbable, and the polymers can be naturally derived materials or synthetic materials. Bone tissue engineering systems include demineralized bone matrix, collagen composites, fibrin, calcium phosphate, polylactide (PLA), poly(lactide-co-glycolide) (PLGA), polylactide-polyethylene glycol, hydroxyapatite, dental plaster, and titanium.<sup>[2]</sup>

In 2000 there were no orthopedic devices, that incorporate tissue-derived components such as cells and/or growth factors, approved by the FDA. There are, however, fillers without tissue-derived components that may be classified as tissue-engineering materials. Current FDA-listed bone void fillers are only based on four materials: calcium sulphate, methyl methacrylate/poly(methyl methacrylate) (for cranioplasty), collagen or porous hydroxyapatite.<sup>[2]</sup>

The criterion of biodegradability excludes the use of most metals and ceramics as scaffold materials. Although biodegradable ceramic materials, such as tri-calcium phosphate and sea coral, have been used with some success, they have two major limitations. First they are difficult to process into porous materials with complex shapes and second, it is difficult to control their rate of degradation.<sup>[53]</sup> A future development in the field is the preparation of calcium-based scaffolds that gradually degrade at the same rate at which the new bone is formed.<sup>[39]</sup>

Polymers on the other hand, are easily formed into any shape.<sup>[53]</sup> Two other attractive properties of polymers are:

- Tailoring of composition and physical properties to the specific need.
- Biodegradability: hydrolysis of chemical bonds, degradation by enzymatic or cellular pathways.

Currently, the design and fabrication of polymeric scaffolds in tissue engineering research makes use of materials that can be categorized as follows<sup>[56]</sup>: 1) Biodegradable and bioresorbable polymers such as collagen, polyglycolide (PGA), poly-L- and poly-D,L-lactides (PLLA, PDLA), poly( $\epsilon$ -caprolactone) (PCL), that are approved by regulatory bodies. 2) Well-known polymers, such as polyorthoesters (POE), polyanhydrides (PAH), that are not approved by regulatory bodies. 3) Novel polymeric biomaterials, such as poly(lactic acid-co-lysine).<sup>[69]</sup>

The biodegradable polymers that are most often being used and/or studied for implants in the medical arena are: PLA, PGA, copolymers of PLA and PGA (PLGA), PAH, POE, PCL, polycarbonates and polyfumarates.<sup>[54]</sup> In addition to the biocompatibility, mechanical properties are perhaps equally important in orthopedic applications secondary to the inherent load bearing requirements. Engelberg and Kohn determined the mechanical and thermal properties of 20 selected degradable polymers. Based on their results, it is clear that PLLA is the preferred polymer for high-strength applications such as orthopedic implants (e.g., degradable bone nails). In terms of tensile strength, high molecular weight PLLA is one of the strongest medical polymers currently available. However, these degradable polymers are inferior in terms of mechanical strength to those of advanced biostable polymers such as PEEK and Kevlar<sup>TM</sup>.<sup>[70]</sup>

Although PEOT/PBT copolymers lack the mechanical strength of polymers like PLLA, they possess several properties that make them interesting candidates as scaffold materials in bone tissue engineering. One of the outstanding features is their bone bonding behavior (especially copolymers with a high PEO content). A major advantage of these materials is that mechanical, biological and physicochemical properties can be tailored by variation of the

composition of the PEOT/PBT copolymers. This offers the opportunity to apply PEOT/PBT block copolymers (also referred to as PolyActive™) at different sites in the body, for both soft and hard tissue applications.

Indeed, extensive research performed with PEOT/PBT in vitro and in animal experiments has led to several clinical studies. The following devices have been applied:

- Ventilation tube (1000PEOT60PBT40)<sup>[71]</sup>
- Tympanic membrane replacement (1000PEOT60PBT40)<sup>[71]</sup>
- Cement retainer (1000PEOT70PBT30)<sup>[72,73]</sup>
- Anti-adhesive barrier (1000PEOT60PBT40)<sup>[74,75]</sup>
- Skin substitute (300PEOT55PBT45)<sup>[76]</sup>
- Bone filler / bone-bonding material (1000PEOT70PBT30)<sup>[77-80]</sup>

Bone bonding has been defined as: ‘The establishment by physicochemical processes of a continuity between implant and bone matrix’.<sup>[81]</sup> The carbonate-containing apatite layer that is formed on PEOT/PBT copolymer matrices shows similarity with the bone/implant interface formed on accepted bone-bonding biomaterials like hydroxyapatite ceramics. This might explain the bone-bonding behavior of PolyActive™. There is a direct relation between bone bonding and calcification of the PEOT/PBT surface.<sup>[82]</sup> In a study on bone bonding of PEOT/PBT copolymers in goats it was shown that 1000PEOT70PBT30 is the polymer composition that exhibits extensive in vivo calcification and bone bonding (bone/biomaterial contact).<sup>[83]</sup> This in contrast to 1000PEOT40PBT60 and 1000PEOT30PBT70 where no in vivo bone bonding or calcification was observed.

Calcification, in turn, is related to the swelling behavior of PEOT/PBT block copolymers.<sup>[84,85]</sup> Both are, therefore, dependent on the weight percentage hydrophilic ‘soft’ segment in the PEOT/PBT block copolymers and on the molecular weight of the used PEO segment.<sup>[86]</sup> An increase in the PEO segment length and mass percentage resulted in a more extensive calcification.

Research on PEO hydrogels<sup>[87]</sup> and PEOT/PBT copolymers<sup>[88,89]</sup> has shown that PEO with a molecular weight of 1000 is optimal for calcification in vitro and in vivo.

The mechanical properties of polymers and porous polymeric structures can often be improved/alterd by the addition of filler materials, mainly fibers<sup>[90]</sup> or particles.<sup>[91]</sup> In bone tissue engineering applications, hydroxyapatite (HA),  $\beta$ -tricalcium phosphate ( $\beta$ -TCP) and other calcium phosphates are often used to improve the mechanical and biological properties of the polymer in question.<sup>[92]</sup> One of the first successful systems is polyethylene reinforced with hydroxyapatite (HAPEX™) as developed by Bonfield and coworkers. HA, the mineral constituent of bone, not only improved the mechanical properties<sup>[93-97]</sup>, but also improved the bioactivity, by acting as a favorable site for osteoblast attachment.<sup>[98-100]</sup> These materials, however, need to function as permanent implants, since polyethylene is non-biodegradable.

The same approach has also been used in designing biodegradable implants and scaffolds for bone tissue engineering. Biodegradable composite systems based on collagen<sup>[101]</sup>, gelatin<sup>[102-104]</sup>, chitosan<sup>[105-107]</sup> and chitin<sup>[108]</sup> have been described in literature. The most extensively studied group of biodegradable composites is based on polyesters, mainly PLLA<sup>[109-117]</sup>, PDLA<sup>[118]</sup>, PGA<sup>[119]</sup>, PCL<sup>[120]</sup> and their copolymers.<sup>[121-123]</sup> PEOT/PBT<sup>[124-126]</sup> and poly(hydroxybutyrate)<sup>[127]</sup> composites have also attracted much attention. Reinforced PLLA (50 wt % HA) is reported to have an E-modulus of 8 GPa.<sup>[110]</sup>

### *Polymer surface modification for the improvement of cell adhesion and growth*

The surface characteristics of materials, such as topography, roughness, chemistry and surface energy, play an essential part in the adhesion of cells to biomaterials. Attachment, adhesion

and spreading characterize the first phase of cell-material interactions and have an effect on the cell's capability to proliferate and to differentiate upon contact with the implant.<sup>[128]</sup> Adhesion involves two different phenomena: 1) the attachment phase, which occurs rapidly and involves short term events like physico-chemical linkages between cells and adsorbed proteins or materials, involving ionic forces, van der Waals forces etc. and 2) the adhesion phase occurring in the longer term and involving various biological molecules: extracellular matrix proteins, cell membrane proteins and cytoskeletal proteins, which interact to induce signal transduction, promote the action of transcription factors and consequently regulate gene expression.<sup>[128]</sup> The surface characteristics of the material determine how biological molecules will adsorb to the surface and more particularly determine the orientation of adsorbed molecules. They also determine the cell behavior on contact.

Poly(ethylene glycol) is recognized as a biocompatible polymer that is able to modify surface properties due to its minimal interaction with proteins and cells.<sup>[129-134]</sup> A study on poly(D,L-lactic acid)-poly(ethylene glycol) diblock copolymers clearly shows the relation between PEO content, protein adsorption and cell attachment. An increase in PEO content caused reduced cell spreading and, consequently, a decrease in cell proliferation.<sup>[129]</sup> There was, however, a more pronounced cell differentiation. Enhanced bioactivity of adsorbed adhesion proteins due to conformational changes might be responsible for this phenomenon.<sup>[129]</sup> In another study the surface modification of polystyrene particles with PEG reduced the amount of protein adsorption (including the amount of adhesion proteins) with 90-95 %. Complete inhibition of protein adsorption was, however, not observed.<sup>[135]</sup>

Many approaches are being applied to modify the surface characteristics of materials. Surfaces can be chemically or physically modified to influence protein adsorption and subsequent cell attachment. Several approaches will be briefly discussed here.

Some bone proteins (fibronectin, osteopontin, type I collagen, vitronectin) have chemotactic or adhesive properties, because they contain an Arg-Gly-Asp (RGD) sequence which is involved in the fixation of cell membrane receptors like integrin.<sup>[128,136,137]</sup> The degree of cell adhesion differs per cell and per adhesion molecule.<sup>[138]</sup> Polymers functionalized with these RGD peptides are able to bind cells.<sup>[139-142]</sup> By blending RGD peptide functionalized polymers with non-functionalized polymers it is possible to tune cell adhesion.<sup>[143-145]</sup>

Studies on PLA and PCL composites with HA have shown an increase in osteoblast attachment and activity, showing the beneficial effect of this mineral.<sup>[120,146]</sup> HA itself is also used as a scaffolding material for the implantation of bone marrow stromal cells.<sup>[2,48,147]</sup>

Material surface properties like hydrophilicity, the presence of positive or negative charges and functional groups are also known to play an important role in cell adhesion.<sup>[148,149]</sup> The degree of hydrophilicity can sometimes be altered by very simple means. Since many of the polymers used as scaffold materials are hydrophobic, it is difficult, due to surface tension forces, to bring a cell suspension into the porous scaffold. One way of overcoming this problem is to pre-wet the polymer scaffold with a liquid that is miscible with the culture medium and easily penetrates into the scaffold pores. This technique has successfully been applied to PLLA, PLGA 85:15 and PLGA 50:50 scaffolds.<sup>[53]</sup> The coating of a porous structure with poly (vinyl alcohol) (PVA) by infiltration with a PVA solution also makes it easier for cell-suspensions to enter the porous structures.<sup>[150]</sup>

Several ways are available to introduce chemical groups at the surfaces of polymers. In the past oxidizing reagents (concentrated acids) have been used to improve cell attachment (Vero cells) to polystyrene<sup>[151]</sup>, sodium hydroxide treatments to improve smooth muscle cell attachment to PGA<sup>[152]</sup> and fibroblast attachment to poly(hydroxy alkanoates).<sup>[153]</sup> Chemical treatments have also improved the adhesive strength of apatite layers to different polymers.<sup>[154-156]</sup>

Gas plasma treatments are a versatile way of chemical surface modification.<sup>[157,158]</sup> Depending on the gas employed and the polymeric surface to be treated a wide range of different functional groups can be introduced at the surface of the material.<sup>[159-161]</sup> Such treatments can have pronounced effects: stronger binding of proteins<sup>[162]</sup>, improved cell attachment<sup>[163]</sup> and a stronger adhesive strength of an apatite layer<sup>[164]</sup> are among the reported results.

It remains, however, difficult to establish a clear correlation between surface chemistry and adsorbed proteins and subsequent cell attachment.<sup>[165,166]</sup>

## Scaffold preparation methods

In industry foaming is without doubt the most often employed method for making polymers with a porous structure. Depending on the blowing agent and the exact processing techniques used, one can obtain polymer foams with open- or closed pores. The use of a blowing agent mostly results in closed-pore structures and often additional processing steps like reticulation are necessary to obtain a structure with open pores. In open-pore structures, the gas phase is air, whereas in foamed polymers the isolated pores may also contain hydrogen, carbon dioxide and volatile liquids, originating from the blowing agent employed.<sup>[64]</sup> In many cases the obtained foams are non-uniform.

The non-uniformity of the density distribution is mainly due to the processing conditions. The actual density of polymer foams depends largely on the amount of blowing agent used.<sup>[64]</sup> However, for each type of blowing agent there is a maximum concentration that can be employed. If this concentration is exceeded the density of the foam will not be reduced further, but the polymer strength will deteriorate, due to plastization of the polymer by degradation products of the blowing agent and due to the unusually rapid pressure rise in the pores.

Based on the mechanism by which they liberate gas, blowing agents can be subdivided in chemical and physical blowing agents, either by a chemical or a physical change. It has to be noted that most industrially used blowing agents are not suitable for biomedical applications, due to issues of toxicity.<sup>[167]</sup> This part will, therefore, mainly focus on other techniques used in the biomaterial field to prepare (interconnected) porous structures. Table 2.3 summarizes different techniques that have been applied in the preparation of porous structures.

### *Fiber structures*

PGA non-woven structures have been prepared by formation of a composite material with non-bonded PGA fibers embedded in a poly(L-lactic acid) (PLLA) matrix.<sup>[168]</sup> Subsequent thermal treatment of the composite and selective dissolution of the PLLA matrix resulted in a bonded PGA fiber network (porosity 81 %). However, the stipulations concerning the choice of solvent, immiscibility of the two polymers, and their relative melting temperatures, restrict the general application of this technique to other polymers than PGA and PLLA. In addition, the technique does not lend itself to easy and independent control of porosity and pore size.<sup>[53]</sup> A more versatile way to obtain bonded fiber networks is by coating the fiber mesh with another polymer. PGA fibers have been stabilized after treatment with PLLA or PLGA solutions in chloroform.<sup>[169]</sup>

Non-woven structures can also be obtained as more intricate devices like porous tubes.<sup>[170]</sup> Fibers can be produced by extrusion of polymer melts or polymer solutions through fine orifices, these fibers are then stretched and wound on a rotating mandril. Fiber-fiber bonding takes place (the fibers are still wet or hot), resulting in the formation of stable porous tubes.

Table 2.3 - Overview of techniques to prepare porous scaffolds for tissue engineering

Technique	Porosity (%)	Pore size (μm)	Remarks	Reference
Foaming using blowing agents	-	20-1000	Non porous outer layer (skin)	[172]
Foaming using CaCO <sub>3</sub>	<80	<350	Pore interconnectivity >99 %	[173]
Foaming using NH <sub>4</sub> HCO <sub>3</sub>	<81	100-1000	Difficult control	[174]
	<94	100-500	Interconnected pores	[175]
Non-wovens			Insufficient mechanical properties	
Woven fabrics	-	-		[176]
Bonded fiber structures	81	-	Described process only possible for PGA-PLLA combination	[168]
	-	-	Coating of fiber mesh with another polymer	[169]
Nanofiber electrospinning	-	-	Interconnected pore structure with a high specific surface area	[177]
Sintered microspheres	32-39	67-150	Interconnected pores	[178,179]
Solvent casting + particulate leaching	20-50	30-425	Spherical pores, salt particles remain in matrix, only thin membranes or small devices	[150]
				[180]
Coagulation + particulate leaching	<92	800-1500	Large interconnections (350 μm)	[181]
	<96	250-1180	Irregular pore morphology	[182]
			Wide range of porosities and pore sizes	
Solvent merging + particulate leaching	<95	250-500	Good interconnectivity	[183]
Fused salt particles + solvent casting + particulate leaching	<97	250-425	Improved interconnectivity compared to solvent casting + particulate leaching	[184]
Fused salt particles + gas foaming + particulate leaching	<94	250-425		[185]
Porous membrane lamination	<88	10-400	Irregular pore size, tedious procedure	[59]
Solvent casting + extrusion	<90	<30	Highly porous. Interconnected pores. Severe breakdown of salt particle during extrusion	[186]
Hydrocarbon templating	<88	100-1000	Allows incorporation of proteins	[187]
	<96	250-420	Control over interconnectivity	[65]
Melt molding	<80	50-500		[56]
Solid-liquid phase separation (freeze drying)	<97	<500	1,4-dioxane, phenol, benzene, naphthalene are toxic solvents	[188-194]
				[195,196]
Emulsion freeze drying	<97	<200	High volume of interconnected micropore structure	[197,198]
Solvent induced phase separation (immersion precipitation)	<95	<10	Only possible for films / tubes	[199]
	<45	<10		[200]
Thermally induced phase separation	<97	<200	High volume of interconnected micropore structure	[191,194,201]
Super critical fluid technology (gas foaming)	<97	10-500	Only partly interconnected pores. Formation of a skin layer	[202]
Super critical fluid technology (gas foaming)	10-30	<100	High volume of non interconnected micropore structure	[203]
Super critical fluid technology (gas foaming) + particulate leaching	<97	Micro <50 Macro <400	Low volume of non-interconnected micropore structure + interconnected macropore structure	[197]
Solid free form fabrication (rapid prototyping)				[204]
3-D printing with or without particle leaching	<60	45-150	100 % interconnected macropore structure	[56,205]
Fused deposition modelling	<80	150-700	100 % interconnected macropore structure	[56,205-208]
	60		Degradation during processing	[209]

The porosity is relatively constant and independent of the fiber diameter. The pore size on the other hand is strongly dependent on fiber diameter and ranges from ca. 40  $\mu\text{m}$  for a fiber diameter of 13  $\mu\text{m}$  to ca. 200  $\mu\text{m}$  for a fiber diameter of 30  $\mu\text{m}$ . Porosity and pore size can be varied by changing the angle of winding, the shape of the pores then also changes.

Spun fibers can be regularly intertwined by knitting, braiding or weaving. The textile stiffness for woven textures is dependent on the technique used.<sup>[171]</sup> Knitted structures can be of interest for structural anisotropic biomaterials.

### *Particulate leaching*

Porosifying agents are used to create the desired pores in a polymer. In this case the polymer (melt or solution) is mixed with a porosifying agent like an inorganic salt, that is insoluble in the polymer matrix. After solidification, due to cooling or evaporation of the polymer solvent, the porosifying agent is leached out by using a non-solvent for the polymer, this results in a porous structure.

Often-used porosifying agents are inorganic salts like sodium chloride. These salts are usually chemically inert and soluble in water, often a typical non-solvent for polymers.<sup>[210]</sup> The desired pore size is usually achieved by using salt particles with the size of the desired pore size. These salt particles are usually obtained by sieving.

Porous membranes have been prepared from poly(L-lactic acid) (PLLA) using sodium chloride, sodium citrate and sodium tartrate sieved particles, by mixing the salt particles with a PLLA solution in chloroform.<sup>[211]</sup> Membranes were prepared by casting the solution in a Petri dish, followed by evaporation of the solvent. The PLLA membrane properties are independent of the salt type and are related to the salt weight fraction and particle size. Porosity increases with the salt weight fraction, and the median pore diameter increases as the salt particle size increases. When 70-90 wt % salt was used, the membranes were homogeneous with interconnected pores. All prepared PLLA foams were 99.9 wt % salt-free and had porosities as high as 93 % and median pore diameters up to 150  $\mu\text{m}$ . The observed porosity is somewhat higher than expected on the salt content alone, because additional pores were formed during solvent evaporation and polymer solidification.

These porous PLLA membranes can be stacked to form three-dimensional polymer foams with precise anatomical shapes.<sup>[59]</sup> Careful processing of the porous films did not lead to closure of the pores between adjacent layers, resulting in a continuous pore structure. The same technique was also used to produce porous PLLA cylinders of 1-5 mm thick (diameter 2 cm), with device porosities ranging from 90-95 %.<sup>[150]</sup>

In combination with extrusion, it is possible to obtain porous tubular conduits.<sup>[186]</sup> After solvent evaporation the solution cast polymer/salt composite was extruded, after which the salt particles were leached out. The high temperatures of extrusion led to polymer degradation and the large shear forces broke up the salt particles resulting in smaller salt particles and hence smaller pore sizes. Large salt particles of 500-700  $\mu\text{m}$  gave mean pore diameters of 30  $\mu\text{m}$ . Increasing the salt particle size and the salt weight fraction both led to an increase in the mean pore diameter.

Cast PLGA composites can also be crushed and placed in a mold. With the application of heat and pressure, the polymer can be molded into the required shape, after which the porogen is leached.<sup>[212]</sup> A comparable approach makes use of precipitation of the composite, followed by compression molding to produce the desired structure.<sup>[181,182]</sup> Scaffolds with high porosities up to 96 % with independent control over pore size (250 to 1180  $\mu\text{m}$ ) can be obtained.<sup>[182]</sup> Fusion of salt particles results in more interconnected pores in the final scaffold.<sup>[185]</sup>

Besides inorganic salts it is possible to use other porosifying agents, like sugars (i.e. glucose, saccharose)<sup>[213]</sup>, gelatin<sup>[53,66]</sup>, ice particles<sup>[214-216]</sup>, palm oil<sup>[214]</sup>, and fused paraffin spheres.<sup>[65,187]</sup> In supramolecular chemistry amphiphiles or amphiphilic block copolymers have been used as nano-sized templates for pores.<sup>[217,218]</sup>

### *Gas foaming*

Mooney *et al.* have reported the fabrication of macroporous sponges from synthetic biodegradable polymers (PLGA) using high pressure carbon dioxide processing at room temperature.<sup>[202]</sup> Solid discs of polymer were saturated with CO<sub>2</sub> (5.5 MPa, 72 h). The solubility of the gas in the polymer was then rapidly decreased by reducing the CO<sub>2</sub> gas pressure to atmospheric levels. This creates thermodynamic instability and results in the nucleation and growth of gas cells within the polymer matrix.

Nucleation can occur homogeneously or heterogeneously. In homogeneous nucleation, the gas molecules cluster together within the continuous material, the associated activation energy is the free energy required to form a stable new surface and the work performed to generate the volume change. In heterogeneous nucleation, the cells nucleate at discrete interfaces in the polymer matrix. The nucleation free energy barrier at the interface is lower than that for homogeneous materials owing to surface tension effects. Heterogeneous nucleation rates are thus faster. Compared to homogeneous nucleation this leads to fewer but larger pores. Polymer sponges with large pores (up to 100  $\mu\text{m}$ ) and porosities up to 93 % could be fabricated by this technique. This procedure yielded structures with largely non-porous surface films and both open and closed cells in the central portion of the matrix.

For semi-crystalline thermoplastic elastomers the polymer/gas solution formation is notably more complex.<sup>[219]</sup> In the fabrication of microcellular (cell size 1-10  $\mu\text{m}$ ) poly (ethylene terephthalate) (PET) it was found that PET crystallizes in the presence of high CO<sub>2</sub> solution concentrations. A downside of gas foaming is that only 10-30 % of the pores are interconnected.<sup>[53]</sup>

Harris *et al.* reported the preparation of highly porous (porosities up to 97 %) PLGA by using a combination of gas foaming (CO<sub>2</sub>) and salt leaching (NaCl).<sup>[203]</sup> Blends of PLGA particles (106-250  $\mu\text{m}$ ) and NaCl crystals were compressed and subsequently foamed using CO<sub>2</sub>. The NaCl was removed by leaching. The most important advantage of the foams prepared by this technique over the combination of solvent casting and particulate leaching are the improved compression strengths (+ 82 %) and tensile strengths (+ 229 %). Also this technique might lead to less denaturation of proteins like growth factors, if these are to be incorporated in the porous structure.

### *Thermally induced phase separation*

The principles of thermally induced phase separation as a technique to obtain polymeric foams have been described by Aubert *et al.*<sup>[220]</sup> The basic process is to first dissolve a polymer (Aubert and coworkers used polystyrene) in a suitable solvent. The solution is then placed into a mold and the mold is cooled rapidly. Next the solvent is removed from the resulting solid either by evaporation, sublimation or replacement (by a non-solvent for the polymer). The density of the foam is determined by the initial concentration of polymer in solution. The morphology of the resulting foam is determined either by liquid-liquid phase separation, which may occur prior to freezing of the solvent, or liquid-solid phase separation, which occurs when the solvent freezes. In the case of the studied polystyrene/cyclohexane system, liquid-liquid phase separation resulted in an isotropic foam with small cells (10  $\mu\text{m}$ ). Upon quenching liquid-solid phase separation led to an anisotropic foam with a sheet-like



morphology and a large separation between the folds in the sheets (100  $\mu\text{m}$ ). In the case of liquid-solid phase separation the crystallizing solvent excludes the polymer to the grain boundaries, resulting in a sheet-like morphology.

### *Liquid-liquid phase separation*

In the biomedical field liquid-liquid phase separation was successfully used for the preparation of isotropic foams from amorphous PDLLA and semicrystalline PLLA in dioxane/water mixtures.<sup>[201]</sup> Freeze-drying of the poly(lactide) solutions produced foams with interconnected pores of 1-10  $\mu\text{m}$  in diameter. Better foams were formed with higher molecular weight poly(lactides). The major effect of polymer molecular weight is to allow for lower polymer concentrations and therefore a decrease in foam density, and an increase in the foam porosity (all other conditions being the same). At higher poly(lactide) concentrations gel formation is observed. Solutions of semicrystalline polymers usually form a gel as a result of liquid-liquid phase separation.

### *Liquid-solid phase separation*

Liquid-solid phase separation can occur when either the solvent or the polymer<sup>[188,189]</sup> crystallizes before liquid-liquid phase separation can take place. Due to the crystallization of one fraction the other fraction will be expelled to the grain boundaries of the forming crystals, thereby causing phase separation of the components of the polymer/solvent mixture.

An often used solvent for this purpose is 1,4-dioxane, which has a melting point of 11.8  $^{\circ}\text{C}$  and can be readily removed by sublimation (freeze-drying). Phase separation of PDLLA or PLLA/dioxane mixtures yielded highly anisotropic foams with bundles of channels with a diameter of 100  $\mu\text{m}$  with a porous substructure (10  $\mu\text{m}$ ) in the internal walls.<sup>[190]</sup> Higher polymer concentrations gave more regular porous structures. The polymer molecular weight had no significant influence on the pore morphology of the porous structure. The crystallization of 1,4-dioxane (depending on the cooling rates) had the strongest effect on foam morphology. Using a uniaxial temperature gradient, it is possible to obtain a parallel array of microtubular architectures (open pores), with anisotropic mechanical properties.<sup>[196]</sup>

Also using 1,4-dioxane, it was possible to produce highly porous composite foams of PLLA and HA with interconnected pores.<sup>[191]</sup> Addition of HA to the PLLA/dioxane solution, perturbs the crystallization of the solvent, making the crystals of the solvent more irregular. Because of the greater irregularity, the foam is more isotropic and no channel structure or repeating partitions are observed for foams with 50 % HA or more. Foams with a porosity as high as 95 % and pore sizes from several microns to a few hundred microns were obtained. The addition of HA significantly improved the mechanical properties (almost a doubling of the compressive modulus and yield strength of the porous structures).

Combined with injection molding it is possible to prepare uniform and non-uniform tubular structures from polyurethane/dioxane solutions with pore sizes up to 200  $\mu\text{m}$  and a porosity up to 51 %.<sup>[192]</sup>

PLLA foams<sup>[193]</sup> and PLLA/HA composite foams<sup>[194]</sup> also have been made from solutions with naphthalene (m.p. 80  $^{\circ}\text{C}$ ) and phenol (m.p. 43  $^{\circ}\text{C}$ ). Naphthalene and phenol have the following advantages:

1. The combination of molten naphthalene and phenol dissolves a wide range of polymers used in the field of tissue engineering.
2. The melting points of these reagents are low enough to minimize the thermal degradation of polymers and of incorporated bioactive agents.

3. The progress of phase separation can be controlled by quenching the solution to a temperature below the melting point of the solvent, thereby preserving the foam morphology.
4. Both solvents are exceptionally easy to remove by sublimation.

The PLLA foams obtained from naphthalene had a porosity greater than 87 % and pore sizes up to 100  $\mu\text{m}$ . With phenol pore sizes up to 500  $\mu\text{m}$  could be obtained. The residual amounts of solvent were very low as determined by DSC measurements (naphthalene 0.2 wt % after 220 h of freeze drying and phenol 0.01 wt %). Naphthalene and phenol are, however, very toxic solvents.

De Groot *et al.* used a combination of freeze-drying and salt leaching to obtain porous polyurethanes (PU).<sup>[221,222]</sup> PUs were typically dissolved in 1,4-dioxane, after which cyclohexane was added to induce phase separation. After addition of the porosifying agents (NaCl or saccharose particles), the mixture was frozen and freeze-dried. The salt or sugar crystals were subsequently leached out with water.

Although polymer structures with pores of about 200  $\mu\text{m}$  could be prepared by freeze-drying alone, the resulting foams lacked sufficient mechanical strength. A suitable foam was obtained when saccharose was used as a porosifying agent. Addition of some water to the PU-solvent (dioxane/cyclohexane)-sugar mixture, led to partial dissolution of the sugar crystals, resulting in a better connection between small and large pores. Implants with a macroporous structure (100-300  $\mu\text{m}$ ) highly interconnected with a microporous structure (<50  $\mu\text{m}$ ) were obtained with porosities up to 86 %. The freeze-drying step is of great importance in order to obtain highly interconnected porous polymer materials with good mechanical properties. More needle-like pores were obtained by using trioxane in the solvent mixture. Sugar particles can also be sintered into a sugar template that ensures the interconnectivity of the resulting porous network.<sup>[184]</sup>

### *Emulsion freeze-drying*

Wang *et al.* developed an emulsion freeze-drying method for the preparation of porous biodegradable PLGA scaffolds.<sup>[197]</sup> Scaffolds with porosities in the range of 91-95 % and median pore diameters from 13 to 35  $\mu\text{m}$  (with large pores up to 200  $\mu\text{m}$ ) were obtained. The method consists of creating an emulsion by homogenization of a polymer-solvent solution and water, rapidly cooling the emulsion to lock in the liquid-state structure (freezing in a copper mold), and removing the solvent and water by freeze-drying. Two different types of pores are obtained, those larger than 1  $\mu\text{m}$  (mostly due to the emulsion) and those smaller than 0.01  $\mu\text{m}$  (probably due to the inherent porosity of the polymer itself from the evaporation of the solvent). The use of high molecular weight polymer gives the emulsion structure high stability, this allows for the formation of larger pores. The scaffolds made with this method can be made more than 1 cm in thickness, much thicker than those made via a solvent casting/salt leaching method. The use of an emulsion makes it possible to incorporate proteins.

### *Rapid prototyping*

Rapid Prototyping technologies (RP) or Solid Free Form fabrication (SFF) methods are defined as a set of manufacturing processes that are capable of producing complex free-form parts directly from a computer-aided design (CAD) model of an object. RP systems join together liquid, powder and sheet materials to form parts. Several RP systems have been developed over the years, examples are stereolithography, selective laser sintering, laminated

object manufacturing, three-dimensional printing and fused deposition modeling.<sup>[205]</sup> The last two will be discussed in more detail.

Three-dimensional printing is a rapid prototyping technology that has been used to process bioresorbable scaffolds for tissue engineering applications. The technology is based on the printing of a binder material (mostly solvents) through a print head nozzle onto a powder bed, with no tooling required. The part is built sequentially in layers. The entire process is performed at ambient conditions. Biological agents, such as cells, growth factors etc. could be incorporated into a porous scaffold without inactivation if non-toxic solvents can be used. Unfortunately, aliphatic polyesters can often only be dissolved in highly toxic solvents, such as chloroform and methylene chloride.<sup>[56,205]</sup>

In fused deposition modeling the thermoplastic polymer material feeds into a temperature-controlled extrusion head, where it is heated to a semi-liquid state. The head extrudes and deposits the fiber in ultra-thin layers onto a support. The head directs the material precisely into place. The fiber solidifies, bonding to the fibers in the preceding layer.<sup>[56,205]</sup>

The scaffold can be designed using a CAD file or digital data derived from CT or MRI scans, permitting custom-made fabrication of bioresorbable hybrid scaffold systems.<sup>[56,205]</sup> Inactivation of bioactive molecules by exposure to high temperatures or toxic solvents, is the major obstacle to successful drug incorporation and delivery from degradable scaffolds prepared in these ways.<sup>[53]</sup>

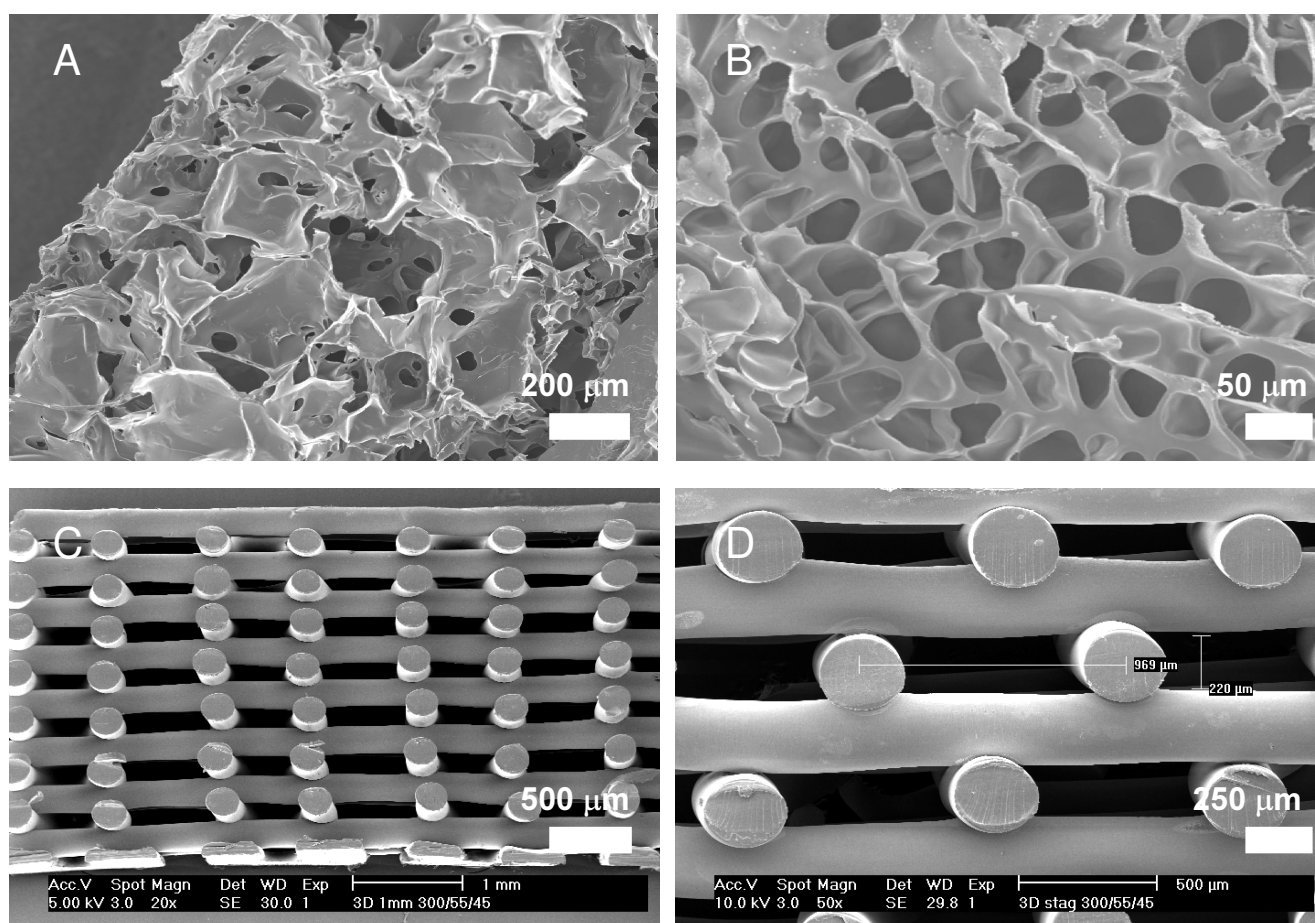


Figure 2.3 – Porous PEOT/PBT scaffolds prepared by different fabrication techniques. A: solution casting combined with salt leaching (1000PEOT70PBT30), B: liquid-solid phase separation, freeze-drying using 1,4-dioxane (600PEOT70PBT30), C and D: fused deposition modeling (300PEOT55PBT45, by courtesy of T.B.F. Woodfield, Isotis S.A., Bilthoven, The Netherlands).

### *Preferred ways of scaffold fabrication*

Of the different techniques available those that are based on particulate leaching and liquid-solid phase separation (freeze-drying) are the most versatile ones. With both techniques it is possible to prepare scaffolds with a wide range of porosities and pore sizes, without the need for specialized equipment, like in the case of rapid prototyping.

Figure 2.3 shows some examples of PEOT/PBT scaffolds prepared by different scaffold fabrication techniques as described in this section. The differences in morphology are clearly observed.

Although this chapter reviews the different materials and techniques for preparing scaffolds for (bone) tissue engineering, it is impossible to address all the publications written on this subject. For more information the reader is advised to consult some excellent reviews written on bone substitution,<sup>[40,68,147,223]</sup> cells in (bone) tissue engineering<sup>[2,38,39,41,53,224]</sup>, biomaterials<sup>[2,53,54,225]</sup> and scaffold fabrication methods.<sup>[53,54,56,205,226]</sup>

## References

1. R.O.C. Oreffo, J.T. Triffitt *Future potentials for using osteogenic stem cells and biomaterials in orthopedics* Bone **1999**, 25, 5S-9S.
2. K.J.L. Burg, S. Porter, J.F. Kellam *Biomaterial developments for bone tissue engineering* Biomaterials **2000**, 21, 2347-2359.
3. J.E. Babensee, L.V. McIntire, A.G. Mikos *Growth factor delivery for tissue engineering* Pharm. Res. **2000**, 17, 497-504.
4. A. Yamaguchi *Regulation of differentiation pathway of skeletal mesenchymal cells in cell-lines by transforming growth-factor-beta superfamily* Semin. Cell Biol. **1995**, 6, 165-173.
5. P.B. Malafaya, G.A. Silva, E.T. Baran, R.L. Reis *Drug delivery therapies I - General trends and its importance on bone tissue engineering applications* Curr. Opin. Solid State Mat. Sci. **2002**, 6, 283-295.
6. M.R. Urist, B.F. Silverman, K. Buering, F.L. Dubuc, J.M. Rosenberg *The bone induction principle* Clin. Orthop. Rel. Res. **1967**, 53, 243-283.
7. M.R. Urist, B.S. Strates *Bone morphogenetic protein* J. Dent. Res. **1971**, 50, 1392-1406.
8. N. Saito, K. Takaoka *New synthetic biodegradable polymers as BMP carriers for bone tissue engineering* Biomaterials **2003**, 24, 2287-2293.
9. P.B. Malafaya, G.A. Silva, E.T. Baran, R.L. Reis *Drug delivery therapies II. Strategies for delivering bone regenerating factors* Curr. Opin. Solid State Mat. Sci. **2002**, 6, 297-312.
10. G. Zellin, A. Linde *Effects of recombinant human fibroblast growth factor-2 on osteogenic cell populations during orthopic osteogenesis in vivo* Bone **2000**, 26, 161-168.
11. G. Lisignoli, M. Fini, G. Giavaresi, N.N. Aldini, S. Toneguzzi, A. Facchini *Osteogenesis of large segmental radius defects enhanced by basic fibroblast growth factor activated bone marrow stromal cells grown on non-woven hyaluronic acid-based polymer scaffold* Biomaterials **2002**, 23, 1043-1051.
12. Y.J. Park, Y.M. Lee, S.N. Park, S.Y. Sheen, C.P. Chung, S.J. Lee *Platelet derived growth factor releasing chitosan sponge for periodontal bone regeneration* Biomaterials **2000**, 21, 153-159.
13. J.Y. Lee, S.H. Nam, S.Y. Im, Y.J. Park, Y.M. Lee, Y.J. Seol, C.P. Chung, S.J. Lee *Enhanced bone formation by controlled growth factor delivery from chitosan-based biomaterials* J. Control. Release **2002**, 78, 187-197.
14. S.J. Lee, Y.J. Park, S.N. Park, Y.M. Lee, Y.J. Seol, Y. Ku, C.P. Chung *Molded porous poly (L-lactide) membranes for guided bone regeneration with enhanced effects by controlled growth factor release* J. Biomed. Mater. Res. **2001**, 55, 295-303.
15. M. Raschke, B. Wildemann, P. Inden, H. Bail, A. Flyvbjerg, J. Hoffmann, N.P. Haas, G. Schmidmaier *Insulin-like growth factor-1 and transforming growth factor- beta 1 accelerates osteotomy healing using polylactide-coated implants as a delivery system: A biomechanical and histological study in minipigs* Bone **2002**, 30, 144-151.
16. G. Schmidmaier, B. Wildemann, A. Stemberger, N.P. Haas, M. Raschke *Biodegradable poly(D,L-lactide) coating of implants for continuous release of growth factors* J. Biomed. Mater. Res. **2001**, 58, 449-455.
17. G. Schmidmaier, B. Wildemann, H. Bail, M. Lucke, T. Fuchs, A. Stemberger, A. Flyvbjerg, N.P. Haas, M. Raschke *Local application of growth factors (insulin-like growth factor-1 and transforming growth factor-*

- beta 1) from a biodegradable poly(D,L-lactide) coating of osteosynthetic implants accelerates fracture healing in rats* Bone **2001**, 28, 341-350.
18. J.W.M. Vehof, J.P. Fisher, D. Dean, J. van der Waerden, P.H.M. Spauwen, A.G. Mikos, J.A. Jansen *Bone formation in transforming growth factor beta-1-coated porous poly(propylene fumarate) scaffolds* J. Biomed. Mater. Res. **2002**, 60, 241-251.
19. G. Li, M.L. Bouxsein, C. Luppen, X.J. Li, M. Wood, H.J. Seeherman, J.M. Wozney, H. Simpson *Bone consolidation is enhanced by rhBMP-2 in a rabbit model of distraction osteogenesis* J. Orthop. Res. **2002**, 20, 779-788.
20. W. Friess, H. Uludag, S. Foskett, R. Biron, C. Sargeant *Characterization of absorbable collagen sponges as recombinant human bone morphogenetic protein-2 carriers* Int. J. Pharm. **1999**, 185, 51-60.
21. W. Friess, H. Uludag, S. Foskett, R. Biron, C. Sargeant *Characterization of absorbable collagen sponges as rhBMP-2 carriers* Int. J. Pharm. **1999**, 187, 91-99.
22. T.J. Gao, H. Uludag *Effect of molecular weight of thermoreversible polymer on in vivo retention of rhBMP-2* J. Biomed. Mater. Res. **2001**, 57, 92-100.
23. G.E. Pluhar, P.A. Manley, J.P. Heiner, R. Vanderby, H.J. Seeherman, M.D. Markel *The effect of recombinant human bone morphogenetic protein-2 on femoral reconstruction with an intercalary allograft in a dog model* J. Orthop. Res. **2001**, 19, 308-317.
24. A.G. Zabka, G.E. Pluhar, R.B. Edwards, P.A. Manley, K. Hayashi, J.P. Heiner, V.L. Kalscheur, H.J. Seeherman, M.D. Markel *Histomorphometric description of allograft bone remodeling and union in a canine segmental femoral defect model: a comparison of rhBMP-2, cancellous bone graft, and absorbable collagen sponge* J. Orthop. Res. **2001**, 19, 318-327.
25. S. Itoh, M. Kikuchi, K. Takakuda, Y. Koyama, H.N. Matsumoto, S. Ichinose, J. Tanaka, T. Kawauchi, K. Shinomiya *The biocompatibility and osteoconductive activity of a novel hydroxyapatite/collagen composite biomaterial, and its function as a carrier of rhBMP-2* J. Biomed. Mater. Res. **2001**, 54, 445-453.
26. J. Louis-Ugbo, H.S. Kim, S.D. Boden, M.T. Mayr, R.C. Li, H. Seeherman, D. D'Augusta, C. Blake, A.P. Jiao, S. Peckham *Retention of I-125-labeled recombinant human bone morphogenetic protein-2 by biphasic calcium phosphate or a composite sponge in a rabbit posterolateral spine arthrodesis model* J. Orthop. Res. **2002**, 20, 1050-1059.
27. X.Q. Chen, L.S. Kidder, W.D. Lew *Osteogenic protein-1 induced bone formation in an infected segmental defect in the rat femur* J. Orthop. Res. **2002**, 20, 142-150.
28. M. Lind, S. Overgaard, T.B. Jensen, Y. Song, S.B. Goodman, C. Bunger, K. Soballe *Effect of osteogenic protein 1/collagen composite combined with impacted allograft around hydroxyapatite-coated titanium alloy implants is moderate* J. Biomed. Mater. Res. **2001**, 55, 89-95.
29. H. Uludag, D. D'Augusta, J. Golden, J. Li, G. Timony, R. Riedel, J.M. Wozney *Implantation of recombinant human bone morphogenetic proteins with biomaterial carriers: A correlation between protein pharmacokinetics and osteoinduction in the rat ectopic model* J. Biomed. Mater. Res. **2000**, 50, 227-238.
30. A. Chenite, C. Chaput, D. Wang, C. Combes, M.D. Buschmann, C.D. Hoemann, J.C. Leroux, B.L. Atkinson, F. Binette, A. Selmani *Novel injectable neutral solutions of chitosan form biodegradable gels in situ* Biomaterials **2000**, 21, 2155-2161.
31. J.A. Cadee, C.J. de Groot, W. Jiskoot, W. den Otter, W.E. Hennink *Release of recombinant human interleukin-2 from dextran-based hydrogels* J. Control. Release **2002**, 78, 1-13.
32. D. Logeart-Avramoglou, R. Huynh, F. Chaubet, L. Sedel, A. Meunier *Interaction of specifically chemically modified dextrans with transforming growth factor beta 1: potentiation of its biological activity* Biochem. Pharmacol. **2002**, 63, 129-137.
33. S. Tamura, H. Kataoka, Y. Matsui, Y. Shionoya, K. Ohno, K.I. Michi, K. Takahashi, A. Yamaguchi *The effects of transplantation of osteoblastic cells with bone morphogenetic protein (BMP)/carrier complex on bone repair* Bone **2001**, 29, 169-175.
34. G. Lisignoli, N. Zini, G. Remiddi, A. Piacentini, A. Puggioli, C. Trimarchi, M. Fini, N.M. Maraldi, A. Facchini *Basic fibroblast growth factor enhances in vitro mineralization of rat bone marrow stromal cells grown on non-woven hyaluronic acid based polymer scaffold* Biomaterials **2001**, 22, 2095-2105.
35. D.D. Hile, M.L. Amirpour, A. Akgerman, M.V. Pishko *Active growth factor delivery from poly(D,L-lactide-co-glycolide) foams prepared in supercritical CO<sub>2</sub>* J. Control. Release **2000**, 66, 177-185.
36. W.L. Murphy, M.C. Peters, D.H. Kohn, D.J. Mooney *Sustained release of vascular endothelial growth factor from mineralized poly(lactide-co-glycolide) scaffolds for tissue engineering* Biomaterials **2000**, 21, 2521-2527.
37. M.H. Sheridan, L.D. Shea, M.C. Peters, D.J. Mooney *Bioadsorbable polymer scaffolds for tissue engineering capable of sustained growth factor delivery* J. Control. Release **2000**, 64, 91-102.

38. A.I. Caplan, S.P. Bruder *Mesenchymal stem cells: building blocks for molecular medicine in the 21st century* Trends Mol. Med **2001**, 7, 259-264.
39. R. Cancedda, B. Dozin, P. Giannoni, R. Quarto *Tissue engineering and cell therapy of cartilage and bone* Matrix Biol. **2003**, 22, 81-91.
40. S.P. Bruder, N. Jaiswal, N.S. Ricalton, J.D. Mosca, K.H. Kraus, S. Kadiyala *Mesenchymal stem cells in osteobiology and applied bone regeneration* Clin. Orthop. Rel. Res. **1998**, S247-S256.
41. F. Rose, R.O.C. Oreffo *Bone tissue engineering: Hope vs hype* Biochem. Biophys. Res. Commun. **2002**, 292, 1-7.
42. C. Maniopoulos, J. Sodek, A.H. Melcher *Bone-formation in vitro by stromal cells obtained from bone marrow of young-adult rats* Cell Tissue Res. **1988**, 254, 317-330.
43. S.J. Peter, C.R. Liang, D.J. Kim, M.S. Widmer, A.G. Mikos *Osteoblastic phenotype of rat marrow stromal cells cultured in the presence of dexamethasone,  $\beta$ -glycerolphosphate, and L- ascorbic acid* J. Cell. Biochem. **1998**, 71, 55-62.
44. P.S. Leboy, J.N. Beresford, C. Devlin, M.E. Owen *Dexamethasone induction of osteoblast messenger-RNAs in rat marrow stromal cell-cultures* J. Cell. Physiol. **1991**, 146, 370-378.
45. D.J. Rickard, T.A. Sullivan, B.J. Shenker, P.S. Leboy, I. Kazhdan *Induction of rapid osteoblast differentiation in rat bone-marrow stromal cell-cultures by dexamethasone and BMP-2* Dev. Biol. **1994**, 161, 218-228.
46. A.E. Grigoriadis, J.N.M. Heersche, J.E. Aubin *Differentiation of muscle, fat, cartilage, and bone from progenitor cells present in a bone-derived clonal cell population: effect of dexamethasone* J. Cell. Biol. **1988**, 106, 2139-2151.
47. S.C. Mendes, J.M. Tibbe, M. Veenhof, K. Bakker, S. Both, P.P. Platenburg, F.C. Oner, J.D. de Bruijn, C.A. van Blitterswijk *Bone tissue-engineered implants using human bone marrow stromal cells: Effect of culture conditions and donor age* Tissue Eng. **2002**, 8, 911-920.
48. E. Kon, A. Muraglia, A. Corsi, P. Bianco, M. Marcacci, I. Martin, A. Boyde, I. Ruspanini, P. Chistolini, M. Rocca, R. Giardino, R. Cancedda, R. Quarto *Autologous bone marrow stromal cells loaded onto porous hydroxyapatite ceramic accelerate bone repair in critical-size defects of sheep long bones* J. Biomed. Mater. Res. **2000**, 49, 328-337.
49. S. Kadiyala, N. Jaiswal, S.P. Bruder *Culture-expanded, bone marrow-derived mesenchymal stem cells can regenerate a critical-sized segmental bone defect* Tissue Eng. **1997**, 3, 173-185.
50. S.L. Ishaug-Riley, G.M. Crane, A. Gurlek, M.J. Miller, A.W. Yasko, M.J. Yaszemski, A.G. Mikos *Ectopic bone formation by marrow stromal osteoblast transplantation using poly(DL-lactic-co-glycolic acid) foams implanted into the rat mesentery* J. Biomed. Mater. Res. **1997**, 36, 1-8.
51. T. Livingston, P. Ducheyne, J. Garino *In vivo evaluation of a bioactive scaffold for bone tissue engineering* J. Biomed. Mater. Res. **2002**, 62, 1-13.
52. S.C. Mendes, M. Sleijster, A. van den Muysenberg, J.D. de Bruijn, C.A. van Blitterswijk *A cultured living bone equivalent enhances bone formation when compared to a cell seeding approach* J. Mater. Sci.-Mater. Med. **2002**, 13, 575-581.
53. R.C. Thomson, M.C. Wake, M.J. Yaszemski, A.G. Mikos *Biodegradable polymer scaffolds to regenerate organs* Adv. Polym.Sci. **1995**, 122, 245-274.
54. C.M. Agrawal, R.B. Ray *Biodegradable polymeric scaffolds for musculoskeletal tissue engineering* J. Biomed. Mater. Res. **2001**, 55, 141-150.
55. J.H. Brekke, J.M. Toth *Principles of tissue engineering applied to programmable osteogenesis* J. Biomed. Mater. Res. (Appl. Biomater.) **1998**, 43, 380-398.
56. D.W. Hutmacher *Scaffolds in tissue engineering bone and cartilage* Biomaterials **2000**, 21, 2529-2543.
57. L.E. Freed, G. Vunjaknovakovic, R. Langer *Cultivation of Cell-Polymer Cartilage Implants in Bioreactors* J. Cell. Biochem. **1993**, 51, 257-264.
58. L.E. Freed, G. Vunjaknovakovic, J.C. Marquis, R. Langer *Kinetics of Chondrocyte Growth in Cell-Polymer Implants* Biotechnol. Bioeng. **1994**, 43, 597-604.
59. A.G. Mikos, G. Sarakinos, S.M. Leite, J.P. Vacanti, R. Langer *Laminated three-dimensional biodegradable foams for use in tissue engineering* Biomaterials **1993**, 14, 323-330.
60. L.J. Gibson *The mechanical behaviour of cancellous bone* J. Biomechanics **1985**, 18, 317-328.
61. T.M. Keaveny, W.C. Hayes *A 20-year perspective on the mechanical-properties of trabecular bone* J. Biomech. Eng.-Trans. ASME **1993**, 115, 534-542.
62. J.H. Saunders *Fundamentals of foam formation* in "Polymeric foams: Handbook of polymeric foams and foam technology" 1st ed.; D. Klempner, and K.C. Frisch, Ed.; Carl Hanser Verlag: Munich, Germany **1991**; pp 5-15.

63. F.H. Shutov *Cellular structure and properties of foamed polymers* in "Polymeric foams: Handbook of polymeric foams and foam technology" 1st ed.; D. Klemmner, and K.C. Frisch, Ed.; Carl Hanser Verlag: Munich, Germany **1991**; pp 17-46.
64. F.A. Shutov *Foamed polymers, cellular structure and properties* Adv. Polym. Sci. **1983**, *51*, 155-218.
65. P.X. Ma, J.W. Choi *Biodegradable polymer scaffolds with well-defined interconnected spherical pore network* Tissue Eng. **2001**, *7*, 23-33.
66. R.C. Thomson, M.J. Yaszemski, J.M. Powers, A.G. Mikos *Fabrication of biodegradable polymer scaffolds to engineer trabecular bone* J. Biomater. Sci.-Polym. Ed. **1995**, *7*, 23-38.
67. M.W.D. Van der Burg, V. Shulmeister, E. Van der Geissen, R. Marissen *On the linear elastic properties of regular and random open-cell foam models* J. Cell. Plast. **1997**, *33*, 31-54.
68. M.J. Yaszemski, R.G. Payne, W.C. Hayes, R. Langer, A. Mikos, G. *Evolution of bone transplantation: molecular, cellular and tissue strategies to engineer human bone* Biomaterials **1996**, *17*, 175-185.
69. J. Helder *Polydepsipeptides: copolymers of  $\alpha$ -amino acids and  $\alpha$ -hydroxy acids*, Thesis, University of Twente, Enschede, The Netherlands, **1988**.
70. I. Engelberg, J. Kohn *Physicomechanical properties of degradable polymers used in medical applications - a comparative-study* Biomaterials **1991**, *12*, 292-304.
71. D. Bakker, C.A. van Blitterswijk *Prothetische voortbrengsels met botbindende eigenschappen* NL Patent 8802178 **1988**.
72. S.K. Bulstra, R.G.T. Geesink, D. Bakker, T.H. Bulstra, S.J.M. Bouwmeester, A.J. van der Linden *Femoral canal occlusion in total hip replacement using a resorbable and flexible cement restrictor* J. Bone Joint Surg.-Br. Vol. **1996**, *78B*, 892-898.
73. K.G. Freund, N. Herold, N.D. Rock, P. Riegels-Nielsen *Poor results with the Shuttle Stop - Resorbable versus nonresorbable intramedullar cement restrictor in a prospective and randomized study with a 2-year follow-up* Acta Orthop. Scand. **2003**, *74*, 37-41.
74. E.A. Bakkum, J.B. Trimbos, R.A.J. Dalmeijer, C.A. Van Blitterswijk *Preventing postoperative intraperitoneal adhesion formation with Polyactive(Tm), a degradable copolymer acting as a barrier* J. Mater. Sci.-Mater. Med. **1995**, *6*, 41-45.
75. D. Bakker, E.A. Bakkum, C.A. van Blitterwijk *Devices for preventing tissue adhesion* U.S. Patent 5508036 **1996**.
76. G.J. Beumer *Synthetic biodegradable polymers in the regeneration of skin*, Thesis, University of Leiden, Leiden, The Netherlands, **1993**.
77. M.L. Gaillard *The Role of Calcium Phosphate in a Bone-Bonding Polymer*, Thesis, University of Leiden, Leiden, The Netherlands, **1995**.
78. G.J. Meijer *Flexible Bone-Bonding Implants: A study of Polyactive applied as dental implant and bone filler*, Thesis, University of Utrecht, Utrecht, The Netherlands, **1996**.
79. A.M. Radder *Bone-bonding copolymers for hard tissue replacement*, Thesis, University of Leiden, Leiden, The Netherlands, **1994**.
80. J.D. de Bruijn *Calcium Phosphate Biomaterials: Bone-bonding and Biodegradation Properties*, Thesis, University of Leiden, Leiden, The Netherlands, **1993**.
81. A.M. Radder, J.E. Davies, H. Leenders, S.A.T. van der Meer, C.A. van Blitterswijk *Proceedings of the 6th international symposium on ceramics in medicine* Bioceramics **1993**, *6*, 345-351.
82. M. Okumura, C.A. van Blitterswijk, H.K. Koerten, D. Bakker, S.C. Hesselting, K. de Groot *Bone-bonding materials*; P. Ducheyne, T. Kokubo and C.A. van Blitterswijk, Ed.; Reed Healthcare Communications: Leiderdorp, The Netherlands **1992**; pp 13-30.
83. A.M. Radder, H. Leenders, C.A. van Blitterswijk *Interface reactions to PEO/PBT copolymers (Polyactive(R)) after implantation in cortical bone* J. Biomed. Mater. Res. **1994**, *28*, 141-151.
84. C.A. van Blitterswijk, J. van der Brink, H. Leenders, D. Bakker *The effect of PEO ratio on degradation, calcification and bone bonding of PEO/PBT copolymer (Polyactive)* Cells and Materials **1993**, *3*, 23-36.
85. A.M. Radder, J.A. Vanloon, G.J. Puppels, C.A. van Blitterswijk *Degradation and calcification of a PEO/PBT copolymer series* J. Mater. Sci.-Mater. Med. **1995**, *6*, 510-517.
86. M.L. Gaillard, J.R. de Wijn, C.A. van Blitterswijk *Proceeding of the 6th international symposium on ceramics in medicine* Bioceramics **1993**, *6*, 53-58.
87. S.F.A. Hossainy, J.A. Hubbell *Molecular weight dependence of calcification of polyethylene glycol hydrogels* Biomaterials **1994**, *15*, 921-925.
88. P. Li, D. Bakker, C.A. van Blitterswijk *The bone-bonding polymer Polyactive(R) 80/20 induces hydroxycarbonate apatite formation in vitro* J. Biomed. Mater. Res. **1997**, *34*, 79-86.
89. A.M. Radder, C.A. van Blitterswijk *Abundant postoperative calcification of an elastomer - matrix calcium phosphate-polymer composite for bone reconstruction* J. Mater. Sci.-Mater. Med. **1994**, *5*, 320-325.

90. G.C. McGrath, D.W. Clegg *Reinforced thermoplastic foams (chapter 10)* in "Mechanical properties of reinforced thermoplastics; 1st ed.; D.W. Clegg, Ed.; Elsevier Applied Science Publishers Ltd.: London, United Kingdom **1986**; pp 295-317.
91. R. Mushack, R. Lüttich, W. Bachmann *White fillers in elastomers* Eur. Rubber J. **1996**, July/August, 24-29.
92. M. Kobayashi, T. Nakamura, S. Shinzato, W.F. Mousa, K. Nishio, K. Ohsawa, T. Kokubo, T. Kikutani *Effect of bioactive filler content on mechanical properties and osteoconductivity of bioactive bone cement* J. Biomed. Mater. Res. **1999**, 46, 447-457.
93. M. Wang, R. Joseph, W. Bonfield *Hydroxyapatite-polyethylene composites for bone substitution: effects of ceramic particle size and morphology* Biomaterials **1998**, 19, 2357-2366.
94. M. Wang, D. Porter, W. Bonfield *Processing, characterisation, and evaluation of hydroxyapatite reinforced polyethylene composites* Brit. Ceram. Trans. **1994**, 93, 91-95.
95. M. Wang, C. Berry, M. Braden, W. Bonfield *Young's and shear moduli of ceramic particle filled polyethylene* J. Mater. Sci.-Mater. Med. **1998**, 9, 621-624.
96. Y. Zhang, K.E. Tanner *Impact behavior of hydroxyapatite reinforced polyethylene composites* J. Mater. Sci.-Mater. Med. **2003**, 14, 63-68.
97. S.N. Nazhat, R. Joseph, M. Wang, R. Smith, K.E. Tanner, W. Bonfield *Dynamic mechanical characterization of hydroxyapatite reinforced polyethylene: effect of particle size* J. Mater. Sci.-Mater. Med. **2000**, 11, 621-628.
98. J. Huang, L. DiSilvio, M. Wang, K.E. Tanner, W. Bonfield *In vitro mechanical and biological assessment of hydroxyapatite-reinforced polyethylene composite* J. Mater. Sci.-Mater. Med. **1997**, 8, 775-779.
99. M.J. Dalby, L. Di Silvio, G.W. Davies, W. Bonfield *Surface topography and HA filler volume effect on primary human osteoblasts in vitro* J. Mater. Sci.-Mater. Med. **2000**, 11, 805-810.
100. L. Di Silvio, M. Dalby, W. Bonfield *In vitro response of osteoblasts to hydroxyapatite-reinforced polyethylene composites* J. Mater. Sci.-Mater. Med. **1998**, 9, 845-848.
101. C. Du, F.Z. Cui, Q.L. Feng, X.D. Zhu, K. de Groot *Tissue response to nano-hydroxyapatite/collagen composite implants in marrow cavity* J. Biomed. Mater. Res. **1998**, 42, 540-548.
102. K.S. ten Huysen, P.W. Brown *The formation of hydroxyapatite-gelatin composites at 38- Degrees-C* J. Biomed. Mater. Res. **1994**, 28, 27-33.
103. A. Bigi, S. Panzavolta, N. Roveri *Hydroxyapatite-gelatin films: a structural and mechanical characterization* Biomaterials **1998**, 19, 739-744.
104. N. Sasaki, H. Umeda, S. Okada, R. Kojima, A. Fukuda *Mechanical-properties of hydroxyapatite-reinforced gelatin as a model system of bone* Biomaterials **1989**, 10, 129-132.
105. T. Kawakami, M. Antoh, H. Hasegawa, T. Yamagishi, M. Ito, S. Eda *Experimental-study on osteoconductive properties of a chitosan- bonded hydroxyapatite self-hardening paste* Biomaterials **1992**, 13, 759-763.
106. M. Ito *In vitro properties of a chitosan-bonded hydroxyapatite bone- filling paste* Biomaterials **1991**, 12, 41-45.
107. Y.J. Yin, F. Zhao, X.F. Song, K.D. Yao, W.W. Lu, J.C. Leong *Preparation and characterization of hydroxyapatite/chitosan- gelatin network composite* J. Appl. Polym. Sci. **2000**, 77, 2929-2938.
108. A.C.A. Wan, E. Khor, G.W. Hastings *Hydroxyapatite modified chitin as potential hard tissue substitute material* J. Biomed. Mater. Res. **1997**, 38, 235-241.
109. S. Higashi, T. Yamamuro, T. Nakamura, Y. Ikada, S.-H. Hyon, K. Jamshidi *Polymer-hydroxyapatite composites for biodegradable bone fillers* Biomaterials **1986**, 7, 183-187.
110. C.C.P.M. Verheyen, J.R. de Wijn, C.A. van Blitterswijk, K. de Groot *Evaluation of hydroxylapatite poly(L-lactide) composites - mechanical-behavior* J. Biomed. Mater. Res. **1992**, 26, 1277-1296.
111. C.C.P.M. Verheyen, J.R. de Wijn, C.A. van Blitterswijk, K. de Groot, P.M. Rozing *Hydroxylapatite poly(L-lactide) composites - an animal study on push-out strengths and interface histology* J. Biomed. Mater. Res. **1993**, 27, 433-444.
112. C.C.P.M. Verheyen, C.P.A.T. Klein, J.M.A. de Bleeck-Hogervorst, J.G.C. Wolke, C.A. van Blitterswijk, K. de Groot *Evaluation of hydroxylapatite poly(L-lactide) composites - physicochemical properties* J. Mater. Sci.-Mater. Med. **1993**, 4, 58-65.
113. Y. Shikinami, M. Okuno *Bioresorbable devices made of forged composites of hydroxyapatite (HA) particles and poly-L-lactide (PLLA): Part I. Basic characteristics* Biomaterials **1999**, 20, 859-877.
114. Y. Shikinami, M. Okuno *Bioresorbable devices made of forged composites of hydroxyapatite (HA) particles and poly L-lactide (PLLA). Part II: practical properties of miniscrews and miniplates* Biomaterials **2001**, 22, 3197-3211.
115. N.C. Bleach, K.E. Tanner, M. Kellomaki, P. Tormala *Effect of filler type on the mechanical properties of self- reinforced polylactide-calcium phosphate composites* J. Mater. Sci.-Mater. Med. **2001**, 12, 911-915.



116. N. Ignjatovic, S. Tomic, M. Dakic, M. Miljkovic, M. Plavsic, D. Uskokovic *Synthesis and properties of hydroxyapatite/poly-L-lactide composite biomaterials* Biomaterials **1999**, 20, 809-816.
117. M. Matsumoto, E. Chosa, K. Nabeshima, Y. Shikunami, N. Tajima *Influence of bioresorbable, unsintered hydroxyapatite/poly-L-lactide composite films on spinal cord, nerve roots, and epidural space* J. Biomed. Mater. Res. **2002**, 60, 101-109.
118. S.A.T. van der Meer, J.R. de Wijn, J.G.C. Wolke *The influence of basic filler materials on the degradation of amorphous D- and L-lactide copolymer* J. Mater. Sci.-Mater. Med. **1996**, 7, 359-361.
119. W. Linhart, F. Peters, W. Lehmann, K. Schwarz, A.F. Schilling, M. Amling, J.M. Rueger, M. Epple *Biologically and chemically optimized composites of carbonated apatite and polyglycolide as bone substitution materials* J. Biomed. Mater. Res. **2001**, 54, 162-171.
120. S.C. Rizzi, D.T. Heath, A.G.A. Coombes, N. Bock, M. Textor, S. Downes *Biodegradable polymer/hydroxyapatite composites: Surface analysis and initial attachment of human osteoblasts* J. Biomed. Mater. Res. **2001**, 55, 475-486.
121. C. Durucan, P.W. Brown *Low temperature formation of calcium-deficient hydroxyapatite- PLA/PLGA composites* J. Biomed. Mater. Res. **2000**, 51, 717-725.
122. E. Ural, K. Kesenci, L. Fambri, C. Migliaresi, E. Piskin *Poly(D,L-lactide/epsilon-caprolactone)/hydroxyapatite composites* Biomaterials **2000**, 21, 2147-2154.
123. A. Senkoylu, E. Ural, K. Kesenci, A. Simsek, S. Ruacan, L. Fambri, C. Migliaresi, E. Piskin *Poly(D,L-lactide/epsilon-caprolactone)/hydroxyapatite composites as bone filler: An in vivo study in rats* Int. J. Artif. Organs **2002**, 25, 1174-1179.
124. Q. Liu, J.R. de Wijn, C.A. van Blitterswijk *Nano-apatite/polymer composites: mechanical and physicochemical characteristics* Biomaterials **1997**, 18, 1263-1270.
125. Q. Liu, J.R. de Wijn, D. Bakker, C.A. van Blitterswijk *Surface modification of hydroxyapatite to introduce interfacial bonding with polyactive 70/30 in a biodegradable composite* J. Mater. Sci.-Mater. Med. **1996**, 7, 551-557.
126. Q. Liu, J.R. de Wijn, D. Bakker, M. van Toledo, C.A. van Blitterswijk *Polyacids as bonding agents in hydroxyapatite polyester-ether (Polyactive (TM) 30/70) composites* J. Mater. Sci.-Mater. Med. **1998**, 9, 23-30.
127. C. Doyle, E.T. Tanner, W. Bonfield *In vitro and in vivo evaluation of polyhydroxybutyrate and of polyhydroxybutyrate reinforced with hydroxyapatite* Biomaterials **1991**, 12, 841-847.
128. K. Anselme *Osteoblast adhesion on biomaterials* Biomaterials **2000**, 21, 667-681.
129. E. Lieb, J. Tessmar, M. Hacker, C. Fischbach, D. Rose, T. Blunk, A.G. Mikos, A. Gopferich, M.B. Schulz *Poly(D,L-lactic acid)-poly(ethylene glycol)-monomethyl ether diblock copolymers control adhesion and osteoblastic differentiation of marrow stromal cells* Tissue Eng. **2003**, 9, 71-84.
130. R.J. Green, M.C. Davies, C.J. Roberts, S.J.B. Tendler *A surface plasmon resonance study of albumin adsorption to PEO- PPO-PEO triblock copolymers* J. Biomed. Mater. Res. **1998**, 42, 165-171.
131. M.-S. Sheu, A.S. Hoffman, J.G.A. Terlingen, J. Feijen *A new gas discharge process for preparation of non-fouling surfaces on biomaterials* Clin. Mater. **1993**, 13, 41-46.
132. B.D. Ratner *The engineering of biomaterials exhibiting recognition and specificity* J. Mol. Recognit. **1996**, 9, 617-625.
133. K. Holmberg, K. Bergstrom, C. Brink, E. Osterberg, F. Tiberg, J.M. Harris *Effects on protein adsorption, bacterial adhesion and contact- angle of grafting PEG chains to polystyrene* J. Adhes. Sci. Technol. **1993**, 7, 503-517.
134. D.K. Han, K.D. Park, J.A. Hubbell, Y.H. Kim *Surface characteristics and biocompatibility of lactide-based poly(ethylene glycol) scaffolds for tissue engineering* in "Polymers for tissue engineering"; M.S. Shoichet and J.A. Hubbell, Ed.; VSP BV: Utrecht, The Netherlands **1998**; pp 221-234.
135. F.H. Meng *Artificial cells based on biodegradable polymersomes*, Thesis, University of Twente, Enschede, The Netherlands, **2003**.
136. M.D. Piersbacher *Cell attachment activity of fibronectin can be duplicated by small synthetic fragments of the molecule* Nature **1984**, 309, 30-33.
137. K. Bhadriraju, L.K. Hansen *Hepatocyte adhesion, growth and differentiated function on RGD- containing proteins* Biomaterials **2000**, 21, 267-272.
138. K. Tsuchiya, G.P. Chen, T. Ushida, T. Matsuno, T. Tateishi *Effects of cell adhesion molecules on adhesion of chondrocytes, ligament cells and mesenchymal stem cells* Mater. Sci. Eng. C-Biomimetic Supramol. Syst. **2001**, 17, 79-82.
139. W.G. Dai, J. Belt, W.M. Saltzman *Cell-binding peptides conjugated to poly(ethylene glycol) promote neural cell-aggregation* Bio-Technology **1994**, 12, 797-801.
140. W.G. Dai, W.M. Saltzman *Fibroblast aggregation by suspension with conjugates of poly(ethylene glycol) and RGD* Biotechnol. Bioeng. **1996**, 50, 349-356.

141. R.G. Lebaron, K.A. Athanasiou *Extracellular matrix cell adhesion peptides: Functional applications in orthopedic materials* Tissue Eng. **2000**, 6, 85-103.
142. K.M. Shakesheff, S.M. Cannizzaro, R. Langer *Creating biomimetic micro-environments with synthetic polymer-peptide hybrid molecules* J. Biomater. Sci.-Polym. Ed. **1998**, 9, 507-518.
143. D.J. Irvine, A.M. Mayes, L.G. Griffith *Nanoscale clustering of RGD peptides at surfaces using comb polymers. 1. Synthesis and characterization of comb thin films* Biomacromolecules **2001**, 2, 85-94.
144. D.J. Irvine, A.G. Ruzette, A.M. Mayes, L.G. Griffith *Nanoscale clustering of RGD peptides at surfaces using comb polymers. 2. Surface segregation of comb polymers in polylactide* Biomacromolecules **2001**, 2, 545-556.
145. G. Maheshwari, G. Brown, D.A. Lauffenburger, A. Wells, L.G. Griffith *Cell adhesion and motility depend on nanoscale RGD clustering* J. Cell Sci. **2000**, 113, 1677-1686.
146. L. Calandrelli, B. Immirzi, M. Malinconico, M.G. Volpe, A. Oliva, F. Della Ragione *Preparation and characterisation of composites based on biodegradable polymers for "in vivo" application* Polymer **2000**, 41, 8027-8033.
147. S.P. Bruder, B.S. Fox *Tissue engineering of bone - Cell based strategies* Clin. Orthop. Rel. Res. **1999**, S68-S83.
148. M.J. Lydon, T.W. Minett, B.J. Tighe *Cellular interactions with synthetic polymer surfaces in culture* Biomaterials **1985**, 6, 396-402.
149. P.B. van Wachem, T. Beugeling, J. Feijen, A. Bantjes, J.P. Detmers, W.G. van Aken *Interaction of cultured human endothelial cells with polymeric surfaces of different wettabilities* Biomaterials **1985**, 6, 403-408.
150. D.J. Mooney, S. Park, P.M. Kaufmann, K. Sano, K. McNamara, J.P. Vacanti, R. Langer *Biodegradable sponges for hepatocyte transplantation* J. Biomed. Mater. Res. **1995**, 29, 959-965.
151. W.S. Ramsey, W. Hertl, E.D. Nowlan, N.J. Binkowski *Surface treatments and cell attachment* In vitro **1984**, 20, 802-808.
152. J.M. Gao, L. Niklason, R. Langer *Surface hydrolysis of poly(glycolic acid) meshes increases the seeding density of vascular smooth muscle cells* J. Biomed. Mater. Res. **1998**, 42, 417-424.
153. X. Yang, K. Zhao, G.-Q. Chen *Effect of surface treatment on the biocompatibility of microbial polyhydroxyalkanoates* Biomaterials **2001**, 23, 1391-1397.
154. M. Tanahashi, T. Yao, T. Kokubo, M. Minoda, T. Miyamoto, T. Nakamura, T. Yamamuro *Apatite coated on organic polymers by biomimetic process - improvement in its adhesion to substrate by NaOH treatment* J. Appl. Biomater. **1994**, 5, 339-347.
155. M. Tanahashi, T. Yao, T. Kokubo, M. Minoda, T. Miyamoto, T. Nakamura, T. Yamamuro *Apatite coated on organic polymers by biomimetic process - improvement in adhesion to substrate by HCl treatment* J. Mater. Sci.-Mater. Med. **1995**, 6, 319-326.
156. W.L. Murphy, D.J. Mooney *Bioinspired growth of crystalline carbonate apatite on biodegradable polymer substrata* J. Am. Chem. Soc. **2002**, 124, 1910-1917.
157. W.R. Gombotz, A.S. Hoffman *Gas-discharge techniques for biomaterial modification* Crit. Rev. Biocomp. **1987**, 4, 1-42.
158. P.K. Chu, J.Y. Chen, L.P. Wang, N. Huang *Plasma-surface modification of biomaterials* Mater. Sci. Eng. R-Rep. **2002**, 36, 143-206.
159. J.G.A. Terlingen, H.F.C. Gerritsen, A.S. Hoffman, F.J. Jen *Introduction of functional-groups on polyethylene surfaces by a carbon-dioxide plasma treatment* J. Appl. Polym. Sci. **1995**, 57, 969-982.
160. G.A.J. Takens, J.G.A. Terlingen, G.H.M. Engbers, J. Feijen *Introduction of functional groups on polyethylene surfaces in a low pressure carbon dioxide glow discharge; a mechanistic study* Proceedings ISPC-12, Minneapolis, Minnesota, USA **1995**, 1, 33-38.
161. A.J.A. Klomp, J.G.A. Terlingen, G.A.J. Takens, A. Strikker, G.H.M. Engbers, J. Feijen *Treatment of PET nonwoven with a water vapor or carbon dioxide plasma* J. Appl. Polym. Sci. **2000**, 75, 480-494.
162. A.J.A. Klomp, G.H.M. Engbers, J. Mol, J.G.A. Terlingen, J. Feijen *Adsorption of proteins from plasma at polyester non-wovens* Biomaterials **1999**, 20, 1203-1211.
163. G. Khang, J.H. Jeon, J.W. Lee, S.C. Cho, H.B. Lee *Cell and platelet adhesions on plasma glow discharge-treated poly(lactide-co-glycolide)* Bio-Med. Mater. Eng. **1997**, 7, 357-368.
164. M. Tanahashi, T. Yao, T. Kokubo, M. Minoda, T. Miyamoto, T. Nakamura, T. Yamamuro *Apatite coated on organic polymers by biomimetic process - improvement in its adhesion to substrate by glow-discharge treatment* J. Biomed. Mater. Res. **1995**, 29, 349-357.
165. M.C. Shen, T.A. Horbett *The effects of surface chemistry and adsorbed proteins on monocyte/macrophage adhesion to chemically modified polystyrene surfaces* J. Biomed. Mater. Res. **2001**, 57, 336-345.
166. S.I. Ertel, B.D. Ratner, T.A. Horbett *The adsorption and elutability of albumin, IgG, and fibronectin on radiofrequency plasma deposited polystyrene* J. Colloid Interface Sci. **1991**, 147, 433-442.

167. F.H. Shutov *Blowing agents for polymer foams* in "Polymeric foams: Handbook of polymeric foams and foam technology" 1st ed.; D. Klemmner, and K.C. Frisch, Ed.; Carl Hanser Verlag: Munich, Germany **1991**; pp 375-409.
168. A.G. Mikos, Y. Bao, L.G. Cima, D.E. Ingber, J.P. Vacanti, R. Langer *Preparation of poly(glycolic acid) bonded fiber structures for cell attachment and transplantation* J. Biomed. Mater. Res. **1993**, 27, 183-189.
169. D.T. Mooney, C.L. Mazzoni, C. Breuer, K. McNamara, D. Hern, J.P. Vacanti, R. Langer *Stabilized polyglycolic acid fibre based tubes for tissue engineering* Biomaterials **1996**, 17, 115-124.
170. J. Leidner, E.W.C. Wong, D.C. MacGregor, G.J. Wilson *A novel process for the manufacturing of porous grafts: Process description and product evaluation* J. Biomed. Mater. Res. **1983**, 17, 229-247.
171. E. Wintermantel, J. Mayer, J. Blum, K.-L. Eckert, P. Lüscher, M. Mathey *Tissue engineering scaffolds using superstructures* Biomaterials **1996**, 17, 83-91.
172. C.S. Pereira, M.E. Gomes, R.L. Reis, A.M. Cunha *Hard cellular materials in the human body: properties and production of foamed polymers for bone replacement* in "Foams, emulsions and cellular materials"; F. Sapoc and N. Rivier, Ed.; Kluwer Press: Dordrecht, The Netherlands **1997**.
173. A.S.P. Lin, T.H. Barrows, S.H. Cartmell, R.E. Guldberg *Microarchitectural and mechanical characterization of oriented porous polymer scaffolds* Biomaterials **2003**, 24, 481-489.
174. K.S. Chow, E. Khor *Novel fabrication of open-pore chitin matrixes* Biomacromolecules **2000**, 1, 61-67.
175. Y.S. Nam, J.J. Yoon, T.G. Park *A novel fabrication method of macroporous biodegradable polymer scaffolds using gas foaming salt as a porogen additive* J. Biomed. Mater. Res. **2000**, 53, 1-7.
176. G.P. Chen, T. Ushida, T. Tateishi *A hybrid network of synthetic polymer mesh and collagen sponge* Chem. Commun. **2000**, 1505-1506.
177. H. Yoshimoto, Y.M. Shin, H. Terai, J.P. Vacanti *A biodegradable nanofiber scaffold by electrospinning and its potential for bone tissue engineering* Biomaterials **2003**, 24, 2077-2082.
178. M. Borden, M. Attawia, C.T. Laurencin *The sintered microsphere matrix for bone tissue engineering: In vitro osteoconductivity studies* Journal of Biomedical Materials Research **2002**, 61, 421-429.
179. M. Borden, M. Attawia, Y. Khan, C.T. Laurencin *Tissue engineered microsphere-based matrices for bone repair: design and evaluation* Biomaterials **2002**, 23, 551-559.
180. G.P. Chen, T. Ushida, T. Tateishi *Fabrication of PLGA-collagen hybrid sponge* Chem. Lett. **1999**, 561-562.
181. C.E. Holy, S.M. Dang, J.E. Davies, M.S. Shoichet *In vitro degradation of a novel poly(lactide-co-glycolide) 75/25 foam* Biomaterials **1999**, 20, 1177-1185.
182. Q. Hou, D.W. Grijpma, J. Feijen *Porous polymeric structures for tissue engineering prepared by a coagulation, compression moulding and salt leaching technique* Biomaterials **2003**, 24, 1937-1947.
183. C.J. Liao, C.F. Chen, J.H. Chen, S.F. Chiang, Y.J. Lin, K.Y. Chang *Fabrication of porous biodegradable polymer scaffolds using a solvent merging/particulate leaching method* J. Biomed. Mater. Res. **2002**, 59, 676-681.
184. Q. Hou, D.W. Grijpma, J. Feijen *Preparation of interconnected, highly porous polymeric structures by a replication and freeze-drying process* J. Control. Release **2003**, 87, 304-307.
185. W.L. Murphy, R.G. Dennis, J.L. Kileny, D.J. Mooney *Salt fusion: An approach to improve pore interconnectivity within tissue engineering scaffolds* Tissue Eng. **2002**, 8, 43-52.
186. M.S. Widmer, P.K. Gupta, L. Lu, R.K. Meszlenyi, G.R.D. Evans, K. Brandt, T. Savel, A. Gurlek, C.W. Patrick Jr, A.G. Mikos *Manufacture of porous biodegradable polymer conduits by an extrusion process for guided tissue regeneration* Biomaterials **1998**, 19, 1945-1955.
187. V.P. Shastri, I. Martin, R. Langer *Macroporous polymer foams by hydrocarbon templating* Proc. Natl. Acad. Sci. U. S. A. **2000**, 97, 1970-1975.
188. S.S. Kim, D.R. Lloyd *Thermodynamics of polymer/diluent systems for thermally induced phase separation: 1. Determination of equation of state parameters* Polymer **1992**, 33, 1026-1035.
189. S.S. Kim, D.R. Lloyd *Thermodynamics of polymer/diluent systems for thermally induced phase separation: 2. Solid-liquid phase separation systems* Polymer **1992**, 33, 1036-1046.
190. C. Schugens, V. Maquet, C. Grandfils, R. Jerome, P. Teyssie *Biodegradable and macroporous polylactide implants for cell transplantation: 1. Preparation of macroporous polylactide supports by solid-liquid phase separation* Polymer **1996**, 37, 1027-1038.
191. R. Zhang, P.X. Ma *Poly( $\alpha$ -hydroxyl acids)/hydroxyapatite porous composites for bone-tissue engineering. I. Preparation and morphology* J. Biomed. Mater. Res. **1999**, 44, 446-455.
192. S.Q. Liu, M. Kodama *Porous polyurethane vascular prostheses with variable compliance* J. Biomed. Mater. Res **1992**, 26, 1489-1502.
193. H. Lo, S. Kadiyala, S.E. Guggino, K.W. Leong *Poly(L-lactic acid) foams with cell seeding and controlled-release capacity* J. Biomed. Mater. Res. **1996**, 30, 475-484.

194. H. Lo, M.S. Ponticciello, B.S. Leong, K.W. Leong *Fabrication of controlled release biodegradable foams by phase separation* Tissue Eng. **1995**, 1, 15-28.
195. R. Zhang, P.X. Ma *Porous poly(L-lactic acid)/apatite composites created by biomimetic process* J. Biomed. Mater. Res. **1999**, 45, 285-293.
196. P.X. Ma, R.Y. Zhang *Microtubular architecture of biodegradable polymer scaffolds* J. Biomed. Mater. Res. **2001**, 56, 469-477.
197. K. Whang, C.H. Thomas, K.E. Healy, G. Nuber *A novel method to fabricate bioabsorbable scaffolds* Polymer **1995**, 36, 837-842.
198. K. Whang, D.C. Tsai, E.K. Nam, M. Aitken, S.M. Sprague, P.K. Patel, K.E. Healy *Ectopic bone formation via rhBMP-2 delivery from porous bioabsorbable polymer scaffolds* J. Biomed. Mater. Res. **1998**, 42, 491-499.
199. R.A. Zoppi, S. Contant, E.A.R. Duek, F.R. Marques, M.L.F. Wada, S.P. Nunes *Porous poly(L-lactide) films obtained by immersion precipitation process: morphology, phase separation and culture of VERO cells* Polymer **1999**, 40, 3275-3289.
200. J.-H. Chen, R.-F. Laiw, S.-F. Jiang, Y.-D. Lee *Microporous segmented polyetherurethane vascular graft: I. dependency of graft morphology and mechanical properties on compositions and fabrication conditions* J. Biomed. Mater. Res. (Appl. Biomater.) **1999**, 48, 235-245.
201. C. Schugens, V. Maquet, C. Grandfils, R. Jerome, P. Teyssie *Polylactide macroporous biodegradable implants for cell transplantation. II. Preparation of polylactide foams by liquid-liquid phase separation* J. Biomed. Mater. Res. **1996**, 30, 449-461.
202. D.J. Mooney, D.F. Baldwin, N.P. Suh, J.P. Vacanti, R. Langer *Novel approach to fabricate porous sponges of poly(D,L-lactic-co-glycolic acid) without the use of organic solvents* Biomaterials **1996**, 17, 1417-1422.
203. L.D. Harris, B.-S. Kim, D.J. Mooney *Open pore biodegradable matrices formed with gas foaming* J. Biomed. Mater. Res. **1998**, 42, 396-402.
204. K.F. Leong, C.M. Cheah, C.K. Chua *Solid freeform fabrication of three-dimensional scaffolds for engineering replacement tissues and organs* Biomaterials **2003**, 24, 2363-2378.
205. D.W. Hutmacher *Scaffold design and fabrication technologies for engineering tissues - state of the art and future perspectives* J. Biomater. Sci.-Polym. Ed. **2001**, 12, 107-124.
206. I. Zein, D.W. Hutmacher, K.C. Tan, S.H. Teoh *Fused deposition modeling of novel scaffold architectures for tissue engineering applications* Biomaterials **2002**, 23, 1169-1185.
207. D.W. Hutmacher, T. Schantz, I. Zein, K.W. Ng, S.H. Teoh, K.C. Tan *Mechanical properties and cell cultural response of polycaprolactone scaffolds designed and fabricated via fused deposition modeling* J. Biomed. Mater. Res. **2001**, 55, 203-216.
208. Y.N. Yan, Z. Xiong, Y.Y. Hu, S.G. Wang, R.J. Zhang, C. Zhang *Layered manufacturing of tissue engineering scaffolds via multi-nozzle deposition* Mater. Lett. **2003**, 57, 2623-2628.
209. Z. Xiong, Y.N. Yan, R.J. Zhang, L. Sun *Fabrication of porous poly(L-lactic acid) scaffolds for bone tissue engineering via precise extrusion* Scr. Mater. **2001**, 45, 773-779.
210. W.L.J. Hinrichs *Porous Polymer Structures for Tissue Regeneration*, Thesis, University of Twente, Enschede, The Netherlands, **1992**.
211. A.G. Mikos, A.J. Thorsen, L.A. Czerwonka, Y. Bao, R. Langer, D.N. Winslow, J.P. Vacanti *Preparation and characterization of poly(L-lactid acid) foams* Polymer **1994**, 35, 1068-1077.
212. S.J. Peter, M.J. Miller, A.W. Yasko, M.J. Yaszemski, A.G. Mikos *Polymer concepts in tissue engineering* J. Biomed. Mater. Res. (Appl. Biomater.) **1998**, 43, 422-427.
213. J.H. De Groot, F.M. Zijlstra, H.W. Kuipers, A.J. Pennings, J. Klompmaker, R.P.H. Veth, H.W.B. Jansen *Meniscal tissue regeneration in porous 50/50 copoly(L-lactide/epsilon-caprolactone) implants* Biomaterials **1997**, 18, 613-622.
214. J. McGregor, P.W. Watt, N.D. Light, W. Harvey *Absorbable implant materials having controlled porosity* US Patent 5,869,080 **1999**.
215. G.P. Chen, T. Ushida, T. Tateishi *Development of biodegradable porous scaffolds for tissue engineering* Mater. Sci. Eng. C-Biomimetic Supramol. Syst. **2001**, 17, 63-69.
216. G.P. Chen, T. Ushida, T. Tateishi *Preparation of poly(L-lactic acid) and poly(DL-lactic-co-glycolic acid) foams by use of ice microparticulates* Biomaterials **2001**, 22, 2563-2567.
217. U. Beginn *Supramolecular templates as porogenes* Adv. Mater. **1998**, 10, 1391-1394.
218. R. Hafkamp *Supramolecular structures from gluconamide building blocks*, Thesis, University of Nijmegen, Nijmegen, The Netherlands, **1996**.
219. D.F. Baldwin, M. Shimbo, N.P. Suh *The role of gas dissolution and induced crystallization during microcellular polymer processing: a study of poly(ethylene terephthalate) and carbon dioxide systems* J. Eng. Mater. - T. ASME **1995**, 117, 62-74.

- 220. J.H. Aubert, R.L. Clough *Low-density, microcellular polystyrene foams* Polymer **1985**, 26, 2047-2054.
- 221. J.H. De Groot, A.J. Nijenhuis, P. Bruin, A.J. Pennings, R.P.H. Veth, J. Klompmaker, H.W.B. Jansen *Use of porous biodegradable polymer implants in meniscus reconstruction. 1) Preparation of porous biodegradable polyurethanes for the reconstruction of meniscus lesions* Colloid Polym. Sci. **1990**, 268, 1073-1081.
- 222. J.H. De Groot, R. De Vrijer, A.J. Pennings, J. Klompmaker, R.P.H. Veth, H.W.B. Jansen *Use of porous polyurethanes for meniscal prostheses* Biomaterials **1996**, 17, 163-173.
- 223. C.J. Damien, J.R. Parsons *Bone-graft and bone-graft substitutes - a review of current technology and applications* J. Appl. Biomater. **1991**, 2, 187-208.
- 224. P. Bianco, P.G. Robey *Stem cells in tissue engineering* Nature **2001**, 414, 118-121.
- 225. J.S. Temenoff, A.G. Mikos *Injectable biodegradable materials for orthopedic tissue engineering* Biomaterials **2000**, 21, 2405-2412.
- 226. H.-P. Hentze, M. Antonietti *Porous polymers and resins for biotechnological and biomedical applications* Rev. Mol. Biotech. **2002**, 90, 27-53.



# Chapter 3

## Synthesis, processing and characterization of poly(ethylene oxide)/poly(butylene terephthalate) block copolymers

*A tower of nine storeys begins with a heap of earth.  
The journey of a thousands li starts from where one stands.*

Lao Tzu (604 –531 BC)

### Abstract

Poly(ethylene oxide)/poly(butylene terephthalate) (PEOT/PBT) block copolymers have been prepared by two-step polycondensation on a 50-100 g and on a 1 kg scale. Copolymers with weight average molecular weights (relative to poly(methyl methacrylate)) of 110,000 to 150,000 g/mol have been obtained. Molecular weights were determined by gel permeation chromatography using a solution of sodium trifluoroacetate in 1,1,1,3,3,3-hexafluoro-2-propanol as a solvent. PEOT/PBT copolymers with higher molecular weights could be obtained after postcondensation of purified and precipitated copolymer. Thermal processing in the form of compression molding results in films and porous structures with molecular weights slightly lower than the ones of the original copolymers.

Due to the uptake of water PEOT/PBT copolymers in the water-swollen state have significantly decreased tensile and creep properties as compared to those in the dry state.

### Introduction

#### *Segmented poly(ether ester) elastomers*

Segmented poly(ether ester) elastomers contain repeating blocks that are phase separated into domains of hard segments with a high  $T_g$  or  $T_m$ , acting as physical cross-links, and domains of soft segments with a low  $T_g$ . Typically, the hard segments are composed of aromatic esters of short chain diols, such as butylene terephthalate, and the soft segments are derived from aliphatic polyether glycols. By varying the ratio of hard to soft segments and the relative length of the soft segment, polymers ranging from soft elastomers to relatively hard thermoplastics can be obtained.<sup>[1]</sup>

The first research on block copoly(ether ester) elastomers started around 1950, with the principal efforts being directed towards modifying or developing new melt spinnable synthetic fibers. In 1949 Coleman at ICI prepared block copolymers by copolymerisation of ethylene

glycol, dimethyl terephthalate (DMT) and poly(ethylene oxide) (PEO) with different molecular weights.<sup>[2,3]</sup> The synthesized poly(ethylene oxide)/poly(ethylene terephthalate) (PEO/PET) block copolymers were meant to have a better dye receptivity than PET fibers. In 1967 Nishimura and Komogata studied polyester elastomer fibers prepared by block copolymerization of dimethyl terephthalate, 1,4-butanediol and polytetramethylene oxide (PTMO). These elastomers were melt-spun to give elastic fibers.<sup>[4]</sup> Witsiepe at DuPont started research on these PTMO/PBT block copolymers for molding and extrusion applications.<sup>[5-7]</sup> He obtained a variety of polymers by varying the weight percentage of PBT and adding different monomers, thereby obtaining polymers where part of the butylene terephthalate units were replaced by butylene isophthalate or butylene phthalate units. This family of polyester elastomers exhibits outstanding elasticity, tear strength, solvent resistance, low-temperature flexibility and strength at elevated temperatures. In 1972, they were commercialized under the trademark Hytrel polyester elastomer by DuPont. Other copoly(ether ester)s currently on the market are Arnitel (manufactured by DSM) and Ecdel (manufactured by Eastman).<sup>[1]</sup>

The first report on the use of such poly(ether ester)s as a biomaterial was in 1979, when Gilding and Reed discussed the synthesis<sup>[8]</sup> and degradation<sup>[9]</sup> of PEO/PET block copolymers. In 1988 Van Blitterswijk *et al.* found that PEOT/PBT block copolymers can be used for prosthetic devices with bone-bonding properties.<sup>[10]</sup> Like other poly(ether ester)s, PEOT/PBT contains blocks that are capable of phase separation: 'hard' PBT segments with a high  $T_g$  or  $T_m$ , acting as physical crosslinks, and 'soft' hydrophilic PEOT segments with a low  $T_g$ , forming amorphous domains.

A PEOT/PBT family of polymers can be prepared by varying PEO molecular weight and weight percentage. The dependence of some physical and mechanical properties on the composition of these PEOT/PBT polymers was studied by Fakirov *et al.*<sup>[11,12]</sup>

#### *Copoly(ether ester) synthesis*

The synthesis of block copoly(ether ester)s has been thoroughly studied by Hoeschele *et al.* at DuPont.<sup>[13,14]</sup> Segmented poly(ether ester)s were prepared by an ester interchange reaction of dimethyl terephthalate, excess 1,4-butanediol and either hydroxyl terminated poly(ethylene oxide) (PEO), poly(propylene oxide) (PPO) or poly(tetramethylene oxide) (PTMO). The reaction can be divided into two steps, namely transesterification and polycondensation.

In these reactions an excess of removable diol is used. It speeds up the trans-esterification step (due to an increase in reactant concentration) and in the second polycondensation step drives the reaction to completion (resulting in polymers of high molecular weight) by distilling off the extra added amount of diol. At the beginning of the reaction an excess of diol is used, since starting with a 1:1 stoichiometry would lead to a low conversion, resulting in a low molecular weight polymer. This reaction is analogous to that for the synthesis of PET, however in the case of PBT somewhat different catalysts and reaction conditions are used. To accelerate the transesterification as well as the polycondensation reactions in the synthesis of polyalkylene terephthalates (PET, PBT) titanium complexes like  $Ti(OBu)_4$  have proven to be effective catalysts.<sup>[15]</sup>

These alkoxides are very sensitive to traces of water that can coordinate to the metal as shown in Figure 3.1 leading to an inactive catalyst complex.

The exact mechanism of the polycondensation and the participation of the catalyst in it are not quite clear. Apicella *et al.* propose different mechanisms for bivalent (like  $Zn^{2+}$ ) and tri- or tetravalent catalysts (like  $Ti^{4+}$ , see Figure 3.2).<sup>[16]</sup> It has previously been suggested that the catalyst metal interacts with the carbonyl group. In the synthesis of PET however there are no spectroscopic (NMR or IR) indications for such an interaction.



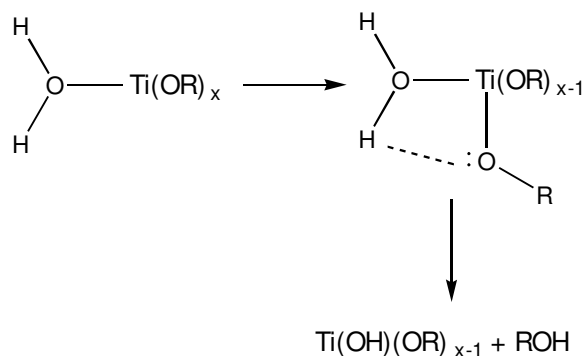
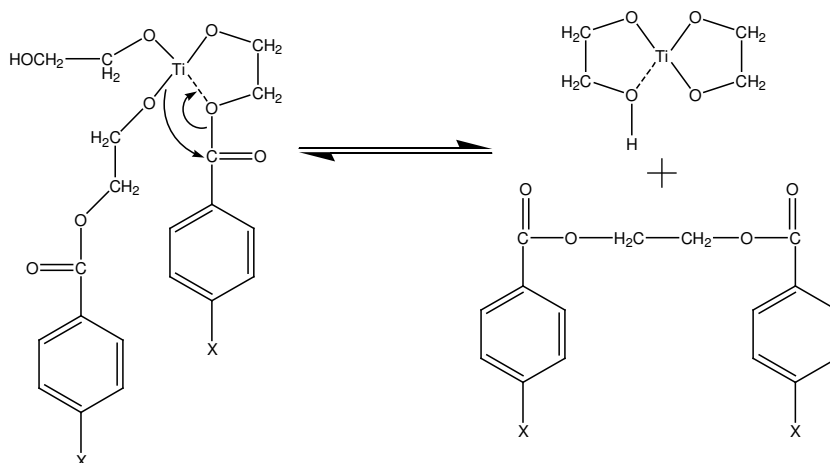


Figure 3.1 - Hydrolysis of titanium alkoxides.

Apicella *et al.* found that the effect of substituent  $x$  on the activity in the tri- and tetravalent metal systems was negligible, a finding that one would not expect in the case of titanium/carbonyl interaction.

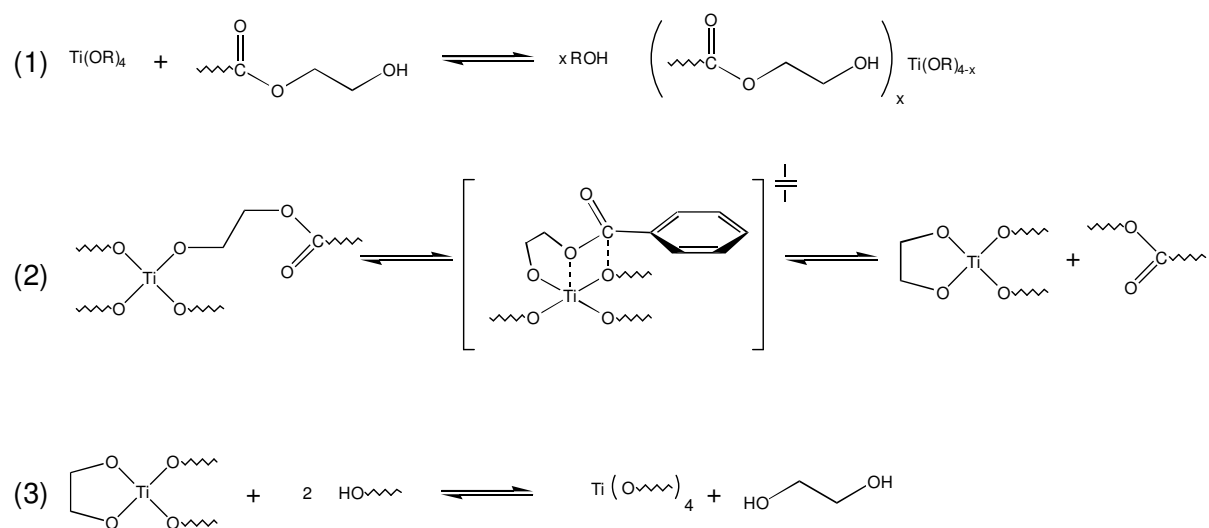

 Figure 3.2 - Part of the proposed mechanism for the synthesis of PET catalysed by  $\text{Ti}(\text{OBu})_4$ , as described by Apicella *et al.*<sup>[16]</sup>

The authors propose that tri- and tetravalent metals are coordinated to the acyclic oxygen, in contrast to divalent metals that coordinate to the carbonyl oxygen, in line with a previously described model by Weingart *et al.* Based on NMR and IR data, Weingart *et al.* suggested the following mechanism, as indicated in Figure 3.3.<sup>[15]</sup>

It is very likely that a comparable mechanism is operative in the synthesis of PBT and in our case in the synthesis of PEOT/PBT block copolymers.

PEO<sup>[17]</sup> and to a much lesser extent PBT<sup>[18]</sup> are known to be sensitive to degradation at high temperatures. Due to the high temperatures during the synthesis it is necessary to add an antioxidant to the reaction mixture to prevent oxidative degradation of PEO.

Often used antioxidants are based on secondary aromatic amines and or substituted phenols.<sup>[11,13,19]</sup> In our case the naturally occurring hindered phenol vitamin E ( $\alpha$ -tocopherol) is used.

Figure 3.3 - Mechanism for the synthesis of PET, as proposed by Weingart *et al.*[15]

## Materials and methods

### Synthesis

**50-100 g scale synthesis.** The copolymers were prepared by two-step polycondensation in the presence of titanium tetrabutoxide ( $\text{Ti(OBu)}_4$ , Merck, Germany) as catalyst, as previously described<sup>[19]</sup>, with the exception that vitamin E (Sigma-Aldrich, Germany, approx. 95 % pure) was used as antioxidant. The composition was adjusted by varying the poly (ethylene glycol) (Fluka, Switzerland) to dimethyl terephthalate (DMT, Merck, Germany)/1,4-butanediol (Acros, Belgium) ratio. The catalyst (0.1 wt % of DMT weight) was added as a solution in toluene (Biosolve, The Netherlands). Synthesis was performed on a 50-100 g scale using standard laboratory glassware.

The composition of these copolymers is indicated as  $a\text{PEOT}b\text{PBT}c$ , with  $a$  the molecular weight of the poly (ethylene glycol) starting compound,  $b$  the weight percentage of the PEOT soft segments and  $c$  the weight percentage of the PBT hard segments. The copolymer composition was determined by  $^1\text{H-NMR}$  ( $\text{CDCl}_3$ , Varian Inova 300 MHz). The copolymers were used without further purification unless otherwise mentioned.

**1 kg scale synthesis.** Copolymer batches up to 1 kg were prepared in a 2 L stainless steel conical shaped reaction vessel (Büchi, Flawil, Switzerland) equipped with a 800 Ncm magnetic coupling, a helical shaped stirrer (both Büchi), an Unistat T 325 oil heater (Huber, Offenburg, Germany) and an oil-filled rotary vane E2M18 vacuum pump (BOC Edwards, Crawley, United Kingdom) (see Figure 3.4).

Copolymers were prepared analogous to the small scale synthesis, except that the pure  $\text{Ti(OBu)}_4$  catalyst was added to the reaction mixture at a higher concentration (0.2 wt % of DMT weight). Polymer melt temperature, reactor pressure, condensor temperature and the torque of the stirrer were recorded and logged during the polymerization using Labview (version 5.1, National Instruments, U.S.A.).

Methanol and excess 1,4-butanediol were collected in a glass cold trap. The polymer was discharged once the measured torque reached a plateau value. The copolymer composition was determined by  $^1\text{H-NMR}$  ( $\text{CDCl}_3$ , Varian Inova 300 MHz).

The copolymers were used without further purification unless otherwise mentioned.

For the synthesis of 1000PEOT70PBT30 the typical procedure was as follows:

After purging of the reaction vessel with nitrogen, all chemicals (as described in the 50-100 g scale synthesis) are put into the reaction vessel. As soon as possible the stirring speed is set to 100 rpm. The reactor is slowly heated to 200 °C, when the melt temperature reaches 150 °C methanol distillation starts. After approximately 30 min, the distillation ends and the temperature is further increased to 260 °C. The distillation of excess 1,4-butanediol starts at 250 °C. After approximately 90 min (after the temperature increase) the nitrogen inlet is closed and the pressure is slowly reduced, over a time period of approximately 30 min, reaching a value of approximately 25 mbar. Cooling the cold traps with liquid nitrogen further decreases the pressure to 3-4 mbar. The torque gradually increases, leveling off at a value around 450-510 Ncm after 2 h (after cooling with liquid nitrogen). At that time the polymer is discharged from the reaction vessel and cooled using an ice/water bath.

*Post condensation.* A post condensation experiment was carried out with 1000PEOT70PBT30. This polymer was heated at 150 °C at a pressure of 7.5 mbar. After dissolution of the copolymer in chloroform and precipitation in a tenfold excess of ethanol, three samples of the purified polymer were heated in three different glass tubes: one for 1 h, one for 3 h and one for 5 h. The samples were allowed to cool under dry nitrogen, after which the intrinsic viscosity was determined by a single point measurement<sup>[20,21]</sup> (Ubbelohde OC viscometer, 25 °C, copolymer solutions in CHCl<sub>3</sub> with a concentration of approximately 0.3 g/dL).



Figure 3.4 – 1 Kg scale synthesis unit. Left: overview. Top right: helical shaped stirrer. Bottom right: Cover plate of the reaction vessel, showing inlet valves and various sensors and the stirrer equipped with a 800 Ncm magnetic coupling fitted with a sensor for registering the torque. Next to the manometer is the connection for the condensor and cold trap (not shown). [Color figure on p. 168].

### Processing

*Films prepared by solution casting.* PEOT/PBT block copolymers were dissolved in chloroform ( $\text{CHCl}_3$ , Biosolve, The Netherlands) to obtain a polymer solution of approximately 10 % (w/v). All polymers, were soluble in chloroform, except for the 4000PEOT70PBT30, which was soluble in a 20 % (w/v) solution of 1,1,1,3,3,3-hexafluoro-2-propanol (HFIP, Biosolve, The Netherlands) in  $\text{CHCl}_3$ . The resulting polymer solutions were cast on a glass plate using a 0.75 mm casting knife. All PEOT/PBT copolymers readily formed films within min. All films were dried for 2 d in a vacuum oven at room temperature.

*Films prepared by compression molding.* Copolymer films were prepared by compression molding for 4 min at 140 °C (1000PEOT70PBT30), 150 °C (300PEOT55PBT45) or 175 °C (1000PEOT55PBT45) in a laboratory hot press (THB 008, Fontijne Holland BV, The Netherlands).

*Porous structures prepared by compression molding of polymer/salt mixtures followed by salt leaching.* 1000PEOT70PBT30 copolymer granulate was cryogenically ground using an IKA Labortechnik (Germany) A10 grinder. Polymer powder and sodium chloride crystals (Merck, Germany) were sieved using Endecotts (England) test sieves of 250, 425, 500, 710, 1000 and 1180  $\mu\text{m}$  mesh size. The desired salt volume fractions (425-500  $\mu\text{m}$  particle size) were calculated using a salt density of 2.165  $\text{g/cm}^3$ . The powders were mixed and subsequently compression molded in a laboratory hot press (THB 008, Fontijne Holland BV, The Netherlands) into 4 mm thick blocks. Mixed powders were heated at 180 °C for 3 min and subsequently pressed for 1 min at 2.9 MPa. Samples were leached with milliQ water for 48 h and dried under reduced nitrogen pressure in a vacuum oven.

### Characterization

*Water uptake.* The water uptake of the different PEOT/PBT polymers was determined at regular intervals during 14 d. The samples (solution cast films) were weighed at regular intervals after blotting the surface of the film with a tissue to remove any residual water. For every polymer, three film samples of 15 mm diameter were swollen in demineralized water (milliQ) and put in a shaking bath at 37 °C.

*Tensile testing of solution cast films.* Dumb-bell shaped specimens were cut according to DIN 53504 (dumb-bell S2). Films had a thickness ranging from 0.08 (dry) to 0.18 mm (wet). The thickness of the films was measured in triplicate using a spring-loaded micrometer (Mitutoyo, Tokyo, Japan). To prepare wet films, films were swollen in water for at least 24 h, after which the samples were cut.

A Zwick Z020 universal tensile testing machine was equipped with a 10 N load cell. A grip-to-grip separation of 25 mm, a pre-load of 0.05 N and a crosshead speed of 200 mm/min were used. The tensile modulus was determined from the initial part (0.1- 0.3 % elongation) of the stress-strain curve. The sample deformation was derived from the grip-to-grip separation, therefore the presented values of the E-modulus give only an indication of the stiffness of the different composites.

*Tensile testing of compression molded films.* Strips of 50 x 1000 mm were cut from compression molded films and subjected to tensile testing. A Zwick Z020 universal tensile testing machine was equipped with a 500 N load cell and the strips were clamped in pneumatic clamps with sandpaper (to prevent slippage). A grip-to-grip separation of 50 mm, a pre-load of 0.1 N and a crosshead speed of 50 mm/min were used. The tensile modulus was determined from the initial part (0.1-0.3 % elongation) of the stress-strain curve. The sample deformation was derived from the grip-to-grip separation, therefore the presented values of the E-modulus give only an indication of the stiffness of the different composites.

*Creep tests.* Compression molded 1000PEOT70PBT30 strips of 5 x 50 mm with a thickness of 1.0 mm were statically loaded with a weight corresponding to 2.5, 5.0, 10 or 20 N. Grip-to-

grip distance was 4.0 cm. At regular time intervals the elongation was measured between two marks initially placed at 3 cm distance. The constant creep rate was determined from the creep curve. Samples were measured both dry and water swollen at room temperature (approximately 18 °C).

*Viscometry.* Intrinsic viscosities of the PEOT/PBT copolymers were determined by single-point measurements<sup>[20,21]</sup>, using an Ubbelohde 0C viscometer at 25 °C and copolymer solutions in CHCl<sub>3</sub> with a concentration of approximately 0.3 g/dL.

*Gel permeation chromatography (GPC).* Copolymers were dissolved in HFIP containing 0.02 M of sodium trifluoroacetate (CF<sub>3</sub>COONa, Aldrich, U.S.A.), at a typical concentration of 5 mg/mL. Number average and weight average molecular weights were calculated relative to poly(methyl methacrylate) standards (PMMA, Polymer Standards Service GmbH, Mainz, Germany). Samples were measured with a flow rate of 0.8 mL/min at 30 °C. Measurements were performed on a Polymer Laboratories PL-GPC 120 High temperature chromatograph with PL HFIPgel columns, a refractive index detector and a Spark Basic + Marathon autosampler. Data were analyzed using Cirrus GPC Offline GPC/SEC Software (version 1.11, release 32, build 1.0.0.10).

## PEOT/PBT block copolymer synthesis

PEOT/PBT copolymers were prepared on a 50-100 g and on a 1 kg scale. By varying the PEO molecular weight and the soft to hard segment ratio a series of block copolymers can be prepared. Table 3.1 shows the compositions and intrinsic viscosities of copolymers based on different PEO molecular weights. The compositions of the copolymers are close to the intended ones. Most copolymers containing a high weight % of PEO are soluble in CHCl<sub>3</sub>.

Table 3.1 - Composition and intrinsic viscosity of PEOT/PBT block copolymers prepared on a 50-100 g scale.

Intended composition	Composition ( <sup>1</sup> H-NMR)	Intrinsic viscosity [η] in CHCl <sub>3</sub> (dL/g) at 25 °C
300PEOT70PBT30	67/33	0.75
600PEOT70PBT30	63/37	0.80
1000PEOT70PBT30	70/30	1.07
1000PEOT70PBT30	70/30	1.10
2000PEOT70PBT30	74/26	0.68
4000PEOT70PBT30	80/20	0.95

Purification by dissolution and precipitation of the synthesized copolymer leads to a small increase in intrinsic viscosity, the shorter and more soluble oligomers dissolve during precipitation. During the last stages of polycondensation, the last fraction of 1,4-butanediol is removed from the oligomers/polymer chains of low molecular weight, resulting in chain extension. As indicated in Figure 3.5, the pressure at the end of the reaction is a measure for the polymer intrinsic viscosity, the lower the pressure the higher the intrinsic viscosity.

Although the measured intrinsic viscosities (and hence molecular weights) for the PEO/PBT block copolymers are reasonably high, they can be further increased by post condensation. During post condensation 1000PEOT70PBT is heated at a temperature slightly below its melting point (157 °C)<sup>[22]</sup> at reduced pressure or under an inert gas like nitrogen or argon.

During post condensation the polymer chains can react further to give a higher molecular weight.<sup>[14]</sup> Purification by precipitation of the polymers before post condensation reduces the

amount of low boiling oligomers, which favors the evaporation of 1,4-butanediol, thus resulting in higher polycondensation rates during post condensation.<sup>[23]</sup> The increased surface area of the precipitated polymer fibers as compared to the area present during melt polymerization also favors the evaporation of 1,4-butanediol. As indicated in Figure 3.6 there is an increase in intrinsic viscosity from 1.10 to 1.21 dL/g after 5 h of postcondensation. Figure 3.6 suggests that a post condensation longer than 5 h will result in even higher polymer molecular weights.

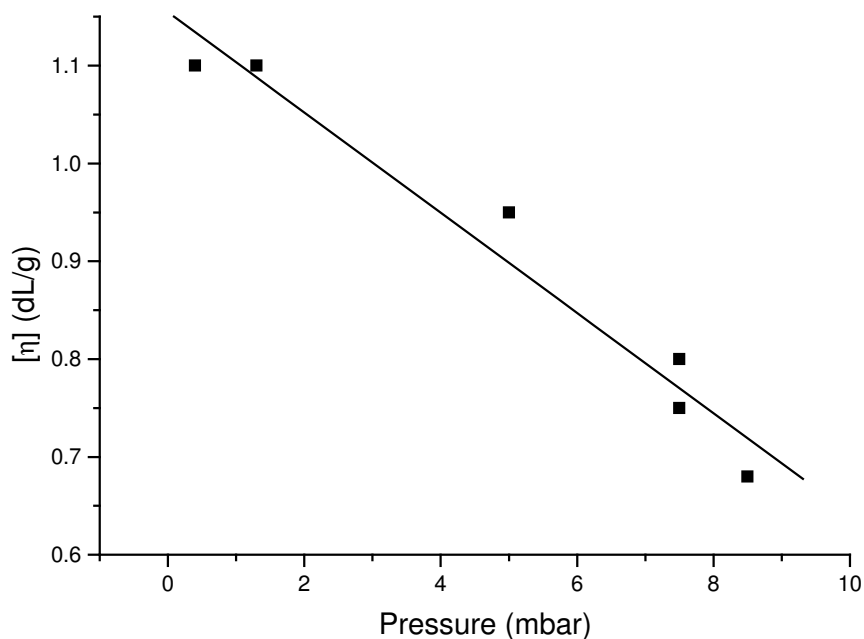


Figure 3.5 - Intrinsic viscosity as a function of pressure, as measured during the last stages of polycondensation for copolymers of various compositions.

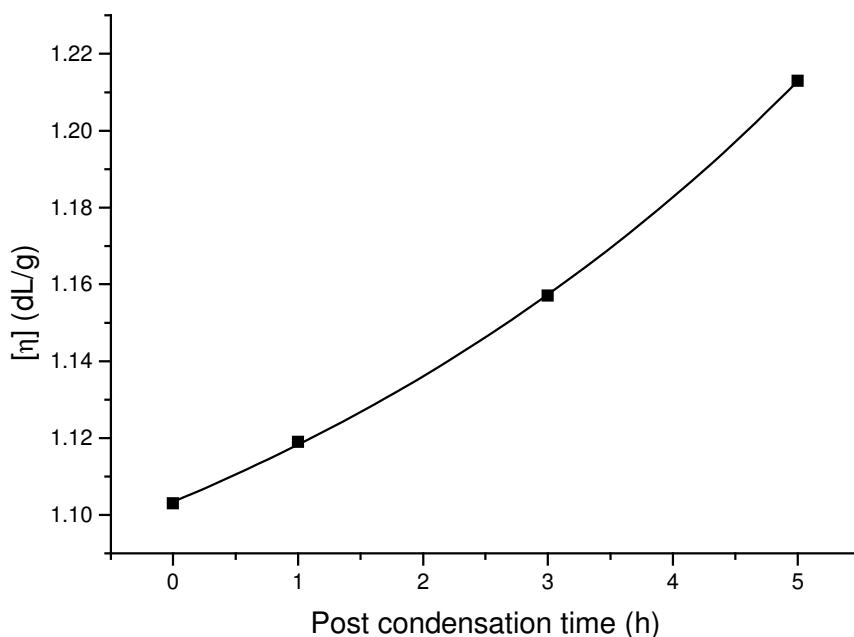


Figure 3.6 - Post condensation of precipitated 1000PEOT70PBT30 at 150 °C and 7.5 mbar. [η] in CHCl<sub>3</sub> at 25 °C.

1 Kg scale synthesis also showed good control over the copolymer composition, as shown in Table 3.2 (later in this chapter); the copolymer compositions are close to the intended ones.

#### *Gel permeation chromatography (GPC)*

In order to determine the molecular weight of the synthesized copolymers, attempts have been made to setup a GPC system that is suitable for all PEOT/PBT copolymers, including those with a high PBT content. Although PEOT/PBT copolymers with a high PEO content are soluble in  $\text{CHCl}_3$ , those with a high PBT content are not. To dissolve copolymers with high amounts of PBT, it is necessary to use other solvents, for instance 1,1,1,3,3,3-hexafluoro-2-propanol (HFIP).<sup>[22]</sup> It has been shown that HFIP is a suitable solvent for various polyesters, polyamides and other polar polymers.<sup>[24,25]</sup> Addition of an electrolyte like sodium trifluoroacetate ( $\text{CF}_3\text{COONa}$ ) to HFIP gives additional benefits like peak-narrowing and better polymer chain dissociation by breaking down hydrogen bonding.<sup>[26]</sup>

HFIP is a volatile and corrosive organic solvent. Previous studies on the degradation of PEOT/PBT copolymers by Deschamps et al. showed that these copolymers are susceptible to degradation both by hydrolysis and oxidation.<sup>[19]</sup>

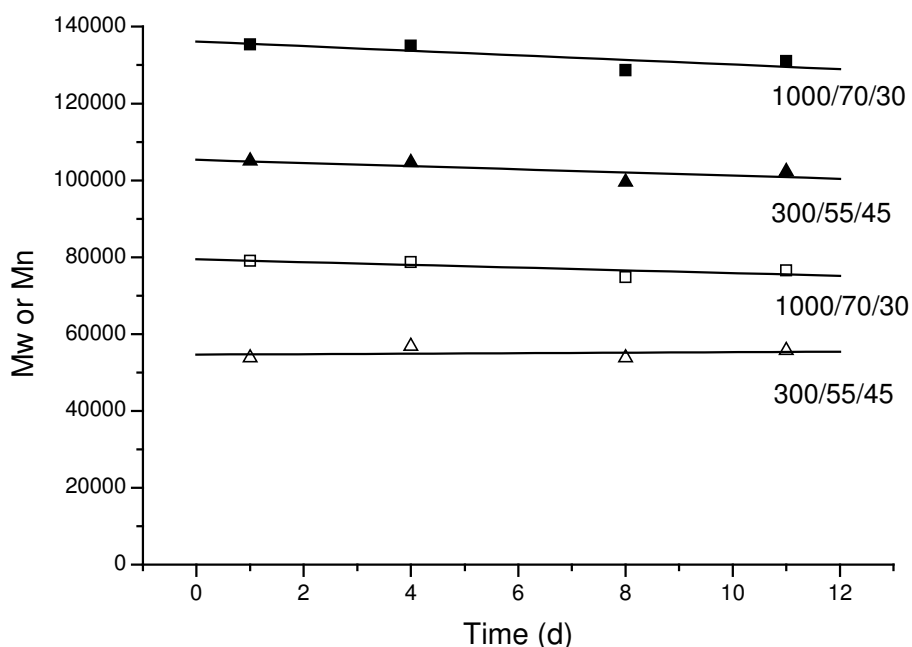


Figure 3.7 - Weight (closed symbols) and number (open symbols) average molecular weights as determined by GPC of 300PEOT55PBT45 and 1000PEOT70PBT30 dissolved in a solution of HFIP and 0.02 M  $\text{CH}_3\text{COONa}$  kept for different times at room temperature.

To study if PEOT/PBT copolymers degrade in HFIP, two different copolymers were dissolved in a solution of HFIP and 0.02 M  $\text{CH}_3\text{COONa}$  and their molecular weights were determined by GPC at regular time intervals. As indicated in Figure 3.7 only a slight decrease was observed in the molecular weights of 1000PEOT70PBT30 and 300PEOT55PBT45 over a period of 11 d. The GPC data for the different copolymers (Table 3.2) was typically obtained by dissolving the copolymers overnight in a solution of HFIP and 0.02 M  $\text{CH}_3\text{COONa}$ , so no noticeable decrease in molecular weight is expected for these measurements. All GPC measurements were performed at 30 °C and the molecular weights were calculated relative to a PMMA calibration line.

Previously intrinsic viscosities of these copolymers have been reported: Hoeschele *et al.* reported values of 1.2-1.5 dL/g (m-cresol, 30 °C)<sup>[14]</sup>, Fakirov *et al.* values of 1.0-1.4 dL/g

(phenol:1,1,2,2-tetrachloroethane 1:1 at 20 °C)<sup>[11]</sup>, and Deschamps *et al.* values of 1.0-1.6 dL/g (chloroform, 25 °C) <sup>[19]</sup> and values up to 1.9 dL/g (HFIP + 0.02 M CF<sub>3</sub>COONa, 40 °C)<sup>[22]</sup>. These reported values would roughly correspond to weight average molecular weights of 50,000 to 150,000 g/mol, as can be expected for a polycondensation reaction.<sup>[14,19]</sup> The obtained relative values from our GPC measurements correspond well with these reported values.

Table 3.2 - PEOT/PBT copolymers prepared on a 1 kg scale. Compositions and molecular weights relative to PMMA measured in HFIP with 0.02 M CF<sub>3</sub>COONa at 30 °C.

Intended Composition	Composition ( <sup>1</sup> H- NMR)	$\overline{M}_n$	$\overline{M}_w$	PDI
300PEOT55PBT45	299/56/44	9.2×10 <sup>4</sup>	15.0×10 <sup>4</sup>	1.66
300PEOT70PBT30	298/69/31	6.8×10 <sup>4</sup>	12.0×10 <sup>4</sup>	1.74
300PEOT70PBT30	302/68/32	7.4×10 <sup>4</sup>	13.0×10 <sup>4</sup>	1.73
1000PEOT30PBT70	-§	5.6×10 <sup>4</sup>	11.0×10 <sup>4</sup>	1.92
1000PEOT55PBT45	924/57/43	7.7×10 <sup>4</sup>	13.0×10 <sup>4</sup>	1.71
1000PEOT70PBT30	945/71/29	7.8×10 <sup>4</sup>	13.0×10 <sup>4</sup>	1.69
1000PEOT70PBT30	945/71/29	9.2×10 <sup>4</sup>	15.0×10 <sup>4</sup>	1.68
1000PEOT70PBT30	899/72/28	8.4×10 <sup>4</sup>	15.0×10 <sup>4</sup>	1.73
1000PEOT70PBT30	945/71/29	8.3×10 <sup>4</sup>	14.0×10 <sup>4</sup>	1.72
1000PEOT70PBT30	917/70/30	8.3×10 <sup>4</sup>	14.0×10 <sup>4</sup>	1.71

§: insoluble in CDCl<sub>3</sub>

## Thermal processing

To obtain functional objects the copolymer needs to be processed into films and/or scaffolds. Although for many processing routes solvents are used, a more convenient way of processing these thermoplastic elastomers is by injection and compression molding.

Table 3.3 - Molecular weights as determined by GPC (HFIP + 0.02 M CF<sub>3</sub>COONa, relative to PMMA) of various PEOT/PBT copolymers before and after compression molding.

	300PEOT55 PBT45		1000PEOT55 PBT45		1000PEOT70 PBT30		1000PEOT70 PBT30	
	1 mm thick film		1 mm thick film		1 mm thick film		4 mm thick porous structure <sup>§</sup>	
Process temp.	4 min 150 °C		4 min 175 °C		4 min 140 °C		4 min 180 °C	
	before	after	Before	after	Before	after	before	after
$\overline{M}_n$	5.7×10 <sup>4</sup>	5.5×10 <sup>4</sup>	7.7×10 <sup>4</sup>	7.3×10 <sup>4</sup>	8.3×10 <sup>4</sup>	7.5×10 <sup>4</sup>	7.8×10 <sup>4</sup>	6.6×10 <sup>4</sup>
$\overline{M}_w$	10.0×10 <sup>4</sup>	10.0×10 <sup>4</sup>	13.0×10 <sup>4</sup>	12.0×10 <sup>4</sup>	14.0×10 <sup>4</sup>	13.0×10 <sup>4</sup>	13.0×10 <sup>4</sup>	13.0×10 <sup>4</sup>
PDI	1.84	1.85	1.71	1.70	1.71	1.73	1.69	1.90

§: 80 vol % sodium chloride crystals of 425-500 µm

Many of the films and porous structures described in this thesis were prepared by compression molding. Like with the copolymer synthesis care needs to be taken that the copolymers do not degrade during the exposure to high temperatures.<sup>[27]</sup> Table 3.3 summarizes the molecular



weights of several copolymers before and after compression molding. For the different copolymers, only small decreases in molecular weights were measured. For the process conditions described, the lowest possible temperatures that still enable the production of homogeneous films or stable scaffolds are applied.

## Mechanical properties

Although the hydrophilic nature of some of the PEOT/PBT copolymers is an important factor in their *in vivo* bone bonding<sup>[28]</sup> and calcification<sup>[29]</sup>, one should realize that the high water uptake of the hydrophilic materials has a prominent effect on their mechanical properties in the water-swollen state. An elaborate study on the effects of copolymer composition and molecular weight on the physical, mechanical and degradation properties was previously reported by Deschamps *et al.*<sup>[19]</sup> With increasing PEO length there is an increase in the actual PEO weight % present in the copolymer. With increasing PEO weight % a strong increase in the water uptake was observed (Figure 3.8).

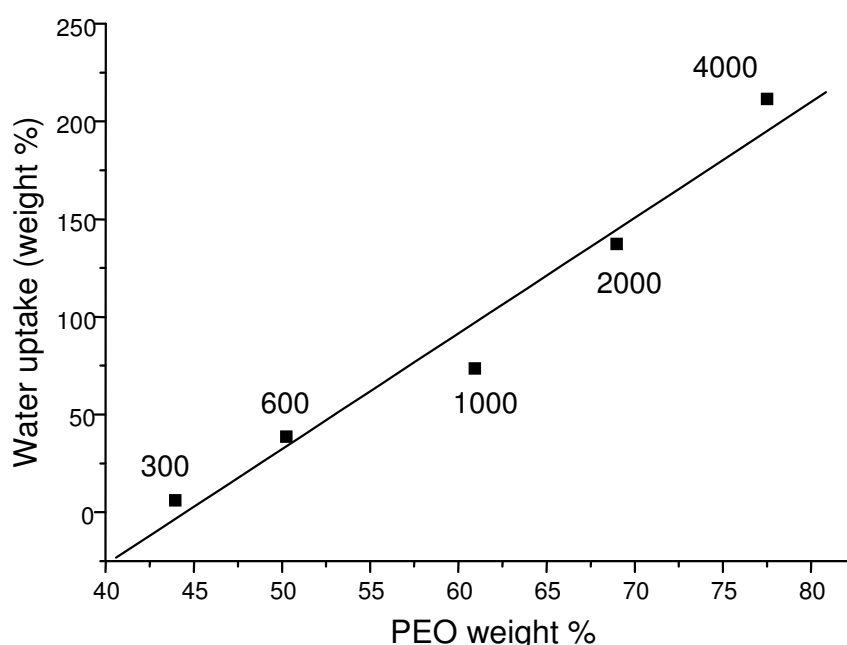


Figure 3.8 - Water uptake as a function of PEO weight % for PEOT70PBT30 copolymers. The PEO  $\overline{M}_w$  is indicated next to the data points.

To determine tensile characteristics like the elastic modulus, dry (stored at ambient conditions) and wet films of the PEOT/PBT block copolymers were subjected to tensile testing. For water swollen samples there is a decrease in E-modulus with increasing PEO molecular weight. A comparable relation also applies to dry samples (Figure 3.9).

Polymers with a PEO molecular weight of 4000 in the dry state have an E-modulus of 325 N/mm<sup>2</sup> (data not shown in Figure 3.9), which is much higher than the E-modulus of polymers based on PEO's with lower molecular weight. Crystallization of PEO, due to the high molecular weight of the PEOT segment, is expected to play an important role here. The crystallinity is probably lost in the water-swollen samples ( $E = 3.8$  N/mm<sup>2</sup>), due to swelling of the hydrophilic PEO domains (water uptake over 200 mass %).

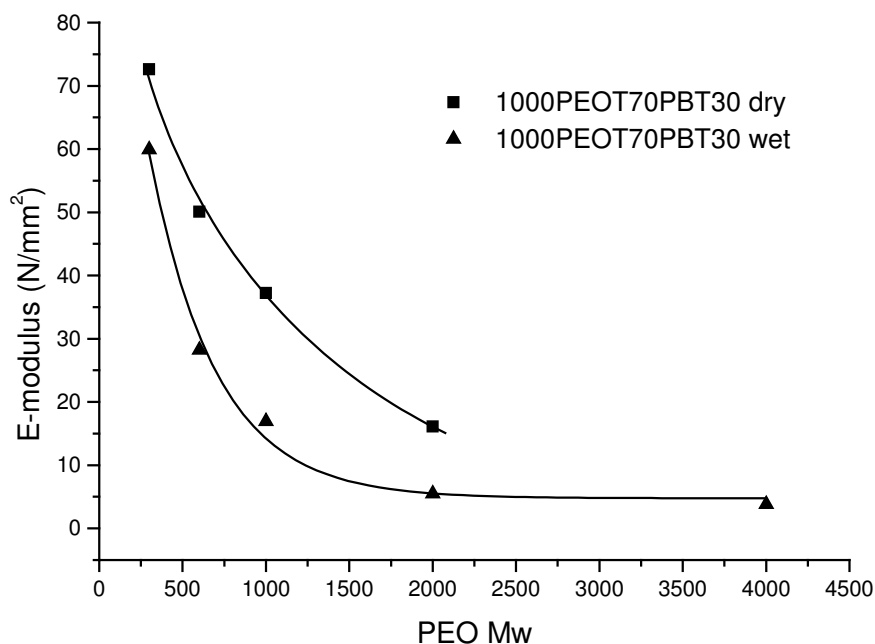


Figure 3.9 - E-moduli of dry and water-swollen samples (solution cast films) as a function of PEO molecular weight in PEOT70PBT30 copolymers.

Besides a decrease in E-modulus, water uptake also has a pronounced effect on the strength of the material. In Table 3.4 the tensile properties of 1000PEOT70PBT30 in the dry and water-swollen state are compared.

Besides tensile properties, where the samples are subjected to a relatively fast deformation, the properties of these copolymers with respect to static or cyclic loading for extended time periods are of importance. Under dynamic culture conditions in a bioreactor, the scaffold material can be exposed to long term static loads, mainly due to shear forces.<sup>[30-35]</sup>

Mechanical stimulation has been successfully applied in the culture of skeletal muscle<sup>[36,37]</sup>, cartilage<sup>[38,39]</sup>, smooth muscle tissue and blood vessels<sup>[40-42]</sup> to improve the physical properties of the resulting tissues.

Table 3.4 - Selected tensile properties of compression molded 1000PEOT70PBT30 copolymer films.

	Dry	Water swollen
E-modulus (N/mm <sup>2</sup> )	26.5 ± 1.3	14.7 ± 0.2
$\epsilon_{\text{break}}$ (%)	805 ± 5	288 ± 32
$\sigma_{\text{max}}$ (N/mm <sup>2</sup> )	12.1 ± 0.3	7.8 ± 0.2
Energy up to break (Nmm)	(18.3 ± 0.6) × 10 <sup>3</sup>	(5.0 ± 0.7) × 10 <sup>3</sup>

To evaluate the mechanical properties of 1000PEOT70PBT30 under static loads, creep tests were carried out. Figure 3.10 shows parts of creep curves of 1000PEOT70PBT30 both in the dry and water-swollen state. The constant creep rate was determined over the time period 60-3600 s of the test for the water-swollen samples and over the time period of  $6.8 \times 10^3$ - $1 \times 10^6$  s for the dry samples.

Especially in the dry state this material shows low creep rates. (Table 3.5). Unfortunately in the water-swollen state the creep rate is considerably higher and the samples break before the

end of the test (after approximately 3-4 h compared to 21 d for the dry samples), in line with the lower tensile strength in the water-swollen state.

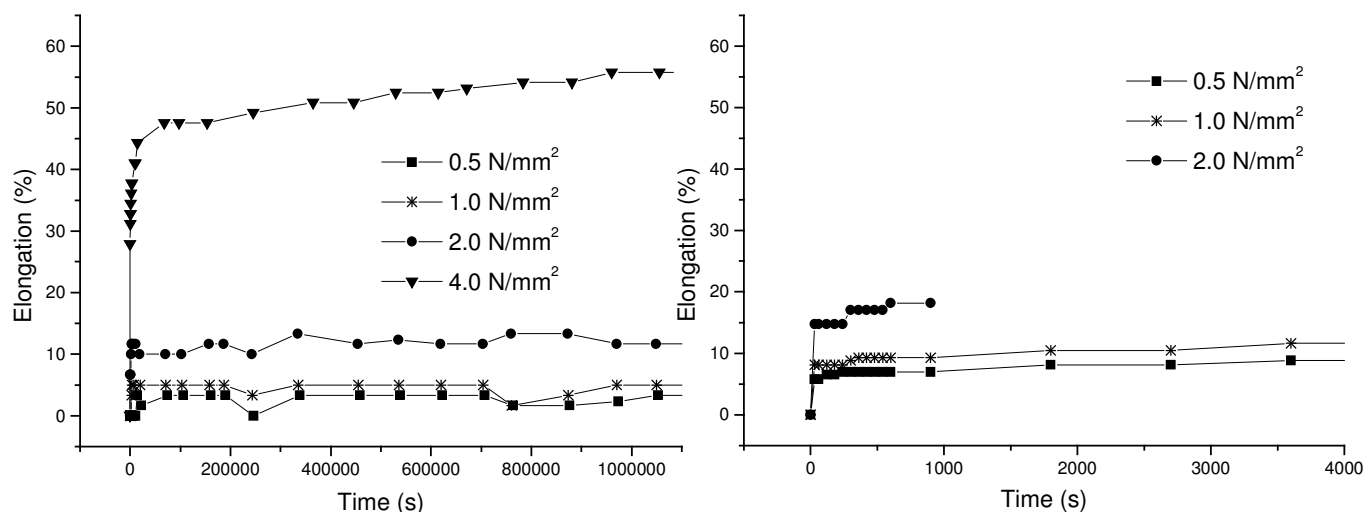


Figure 3.10 - Creep curves of 1000PEOT70PBT30. Left: dry. Right: wet. Swollen 1000PEOT70PBT30 was unable to sustain a load of 4 N/mm<sup>2</sup>. Measurements were performed at room temperature (18 °C).

Table 3.5 - Creep rates of 1000PEOT70PBT30 copolymer films. For the dry samples the creep rate was determined during the first 1×10<sup>6</sup> s of the test, for the water-swollen samples during the first 3600 s.

	Load (N/mm <sup>2</sup> ) <sup>¶</sup>	Creep rate (s <sup>-1</sup> )	Residual strain (%) (after 21 d)
1000PEOT70PBT30 Dry	0.5 (10 %)	1 × 10 <sup>-7</sup>	0
	1.0 (20 %)	1 × 10 <sup>-7</sup>	0
	2.0 (40 %)	1 × 10 <sup>-6</sup>	0
	4.0 (80 %)	9 × 10 <sup>-6</sup>	13
1000PEOT70PBT30 Water swollen	0.5 (10 %)	7 × 10 <sup>-4</sup>	-§
	1.0 (20 %)	9 × 10 <sup>-4</sup>	-§
	2.0 (40 %)	5 × 10 <sup>-3</sup>	-§

¶: percentage of yield stress as indicated in parentheses

§: wet samples broke during testing, hence no residual strain could be determined

## Conclusions

PEOT/PBT block copolymers were prepared on a 50-100 g and on a 1 kg scale. Copolymers with weight average molecular weights of 110,000 to 150,000 g/mol (relative to PMMA) have been obtained. A further increase (if desired) in molecular weight can be obtained by postcondensation of the precipitated copolymer.

Dissolution of the copolymers in a solution of HFIP and 0.02 M CH<sub>3</sub>COONa results in a limited decrease in molecular weight in time, showing the suitability of this solvent for GPC measurements to determine PEOT/PBT molecular weights. Thermal processing in the form of compression molding results in films and porous structures with molecular weights of the copolymers slightly lower than the original ones. The tensile and creep properties of PEOT/PBT copolymers in the water-swollen state are significantly lower as compared to those in the dry state.

## Acknowledgements

We thank C.J. Padberg for the technical assistance in the GPC measurements (University of Twente). This study was financially supported by the European Community (Brite-Euram project BE97-4612).

## References

1. R.K. Adams, G.K. Hoeschele, W.K. Witsiepe *Thermoplastic Polyether Ester Elastomers* in "Thermoplastic Elastomers", 2nd ed.; G. Holden, N.R. Legge, R. Quirk, and H.E. Schroeder, Ed.; Hanser Publishers: Munich, Germany **1996**; pp 191-225.
2. D. Coleman *Block copolymers: Copolymerization of ethylene terephthalate and polyoxyethylene glycols* J. Polym. Sci. **1954**, *14*, 15-28.
3. D. Coleman (to ICI) U.K. Patent 682866 **1952**.
4. A.A. Nishimura, H. Komagata *Elastomers based on polyester* J. Macromol. Sci. (Chem.) **1967**, *A1*, 617-625.
5. W.K. Witsiepe (to DuPont) *Segmented thermoplastic copolyester elastomers* U.S. Patent 3651014 **1972**.
6. W.K. Witsiepe (to DuPont) *Segmented thermoplastic copolyesters* U.S. Patent 3763109 **1973**.
7. W.K. Witsiepe (to DuPont) *Segmented thermoplastic copolyester elastomers* U.S. Patent 3766146 **1973**.
8. D.K. Gilding, A.M. Reed *Biodegradable polymers for use in surgery-poly(ethylene oxide) poly(ethylene terephthalate) (PEO/PET) copolymers: 1* Polymer **1979**, *20*, 1454-1458.
9. A.M. Reed, D.K. Gilding *Biodegradable polymers for use in surgery-poly(ethylene oxide)/poly(ethylene terephthalate) (PEO/PET) copolymers: 2. in vitro degradation* Polymer **1981**, *22*, 499-504.
10. D. Bakker *Alloplastic tympanic membrane*, Thesis, University of Leiden, Leiden, The Netherlands, **1988**.
11. S. Fakirov, T. Gogeva *Poly(ether/ester)s based on poly(butylene terephthalate) and poly(ethylene glycol), 1 Poly(ether/ester)s with various polyether:polyester ratios* Makromol. Chem. **1990**, *191*, 603-614.
12. S. Fakirov, T. Gogeva *Poly(ether/ester)s based on poly(butylene terephthalate) and poly(ethylene glycol), 2 Effect of polyether segment length* Makromol. Chem. **1990**, *191*, 615-624.
13. G.K. Hoeschele, W.K. Witsiepe *Polyaetherester-Block-Copolymere - Eine Gruppe neuartiger thermoplastischer Elastomere* Angew. Makromol. Chem. **1973**, *29/30*, 267-289.
14. G.K. Hoeschele *Ueber die Synthese von Polyaetherester-Block-Copolymeren* Chimia **1974**, *28*, 544-552.
15. F. Weingart, P. Hirt, H. Herlinger *Titanium catalysts in the manufacture of polyethylene terephthalate* Chem. Fibers Inter. **1996**, *2*, 96-97.
16. B. Apicella, M. Di Serio, L. Fiocca, R. Po, E. Santacesaria *Kinetic and catalytic aspects of the formation of poly(ethylene terephthalate) (PET) investigated with model molecules* J. Appl. Polym. Sci. **1998**, *69*, 2423-2433.
17. M. Bounekhel, I.C. McNeill *Thermal-Degradation Studies of Terephthalate Polyesters .2. Poly(Ether-Esters)* Polym. Degrad. Stabil. **1995**, *49*, 347-352.
18. V. Passalacqua, F. Pilati, V. Zamboni, B. Fortunato, P. Manaresi *Thermal degradation of poly(butylene terephthalate)* Polymer **1976**, *17*, 1044-1048.
19. A.A. Deschamps, D.W. Grijpma, J. Feijen *Poly(ethylene oxide)/poly(butylene terephthalate) segmented block copolymers: the effect of copolymer composition on physical properties and degradation* Polymer **2001**, *42*, 9335-9345.
20. O.F. Solomon, I.Z. Ciuta *Determination de la viscosité intrinsèque de solutions de polymères par une simple détermination de la viscosité* J. Appl. Polym. Sci. **1962**, *6*, 683-686.
21. R.N. Shroff *Single-point determination of intrinsic viscosity* J. Appl. Polym. Sci. **1965**, *9*, 1547-1551.
22. A.A. Deschamps, A.A. van Apeldoorn, H. Hayen, J.D. de Bruijn, U. Karst, D.W. Grijpma, J. Feijen *In vitro and in vivo degradation of poly(ether ester) block copolymers based on poly(ethylene glycol) and poly(butylene terephthalate)* Biomaterials **2004**, *25*, 247-258.
23. H.R. Stapert *Environmentally Degradable Polyesters, Poly(ester-amide)s and Poly(ester-urethane)s*, Thesis, University of Twente, Enschede, The Netherlands, **1998**.
24. T.H. Mourey, T.G. Bryan *Size-exclusion chromatography in 1,1,1,3,3,3-hexafluoro-2-propanol* J. Chromatogr. A **2002**, *964*, 169-178.
25. S. Mori *Size Exclusion Chromatography of Poly(Ethylene-Terephthalate) Using Hexafluoro-2-Propanol As the Mobile Phase* Anal. Chem. **1989**, *61*, 1321-1325.
26. S. Mori, Y. Nishimura *Effects of Addition of an Electrolyte On Size-Exclusion Chromatography of Polyamides Using Hexafluoro-2-Propanol As Mobile-Phase* J. Liq. Chromatogr. **1993**, *16*, 3359-3370.
27. G. Botelho, A. Queiros, P. Gijsman *Thermooxidative studies of poly(ether-esters) 1. Copolymer of poly(butylene terephthalate) and poly(ethylene oxide)* Polym. Degrad. Stabil. **2000**, *67*, 13-20.

28. R.J.B. Sackers, R.A.J. Dalmeyer, J.R. de Wijn, C.A. van Blitterswijk *Use of bone-bonding hydrogel copolymers in bone: An in vitro and in vivo study of expanding PEO-PBT copolymers in goat femora* J. Biomed. Mater. Res. **2000**, 49, 312-318.
29. C.A. van Blitterswijk, J. van der Brink, H. Leenders, D. Bakker *The effect of PEO ratio on degradation, calcification and bone bonding of PEO/PBT copolymer (Polyactive)* Cells and Materials **1993**, 3, 23-36.
30. G.N. Bancroft, V.I. Sikavitsast, J. van den Dolder, T.L. Sheffield, C.G. Ambrose, J.A. Jansen, A.G. Mikos *Fluid flow increases mineralized matrix deposition in 3D perfusion culture of marrow stromal osteoblasts in a dose- dependent manner* Proc. Natl. Acad. Sci. U. S. A. **2002**, 99, 12600-12605.
31. E.H. Burger, J. Kleinulend, J.P. Veldhuijzen *Modulation of Osteogenesis in Fetal Bone Rudiments By Mechanical-Stress Invitro* J. Biomech. **1991**, 24, 101-&.
32. S. Saini, T.M. Wick *Concentric cylinder bioreactor for production of tissue engineered cartilage: Effect of seeding density and hydrodynamic loading on construct development* Biotechnol. Prog. **2003**, 19, 510-521.
33. S. Jockenhoevel, G. Zund, S.P. Hoerstrup, A. Schnell, M. Turina *Cardiovascular tissue engineering: A new Laminar flow chamber for in vitro improvement of mechanical tissue properties* Asaio J. **2002**, 48, 8-11.
34. S.P. Hoerstrup, R. Sodian, J.S. Sperling, J.P. Vacanti, J.E. Mayer *New pulsatile bioreactor for in vitro formation of tissue engineered heart valves* Tissue Eng. **2000**, 6, 75-79.
35. H.R. Millward, B.J. Bellhouse, I.J. Sobey *The vortex wave membrane bioreactor: Hydrodynamics and mass transfer* Chem. Eng. J. Biochem. Eng. J. **1996**, 62, 175-181.
36. H.H. Vandenburg, S. Hatfaludy, P. Karlisch, J. Shansky *Mechanically Induced Alterations in Cultured Skeletal-Muscle Growth* J. Biomech. **1991**, 24, 91-99.
37. R.G. Dennis, P.E. Kosnik *Excitability and isometric contractile properties of mammalian skeletal muscle constructs engineered in vitro* In Vitro Cell. Dev. Biol.-Anim. **2000**, 36, 327-335.
38. S.E. Carver, C.A. Heath *Increasing extracellular matrix production in regenerating cartilage with intermittent physiological pressure* Biotechnol. Bioeng. **1999**, 62, 166-174.
39. R.L. Mauck, M.A. Soltz, C.C.B. Wang, D.D. Wong, P.H.G. Chao, W.B. Valhmu, C.T. Hung, G.A. Ateshian *Functional tissue engineering of articular cartilage through dynamic loading of chondrocyte-seeded agarose gels* J. Biomech. Eng.-Trans. ASME **2000**, 122, 252-260.
40. B.S. Kim, J. Nikolovski, J. Bonadio, D.J. Mooney *Cyclic mechanical strain regulates the development of engineered smooth muscle tissue* Nat. Biotechnol. **1999**, 17, 979-983.
41. D. Seliktar, R.A. Black, R.P. Vito, R.M. Nerem *Dynamic mechanical conditioning of collagen-gel blood vessel constructs induces remodeling in vitro* Ann. Biomed. Eng. **2000**, 28, 351-362.
42. L.E. Niklason, J. Gao, W.M. Abbott, K.K. Hirschi, S. Houser, R. Marini, R. Langer *Functional arteries grown in vitro* Science **1999**, 284, 489-493.



# Chapter 4

## Enhanced bone marrow stromal cell adhesion and growth on segmented poly(ether ester)s based on poly(ethylene oxide) and poly(butylene terephthalate)\*

*Houston, we've had a problem.*

James Lovell (1928- )

### Abstract

In previous studies in rats and goats, hydrophilic compositions of the PEOT/PBT block copolymer family have shown *in vivo* calcification and bone-bonding. These copolymers are therefore interesting candidates as scaffolding materials in bone tissue engineering applications. Model studies using goat bone marrow stromal cells, however, showed that it was not possible to culture bone marrow stromal cells (BMSCs) *in vitro* on these hydrophilic copolymers. In this paper two ways of surface modifying these materials to improve *in vitro* bone marrow stromal cell attachment and growth are discussed. Two different approaches are described: 1) Blending of hydroxyapatite (HA) followed by CO<sub>2</sub> gas plasma etching. 2) Surface modification using CO<sub>2</sub> gas plasma treatments. It was observed that not only HA, but also the CO<sub>2</sub> plasma treatment by itself has a positive effect on BMSC attachment and growth. Gas plasma treatment appeared to be the most successful approach, resulting in a large increase in the amount of BMSCs present on the surface (determined by a DNA assay). The amount of DNA present on the gas plasma treated copolymer 1000PEOT70PBT30, based on

---

\*Menno B. Claase,<sup>1</sup> Mark B. Olde Riekerink,<sup>1</sup> Martijn C. Huijgen,<sup>1</sup> Joost D. de Bruijn,<sup>3</sup> Dirk W. Grijpma,<sup>1</sup> Gerard H.M. Engbers,<sup>1</sup> Jan Feijen<sup>1</sup>

Published in *Biomacromolecules* **2003**, 4 (1), 57-63.

1) Institute for Biomedical Technology (BMTI) and Department of Polymer Chemistry and Biomaterials, Faculty of Science and Technology, University of Twente, P.O. Box 217, 7500 AE Enschede, The Netherlands

2) IsoTis OrthoBiologics., P.O. Box 98, 3720 AB Bilthoven, The Netherlands

poly(ethylene oxide,  $M_w = 1000$ , 70 weight % soft segment), was comparable to the amount present on PDLLA and significantly higher than the amount present on PCL after 7 d of cell culturing. The fact that after gas plasma treatment BMSCs do attach to PEOT/PBT copolymers, enables in vitro BMSC culturing, making bone tissue engineering applications of these materials possible.

## Introduction

The development of biological substitutes that restore, maintain or improve tissue function and the clinical application thereof is the goal of tissue engineering. Specific cells are harvested from the appropriate tissue and seeded on a biodegradable polymer scaffold. After a period of in vitro cell culture (if desired) to multiply the cells, these constructs can be implanted at the place of the defect.<sup>[1]</sup> This approach is also used in the development of synthetic, manufactured bone graft substitutes.<sup>[2-4]</sup>

In the case of non load-bearing bone tissue, suitable scaffold materials appear to be PEOT/PBT block copolymers, also known under their trade name PolyActive<sup>®</sup>. Here the copolymer compositions will be abbreviated as previously described by Deschamps et al.<sup>[5]</sup>, i.e.  $a\text{PEOT}b\text{PBT}c$ , where  $a$  is the molecular weight of the used poly(ethylene glycol),  $b$  the weight percentage soft segment and  $c$  the weight percentage hard segment.

By varying the copolymer composition, properties like phase separation, in vitro degradation, water uptake<sup>[5]</sup>, but also in vivo degradation, calcification and bone bonding can be tuned.<sup>[6-8]</sup> Copolymer composition also has a pronounced effect on in vitro cell culturing on these materials. Although there is no effect of copolymer composition on chondrocyte attachment and proliferation, significant differences are observed for skeletal muscle cells<sup>[9]</sup> and keratinocytes.<sup>[10]</sup> Both cell types proliferate better on the more hydrophobic compositions (i.e. 300PEOT55PBT45). Similar behavior is seen for goat BMSCs<sup>[11,12]</sup> cultured in the presence of dexamethasone to induce differentiation into the osteogenic lineage.<sup>[13]</sup> The more hydrophilic copolymers, however, show better in vivo degradation, calcification and bone bonding and are therefore the preferred materials as scaffolds in bone tissue engineering. To use these hydrophilic compositions in bone tissue engineering, the copolymer surface needs to be modified to improve in vitro cell attachment. Several approaches towards this end can be taken.

An attempt to improve BMSC attachment by use of PEO-RGD conjugates is described in Appendix A. Surface properties like hydrophilicity, the presence of positive or negative charges and surface roughness play a key role in osteoblast adhesion to biomaterials.<sup>[14]</sup> We therefore explored various ways to modify the surface properties of PEOT/PBT copolymers by use of acidic and alkaline solutions. In the past strongly oxidizing reagents (concentrated acids) have been used to improve cell attachment (Vero cells) to polystyrene<sup>[15]</sup>, sodium hydroxide treatments to improve smooth muscle cell attachment to poly(glycolic acid)<sup>[16]</sup> and fibroblast attachment to poly(hydroxyalkanoates).<sup>[17]</sup>

Acid treatments (solutions in ethanol to prevent bulk hydrolysis) did not result in an improved cell attachment and growth onto 1000PEOT70PBT30. Alkaline treatments resulted in severe surface degradation, even at treatments of one minute in 0.1 N NaOH in ethanol. Also in these cases no improvement in cell attachment and growth was observed.

Studies on PLA and PCL composites with hydroxyapatite (HA) have shown an increase in osteoblast attachment and activity, showing the beneficial effect of this mineral in composite systems.<sup>[18,19]</sup> HA is also used as a scaffolding material for the implantation of BMSCs.<sup>[3,4,20]</sup> It is therefore to be expected that incorporation of this material can have a positive effect on the BMSC attachment to PEOT/PBT copolymer systems. The grafting of 1000PEOT70PBT30 onto HA particles is described in Appendix B. Two ways of surface modification will be



discussed in this paper: 1) Blending of HA and etching with CO<sub>2</sub> gas plasma treatments. 2) Surface modification using CO<sub>2</sub> gas plasma treatments.

The focus of this paper will be on the improvement of cell attachment of the 1000PEOT70PBT30 copolymer since this copolymer composition shows the most favorable in vivo properties (i.e. bone bonding, calcification and degradation) of the PEOT/PBT copolymer family.<sup>[6-8]</sup> The obtained data will be compared with well known biomaterials like poly(D,L-lactide) and poly(ε-caprolactone).

## Materials and methods

### Materials

All solvents used were of analytical grade and all chemicals were at least 99 % pure and used as received, unless otherwise mentioned. <sup>1</sup>H-NMR spectra were taken using a Varian 300 MHz apparatus. <sup>13</sup>C-NMR spectra were obtained using a Varian 400 MHz apparatus.

1000PEOT70PBT30 and 300PEOT55PBT45 were synthesized as previously described, using vitamin E as an antioxidant.<sup>[5]</sup> Compositions according to <sup>1</sup>H-NMR were 945PEOT71PBT29 and 296PEOT53PBT47 respectively. PEOT/PBT copolymers were used without further purification.

Poly(D,L-lactide) (PDLLA,  $M_n = 1.16 \times 10^4$ ) was synthesized using a ring opening polymerization of a 50/50 mixture of D and L-lactide. Poly(ε-caprolactone) (PCL) Capa 680 (lot 96,  $M_n = 7.67 \times 10^4$ ,  $M_w = 1.20 \times 10^5$ ) was obtained from Solvay Interlox Ltd. (Warrington, U.K.).<sup>[21]</sup> Both polymers were purified by precipitation in 96 % ethanol to remove residual monomer. Sintered hydroxyapatite with a particle size of 38-53 μm was provided by professor F.J. Monteiro (Instituto de Engenharia Biomédica (INEB), Porto, Portugal) and was used as received.

### Polymer film preparation

*Films prepared by solution casting.* PEOT/PBT films (75-100 μm thick) were prepared by casting 20 % (w/v) polymer solutions in chloroform (1000PEOT70PBT30) or chloroform/1,1,1,3,3,3-hexafluoro-2-propanol mixtures (300PEOT55PBT45) on a glass plate using a casting knife. All films were placed in ethanol (overnight) to remove any residual 1,1,1,3,3,3-hexafluoro-2-propanol and/or chloroform. Films were dried in a vacuum oven at reduced nitrogen pressure for 5 d.

*Films prepared by compression molding.* Polymer films of PEOT/PBT, PCL and PDLLA were prepared by compression molding for 4 min at 140 °C in a laboratory hot press (THB 008, Fontijne Holland BV, The Netherlands). Subsequently the 1 mm thick films were washed 24 h in hexane, 48 h in ethanol and dried in a vacuum oven at reduced nitrogen pressure for 5 d.

### Composite films with HA

1000PEOT70PBT30 composite films (75-100 μm thick) were prepared by casting of 20 % (w/v) polymer solutions in chloroform on a glass plate using a casting knife. The solutions contained 5, 10 or 25 vol % HA.

To show the effect of HA on cell adhesion and proliferation, a second type of composite film was prepared. HA powder was deposited on the freshly cast (wet) film by sprinkling. All films were placed in ethanol for 24 h to remove any residual chloroform. Films were dried in a vacuum oven at reduced nitrogen pressure for 4 d.

*Gas plasma etching.* Composite films were placed in a tubular reactor (length 80 cm, internal diameter 6.5 cm). Three externally placed capacitively coupled copper electrodes were attached to the reactor: a 'hot' electrode in the center and a 'cold' electrode at both sides of the 'hot' electrode at 12 cm distance. The electrodes were connected to a RF (13.56 MHz) generator through a matching network. Samples were placed in between the 'hot' and 'cold' electrode and treated for 5, 15 or 30 min using a CO<sub>2</sub> gas plasma (plasma pressure: 0.08 mbar). Discharge power was 50 W. A gas flow of 10 cm<sup>3</sup>/min was used. Samples were treated with a pre-delay of 5 min and a post-delay of 2 min.<sup>[11,22]</sup>

### CO<sub>2</sub> gas plasma treatment

Compression molded films (treated on both sides) were treated for 30 min. Discharge power was 50 W. CO<sub>2</sub> gas plasma pressure: 0.06-0.07 mbar. A gas flow of 10 cm<sup>3</sup>/min was used. Samples were treated with a pre-delay of 5 min and a post-delay of 2 min.<sup>[11,22]</sup> After treatment, samples were rinsed using demineralized water, followed by ethanol (p.a.). Samples were washed with ethanol (p.a.) overnight and dried in a vacuum oven for 3 d at room temperature.

### Surface characterization

*XPS analysis.* The measurements were performed using a Quantum 2000 Scanning ESCA microprobe (Physical Electronics, USA) with a monochromatic Al K<sub>α</sub> source (1486.6 eV). The input power was 25 W and the analyzed spot size was 1400 x 500 μm. Survey scans (0-700 eV) were recorded with a pass energy of 117 eV. The concentrations of the various elements were calculated from the relative peak areas, using sensitivity factors from the machine manufacturer. Subsequently, high resolution detail scans of the C1s peak region (278-298 eV) were recorded with a pass energy of 29 eV. The C1s peak was normalized and the first sub-peak (C-C) was set at 284.8 eV. For peak deconvolution, spectra were fitted with the minimal amount of peaks. Samples of the same compositions were fitted with the same settings.

*Contact angle measurements.* Solution cast and compression molded polymer films were characterized by static water contact angle measurements using the captive bubble and the sessile drop method. The measurements were performed with a Video-based Optical Contact Angle Meter OCA 15 Plus (DataPhysics Instruments GmbH, Germany). Samples were fixed onto glass slides with double sided tape. For captive bubble measurements samples were immersed in water overnight and placed in an optical cuvette filled with water, with the polymer film facing downward. Contact angles were determined by placing an air bubble on the sample with an electronically regulated syringe fitted with a hook-shaped needle. For the sessile drop measurements a water droplet of approximately 10 μL was placed on dry surfaces. Contact angles were calculated by SCA 20 software (DataPhysics, version 1.60) using ellipse fitting. Results are the average of at least four measurements (± s.d.).

### Bone marrow stromal cell culturing

*Goat bone marrow stromal culturing on copolymer films.* Samples with a diameter of 10 mm were cut from the copolymer film covered with HA. Before culturing, samples were washed with demineralized water (2x), 70 % ethanol/water and sterile PBS (3x). For preliminary screening experiments goat BMSCs, passage 3 were used. The cells were seeded with a density of 10,000 cells/cm<sup>2</sup>, in the presence of 3 mL minimal essential medium (α-MEM, Life Technologies, The Netherlands) containing<sup>[13]</sup>: 15 % (v/v) fetal bovine serum (Life Technologies, The Netherlands), 100 units/mL penicillin, 100 μg/mL streptomycin (Life Technologies, The Netherlands), 2 mM L-glutamine (Life Technologies, The Netherlands),

0.2 mM ascorbic acid 2-phosphate (Life Technologies, The Netherlands), 10 mM  $\beta$ -glycerophosphate (Sigma, The Netherlands),  $10^{-8}$  M dexamethasone (Sigma, The Netherlands).

*Rat bone marrow stromal cell culturing.* Samples were cut from the compression molded films and put into 24-well plates. Before culturing, samples were washed with demineralised water (2x), 70 % ethanol/water and sterile PBS (3x). BMSCs were isolated from 2 femora and 2 tibia from 2 male Wistar-rats. The femora were cut on both sides and the marrow was flushed out using 9 mL of medium. The collected cells were re-suspended with a 21G needle and cultured at 37 °C, 5 % CO<sub>2</sub> for 7 d, with periodic medium changes every other day. The culture medium was identical to the one used for goat BMSC culturing. After 7 d, cells were confluent and were washed with PBS (Life Technologies, The Netherlands) and treated with trypsin/EDTA (Sigma, The Netherlands), yielding  $2.3 \times 10^6$  rat BMSCs. Cells were seeded at a density of 10,000 cells/cm<sup>2</sup> and cultured up to 7 d. Samples were analyzed after 1, 3 and 7 d.

*Methylene blue staining.* Samples were analyzed at day 1, 3 and 7. Films were washed with warm PBS (containing 100 units/mL penicillin and 100  $\mu$ g/mL streptomycin) and subsequently fixed with glutaraldehyde (Merck, Germany, 1.5 % solution in 0.14 M cacodylic acid (Fluka, Germany, buffer pH = 7.35)). The samples were washed with water and stained for 30 s using a 1 % methylene blue solution in 0.1 M borax buffer (Sigma/Aldrich, Germany, pH = 8.5). Scaffolds were subsequently washed with demineralized water, until the water was clear. Samples were stored in a refrigerator until further analysis. Samples were evaluated using a Nikon SM2-10A stereomicroscope (1x objective). Digital photographs were taken using a Sony progressive 3 CCD camera.

*DNA-assay.* Films were washed with sterile PBS at 37 °C and stored in a freezer (-80 °C) until further analysis. Films were incubated at 56 °C overnight in 1.0 mL of lysis-medium to lyse all cells. The lysis-medium consisted of proteinase K (Sigma, The Netherlands) in Tris/EDTA buffer (1 mg/mL).

The next day 250  $\mu$ L of these suspensions were mixed with 250  $\mu$ L RNase-solution. The RNase solution was prepared from 60  $\mu$ L RNase (Sigma, The Netherlands, 1.35 Kunitz/ $\mu$ l) and 100  $\mu$ L heparin (Leopharma, The Netherlands, 5.000 IE/mL) in 30 mL PBS, and incubated at 37 °C for 70 min to remove the single stranded RNA and DNA. Various dilutions were prepared with PBS. Dilutions were mixed with CyQUANT<sup>®</sup> dye. After 15 min fluorescence was measured in 96 well plates using a Perkin Elmer Luminescence Spectrometer LS 50 B (excitation at 480 nm, slit width 2.5 nm, emission at 520 nm, slit width 7.5 nm). The measured fluorescence intensities were correlated to the amount of DNA using a calibration curve made by using DNA (Sigma) dilutions of known concentration. Data shown are the result of triplicate measurements ( $\pm$  s.d.). Results were analyzed using one-way ANOVA, followed by a Games-Howell Post Hoc Test (assuming unequal variance). Differences were considered statistically significant when  $p < 0.05$ . Statistical calculations were performed using SPSS software for Windows (version 10.0, SPSS, USA).

## Results and discussion

It is well known that chemical treatments can introduce changes at the surface of a material.<sup>[15-17]</sup> Preliminary experiments, however, have shown that treatments with acidic or alkaline solutions of PEOT/PBT copolymers do not improve rat BMSC attachment and growth. Alkaline treatment with 0.1 N NaOH in ethanol for 1 min even causes severe surface degradation. It was, however, observed that there are significant differences in the surface contact angle of the compression molded compared to previously reported solution cast films.<sup>[11]</sup>

The fact that different processing techniques give significantly different surface properties is of interest. For instance in the preparation of porous structures for tissue engineering different techniques are used: thermal processes like heat treatment<sup>[23]</sup>, compression molding<sup>[24]</sup> fiber spinning<sup>[25]</sup> and extrusion<sup>[26]</sup> or techniques involving solvents like solution casting<sup>[27]</sup> and freeze-drying.<sup>[28,29]</sup> Currently we are working on the preparation of porous scaffolds for bone tissue engineering both by freeze-drying and by compression molding combined with salt leaching. In the former technique the solvent is expected to play an important role, where in the latter thermal processes are expected to influence the surface properties.

XPS measurements of the compression molded (untreated) copolymer films (1000PEOT70PBT30 and 300PEOT55PBT45) used in these experiments show that the composition at the surface is the same as for solution cast films, with O/C ratios close to the ones calculated based on the bulk composition (Table 4.1).

Table 4.1 - Selected XPS data from PEOT/PBT copolymers: O/C ratios and C 1s peak deconvolution.

		Solution cast <sup>*</sup>		Compression molded <sup>§</sup>
1000PEOT70PBT30	O/C ratio		0.44	0.440 ± 0.004
	C 1s peak	C-C	29.19 %	30.5 ± 0.8 %
		C-O	65.17 %	63.0 ± 0.7 %
		O-C=O	5.64 %	6.6 ± 0.3 %
1000PEOT70PBT30 30 min CO <sub>2</sub> plasma	O/C ratio		0.49	0.502 ± 0.004
	C 1s peak	C-C	29.47 %	27.2 ± 1.2 %
		C-O	61.88 %	64.0 ± 1.2 %
		O-C=O	8.66 %	8.7 ± 0.2 %
300PEOT55PBT45	O/C ratio		0.41	0.413 ± 0.006
	C 1s peak	C-C	47.8 %	47.9 ± 1.2 %
		C-O	42.39 %	41.4 ± 0.7 %
		O-C=O	9.81 %	10.7 ± 0.6 %

\*: single measurement

§: average of four measurements, ± s.d.

Contact angle measurements however show significant differences between the different films. Table 4.2 compares the contact angle data of solution cast (from chloroform/1,1,1,3,3,3-hexafluoro-2-propanol) and compression molded 1000PEOT70PBT30 and 300PEOT55PBT45 copolymer films as measured by captive bubble and sessile drop measurements. After thorough washing with ethanol, both solution cast and compression molded PEOT/PBT copolymer films of the same composition show the same surface composition as measured by XPS. Based on these findings one could expect comparable surface contact angles, for both solution cast and compression molded films. If one compares the contact angles (sessile drop and captive bubble) of these copolymer films, however, large differences are observed, as shown in Table 4.2. In this table also data on PDLLA and PCL are included, which show the same effects.

In principle sessile drop and captive bubble techniques should give comparable values, since both measure an air/water interface. One should keep in mind, however, that the captive bubble measurements are performed in an aqueous environment allowing the polymers to

absorb water (the wet surfaces in captive bubble measurements can therefore not be directly compared to the dry surfaces in the sessile drop measurements).

But even within the same method large differences are observed between solution cast and compression molded films, both for the PEOT/PBT and PDLA copolymers as for the homopolymer PCL. Different surface morphologies are likely to play a role here.<sup>[30]</sup>

Table 4.2 - Contact angles determined by sessile drop and captive bubble measurement on solution cast and compression molded polymer films.

Material	Water uptake*	Compression molded		Solution cast	
		Captive bubble	Sessile drop	Captive bubble	Sessile drop
1000PEOT70 PBT30	74 %	$32.7 \pm 1.0^0$	$74.6 \pm 4.6^0$	$41 \pm 1^0$	$37 \pm 2^0$
300PEOT 55PBT45	5 %	$39.8 \pm 1.7^0$	$65.9 \pm 0.9^0$	$47 \pm 1^0$	$56 \pm 1^0$
PCL	0.8 %	$49.8 \pm 3.2^0$	$75.3 \pm 3.4^0$	$62 \pm 2^0$	$80 \pm 1^0$
PDLA	0.6 %	$55.3 \pm 1.4^0$	$67.5 \pm 3.0^0$	n.d.	$73^0$

\*: Equilibrium water uptake, measured at room temperature

n.d.: not determined

### *Composites with hydroxyapatite*

To improve cell attachment to the hydrophilic 1000PEOT70PBT30 copolymer system, we investigated the incorporation of non-water soluble materials in the form of hydroxyapatite (HA). HA is used as a scaffolding material for the implantation of BMSCs.<sup>[3,4,20]</sup> It is therefore expected that incorporation of this material can have a positive effect on the BMSC attachment to PEOT/PBT copolymer systems. As shown in Figure 4.1, a stereomicroscopy picture of solution cast 1000PEOT70PBT30 copolymer film, where HA powder was deposited on the surface of the drying film, this is indeed the case.

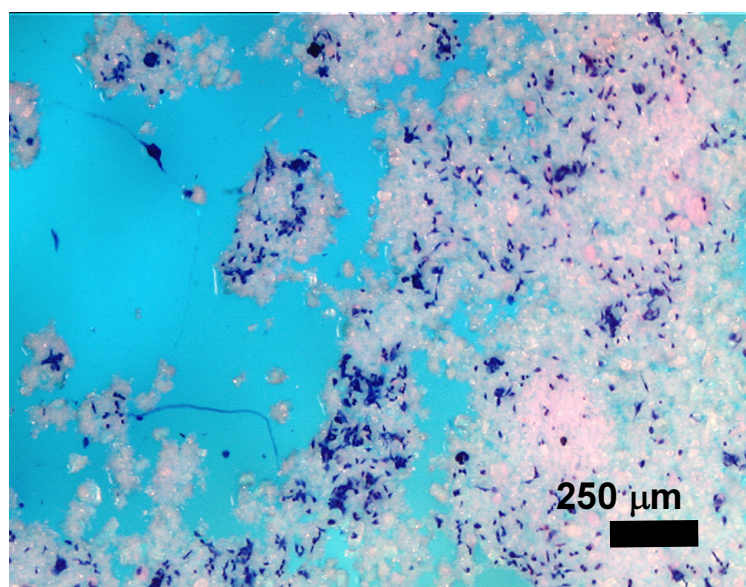


Figure 4.1 - Stereomicroscopic image of a 1000PEOT70PBT30 copolymer film of which the surface is partially covered with hydroxyapatite after 3 d of goat BMSC culturing. The methylene blue stained (dark blue) cells are only present on the white hydroxyapatite. [Color figure on p. 169]

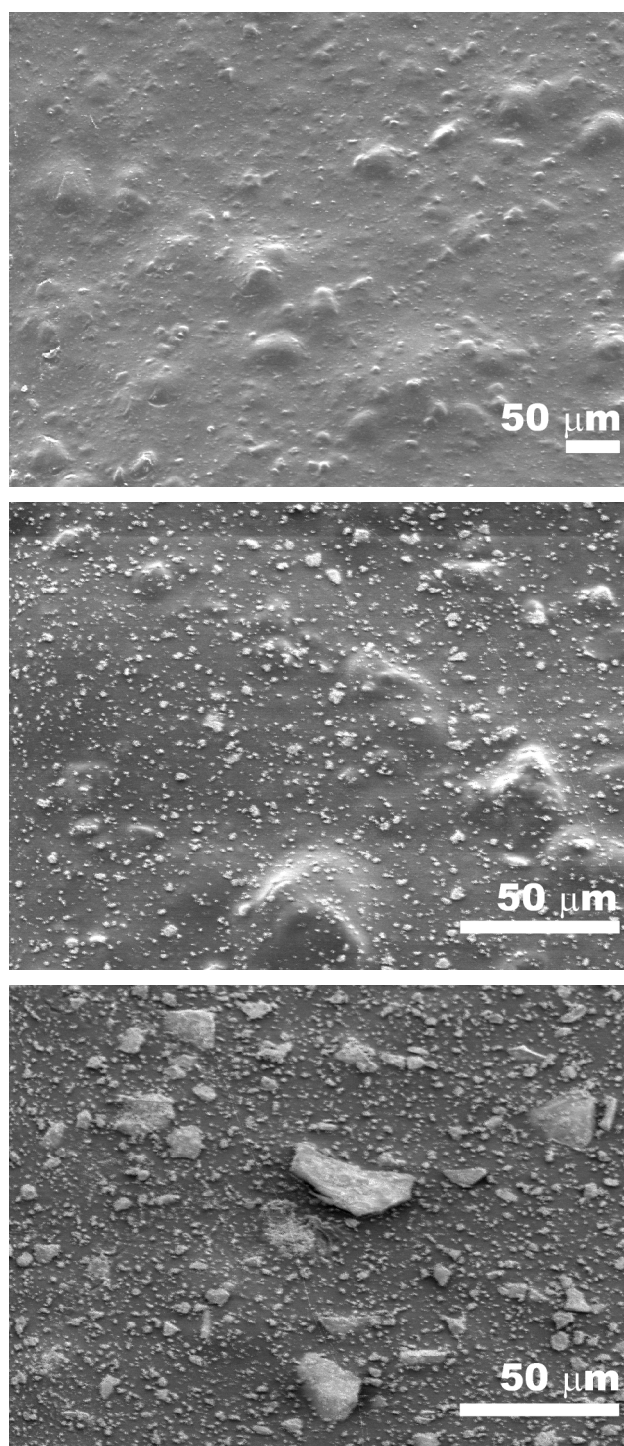


Figure 4.2 - SEM pictures of 1000PEOT70PBT30 composite films with 10 vol % HA. Top: non gas plasma treated, middle: 15 min CO<sub>2</sub> plasma treatment, bottom: 30 min CO<sub>2</sub> gas plasma treatment.

Goat BMSCs are able to attach to the added HA, but not to the copolymer. By blending 1000PEOT70PBT30 chloroform solutions with sintered HA particles (size 38-53  $\mu\text{m}$ ) composites with 5, 10, 25 vol % of HA were prepared. These solution cast composite films, however, hardly showed any cell attachment of goat BMSCs. The reason for this observation becomes clear from SEM. As shown in Figure 4.2 (top picture) for a composite film with 10 vol % HA, almost all HA particles are covered with a layer of copolymer.

To remove this copolymer layer, the composite films were etched using a CO<sub>2</sub> gas plasma treatment for 5, 15 or 30 minutes respectively. As shown in Figure 4.2 (middle and bottom) the covering copolymer layer is etched away. After 30 minutes of treatment, most HA particles are exposed to the surface.

After 3 and 7 d of cell culture, a screening experiment with goat BMSCs showed that on all composite surfaces even after only 5 min of CO<sub>2</sub> gas plasma treatment cells attached and proliferated. Interestingly enough, not only the composite films, but also the 1000PEOT70PBT30 copolymer without added HA, used as control, showed a tremendous improvement in the amount of goat BMSCs after 5, 15 and 30 min of CO<sub>2</sub> gas plasma treatment.

Clearly, not only the exposed HA leads to an improvement in stromal cell attachment and growth, also CO<sub>2</sub> gas plasma treatment of the 1000PEOT70PBT30 copolymer itself has a positive effect on stromal cell attachment and growth.

#### *CO<sub>2</sub> gas plasma treatment*

Based on the good results obtained from the etching experiments the effect of gas plasma treatments on the cell attachment to PEOT/PBT copolymers was investigated. A qualitative assessment of goat BMSC growth on gas plasma treated PEOT/PBT copolymers showed that both CO<sub>2</sub> and Ar plasmas have a positive effect on the cell attachment to solution cast films of different composition.<sup>[11]</sup>

Here, compression molded PEOT/PBT films (CO<sub>2</sub> gas plasma treated and untreated) were compared with PDLLA and PCL with respect to the attachment and growth of BMSCs. In view of future in vivo experiments rat BMSCs were cultured on 300PEOT55PBT45, 1000PEOT70PBT30 and 1000PEOT70PBT30, treated for 30 min with a CO<sub>2</sub> gas plasma, as well as PCL and PDLLA for up to 7 d. The amount of DNA present on the films was determined by means of a fluorescent dye (CyQuant®) at day 1,3 and 7. Results are depicted in Figure 4.3.

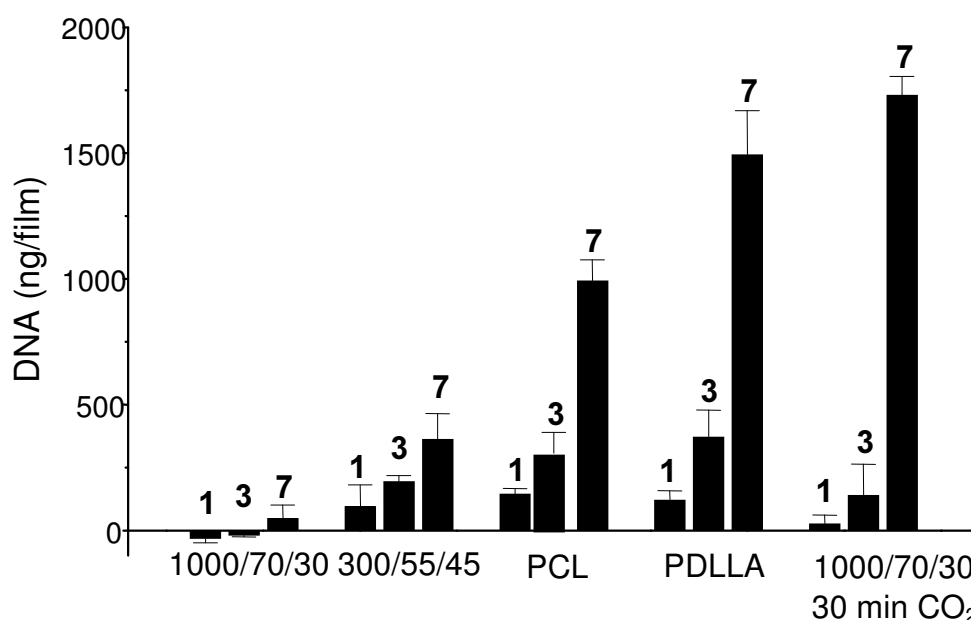


Figure 4.3 - Amount of DNA present after 1,3 and 7 d on 15 mm diameter polymer films of untreated 1000PEOT70PBT30, untreated 300PEOT55PBT45, PCL, PDLLA and 30 min CO<sub>2</sub> plasma treated 1000PEOT70PBT30.

Compared to the untreated copolymer a large increase in the amount of DNA present on the CO<sub>2</sub> gas plasma treated 1000PEOT70PBT30 was observed after 7 d of cell culturing. The amount of DNA present on gas plasma treated 1000PEOT70PBT30 after 7 d was comparable to the value found for PDLLA, but significantly higher than for PCL, 300PEOT55PBT45 and untreated 1000PEOT70PBT30. These results confirm the qualitative results obtained with goat BMSCs previously reported for solution cast and plasma treated PEOT/PBT films.<sup>[11]</sup>

After plasma treatment, a large amount of rat BMSCs attach to the surface of these PEOT/PBT films. After 3 d of cell culture many well spread stromal cells are present on the gas plasma treated 1000PEOT70PBT30 surface, forming extracellular matrix as observed by SEM (Figure 4.4). CO<sub>2</sub> gas plasma treatments result in 1000PEOT70PBT30 copolymer surfaces that attach as many BMSCs as PDLLA.

As shown in Table 4.2, CO<sub>2</sub> gas plasma treatment leads to a significant increase in the O/C ratio (from 0.44 to 0.50) as observed by XPS, showing the introduction of oxygen containing functional groups to the 1000PEOT70PBT30 copolymer surface. The improvement of BMSC attachment to gas plasma treated 1000PEOT70PBT30 and other PEOT/PBT copolymers is possibly related to differences in protein adsorption from the medium used during cell culture to these oxygen containing functional groups on the surfaces.

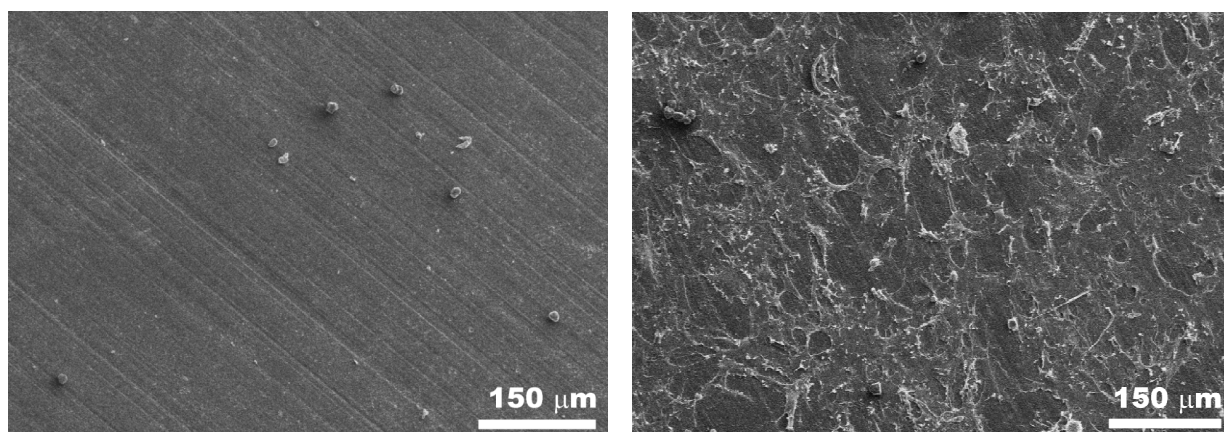


Figure 4.4 - SEM pictures of PEOT/PBT surfaces after 3 d of rat BMSC culturing. Left: untreated 1000PEOT70PBT30, no cells. Right: 1000PEOT70PBT30 after 30 min CO<sub>2</sub> plasma treatment, many cells and extracellular matrix.

Further research in this direction is currently ongoing. Recent data<sup>[24]</sup> have also shown that these kinds of gas plasma treatments are also suitable for the surface modification of porous PEOT/PBT structures.

## Conclusions

Incorporation of HA leads to an increase of BMSCs present on the surface after removal of the copolymer film covering the HA particles. The etching procedure used here (30 min CO<sub>2</sub> gas plasma treatment), however, also improved stromal cell attachment to 1000PEOT70PBT30 copolymer films without HA. XPS data showed the introduction of oxygen containing groups at the material surface.

As determined by means of a DNA-assay, CO<sub>2</sub> gas plasma treatment yielded a surface to which rat BMSCs attached in comparable amounts as to PDLLA. Significantly more cells were observed on CO<sub>2</sub> plasma treated 1000PEOT70PBT30 as compared to PCL. The presented data support previously reported qualitative data on the improvement of goat BMSC attachment to gas plasma treated, solution cast PEOT/PBT films. Gas plasma treatments are



therefore a preferred method of surface modification, resulting in an improvement in cell attachment on both solution cast and thermally processed PEOT/PBT copolymers. The fact that after gas plasma treatment BMSCs attach well to 1000PEOT70PBT30, enables in vitro BMSC culturing as needed for tissue engineering of bone.

## Acknowledgements

We thank Y.J.T. van der Zijpp for the gas plasma treatments, M.A. Smithers for the scanning electron microscopy (University of Twente). Professor F.J. Monteiro (Instituto de Engenharia Biomédica (INEB), Porto, Portugal) for the sintered hydroxyapatite. P.J. Engelberts for the help with the DNA-assay and W. J. Sleijster for the help with the cell culture (IsoTis OrthoBiologics). This study was financially supported by the European Community (Brite-Euram project BE97-4612).

## References

1. J.J. Marler, J. Upton, R. Langer, J.P. Vacanti *Transplantation of cells in matrices for tissue regeneration* Adv. Drug Deliv. Rev. **1998**, 33, 165-182.
2. J.H. Brekke, J.M. Toth *Principles of tissue engineering applied to programmable osteogenesis* J. Biomed. Mater. Res. (Appl. Biomater.) **1998**, 43, 380-398.
3. K.J.L. Burg, S. Porter, J.F. Kellam *Biomaterial developments for bone tissue engineering* Biomaterials **2000**, 21, 2347-2359.
4. S.P. Bruder, B.S. Fox *Tissue engineering of bone - Cell based strategies* Clin. Orthop. Rel. Res. **1999**, S68-S83.
5. A.A. Deschamps, D.W. Grijpma, J. Feijen *Poly(ethylene oxide)/poly(butylene terephthalate) segmented block copolymers: the effect of copolymer composition on physical properties and degradation* Polymer **2001**, 42, 9335-9345.
6. C.A. van Blitterswijk, J. van der Brink, H. Leenders, D. Bakker *The effect of PEO ratio on degradation, calcification and bone bonding of PEO/PBT copolymer (Polyactive)* Cells and Materials **1993**, 3, 23-36.
7. A.M. Radder, H. Leenders, C.A. van Blitterswijk *Bone-bonding behavior of poly(ethylene oxide)-polybutylene terephthalate copolymer coatings and bulk implants - a comparative-study* Biomaterials **1995**, 16, 507-513.
8. A.M. Radder, H. Leenders, C.A. van Blitterswijk *Application of porous PEO/PBT copolymers for bone replacement* J. Biomed. Mater. Res. **1996**, 30, 341-351.
9. M. Papadaki, T. Mahmood, P. Gupta, M.B. Claase, D.W. Grijpma, J. Riesle, C.A. Van Blitterswijk, R. Langer *The different behaviors of skeletal muscle cells and chondrocytes on PEGT/PBT block copolymers are related to the surface properties of the substrate* J. Biomed. Mater. Res. **2001**, 54, 47-58.
10. G.J. Beumer, C.A. van Blitterswijk, D. Bakker, M. Poncet *Cell-seeding and in-vitro biocompatibility evaluation of polymeric matrices of PEO/PBT copolymers and PLLA* Biomaterials **1993**, 14, 598-604.
11. M.B. Olde Riekerink, M.B. Claase, G.H.M. Engbers, D.W. Grijpma, J. Feijen *Gas plasma etching of PEO/PBT segmented block copolymer films* J. Biomed. Mater. Res. **2003**, 65A, 417-428.
12. A.A. Deschamps, M.B. Claase, W.J. Sleijster, J.D. de Bruijn, D.W. Grijpma, J. Feijen *Design of segmented poly(ether ester) materials and structures for the tissue engineering of bone* J. Control. Release **2002**, 78, 175-186.
13. C. Maniopoulos, J. Sodek, A.H. Melcher *Bone-formation in vitro by stromal cells obtained from bone marrow of young-adult rats* Cell Tissue Res. **1988**, 254, 317-330.
14. K. Anselme *Osteoblast adhesion on biomaterials* Biomaterials **2000**, 21, 667-681.
15. W.S. Ramsey, W. Hertl, E.D. Nowlan, N.J. Binkowski *Surface treatments and cell attachment* In vitro **1984**, 20, 802-808.
16. J.M. Gao, L. Niklason, R. Langer *Surface hydrolysis of poly(glycolic acid) meshes increases the seeding density of vascular smooth muscle cells* J. Biomed. Mater. Res. **1998**, 42, 417-424.
17. X. Yang, K. Zhao, G.-Q. Chen *Effect of surface treatment on the biocompatibility of microbial polyhydroxyalkanoates* Biomaterials **2001**, 23, 1391-1397.
18. L. Calandrelli, B. Immirzi, M. Malinconico, M.G. Volpe, A. Oliva, F. Della Ragione *Preparation and characterisation of composites based on biodegradable polymers for "in vivo" application* Polymer **2000**, 41, 8027-8033.

19. S.C. Rizzi, D.T. Heath, A.G.A. Coombes, N. Bock, M. Textor, S. Downes *Biodegradable polymer/hydroxyapatite composites: Surface analysis and initial attachment of human osteoblasts* J. Biomed. Mater. Res. **2001**, 55, 475-486.
20. E. Kon, A. Muraglia, A. Corsi, P. Bianco, M. Marcacci, I. Martin, A. Boyde, I. Ruspantini, P. Chistolini, M. Rocca, R. Giardino, R. Cancedda, R. Quarto *Autologous bone marrow stromal cells loaded onto porous hydroxyapatite ceramic accelerate bone repair in critical-size defects of sheep long bones* J. Biomed. Mater. Res. **2000**, 49, 328-337.
21. Q.P. Hou, D.W. Grijpma, J. Feijen *Porous polymeric structures for tissue engineering prepared by a coagulation, compression moulding and salt leaching technique* Biomaterials **2003**, 24, 1937-1947.
22. M.B. Olde Riekerink *Structural and Chemical Modification of Polymer Surfaces by Gas Plasma Etching*, Thesis, University of Twente, Enschede, The Netherlands, **2001**.
23. A.G. Mikos, Y. Bao, L.G. Cima, D.E. Ingber, J.P. Vacanti, R. Langer *Preparation of poly(glycolic acid) bonded fiber structures for cell attachment and transplantation* J. Biomed. Mater. Res. **1993**, 27, 183-189.
24. M.B. Claase, D.W. Grijpma, S.C. Mendes, J.D. de Bruijn, J. Feijen *Porous PEOT/PBT scaffolds for bone tissue engineering: preparation, characterization and in vitro bone marrow cell culturing* J. Biomed. Mater. Res **2003**, 64A, 291-300.
25. J. Leidner, E.W.C. Wong, D.C. MacGregor, G.J. Wilson *A novel process for the manufacturing of porous grafts: Process description and product evaluation* J. Biomed. Mater. Res. **1983**, 17, 229-247.
26. M.S. Widmer, P.K. Gupta, L. Lu, R.K. Meszlenyi, G.R.D. Evans, K. Brandt, T. Savel, A. Gurlek, C.W. Patrick Jr, A.G. Mikos *Manufacture of porous biodegradable polymer conduits by an extrusion process for guided tissue regeneration* Biomaterials **1998**, 19, 1945-1955.
27. A.G. Mikos, A.J. Thorsen, L.A. Czerwonka, Y. Bao, R. Langer, D.N. Winslow, J.P. Vacanti *Preparation and characterization of poly(L-lactid acid) foams* Polymer **1994**, 35, 1068-1077.
28. C. Schugens, V. Maquet, C. Grandfils, R. Jerome, P. Teyssie *Biodegradable and macroporous polylactide implants for cell transplantation: 1. Preparation of macroporous polylactide supports by solid-liquid phase separation* Polymer **1996**, 37, 1027-1038.
29. P.X. Ma, R.Y. Zhang, G.Z. Xiao, R. Franceschi *Engineering new bone tissue in vitro on highly porous poly(alpha-hydroxyl acids)/hydroxyapatite composite scaffolds* J. Biomed. Mater. Res. **2001**, 54, 284-293.
30. R.D. Hazlett *On surface roughness effects in wetting phenomena in "Contact Angle, Wettability and Adhesion"*; K.L. Mittal, Ed.; VSP: Utrecht, The Netherlands, **1993**; pp 173-181.

# Chapter 5

## Porous PEOT/PBT scaffolds for bone tissue engineering: preparation, characterization and in vitro bone marrow stromal cell culturing\*

*The thirty spokes unite in the one center; but it is on the empty space for the axle that the use of the wheel depends.*

*Clay is fashioned into vessels; but it is on their empty hollowness that their use depends. The door and windows are cut out from the walls to form an apartment; but it is on the empty space that its use depends.*

*Therefore, whatever has being is profitable, but what does not have being can be put to use.*

Lao Tzu (604 –531 BC)

### Abstract

The preparation, characterization and in vitro bone marrow stromal cell (BMSC) culturing on porous PEOT/PBT copolymer scaffolds are described. These scaffolds are meant for use in bone tissue engineering. Previous research showed that PEOT/PBT copolymers showed in vivo degradation, calcification and bone bonding. In spite of this, several of these copolymers do not support BMSC growth in vitro. Surface modification, such as gas plasma treatment, is needed to improve the in vitro cell attachment. Porous structures were prepared using a freeze-drying and a salt-leaching technique, the latter one resulting in highly porous interconnected structures of large pore size. Gas plasma treatment with CO<sub>2</sub> generated an appropriate surface throughout the entire structure, enabling BMSCs to attach. The amount of DNA was determined as a measure for the amount of cells present on the scaffolds. No significant effect of pore size on the amount of DNA present, was seen for scaffolds with pore sizes between 250-1000 µm. Light microscopy data showed cells in the center of the scaffolds, more cells

---

\* Menno B. Claase<sup>1</sup>, Dirk W. Grijpma<sup>1</sup>, Sandra C. Mendes<sup>2</sup>, Joost D. de Bruijn<sup>2</sup>, Jan Feijen<sup>1</sup>

Published in J. Biomed. Mater. Res. **2003**, 64A, 291-300.

1) Institute for Biomedical Technology (BMTI) and Department of Polymer Chemistry and Biomaterials, Faculty of Science and Technology, University of Twente, P.O. Box 217, 7500 AE Enschede, The Netherlands

2) IsoTis OrthoBiologics, P.O. Box 98, 3720 AB Bilthoven, The Netherlands

were observed in the scaffolds of 425-500  $\mu\text{m}$  and 500-710  $\mu\text{m}$  pore size compared to the ones with 250-425  $\mu\text{m}$  and 710-1000  $\mu\text{m}$  pores.

## Introduction

In the restoration of bone defects, the tissue engineering approach<sup>[1]</sup> mimics the natural process of bone repair. The system can be activated or assisted by 1) the delivery of cells capable of differentiating into osteoblasts, 2) inductive growth and differentiation factors or 3) bioresorbable scaffolds which enable cell attachment, migration and proliferation. In many approaches two, sometimes even three of these elements are combined.<sup>[2]</sup>

In the case of non load-bearing bone tissue, a promising scaffold material for this purpose seems to be PEOT/PBT block copolymers also known as Polyactive<sup>®</sup>. The composition of these copolymers is indicated as  $a\text{PEOT}b\text{PBT}c$ , with  $a$  the molecular weight of the poly (ethylene glycol) starting compound,  $b$  the weight percentage of the PEOT soft segments and  $c$  the weight percentage of the PBT hard segments. Mechanical and physical properties of these materials can be tuned by varying the PBT (hard segment) content and PEO (soft segment) molecular weight of these copolymers.<sup>[3,4]</sup> Due to differences in hydrophilicity, water uptake and degradability, the composition of these copolymers is also expected to be of influence on the in vitro cell culturing of bone marrow stromal cells (BMSC) on these materials.

Several subcutaneous and intra-bone (tibia) implantations of dense and porous blocks and porous films in rats showed bone bonding, calcification and degradation for PEOT/PBT copolymers with high PEO content (60 and 70 weight percent PEO containing soft segment).<sup>[5-8]</sup> However, these effects were not seen after implantation of porous blocks into critical size defects in goat<sup>[9]</sup> and human<sup>[10]</sup> ilea. We intend to prepare porous PEOT/PBT scaffolds on which to culture patient-own human BMSCs. These polymer/cell constructs will then be implanted at the site of the defect after a period of in vitro cell culture. For use in bone tissue engineering, the structures need to be highly porous with interconnected pores and a sufficiently large pore size to ensure tissue ingrowth and bone formation.<sup>[11]</sup>

Several ways are known to prepare porous structures, each with their own level of control over pore size, porosity and interconnectivity. Depending on the polymer system each technique has its own advantages and disadvantages.<sup>[12]</sup> A widely applied technique is particulate leaching. Leachable particles, for instance sucrose, sodium chloride or other salts, are mixed with a polymer solution. After solvent evaporation and leaching, porous membranes are obtained.<sup>[13]</sup> These polymer/salt composites can also be molded or extruded into various complex shapes.<sup>[14,15]</sup>

Another versatile technique is liquid-solid phase separation as described by Aubert et al.<sup>[16]</sup> in the preparation of microcellular polystyrene foams. By using solvents that can be freeze-dried, e.g. cyclohexane, naphthalene or 1,4-dioxane, and by use of different freezing temperatures and conditions various pore sizes and pore structures can be obtained.<sup>[17-21]</sup>

We are developing those techniques that give us large flexibility in the preparation of our tissue engineering scaffolds, in terms of pore size and porosity, since the optimal conditions and processing technique for a scaffold vary per material and tissue. Here we describe the preparation and characterization of porous PEOT/PBT structures prepared by liquid-solid phase separation, followed by freeze-drying and by compression molding of polymer and salt particle mixtures, followed by salt leaching. These scaffolds were gas plasma treated using a  $\text{CO}_2$  gas plasma to enable BMSC attachment to these structures.<sup>[22,23]</sup> Scaffolds of varying pore size are evaluated to study the effect of pore size on the gas plasma treatments and on the in vitro rat BMSC culture.

## Materials and methods

All solvents used were analytical grade and all chemicals were at least 99 % pure, unless otherwise mentioned. All were used as received.

### Polymer scaffold preparation

*Synthesis.* PEOT/PBT multiblock copolymers were prepared by two-step polycondensation in the presence of titanium tetrabutoxide (Merck, Germany) as catalyst (0.1 wt %) as previously described<sup>[3]</sup>, with the exception that vitamin E (Sigma-Aldrich, Germany, approx. 95 % pure) was used as antioxidant. Compositions were varied by changing the poly (ethylene glycol) (Fluka, Switzerland) molecular weight and the dimethyl terephthalate (Merck, Germany)/1,4-butanediol (Acros, Belgium) to polyethylene glycol ratio.

Unless otherwise mentioned, the resulting polymers were dissolved in chloroform (Biosolve Ltd., The Netherlands) or chloroform/1,1,1,3,3,3-hexafluoro-2-propanol (Acros, Belgium) mixtures (approximately a 10 % (w/v) solution) and precipitated in a tenfold excess of technical grade ethanol. The copolymer composition was determined by <sup>1</sup>H-NMR (Varian Inova 300 MHz). All copolymers had compositions close to the intended ones. The composition is indicated as *a*PEOT*b*PBT*c*, where *a* is the starting poly (ethylene glycol) molecular weight, *b* the weight percentage of PEOT soft segments and *c*, the weight percentage of PBT hard segments. It has to be noted that terephthalic ester units are present in both the soft and the hard segments.<sup>[3]</sup>

*Film preparation.* Films (75-100 µm thick) were prepared by casting of 20 % (w/v) polymer solutions in chloroform or chloroform/1,1,1,3,3,3-hexafluoro-2-propanol mixtures on a glass plate using a casting knife. All films were placed in ethanol (overnight) to remove any residual 1,1,1,3,3,3-hexafluoro-2-propanol and/or chloroform. Films were dried in a vacuum oven under a small N<sub>2</sub>-current for 5 d.

*Porous structures prepared by freeze-drying.* Typically, 5-20 % (w/v) copolymer solutions were prepared in 1,4-dioxane (Merck, Germany), solutions were heated until a clear solution was obtained (usually between 80 and 110 °C). Solutions were poured into polyethylene vials and frozen at different temperatures: -196 °C (liquid nitrogen), -78 °C (acetone/CO<sub>2</sub>), -28 °C (freezer) and +7 or +10 °C (refrigerator). Subsequent freeze-drying (5 d, 20 mbar) yielded white foams.

*Porous structures prepared by compression molding of polymer/salt mixtures followed by salt leaching.* Copolymer granulate was cryogenically ground using an IKA Labortechnik (Germany) A10 grinder. Polymer powder and sodium chloride (Merck, Germany) was sieved using Endecotts (England) test sieves of 250, 425, 500, 710, 1000 and 1180 µm mesh size. The desired salt volume fractions were calculated using a salt density of 2.165 g/cm<sup>3</sup>. The powders were mixed and subsequently compression molded in a laboratory hot press (THB 008, Fontijne Holland BV, The Netherlands) into the desired shapes. Powders were heated at 180 °C for 3 min and subsequently pressed for 1 min at 2.9 MPa. Samples were leached with milliQ water for 48 h and dried under reduced pressure in a vacuum oven.

*Characterization of porous structures.* Porosity was determined by measurement of scaffold mass and dimensions (volume) in the dry state. The porosity was calculated from the densities of the solid materials, 1000PEOT70PBT30:  $\rho = 1.188 \pm 0.011 \text{ g/cm}^3$ , 300PEOT55PBT30:  $\rho = 1.2437 \pm 0.0029 \text{ g/cm}^3$ . Pore sizes were measured from scanning electron micrographs at a magnification of 100 times. The average diameter of at least 20 pores ( $\pm$  s.d.) was determined. For salt leached samples the pore sizes were found to be in accordance with the sizes of the salt crystals used. Compression moduli were determined at room temperature using a Zwick Z020 tensile tester. Moduli were measured at 10 % strain at a strain rate of 2 mm/min with a

0.1 N preload. The scaffolds had a diameter of 17 mm and a height of 8 mm. Results are averages of at least three measurements ( $\pm$  s.d.).

*Water uptake.* Polymer films were weighed at regular intervals. For every polymer three samples were swollen in milliQ water (shaking bath, 37 °C). All results are averages of triplicate measurements ( $\pm$  s.d.).

*CO<sub>2</sub> gas plasma treatment.* Both solution cast films (treated on both sides) and porous structures were treated for 30 min. Discharge power was 49 W. CO<sub>2</sub> gas plasma pressure: 0.06-0.07 mbar. A gas flow of 10 cm<sup>3</sup>/min was used. Samples were treated with a pre-delay of 2 min and a post-delay of 2 min.<sup>[22]</sup> After treatment samples were rinsed using demineralized water, followed by ethanol (p.a.). Samples were dried in a vacuum oven overnight at room temperature.

### Bone marrow stromal cell culturing

*Goat bone marrow stromal cell culturing on copolymer films.* Samples with a diameter of 10 mm were cut from the copolymer films. For preliminary screening experiments goat BMSCs, passage 3 were used. The cells were seeded with a density of 10,000 cells/cm<sup>2</sup>, on discs in the presence of 3 mL minimal essential medium ( $\alpha$ -MEM, Life Technologies, The Netherlands) containing<sup>[24]</sup>: 15 % fetal bovine serum (Life Technologies, The Netherlands), 100 units/mL penicillin, 100  $\mu$ g/mL streptomycin (Life Technologies, The Netherlands), 2mM L-glutamine (Life Technologies, The Netherlands), 0.2 mM ascorbic acid 2-phosphate (Life Technologies, The Netherlands), 10 mM  $\beta$ -glycerophosphate (Sigma, The Netherlands), 10<sup>-8</sup> M dexamethasone (Sigma, The Netherlands).

*Rat bone marrow stromal cell culturing.* BMSC cells were isolated from 7 femora from 4 male Wistar-rats. The femora were cut on both sides and the marrow was flushed out using 5 mL of medium per femur. The collected cells were re-suspended with a 21G needle and cultured at 37 °C, 5 % CO<sub>2</sub> for 7 d, with periodic medium changes every other day. After 7 d, cells were confluent and were washed with PBS (Life Technologies, The Netherlands) and treated with trypsin/EDTA (Sigma, The Netherlands). The collected cell suspension was cultured for another week, yielding 69 $\times$ 10<sup>6</sup> rat BMSCs.

*Cell seeding and growth on porous scaffolds.* Scaffolds were washed with: distilled water, 100 % ethanol, distilled water, 70 % ethanol/water, 3x sterile PBS containing 100 units/mL penicillin and 100  $\mu$ g/mL streptomycin. The scaffolds were stored in PBS containing 100 units/mL penicillin and 100  $\mu$ g/mL streptomycin until cell culturing (1 1/2 d) and seeded with 2x 150  $\mu$ L of cell suspension ( $\sim$  2 $\times$ 10<sup>5</sup> cells per scaffold). Cell suspensions were ‘injected’ into the scaffolds. Scaffolds were incubated at 37 °C for 3 h, after which 2 mL of cell culture medium was added. Cells were cultured at 37 °C, 5 % CO<sub>2</sub> for 10 d, with periodic medium changes every other day. Samples were analyzed at day 1, 3, 7 (methylene blue staining) and day 10 (alkaline phosphatase staining). The amount of cells seeded was kept constant at approximately 2 $\times$ 10<sup>5</sup> cells per scaffold since the estimated internal surface area was in the same order of magnitude for all the scaffolds: between 13.0 cm<sup>2</sup> (250  $\mu$ m pores) and 3.3 cm<sup>2</sup> (1000  $\mu$ m pores), resulting in a seeding density in the range of 1.5 $\times$ 10<sup>4</sup> - 6 $\times$ 10<sup>4</sup> cells/cm<sup>2</sup>.

### Analysis

*Methylene blue staining.* Samples were analyzed at day 1, 3 and 7. Scaffolds were washed with warm PBS containing 100 units/mL penicillin and 100  $\mu$ g/mL streptomycin and subsequently fixed with glutaraldehyde (Merck, Germany, 1.5 % solution in 0.14 M cacodylic acid buffer, pH = 7.35). Then the samples were washed with water and stained for 30 s using a 1 % methylene blue solution in 0.1 M borax buffer (pH = 8.5). Scaffolds were subsequently

washed with demineralized water, until the water was clear. Samples were stored in a refrigerator until further analysis. Samples were evaluated using a Nikon SM2-10A stereomicroscope (1x objective). Digital photographs were taken using a Sony progressive 3 CCD camera. To obtain a qualitative comparison between the different polymers (concerning the amount of cells present on the film surfaces), the intensity of blue staining of cells on the film surfaces was evaluated. Higher magnifications showed blue staining of the cells. The samples were divided in 4 categories: 1) no cells (-), 2) few cells ( $\pm$ ), 3) cells (+) and 4) many cells at the surface (++/+++). The distribution of cells within the scaffolds was examined using diagonally cut cross-sections of the scaffolds.

*DNA-assay.* Scaffolds were washed with PBS containing 100 units/mL penicillin and 100  $\mu\text{g/mL}$  streptomycin at 37  $^{\circ}\text{C}$  and stored in a freezer (-80  $^{\circ}\text{C}$ ) until further analysis. Scaffolds were cut in at least 4 pieces and incubated at 56  $^{\circ}\text{C}$  overnight in 0.5 mL of lysis-medium to lyse all cells.

The lysis-medium consisted of 26.47 mg iodoacetamide (Sigma, The Netherlands), 1.60 mg pepstatin A (Sigma, The Netherlands) and 150.0 mg proteinase K (Sigma, The Netherlands) in 150 mL Tris/EDTA buffer.

The next day 250  $\mu\text{L}$  of these suspensions were mixed with 250  $\mu\text{L}$  RNase-solution. The RNase solution was prepared from 60  $\mu\text{L}$  RNase (Sigma, The Netherlands, 86 Kunitz units/mg) and 100  $\mu\text{L}$  heparin (Leopharma, The Netherlands, 5.000 IE/mL) in 25 mL PBS, and incubated at 37  $^{\circ}\text{C}$  for 45 min to remove the single stranded RNA and DNA. Various dilutions were prepared with PBS. Dilutions were mixed with CyQUANT<sup>®</sup> dye. After 15 min fluorescence was measured in 96 well plates using a Perkin Elmer Luminescence Spectrometer LS 50 B (excitation at 480 nm, slit width 2.5 nm, emission at 520 nm, slit width 7.5 nm). The measured fluorescence intensities were correlated to the amount of DNA using a calibration curve made by using DNA (Sigma) dilutions of known concentration.

Data shown are the result of triplicate measurements ( $\pm$  s.d.). 6 scaffolds without cells were used as blanks. Results were analyzed using one-way ANOVA, followed by a Tukey's Honestly Significant Difference Post Hoc Test. Differences were considered statistically different when  $p < 0.05$ . ANOVA calculations were performed using SPSS software for Windows (version 10.0, SPSS, USA).

*Alkaline phosphatase (ALP) staining.* Samples were analyzed at day 10. Scaffolds were washed with PBS containing 100 units/mL penicillin and 100  $\mu\text{g/mL}$  streptomycin of 37  $^{\circ}\text{C}$  and subsequently fixed with paraformaldehyde (4 % solution in Sørensen buffer (phosphate buffer)) for 3 1/2 h.

Samples were washed with water (3x) and stained for 35 min using a Fast Blue RR salt (4-benzoylamino-2,5-dimethoxybenzene-diazonium chloride hemi[zinc chloride], Sigma, The Netherlands) in naphthol As-B-1 stock solution (1 g/L). Besides the cultured scaffolds also three blank scaffolds were stained (pore size 500-710  $\mu\text{m}$ ).

Samples were investigated using a Nikon SM2-10A stereomicroscope (1x objective). Digital photographs were taken using a Sony progressive 3 CCD camera.

*Scanning Electron Microscopy (SEM).* Porous scaffolds and films containing BMSCs were fixed (as with methylene blue staining) and stored in 70 % ethanol. Samples were dehydrated using an ethanol/water gradient. Dehydrated samples were dried using a Balzers CPD 030 critical point dryer before coating. Samples were coated with Au/Pd in a Polaron E5600 sputter coater. Pictures were taken with a Hitachi FE-SEM S-800 (6.0 kV).

## Results and discussion

### *Improvement of cell attachment*

Based on literature, the PEOT/PBT multiblock copolymer with a 70 to 30 soft to hard segment ratio and a PEO molecular weight of 1000 (1000PEOT70PBT30) holds promise as a scaffold material for bone tissue engineering. Besides degradation, calcification and bone bonding<sup>[5]</sup>, in vivo studies on porous 1000PEOT70PBT30 also showed bone ingrowth.<sup>[8]</sup> In contrast to our expectation, screening experiments using goat BMSCs however did not show any cell attachment to this 1000PEOT70PBT30 in vitro.

As studies have shown, the hydrophilicity of polymers is an important factor in cell adhesion and growth.<sup>[25,26]</sup> We therefore varied the copolymer compositions to adjust the hydrophilicity. As indicated in Table 5.1 it is possible to vary the physical properties of the tissue engineering scaffolds within a wide range by adjusting the copolymer composition. The water uptake is very much dependent on the PEO molecular weight and the soft to hard segment ratio. To screen for the viability of these materials as scaffold materials for bone tissue engineering, previously frozen goat BMSCs were cultured on these materials. Goat BMSCs only attached to the relatively hydrophobic 300PEOT55PBT45 and somewhat to the 300PEOT70PBT30 but not to the 1000PEOT70PBT30. Interestingly enough, cells did also not attach to the other two copolymers with low PEO contents: 1000PEOT30PBT70 and 1000PEOT40PBT60. Despite their low PEO content these polymers have a considerable water uptake of 32 and 38 mass percent, respectively. This in comparison to the 300PEOT55PBT45 and the 300PEOT70PBT30 that have a much lower water uptake, even though they have a comparable PEO content. Phase separation is likely to play an important role here.<sup>[3]</sup>

Table 5.1 - PEOT/PBT block copolymer films: composition, water uptake and results of goat BMSC attachment experiments, -: no cell attachment, ±: some round, not well attached cells at the surface +: cell attachment, ++ and +++: surface covered with cells.

Copolymer	Soft to hard segment ratio <sup>§</sup>	PEO content (%) <sup>§</sup>	Water uptake (mass %)	BMSC attachment	
				Untreated	30 min. CO <sub>2</sub> plasma
4000PEOT70PBT30	80/20	77.5	212	-	+
1000PEOT30PBT70	30/70	27	32	-	+++
1000PEOT40PBT60	41/59	37	38	-	
1000PEOT55PBT45	55/45	49	46	-	
1000PEOT60PBT40	63/37	54	52	-	
1000PEOT70PBT30	77/23	65	74	-	+ / ++
300PEOT55PBT45	52/48	36	5	+	+ / ++
300PEOT70PBT30	67/33	44	6	±	+++

§: experimental from NMR

An effective way of making PEOT/PBT copolymers more suitable for BMSC attachment is by a 30 min gas plasma treatment with CO<sub>2</sub>.<sup>[22,23,27]</sup> From an assessment of goat BMSC attachment to PEOT/PBT films (cells were stained using methylene blue, data not shown) it could be seen that the amount of cells present on the copolymer surfaces increased



substantially after gas plasma treatment, as qualitatively indicated in Table 5.1. Details of these techniques, like changes in surface chemistry and morphology and other ways of improving cell attachment to these materials are discussed in a Chapter 4 and Appendix A.<sup>[23]</sup> All gas plasma modified PEOT/PBT copolymers tested showed an improvement in goat BMSC attachment, including the 1000PEOT70PBT30 copolymer.

#### *Preparation of porous structures*

An important step towards a tissue-engineered polymer/cell construct is the preparation of a suitable three-dimensional matrix for in vitro cell culturing. We are aiming for methods that enable us to prepare highly porous scaffolds with large pores and good mechanical properties from these hydrophilic copolymers.

A well-known method to prepare porous polymeric scaffolds is by liquid-solid phase separation of a solvent that can easily be removed, for instance by freeze-drying. The resulting porosity of the structures is governed by the polymer concentration of the solution. The obtained pore sizes are mostly governed by the temperature at which the polymer solution is frozen. In correspondence with literature smaller pores are obtained at lower freezing temperatures, due to the faster rate of nucleation of the solvent, leading to more and hence smaller crystals.<sup>[16,21,28]</sup> The effect of freezing temperature of a 1,4-dioxane solution on the pore size of 1000PEOT70PBT30 is shown in Figure 5.1. In this figure the pore size of the pores are shown, as they were observed in SEM pictures (Figure 5.2).

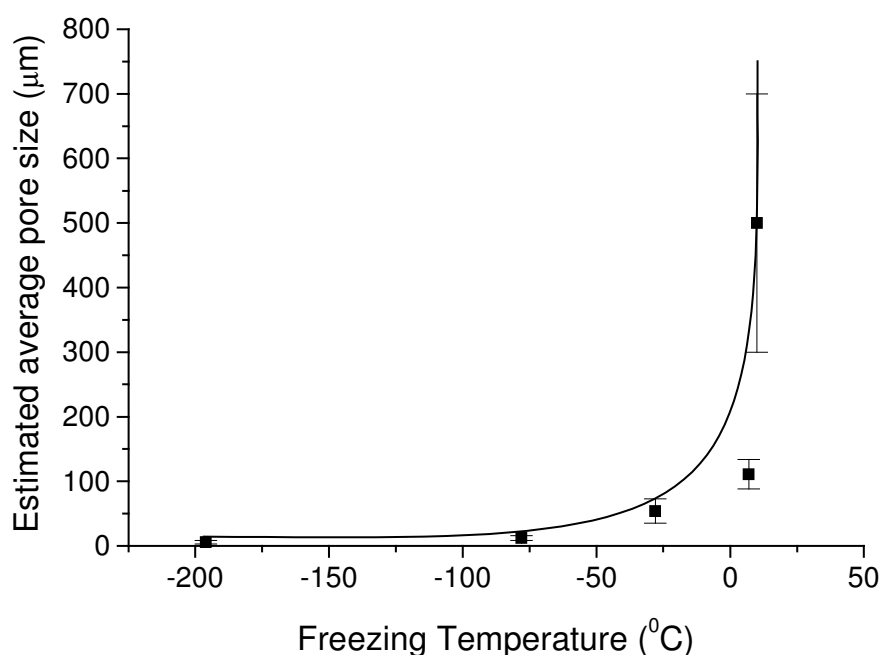


Figure 5.1 - Estimated average pore size ( $\pm$  s.d.) as obtained from SEM pictures of 1000PEOT70PBT30 of 91 % porosity.

Based on in vivo studies it was concluded by Radder et al.<sup>[8]</sup> that 300  $\mu$ m pores were suboptimal for bone ingrowth, probably due to the combination of press-fit implantation and extensive swelling in situ. In order to obtain pores larger than 300  $\mu$ m, we froze 1,4-dioxane solutions at 10 °C, a temperature close to the melting point of the solvent (11 °C). As indicated in Table 5.2 pores well over 300  $\mu$ m are obtained, even pores as large as 1.5 mm were observed.

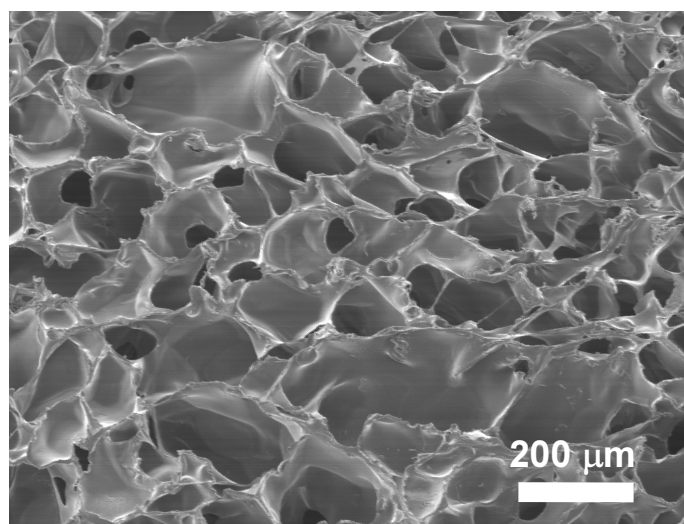


Figure 5.2 - SEM picture from a 92 % porous 1000PEOT70PBT30 scaffold prepared by freeze-drying (frozen at +7 °C, pore size:  $167 \pm 78 \mu\text{m}$ ).

Table 5.2 - Average pore sizes ( $\pm$  s.d.) for 1000PEOT70PBT30 in 1,4-dioxane, frozen at 10 °C, as estimated from SEM.

Volume % 1,4-dioxane	Average pore size (mm)
85	$0.6 \pm 0.3$
90	$0.5 \pm 0.2$
95	$0.6 \pm 0.3$

To our knowledge these are the largest pores reported for porous structures prepared by liquid-solid phase separation.<sup>[12]</sup> The polymer concentration did not seem to have an effect on the obtained pore size. Even though highly porous structures were obtained with porosities ranging from 85 to 95 % most of the pores have a closed pore structure (Figure 5.3), in accordance with previous observations.<sup>[21]</sup> Pore interconnectivity is one of the important parameters for tissue engineering, since it enables tissue ingrowth and vascularization, making the obtained structures not very suitable as tissue engineering scaffolds.

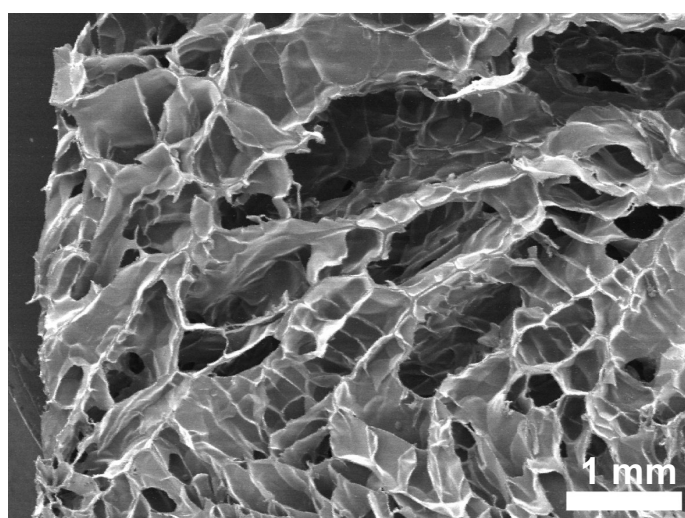


Figure 5.3 - 5 % solution of 1000PEOT70PBT30 frozen at +10 °C, most pores show a closed pore structure.

In order to obtain a well-interconnected structure with large pores a salt-leaching approach was followed. PEOT/PBT granules were cryogenically ground to a powder and subsequently sieved using standard test sieves to obtain powders of known particle size. As leachable porogen sodium chloride was selected which was also sieved to fractions of known sizes.

By compression molding, these polymer powder/salt mixtures can be processed into devices of different sizes and shapes. By varying the polymer powder to salt ratio and the salt size, it was possible to obtain porous structures with porosities ranging from 75 to 90 % and pore sizes of 250 to 1000  $\mu\text{m}$ . Not all polymer/salt mixtures, however, yield coherent structures that stay stable during salt leaching. In Table 5.3 the stability during leaching of 1000PEOT70PBT30 structures is indicated, defining the processing window of this technique.

Table 5.3 - Stability of scaffolds during the leaching process. Scaffolds were prepared by polymer powder mixing/salt leaching. ++ denotes no fragmentation, + single polymer fragment comes off,  $\pm$  several polymer fragments come off, - many polymer fragments come off, -- complete scaffold disintegration.

Intended Porosity	Actual porosity*	250-425 $\mu\text{m}$	425-500 $\mu\text{m}$	500-710 $\mu\text{m}$	710-1000 $\mu\text{m}$
60 %	$74.3 \pm 2.0$	n.p.	++	++	+
70 %	$79.1 \pm 1.3$	++	++	++	++
80 %	$84.8 \pm 2.2$	++	++	++	+
90 %	$91.6 \pm 1.1$	$\pm$	-	$\pm$	--

\* = average of all the scaffolds of all pore sizes, determined by means of density

n.p. = not prepared

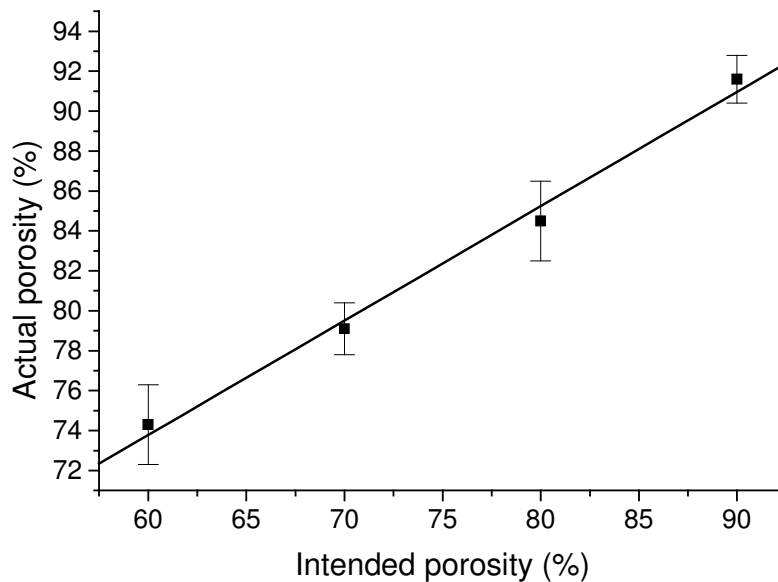


Figure 5.4 - Actual porosity as a function of the salt volume fraction. Values are an average of the porosities of at least 10 scaffolds of various pore size ( $\pm$  s.d.).

The actual porosity was determined by measuring the relative density compared to the density of solid compression molded 1000PEOT70PBT30 ( $\rho = 1.188 \text{ g/cm}^3$ ). The obtained porosity is in almost every case higher than that based on the calculated value. Remaining small air bubbles formed during compression molding within the polymer fraction might be an explanation for this. Nevertheless there is a clear linear relationship, as indicated in Figure 5.4,

giving good control over the porosity in a range of 75-90 %. Interconnectivity of the obtained structures is much better than was the case for the scaffolds prepared by liquid-solid phase separation, as shown in Figure 5.5. The obtained pores are cubic, formed after the shape of the salt crystals used.

Even though both preparation techniques give porous structures of high porosity (up to 90-95 %), the latter described technique of compression molding and leaching shows a better control over pore size and interconnected pores. Therefore, the scaffolds prepared by this technique were thoroughly characterized in terms of mechanical properties and were used in BMSC culturing experiments.

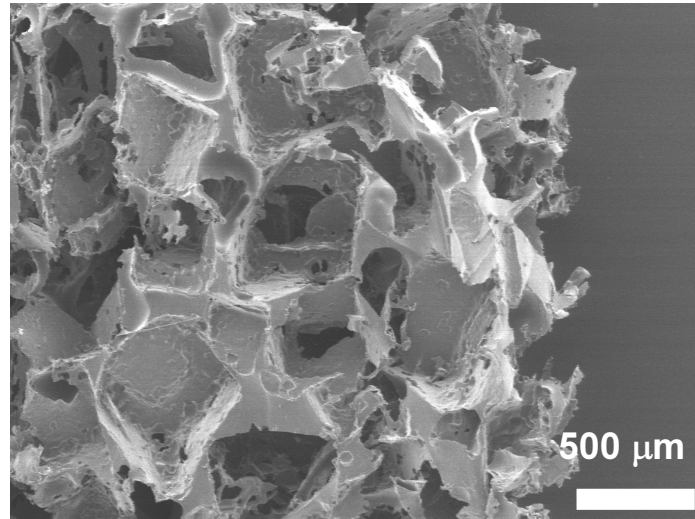


Figure 5.5 - SEM picture of a 1000PEOT70PBT30 scaffold of  $85.1 \pm 3.0$  % porosity, prepared with sodium chloride particles of 500-710  $\mu\text{m}$ .

#### *Mechanical properties of scaffolds prepared by polymer powder/salt mixing*

Although these materials are not intended in load-bearing applications, mechanical properties like scaffold stiffness are of interest. Scaffolds should maintain their structure and stiffness after long periods of cell culture and should maintain their structure for subsequent implantation. Depending on culture medium and culturing time and the place of implantation, very soft or more rigid scaffolds might be required with good handling characteristics up to the time of insertion into the bone defect.

The mechanical properties, especially the compression modulus, of porous materials are mainly governed by porosity. Various empirical relationships relate properties like tensile strength, compressive modulus and flexural modulus to the relative density or porosity.<sup>[29]</sup> From experimental and theoretical studies on trabecular bone it was concluded that the compression modulus of a porous structure ( $C_{\text{foam}}$ ) is related to the relative density ( $\rho_{\text{foam}}/\rho_{\text{solid}}$ ) according to the following formula:<sup>[30]</sup>

$$C_{\text{foam}} = C_{\text{solid}} * \left( \frac{\rho_{\text{foam}}}{\rho_{\text{solid}}} \right)^x \quad (5.1)$$

where  $x$  is an exponent with a value ranging between 2 and 3. The same relation is also valid for polymeric foams.<sup>[29]</sup> Experimentally, the exponent can easily be obtained by preparation of log-log plots of the relative compression modulus versus the relative density.

As shown in Figure 5.6, such relations fit the observed data very well. From our data on 1000PEOT70PBT30 scaffolds of varying porosity an exponent of  $3.2 \pm 0.2$  was obtained, in good correspondence with the previously mentioned value of 2-3, as often seen in literature. Parallel studies on the scaffolds prepared by freeze-drying showed that these porous scaffolds also obey this exponential decrease in modulus with increasing porosity, albeit with a somewhat smaller exponent of 2.2 (1000PEOT70PBT30) or 2.8 (300PEOT55PBT45), depending on the copolymer tested. The obtained relation allows us to accurately predict the compression modulus of a scaffold of a given porosity, enabling us to tune the mechanical properties to a specific need.

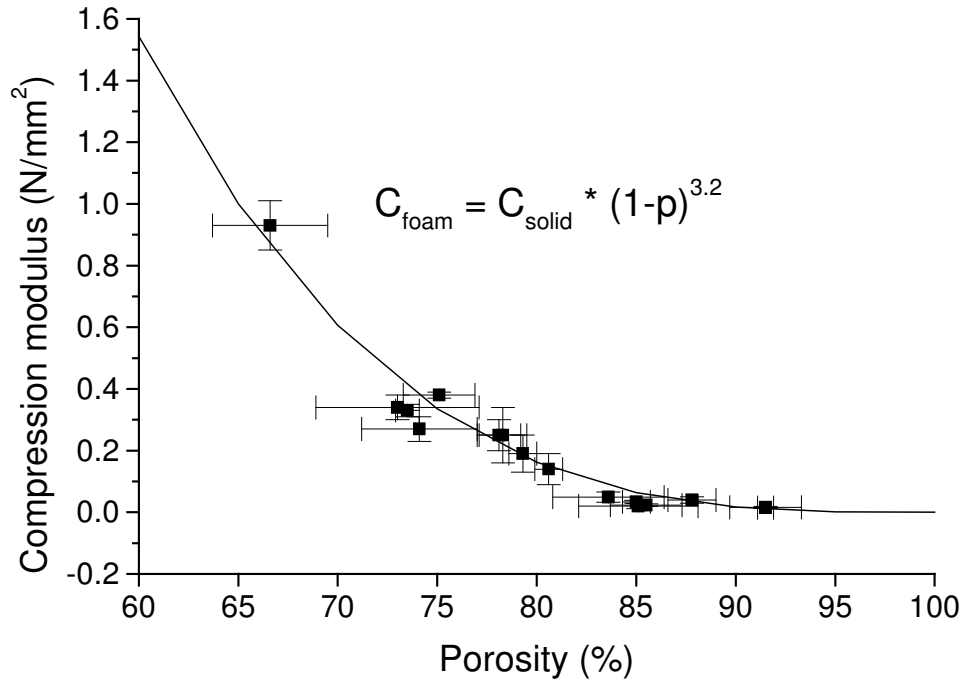


Figure 5.6 - Dependence of compression modulus on scaffold porosity (p) in the case of 1000PEOT70PBT30 foams.  $1-p$  equals the relative density as mentioned in formula 5.1. Moduli are the average of 3 measurements ( $\pm$  s.d.).

#### *In vitro rat bone marrow stromal cell culture on porous scaffolds*

After the initial screening with goat BMSCs, further experiments were carried out using rat BMSCs. Future *in vivo* experiments will be conducted using the rat as a small animal model. To study the effect of scaffold pore size on gas plasma treatment and *in vitro* cell culturing, scaffolds of  $84.5 \pm 2.0$  % porosity of different pore sizes were used. Scaffolds of  $4 \times 4 \times 4$  mm<sup>3</sup> were first treated using a 30 min CO<sub>2</sub> gas plasma to ensure cell attachment. Methylene blue staining (data not shown) and SEM on scaffold cross sections showed that at day 1 of the cell culturing experiments rat BMSCs (obtained from rat femora) attached throughout the entire scaffold, also in the center, showing that the gas plasma is able to reach the center of the scaffold. These results also indirectly show the interconnectivity of pores prepared by the powder mixing/salt leaching technique. Figure 5.7 shows an SEM picture of BMSCs spread on the surface of a 1000PEOT70PBT30 scaffold.

To study the effect of pore size on *in vitro* rat BMSC culture, scaffolds (porosity  $84.5 \pm 2.0$  %) with four different pore sizes were prepared: 250-425, 425-500, 500-710, 710-1000  $\mu$ m. Rat BMSCs were cultured during 7 d, with media refreshments every other day. The amount of

DNA, a direct indication for the amount of cells present in the samples, was then determined. The scaffolds were evaluated at 1, 4 and 7 d as indicated in Figure 5.8.

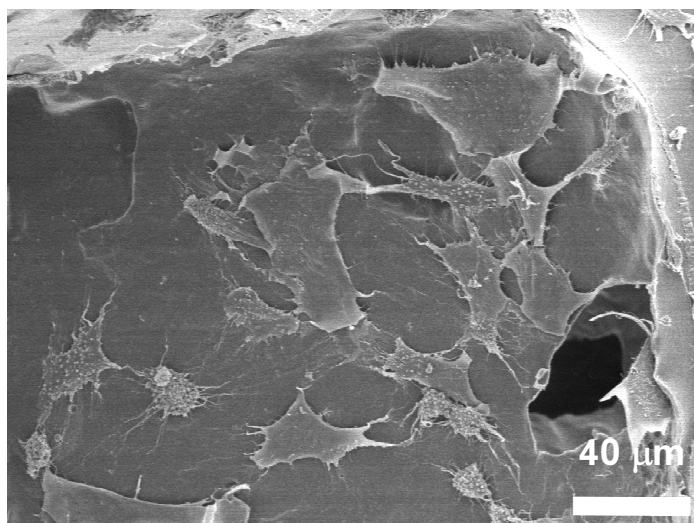


Figure 5.7 - Rat BMSCs attached to the surface of a 1000PEOT70PBT30 scaffold of 85 % porosity and pore size of 250-425  $\mu\text{m}$ .

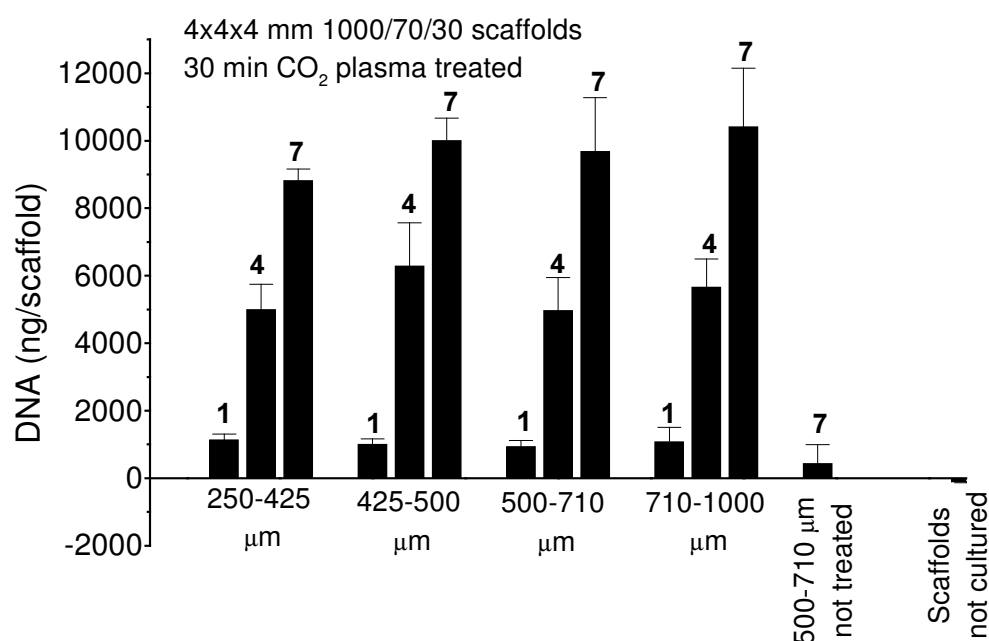


Figure 5.8 - DNA amount (ng) present on 1000PEOT70PBT30 scaffolds (4x4x4 mm) of varying pore size (porosity  $84.5 \pm 2.0$  %), after rat BMSC culturing. DNA amounts are the result of triplicate measurements ( $\pm$  s.d.).

The data show a statistically significant increase in the amount of DNA (and hence in cell numbers) present on the scaffolds after 4 and 7 d. As a reference, a non gas plasma treated scaffold of pore size 500-710  $\mu\text{m}$  was also included in the study, clearly showing the beneficial effect of the gas plasma treatment. After 7 d of culture only  $443 \pm 548$  ng of DNA is

present on these scaffolds, significantly less than the  $9694 \pm 1579$  ng present on the same scaffolds that were gas plasma treated.

The same trend was also observed by light microscopy evaluation of methylene blue stained samples: in time there is a large increase in the amount of cells present on these scaffolds.

Over the culture period no significant differences between the amount of DNA present on the different scaffolds could be observed. On the days of evaluation (1, 4 and 7) all the scaffolds, within the margins of error, have similar amounts of DNA. These data show that for the examined pore ranges, there is no significant effect of pore size on the amount of cells on these scaffolds. Both goat (Table 5.1) and rat (Figure 5.8) BMSCs show improved cell attachment and growth on CO<sub>2</sub> gas plasma treated PEOT/PBT surfaces.

In contrast to in vivo results where it was concluded that 300  $\mu$ m was a suboptimal pore size<sup>[8]</sup>, in our in vitro study, in which pore sizes were varied from 250 to 1000  $\mu$ m, no significant effect of pore size was seen. During in vitro cell culture there is no decrease in pore size due to swelling and press-fit implantation.

Methylene blue staining of scaffold cross sections showed cell attachment in the center of the scaffolds. Although not quantitative, the methylene blue staining suggested the presence of more cells in the scaffolds with pore sizes of 425-500  $\mu$ m and 500-710  $\mu$ m. The presence of BMSCs in the center of these scaffolds indirectly shows the interconnectivity of the pores, allowing cells to attach in the center of the scaffolds.

Rat BMSC differentiation into the osteogenic cell lineage, was verified by staining the cells for alkaline phosphatase activity, an enzyme not present in marrow cells. One of the first signs of differentiation is the presence of alkaline phosphatase. Active cells color purple whereas inactive cells stay yellowish (color of the staining medium). Figure 5.9 shows the alkaline phosphatase active cells present on a 1000PEOT70PBT30 scaffold (710-1000  $\mu$ m) after 10 d of culture, showing the ability of the rat BMSCs to differentiate into the osteogenic lineage on the surface of the gas plasma treated scaffolds.<sup>[24,31,32]</sup>

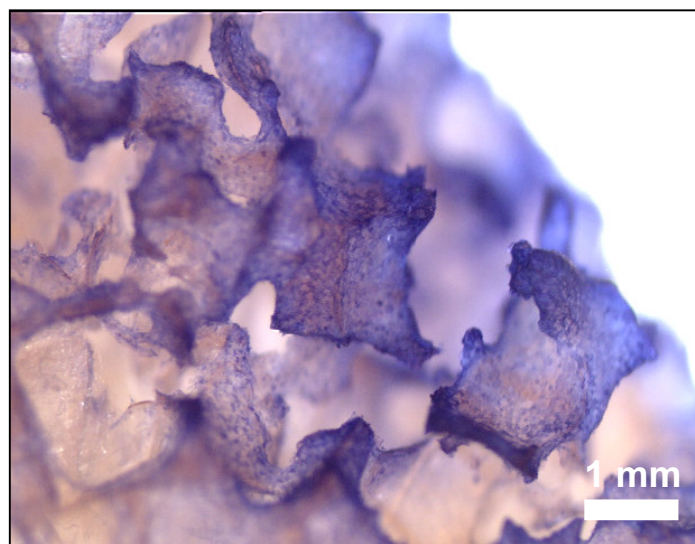


Figure 5.9 - Alkaline phosphatase stained 1000PEOT70PBT30 scaffold of 710-1000  $\mu$ m after 10 d of rat BMSC culturing. Cells containing alkaline phosphatase (differentiated) color purple. [Color figure on p. 170]

## Conclusions

The preparation of porous structures by means of compression molding of polymer powder/salt mixtures followed by salt leaching yields porous structures suitable as scaffold material in in vitro BMSC culturing. Variation of polymer/salt ratio and the salt size gives good control over porosity and pore size respectively, enabling us to prepare scaffolds with pore sizes over 300  $\mu\text{m}$  and porosities over 75 %.

Since during cell culturing rat BMSCs were able to attach in the center of the scaffolds, two points could be proven:

- The structures prepared by powder mixing/salt leaching contain interconnected pores.
- Gas plasma treatments using a  $\text{CO}_2$  gas plasma for 30 min, are effective for the improvement of BMSC attachment to PEOT/PBT porous scaffolds. With gas plasma treatments it is possible to surface modify porous scaffolds both on the outside and the inside.

In the in vitro rat BMSC culturing no significant effect of pore size, in the range of 250 to 1000  $\mu\text{m}$ , on the amount of cells present on the scaffolds was observed. The large increase in the amount of DNA present on the scaffolds over the culture period of 7 d shows the beneficial effect of gas plasma treatments on porous PEOT/PBT scaffolds. Methylene blue stained scaffold cross sections showed cells in the center of the scaffolds, suggesting more cells in the center of the scaffolds of 425-500 and 500-710  $\mu\text{m}$  pore size.

The control over the scaffold preparation, the good cell attachment (after gas plasma treatment) and the previously reported in vivo degradability<sup>[5]</sup> make 1000PEOT70PBT30 a good candidate as a tissue engineering scaffold material.

## Acknowledgements

The authors would like to thank Y.J.T. van der Zijpp for the gas plasma treatments, M.A. Smithers for the scanning electron microscopy (University of Twente) and P.J. Engelberts for the help with the DNA-assay (IsoTis OrthoBiologics). This study was financially supported by the European Community (Brite-Euram project BE97-4612).

## References

1. J.J. Marler, J. Upton, R. Langer, J.P. Vacanti *Transplantation of cells in matrices for tissue regeneration* Adv. Drug Deliv. Rev. **1998**, 33, 165-182.
2. S.P. Bruder, B.S. Fox *Tissue engineering of bone - Cell based strategies* Clin. Orthop. Rel. Res. **1999**, S68-S83.
3. A.A. Deschamps, D.W. Grijpma, J. Feijen *Poly(ethylene oxide)/poly(butylene terephthalate) segmented block copolymers: the effect of copolymer composition on physical properties and degradation* Polymer **2001**, 42, 9335-9345.
4. R.J.B. Sakkers, J.R. de Wijn, R.A.J. Dalmeyer, R. Brand, C.A. van Blitterswijk *Evaluation of copolymers of polyethylene oxide and polybutylene terephthalate (polyactive): mechanical behaviour* J. Mater. Sci.-Mater. Med. **1998**, 9, 375-379.
5. C.A. van Blitterswijk, J. van der Brink, H. Leenders, D. Bakker *The effect of PEO ratio on degradation, calcification and bone bonding of PEO/PBT copolymer (Polyactive)* Cells and Materials **1993**, 3, 23-36.
6. C.A. van Blitterswijk, D. Bakker, S.C. Hesselink, H.K. Koerten *Reactions of cells at implant surfaces* Biomaterials **1991**, 12, 187-193.
7. A.M. Radder, H. Leenders, C.A. van Blitterswijk *Bone-bonding behavior of poly(ethylene oxide)-polybutylene terephthalate copolymer coatings and bulk implants - a comparative-study* Biomaterials **1995**, 16, 507-513.



8. A.M. Radder, H. Leenders, C.A. van Blitterswijk *Application of porous PEO/PBT copolymers for bone replacement* J. Biomed. Mater. Res. **1996**, 30, 341-351.
9. M.L.C. Anderson, W.J.A. Dhert, J.D. de Bruijn, R.A.J. Dalmeijer, H. Leenders, C.A. van Blitterswijk, A.J. Verbout *Critical size defect in the goat's os ilium - A model to evaluate bone grafts and substitutes* Clin. Orthop. Rel. Res. **1999**, 231-239.
10. M. Roessler, A. Wilke, P. Griss, H. Kienapfel *Missing osteoconductive effect of a resorbable PEO/PBT copolymer in human bone defects: A clinically relevant pilot study with contrary results to previous animal studies* J. Biomed. Mater. Res. **2000**, 53, 167-173.
11. J.H. Brekke, J.M. Toth *Principles of tissue engineering applied to programmable osteogenesis* J. Biomed. Mater. Res. (Appl. Biomater.) **1998**, 43, 380-398.
12. D.W. Huttmacher *Scaffolds in tissue engineering bone and cartilage* Biomaterials **2000**, 21, 2529-2543.
13. A.G. Mikos, A.J. Thorsen, L.A. Czerwonka, Y. Bao, R. Langer, D.N. Winslow, J.P. Vacanti *Preparation and characterization of poly(L-lactid acid) foams* Polymer **1994**, 35, 1068-1077.
14. A.G. Mikos, G. Sarakinos, S.M. Leite, J.P. Vacanti, R. Langer *Laminated three-dimensional biodegradable foams for use in tissue engineering* Biomaterials **1993**, 14, 323-330.
15. M.S. Widmer, P.K. Gupta, L. Lu, R.K. Meszlenyi, G.R.D. Evans, K. Brandt, T. Savel, A. Gurlek, C.W. Patrick Jr, A.G. Mikos *Manufacture of porous biodegradable polymer conduits by an extrusion process for guided tissue regeneration* Biomaterials **1998**, 19, 1945-1955.
16. J.H. Aubert, R.L. Clough *Low-density, microcellular polystyrene foams* Polymer **1985**, 26, 2047-2054.
17. K. Whang, C.H. Thomas, K.E. Healy, G. Nuber *A novel method to fabricate bioabsorbable scaffolds* Polymer **1995**, 36, 837-842.
18. H. Lo, S. Kadiyala, S.E. Guggino, K.W. Leong *Poly(L-lactic acid) foams with cell seeding and controlled-release capacity* J. Biomed. Mater. Res. **1996**, 30, 475-484.
19. C. Schugens, V. Maquet, C. Grandfils, R. Jerome, P. Teyssie *Biodegradable and macroporous polylactide implants for cell transplantation: 1. Preparation of macroporous polylactide supports by liquid-solid phase separation* Polymer **1996**, 37, 1027-1038.
20. P.X. Ma, R.Y. Zhang, G.Z. Xiao, R. Franceschi *Engineering new bone tissue in vitro on highly porous poly(alpha-hydroxyl acids)/hydroxyapatite composite scaffolds* J. Biomed. Mater. Res. **2001**, 54, 284-293.
21. P.X. Ma, R.Y. Zhang *Microtubular architecture of biodegradable polymer scaffolds* J. Biomed. Mater. Res. **2001**, 56, 469-477.
22. M.B. Olde Riekerink, M.B. Claase, G.H.M. Engbers, D.W. Grijpma, J. Feijen *Gas plasma etching of PEO/PBT segmented block copolymer films* J. Biomed. Mater. Res. **2003**, 65A, 417-428.
23. M.B. Claase, M.B. Olde Riekerink, D.W. Grijpma, J. Feijen, S.C. Mendes, J.D. de Bruijn *Surface modifications of PEOT/PBT copolymers for the improvement of bone marrow stromal cell attachment* J. Control. Release **2003**, 87, 298-301.
24. C. Maniopoulos, J. Sodek, A.H. Melcher *Bone-formation in vitro by stromal cells obtained from bone marrow of young-adult rats* Cell Tissue Res. **1988**, 254, 317-330.
25. M.J. Lydon, T.W. Minett, B.J. Tighe *Cellular interactions with synthetic polymer surfaces in culture* Biomaterials **1985**, 6, 396-402.
26. P.B. Van Wachem, T. Beugeling, J. Feijen, A. Bantjes, J.P. Detmers, W.G. Van Aken *Interaction of cultured human endothelial cells with polymeric surfaces of different wettabilities* Biomaterials **1985**, 6, 403-408.
27. A.A. Deschamps, M.B. Claase, W.J. Sleijster, J.D. de Bruijn, D.W. Grijpma, J. Feijen *Design of segmented poly(ether ester) materials and structures for the tissue engineering of bone* J. Control. Release **2002**, 78, 175-186.
28. J.H. de Groot, A.J. Nijenhuis, P. Bruin, A.J. Pennings, R.P.H. Veth, J. Klompmaker, H.W.B. Jansen *Use of porous biodegradable polymer implants in meniscus reconstruction. 1) Preparation of porous biodegradable polyurethanes for the reconstruction of meniscus lesions* Colloid Polym. Sci. **1990**, 268, 1073-1081.
29. *Polymeric Foams: Handbook of polymeric foams and foam technology*; 1st ed.; D. Klemmner and K.C. Frisch, Ed.; Carl Hanser Verlag: Munich, Germany **1991**; pp 442.
30. L.J. Gibson *The mechanical behaviour of cancellous bone* J. Biomechanics **1985**, 18, 317-328.
31. S.J. Peter, C.R. Liang, D.J. Kim, M.S. Widmer, A.G. Mikos *Osteoblastic phenotype of rat marrow stromal cells cultured in the presence of dexamethasone,  $\beta$ -glycerolphosphate, and L- ascorbic acid* J. Cell. Biochem. **1998**, 71, 55-62.
32. D.J. Rickard, T.A. Sullivan, B.J. Shenker, P.S. Leboy, I. Kazhdan *Induction of rapid osteoblast differentiation in rat bone-marrow stromal cell-cultures by dexamethasone and BMP-2* Dev. Biol. **1994**, 161, 218-228.



# Chapter 6

## Ectopic bone formation in cell-seeded poly(ethylene oxide)/poly(butylene terephthalate) copolymer scaffolds: I. Effects of pore structure\*

*Men will not be content to manufacture life: they will want to improve on it.*

J.D. Bernal (1901-1971)

### Abstract

Rat bone marrow stromal cells (BMSCs) were seeded and cultured (7 d) on polymer scaffolds. The constructs were subcutaneously implanted in immunodeficient mice for 4 wks and the ectopic formation of bone and bone marrow was evaluated as a model for bone tissue engineering. The scaffolds were prepared from copolymers based on poly(ethylene oxide) and poly(butylene terephthalate), PEOT/PBT, with a PEO molecular weight of 1000 and a PEO content of 70 weight % (1000PEOT70PBT30), using compression molding and salt leaching techniques. The scaffolds were gas plasma treated before cell culturing. Here we report on the effect of the pore structure of 1000PEOT70PBT30 scaffolds with a porosity of approximately 80 % on ectopic bone formation.

The pore size distributions, average pore sizes, the accessible pore volume and accessible surface area (as a function of a simulated permeating sphere with increasing diameter (d)) of the porous scaffolds were determined by micro computed tomography ( $\mu$ -CT). The pore sizes of the different 1000PEOT70PBT30 scaffolds ranged between approximately 0-480  $\mu$ m, 0-648  $\mu$ m, 0-528  $\mu$ m and 0-720  $\mu$ m with corresponding average pore sizes of 260  $\mu$ m, 342  $\mu$ m, 305  $\mu$ m and 447  $\mu$ m. After cell seeding and culturing, all 1000PEOT70PBT30 scaffolds

---

\* Menno B. Claase<sup>1</sup>, Andres Laib<sup>2</sup>, Sanne Both<sup>3</sup>, Joost D. de Bruijn<sup>3</sup>, Dirk W. Grijpma<sup>1</sup>, Jan Feijen<sup>1</sup>

Submitted for publication in Biomaterials 2004

1) Institute for Biomedical Technology (BMTI) and Department of Polymer Chemistry and Biomaterials, Faculty of Science and Technology, University of Twente, P.O. Box 217, 7500 AE Enschede, The Netherlands

2) Scanco Medical AG, Auenring 6-8, CH-8303 Bassersdorf, Switzerland

3) Isotis OrthoBiologics, P.O. Box 98, 3720 AB Bilthoven, The Netherlands

showed the formation of bone and bone marrow upon implantation. By histomorphometry, no significant differences were observed in the amounts of formed bone (5-8 %) and bone marrow (5-13 %) in the middle cross sections of the scaffolds. For simulated sphere diameters (d) up to 100  $\mu\text{m}$ , no significant differences in accessible pore volume (as a fraction of the total volume) of the 1000PEOT70PBT30 scaffolds were observed.

Porous poly(D,L-lactide) (PDLLA, porosity 83.5 %, average pore size 407  $\mu\text{m}$ ) and biphasic calcium phosphate (BCP, porosity 29 %, average pore size 837  $\mu\text{m}$ ) scaffolds, both seeded with rat BMSCs and cultured for 7 d, were used as references. PDLLA and BCP scaffolds showed considerably more bone and bone marrow formation and less fibrous tissue ingrowth and wound exudate retention than the 1000PEOT70PBT30 scaffolds. The accessible pore volume (as a fraction of the total volume) of PDLLA was higher than for the 1000PEOT70PBT30 scaffolds. The scaffold material can also be of great influence on the in vivo bone and bone marrow formation as the swelling properties and stiffness of the polymer can affect the pore structure upon implantation.

## **Introduction**

Bone marrow stromal cells (BMSCs) can be regarded as a mesenchymal progenitor/precursor cell population derived from adult stem cells. Cultured BMSCs can be stimulated to differentiate into bone, cartilage, muscle, marrow stroma, tendon, fat and a variety of other connective tissues.<sup>[1]</sup>

Bone regeneration in large, clinically significant, segmental defects was observed upon implantation of bioceramic scaffolds, which were seeded with in vitro expanded BMSCs. Implantation of bioceramic scaffolds, which were seeded with fresh bone marrow (not expanded in culture), did not result in healing of the segmental defects.<sup>[2]</sup> Because only a very low percentage of mesenchymal stem cells is present in marrow (1 per 100,000 nucleated cells), expansion in vitro is necessary to produce a sufficient number of stem cells for (re)implantation at the surgical site for bone tissue engineering.<sup>[2]</sup>

Poly(ethylene oxide)/poly(butylene terephthalate) (PEOT/PBT) segmented block copolymers have interesting mechanical and physical properties for use in biomedical applications. These properties can be tuned by varying the PBT (hard segment) content and PEO (soft segment) content and molecular weight.<sup>[3,4]</sup> Several subcutaneous and intra-bone (tibia) implantations of dense and porous blocks and porous films in rats and goats showed bone bonding, calcification and degradation for PEOT/PBT copolymers with high PEO content (60 and 70 weight percent PEO containing soft segment).<sup>[5-8]</sup> We therefore investigated the use of these materials as scaffold materials for bone tissue engineering.

Poor bone bonding, limited calcification and limited fragmentation were, however, observed after implantation of porous blocks of the composition with 70 weight % PEOT soft segment and PEO molecular weight 1000 (1000PEOT70PBT30) in goat<sup>[9]</sup> and human<sup>[10]</sup> ilia critical size defects. It is anticipated that seeding these copolymer scaffolds with BMSCs will result in constructs with an osteoinductive effect<sup>[11]</sup>, that are therefore better suited for bone tissue engineering than the scaffolds without BMSCs.<sup>[12,13]</sup> Gas plasma treatment of 1000PEOT70PBT30 scaffolds is an essential step to enable BMSC attachment in vitro to this specific material.<sup>[14,15]</sup> Using a combined technique of polymer powder/salt crystal mixing followed by compression molding and salt leaching, porous scaffolds can easily be prepared. The use of different amounts of salt crystals of various sizes allows for an independent variation of porosity and pore size.<sup>[16]</sup>

Subcutaneous implantation into immunodeficient mice of porous scaffolds seeded with BMSCs to form ectopic bone, can be used as a model for bone tissue engineering.<sup>[11]</sup> Implantation in rats or mice of porous scaffolds, which were first seeded with BMSCs and cultured in vitro in an osteogenic medium for a certain period of time, resulted in enhanced ectopic bone formation as compared to implantation of scaffolds that were only preseeded with BMSCs.<sup>[17-19]</sup> Subcutaneous implantation in nude mice of rat BMSC seeded and cultured (for 7 d in an osteogenic medium) porous 1000PEOT70PBT30 scaffolds of 75 % porosity, prepared by leaching of salt particles of 400-600  $\mu\text{m}$ , showed comparable ectopic bone formation to porous hydroxyapatite, that was also seeded with rat BMSCs and cultured for 7 d in an osteogenic medium containing dexamethasone.<sup>[19]</sup> The effect of scaffold pore structure on the in vivo bone formation was not addressed in that study.

Here we report on the effect of the pore structure of gas plasma treated 1000PEOT70PBT30 scaffolds on ectopic bone formation in immunodeficient mice after subcutaneous implantation of scaffolds preseeded and cultured in vitro (7 d) with rat BMSCs in an osteogenic medium containing dexamethasone. The pore structure of scaffolds with an approximate porosity of 80 % was varied by using salt particles with different size distributions (250-425, 425-500, 500-710 and 710-1000  $\mu\text{m}$ ) in the porosifying process. Poly(D,L-lactide), PDLLA, porosity 83.5 %, prepared with salt particles of 425-500  $\mu\text{m}$  and biphasic calcium phosphate, BCP, porosity 29 %, with an average pore size of 837  $\mu\text{m}$ , as determined by  $\mu\text{-CT}$  were used as controls.

## Materials and methods

### Materials

*1000PEOT70PBT30 copolymer.* The copolymer was prepared by a two-step polycondensation in the presence of titanium tetrabutoxide (Merck, Germany) as catalyst (0.1 wt %) as previously described<sup>[3]</sup>, with the exception that vitamin E (Sigma-Aldrich, Germany, approx. 95 % purity) was used as antioxidant. The copolymer composition was determined by <sup>1</sup>H-NMR (Varian Inova 300 MHz) and a soft to hard segment ratio of 71 to 29 was found. The copolymer was used without further purification.

*PDLLA.* PDLLA was obtained from Purac (Gorinchem, The Netherlands), having an inherent viscosity of 2.96 dL/g (chloroform, 25 °C, concentration 0.1 g/dL).

The polymer was dissolved in chloroform and precipitated in a tenfold excess of technical grade ethanol to remove residual monomer. The precipitate was dried overnight under reduced nitrogen pressure in a vacuum oven and subsequently for 6 h at high vacuum.

*Porous structures prepared by compression molding of polymer/salt mixtures followed by salt leaching.* Both 1000PEOT70PBT30 copolymer granulate and PDLLA copolymer precipitate were cryogenically ground using an IKA Labortechnik (Germany) A10 grinder. Polymer particles and sodium chloride crystals (Merck, Germany) were sieved using Endecotts (United Kingdom) test sieves of 250, 425, 500, 710, 1000 and 1180  $\mu\text{m}$  mesh size. The desired salt volume fractions (250-425, 425-500, 500-710, 710-1000  $\mu\text{m}$  particle size) were calculated using a salt density of 2.165 g/cm<sup>3</sup>. To obtain stable porous structures, the size of the polymer particles needs to be smaller than the size of the salt crystals used. The powders were mixed and subsequently compression molded in a laboratory hot press (THB 008, Fontijne Holland BV, The Netherlands) into 4 mm thick blocks. Mixed powders were heated at 180 °C for 3 min and subsequently pressed for 1 min at 2.9 MPa. Samples were leached with milliQ water for 48 h and dried under reduced nitrogen pressure in a vacuum oven. From the obtained blocks scaffolds of 4×4×4 mm were cut using a razor blade.

*Density determination of porous structures.* Density and porosity were determined by measurement of scaffold mass and dimensions (volume) in the dry state. The porosity was calculated using the following densities of the solid materials 1000PEOT70PBT30:  $\rho = 1.188 \text{ g/cm}^3$ , PDLA:  $\rho = 1.26 \text{ g/cm}^3$ .<sup>[20]</sup>

*CO<sub>2</sub> gas plasma treatment.* 1000PEOT70PBT30 porous structures were gas plasma treated for 30 min according to a previously described procedure.<sup>[15]</sup> Discharge power was 50 W. CO<sub>2</sub> gas plasma pressure: 0.06 mbar. A gas flow of 10 cm<sup>3</sup>/min was used. Samples were treated with a pre-delay of 5 min and a post-delay of 2 min.

*OsSatura<sup>TM</sup> BCP granules.* Biphasic calcium phosphate granules were characterized by mercury intrusion porosimetry and provided by Isotis OrthoBiologics (Bilthoven, The Netherlands).

### Cell culturing and implantation

*Rat bone marrow stromal cell culturing.* BMSCs were isolated from 12 femora of 6 young male Wistar-rats (100-120 g). The osteogenic culture medium was minimal essential medium ( $\alpha$ -MEM, Invitrogen, The Netherlands) containing<sup>[21]</sup>: 15 % (v/v) fetal bovine serum (Invitrogen, The Netherlands), 100 units/mL penicillin, 100  $\mu\text{g/mL}$  streptomycin (Invitrogen, The Netherlands), 2mM L-glutamine (Invitrogen, The Netherlands), 0.2 mM ascorbic acid 2-phosphate (Invitrogen, The Netherlands), 10 mM  $\beta$ -glycerophosphate (Sigma, The Netherlands),  $10^{-8}$  M dexamethasone (Sigma, The Netherlands).

The femora were cut on both sides and the marrow was flushed out using 5 mL of culture medium per femur. The collected cells were re-suspended and cultured in T 75 standard tissue culture flasks (Nunc, Germany) at 37 °C, 5 % CO<sub>2</sub> for 7 d, with periodic medium changes every other day. After 7 d, the cells were confluent, washed with PBS (Invitrogen, The Netherlands) and treated with 0.25 % trypsin/EDTA (Sigma, The Netherlands). The collected cell suspension contained  $9.9 \times 10^7$  rat BMSCs. The suspension was centrifuged at 300 $\times$ g for 10 min at room temperature and re-suspended in medium to obtain a cell concentration of  $6.7 \times 10^5$  cells/mL.

*Cell seeding and growth on porous scaffolds.* Scaffolds were placed in bacteriological well plates (Nunc, Germany) and washed with: distilled water, 100 % ethanol, distilled water, 70 vol % ethanol and 3x sterile PBS, sequentially. Due to swelling in ethanol, PDLA scaffolds were washed with isopropanol instead of ethanol. The scaffolds were put in culture medium overnight and seeded with  $2 \times 150 \mu\text{L}$  of cell suspension (approximately  $2 \times 10^5$  cells per scaffold). Cell suspensions were injected into the scaffolds with a pipette tip. Scaffolds were incubated at 37 °C for 3 h, after which 2 mL of cell culture medium was added. Cells were cultured at 37 °C, 5 % CO<sub>2</sub> for 7 d, with periodic medium changes every other day. At day 7 cultured samples were implanted or analyzed using SEM, alkaline phosphatase staining or a DNA assay.

*In vivo implantation.* Cell-seeded and cultured scaffolds were soaked in serum-free medium and washed with prewarmed PBS (37 °C) before implantation. Six immunodeficient mice (HsdCpb:NMRI-nu) were anaesthetized using a mixture of ketamine/xylazine and atropine, the surgical sites were cleaned with ethanol and subcutaneous pockets were created using blunt incisions. Six sites were created per mouse (3 on each side of the spine) and scaffolds were implanted according to a randomized scheme. After 4 wks the mice were sacrificed by asphyxiation with CO<sub>2</sub> gas. Scaffolds with tissue were removed and fixed with glutaraldehyde (Merck, Germany, 1.5 % solution in 0.14 M cacodylic acid buffer, pH = 7.35)

One mouse showed substantially less bone formation in the 1000PEOT70PBT30 and PDLA scaffolds (BCP was not implanted here) than the other 5. The resulting data were therefore

excluded from the experiment. For each of the 1000PEOT70PBT30 scaffolds 5 samples were analyzed whereas for PDLLA 2 samples and for BCP 3 samples were evaluated. BCP granules with an approximate diameter of 4-5 mm were used for implantation as positive controls.<sup>[22-24]</sup>

### Analyses

*Compression testing.* Compression moduli were determined at room temperature using a Zwick Z020 tensile tester. Moduli were measured at 10 % strain at a strain rate of 2 mm/min with a 0.1 N preload. The scaffolds had a diameter of 17 mm and a height of 8 mm. Results are averages of at least three measurements ( $\pm$  s.d.).

*Micro computed tomography.* The scaffolds were scanned without further sample preparation with a desktop Micro-CT ( $\mu$ CT-40, Scanco Medical, Bassersdorf, Switzerland) at a resolution of 12  $\mu$ m in all three spatial dimensions (X-Ray voltage 45 kVp), with the exception of the BCP and PDLLA scaffolds, which were scanned at a resolution of 20  $\mu$ m. Of every scaffold 300 slices were scanned with 1024x1024 pixels per slice, covering a depth of 3.6 mm. For evaluation, volumes of interest slightly smaller than the diameter of the sample (approximately 4x4x4 mm) were chosen to exclude crushed boundaries. The resulting gray-scale images were segmented using a low-pass filter to remove noise, and a fixed threshold to extract the polymer phase.

For the 3D evaluation of the structure of the scaffold, 'direct' three-dimensional techniques without model-assumptions for the appearance of the structure were used. Pore voxels can be defined as voxels corresponding to the void space and polymer voxels as voxels corresponding to the polymer phase.

Porosity and pore size. In  $\mu$ -CT data analysis, the porosity can be calculated from the number of polymer voxels and the total number of voxels. To determine the pore size, pores are completely filled with modelled spheres of different diameters. The pore diameter assigned to a pore voxel is then the diameter of the largest sphere (still containing that pore voxel) that fits inside the pore.<sup>[25]</sup> In the case of cubic pores, however, as is the case in this study, this underestimates the pore size assigned to pore voxels present in the corners of these pores. Therefore, the algorithm was modified to assign the diameter of the largest sphere fitting in the pore to all voxels within that pore.

The average pore size is calculated by averaging the product of the pore voxels with their assigned pore diameters over the total amount of pore voxels, according to the formula:<sup>[25]</sup>

$$\text{Average pore size} = \frac{\sum_i (\text{pore voxel}_i \times \text{pore size}_i)}{\sum_i \text{pore voxel}_i} \quad (6.1)$$

Accessible pore volume. An algorithm mimicking mercury intrusion porosimetry, by use of a simulated sphere with diameter (d), was used to determine the accessible pore volume. Using a thresholding operation, all the pores not accessible for the sphere with diameter (d) are suppressed. All pores of this thresholded structure not (inter)connected to the outside of the scaffold are discarded with a component labelling operation. The volume of the resulting pore structure is calculated, and plotted versus sphere diameter (d), resulting in a graph of accessible pore volume (as a fraction of the total volume) versus sphere diameter (d).

Accessible surface area. The surface area of the accessible pore volume as a function of sphere diameter (d), was calculated using a triangularization algorithm.<sup>[26]</sup> The calculated surface consists of triangular surfaces contacting the scaffold and triangular surfaces not contacting the scaffold. Triangular surfaces not contacting the scaffold are suppressed, resulting in a

surface area of the pore volume of the scaffold that is accessible for the simulated sphere of diameter (d).

*Scanning Electron Microscopy (SEM).* Scaffolds containing rat BMSCs were fixed and dehydrated using an ethanol/water gradient (isopropanol for PDLLA). Dehydrated samples were dried using a Balzers CPD 030 critical point dryer before coating. The PDLLA scaffolds were air dried. Samples were coated with Au/Pd in a Polaron E5600 sputter coater. Pictures were taken with a Hitachi FE-SEM S-800 (6.0 kV).

*Alkaline phosphatase (ALP) staining.* Duplicate samples were analyzed after 7 days of in vitro culture in an osteogenic medium. Scaffolds were washed with PBS of 37 °C and subsequently fixed with paraformaldehyde (4 % (w/v) solution in Sørensen buffer (phosphate buffer)) for 6 h. Samples were washed with water (3x) and stained for 35 min using a Fast Blue RR salt (4-benzoylamino-2,5-dimethoxybenzene-diazonium chloride hemi[zinc chloride], Sigma, The Netherlands) in naphthol As-B-1 stock solution (1 g/L). Besides the cell-cultured scaffolds, also two unseeded scaffolds (G) were stained. Samples were observed using a Nikon SM2-10A stereomicroscope (1×-4.9× objective). Digital photographs were taken using a Q Image Reticon 1000 camera.

*DNA-assay.* Scaffolds were washed with PBS at 37 °C and stored in a freezer (-80 °C) until further analysis. Scaffolds were cut in at least 4 pieces (except BCP granules) and incubated at 56 °C overnight in 1.0 mL of lysis-medium to lyse all cells. The lysis-medium consisted of proteinase K (Sigma, The Netherlands) in Tris/EDTA buffer (1 mg/mL, pH = 7.6).

The next day 500 µL of these suspensions were mixed with 500 µL RNase-solution. The RNase solution was prepared from 42 µL RNase (Sigma, The Netherlands, 1.35 Kunitz units/µL) and 70 µL heparin (Leopharma, The Netherlands, 5,000 IE/mL) in 17.5 mL PBS, and incubated at 37 °C for 60 min to remove single stranded RNA and DNA. Various dilutions were prepared with PBS. Dilutions were mixed with CyQUANT® dye. After 15 min the fluorescence of the solutions in 96 well plates was measured using a Perkin Elmer Luminescence Spectrometer LS 50 B (excitation at 480 nm, slit width 2.5 nm, emission at 520 nm, slit width 4.0 nm). The measured fluorescence intensities were correlated to the amount of DNA using a calibration curve of DNA (Sigma) dilutions of known concentration. Data shown are the result of triplicate measurements ( $\pm$  s.d.).

To calculate the amount of DNA present in rat BMSCs, the amount of DNA was determined as a function of cell number. Cell batches of the rat BMSCs (passage 1) used to seed the scaffolds were frozen (-80 °C) and analyzed together with the scaffolds that were seeded and cultured in vitro for 7 days. Cell numbers of  $5 \times 10^4$ ,  $10 \times 10^4$ ,  $20 \times 10^4$ ,  $30 \times 10^4$ ,  $40 \times 10^4$ ,  $80 \times 10^4$  were used in duplicate to prepare the DNA-cell calibration line. A slope of  $1.32 \pm 0.03$  pg DNA/cell ( $r = 0.998$ ) was found.

*Histology/histomorphometry.* After 3 d in fixative, scaffolds were dehydrated using an ethanol/water gradient (isopropanol/water for PDLLA) and subsequently embedded in poly(methyl methacrylate) (PMMA). Sections were prepared using a histological diamond saw (Leica SP1600, Leica, Germany) and stained using 1 % methylene blue and 0.3 % basic fuchsin solutions. Samples were investigated using a Nikon SM2-10A stereomicroscope (0.75 and 1× objective). For higher magnifications a Nikon Eclipse E600 with objectives 4-50× was used. Digital photographs were taken using a Q Image Reticon 1000 camera.

To determine the relative amounts of tissue formed, the relative areas of the different tissues were calculated from the number of pixels as determined with Scion Image (version beta 4.02 for Windows, Scion Corporation, USA). Sections from the middle part of the scaffolds were analysed at high magnifications and the relative amounts of the different tissues were calculated with respect to the porosity of the cross section (area of the cross sections



corresponding to the pores). Data shown are the average of 5 scaffolds  $\pm$  s.d., unless otherwise mentioned.

*Statistical analysis.* Results were analyzed using one-way ANOVA, followed by a Games Howell post-hoc test. Results were considered statistically different when  $p < 0.05$ . ANOVA calculations were performed using SPSS software for Windows (version 11.0, SPSS, USA).

## Results and discussion

Four gas plasma treated 1000PEOT70PBT30 scaffolds of approximately 80 % porosity with different pore structures were prepared using different leachable salt fractions. As a comparison, scaffolds were also prepared from poly(D,L-lactide) (PDLA). These polymer scaffolds were seeded and in vitro cultured in an osteogenic medium for 7 d with rat BMSCs, and subsequently subcutaneously implanted in immunodeficient nude mice. OsSatura<sup>TM</sup> BCP (biphasic calcium phosphate) seeded and in vitro cultured in an osteogenic medium for 7 d with rat BMSCs, and gas plasma treated 1000PEOT70PBT30 (unseeded) were used as positive and negative controls respectively. BCP was used as a positive control to confirm the osteogenic potential of the cells used.<sup>[22-24]</sup> The scaffolds and some of their main characteristics are summarized in Table 6.1.

1000PEOT70PBT30 and PDLA scaffolds were prepared by mixing ground and sieved polymer with salt crystals of a 250-425, 425-500, 500-710 or 710-1000  $\mu\text{m}$  size range. The powder mixture was compression molded and salt-leached, resulting in porous structures.<sup>[16]</sup> The technique is known to result in somewhat higher values of the porosity than could be expected on the basis of the volume content of salt used.<sup>[16,20]</sup>

The resulting porosities of the different 1000PEOT70PBT30 scaffolds are similar and therefore these scaffolds show a comparable value of the compression modulus of about 0.2  $\text{N/mm}^2$ . A decrease in compression modulus is observed with increasing porosity, in line with previous observations.<sup>[16]</sup> The PDLA scaffolds are considerably stiffer with a compression modulus of about 2  $\text{N/mm}^2$ . The higher modulus can be directly related to the compression modulus of the starting materials:  $30.2 \pm 1.4 \text{ N/mm}^2$  for 1000PEOT70PBT30<sup>[16]</sup> and  $296.5 \text{ N/mm}^2$  for PDLA.<sup>[20]</sup>

The scaffolds (dry, prior to gas plasma treatment and cell seeding) were characterized by micro computer tomography ( $\mu\text{-CT}$ ), resulting in computer generated 3D pictures as shown in Figure 6.1. Besides this, relevant data like porosity and pore size distribution were calculated. As shown in Table 6.1, the porosity obtained from  $\mu\text{-CT}$  matches the values determined by density measurements quite well. The average pore sizes of 260 to 447  $\mu\text{m}$  as determined by the  $\mu\text{-CT}$  are lower than the size of the salt crystals used for the preparation of these porous structures. This is in line with other reports where  $\mu\text{-CT}$  was used to characterize porous scaffolds.<sup>[27]</sup>

In these previous reports a calculation method was used to calculate the pore size and average pore size from the  $\mu\text{-CT}$  data, that underestimates the assigned pore size for many pore voxels (see Materials and methods). This results in pore size distributions with a relatively high number of small pores and therefore a lower average pore size than expected on the basis of the size of the salt crystals used. In this study, however, the underestimation of the average pore size is less than in previous reports<sup>[27]</sup> due to an improved algorithm more suitable for cubic pores, as is the case in this study for the scaffolds prepared by salt leaching.

For the different 1000PEOT70PBT30 porous scaffolds prepared with salt fractions of 250-

Table 6.1 - Main characteristics of unseeded scaffolds in the dry state, before gas plasma treatment.

Scaffold description	Salt fraction used ( $\mu\text{m}$ )	Salt volume (%)	Average pore size from $\mu\text{-CT}$ ( $\mu\text{m}$ )	Porosity* from $\mu\text{-CT}$ (%)	Compression modulus ( $\text{N/mm}^2$ )
A: 1000PEOT70PBT30 gas plasma treated	250-425	70	260	77.3 (79.3 $\pm$ 0.7)	0.19 $\pm$ 0.06
B <sup>†</sup> : 1000PEOT70PBT30 gas plasma treated	425-500	70	342	78.2 (80.6 $\pm$ 0.7)	0.14 $\pm$ 0.05
C: 1000PEOT70PBT30 gas plasma treated	500-710	70	305	77.6 (78.3 $\pm$ 1.2)	0.25 $\pm$ 0.09
D: 1000PEOT70PBT30 gas plasma treated	710-1000	70	447	73.6 (78.1 $\pm$ 1.1)	0.25 $\pm$ 0.05
E: PDLLA not treated	425-500	80	407	81.7 (83.5 $\pm$ 0.7)	2 <sup>¶</sup>
F: OsSatura <sup>TM</sup> BCP not treated	382 <sup>‡</sup>	-	837	36.2 (29 <sup>§</sup> )	n.d.

\*: porosity as obtained from density measurements is shown in parentheses

†: scaffold G = B not seeded with cells

¶: approximate value based on reference [20]

‡: average pore size, as determined by mercury intrusion porosimetry, pores < 100  $\mu\text{m}$  were excluded

§: average porosity, as determined by mercury intrusion porosimetry, pores < 100  $\mu\text{m}$  were excluded

425, 425-500, 500-710  $\mu\text{m}$  size range, calculations based on  $\mu\text{-CT}$  show that these scaffolds have an average pore size of about 300  $\mu\text{m}$ . The scaffolds prepared with a salt fraction of 710-1000  $\mu\text{m}$  have a higher average pore size of 447  $\mu\text{m}$ .

Although for three 1000PEOT70PBT30 scaffolds the average pore size is comparable, the pore size distribution of the studied scaffolds differs considerably. Figure 6.2 also shows that the pore size distribution for 1000PEOT70PBT30 scaffold D and PDLLA scaffold E are considerably broader (up to 720 and 760  $\mu\text{m}$ ) than for the 1000PEOT70PBT30 scaffolds A, B and C with pore sizes up to 480, 648 and 528  $\mu\text{m}$ , respectively.

The accessible pore volume as a function of a simulated permeating sphere with increasing diameter (d) was determined using  $\mu\text{-CT}$  data, as described in the Materials and methods section. The diameter (d) of the simulated sphere is a direct measure of the size of the interconnecting pore network. The resulting graphs of the accessible pore volume (given as a fraction of the total volume) versus the sphere diameter (d) are shown in Figure 6.3.

The curves for the accessible pore volume for 1000PEOT70PBT30 scaffolds B and D show that a higher pore volume of the scaffold is accessible for simulated spheres with (d) varying from approximately 120 - 650  $\mu\text{m}$  than for scaffolds A and C.

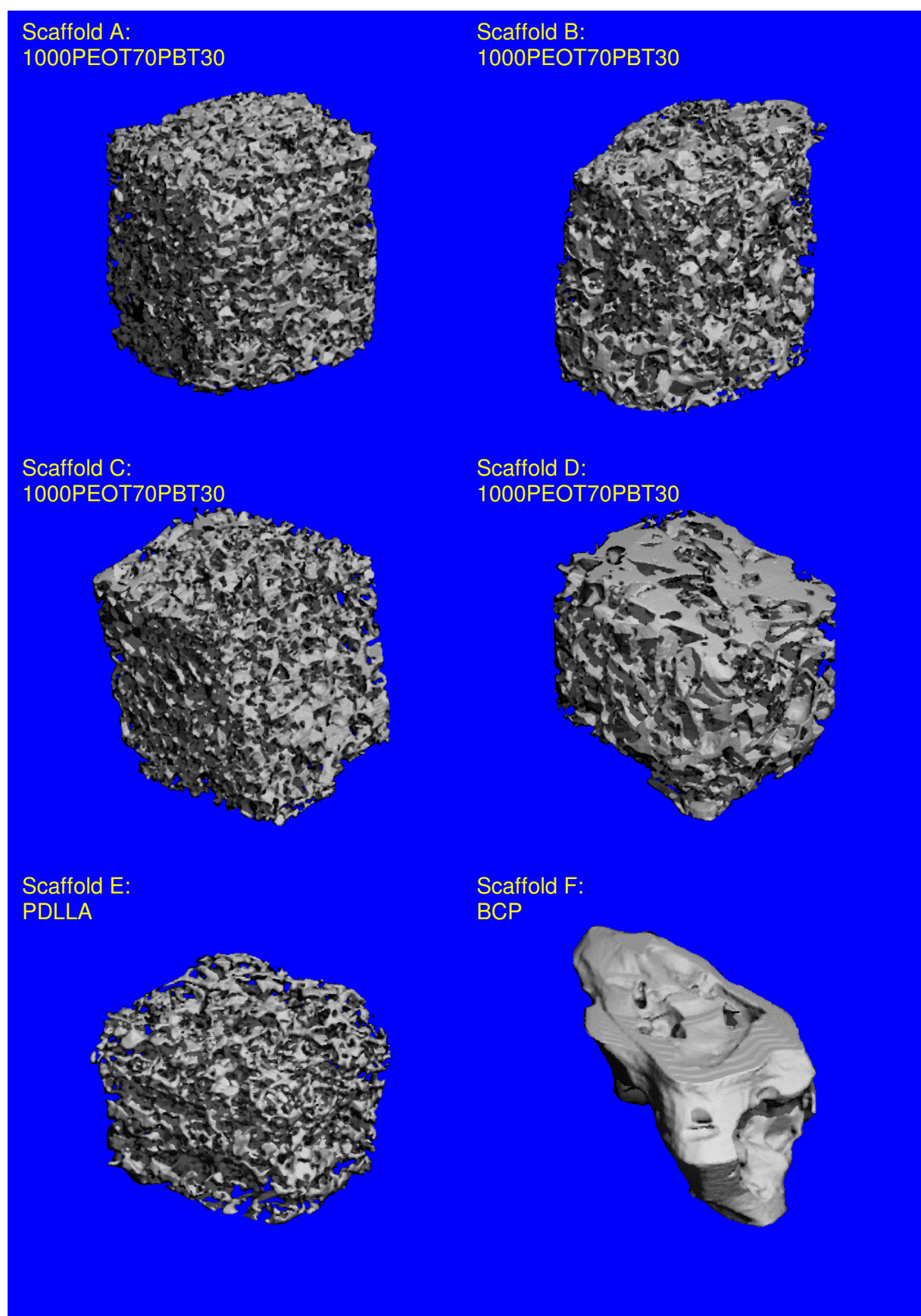


Figure 6.1 - 3D generated computer images of scaffolds constructed from  $\mu$ -CT scans. Dry, unseeded scaffolds before gas plasma treatment, corresponding to scaffolds A, B, C, D, E, F and G (identical to B) as listed in Table 6.1 are shown. [Color figure on p. 171]

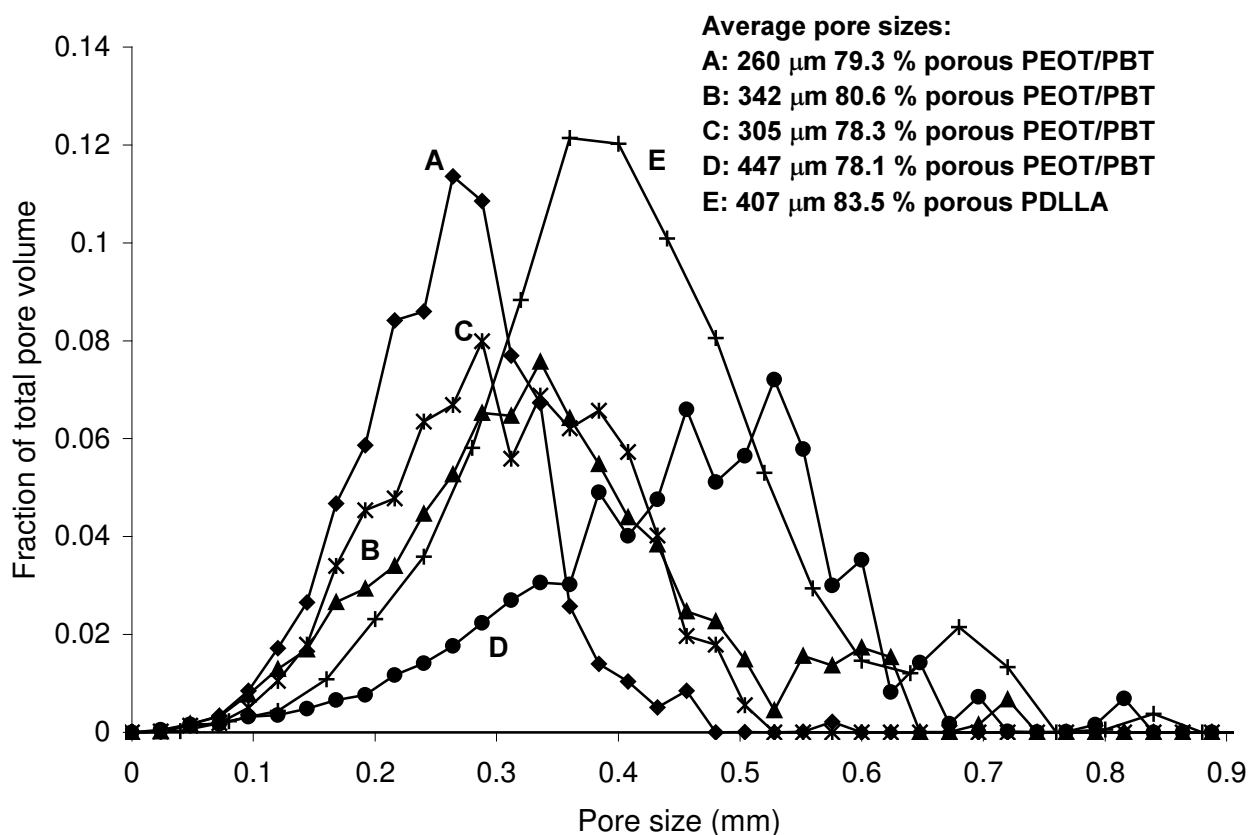


Figure 6.2 - Pore size distributions and average pore sizes derived from  $\mu$ -CT. Scaffold G is identical to scaffold B.

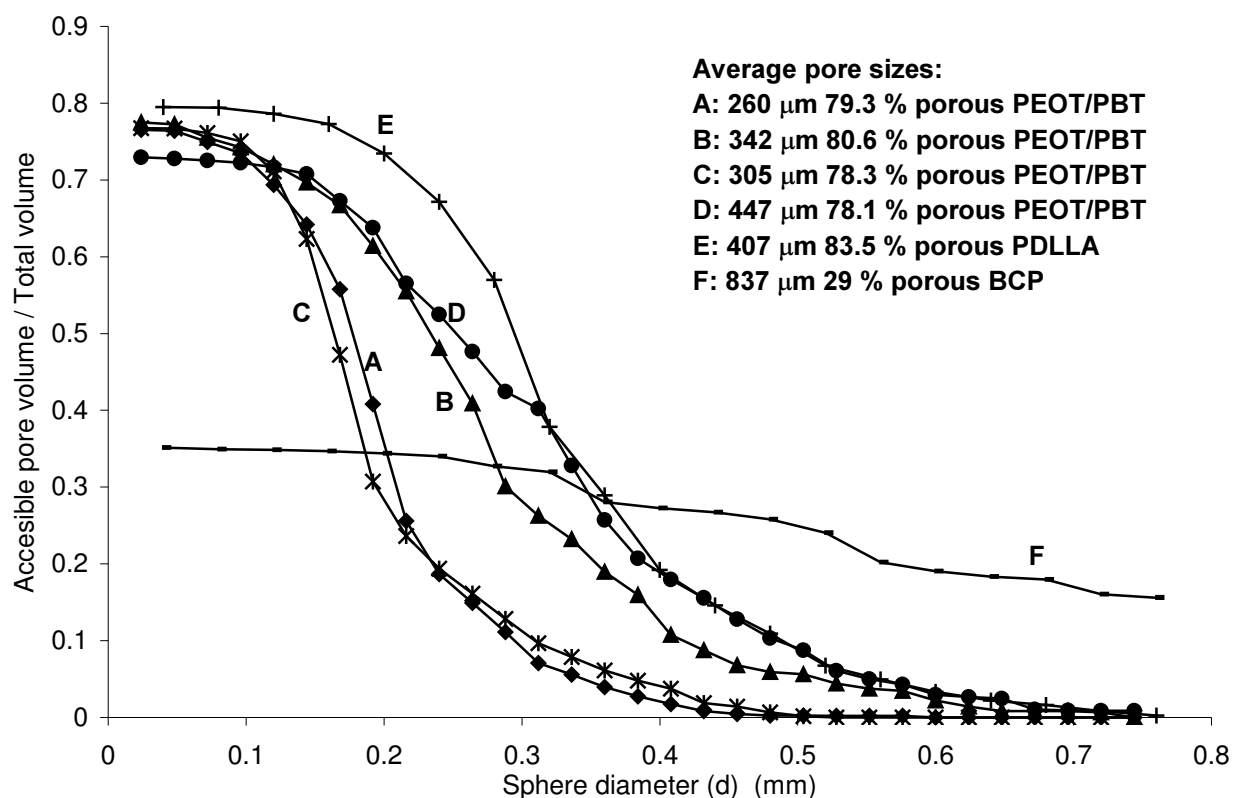


Figure 6.3 - Accessible pore volume (normalized for the total volume) versus sphere diameter (d) for unseeded, dry scaffolds before gas plasma treatment.

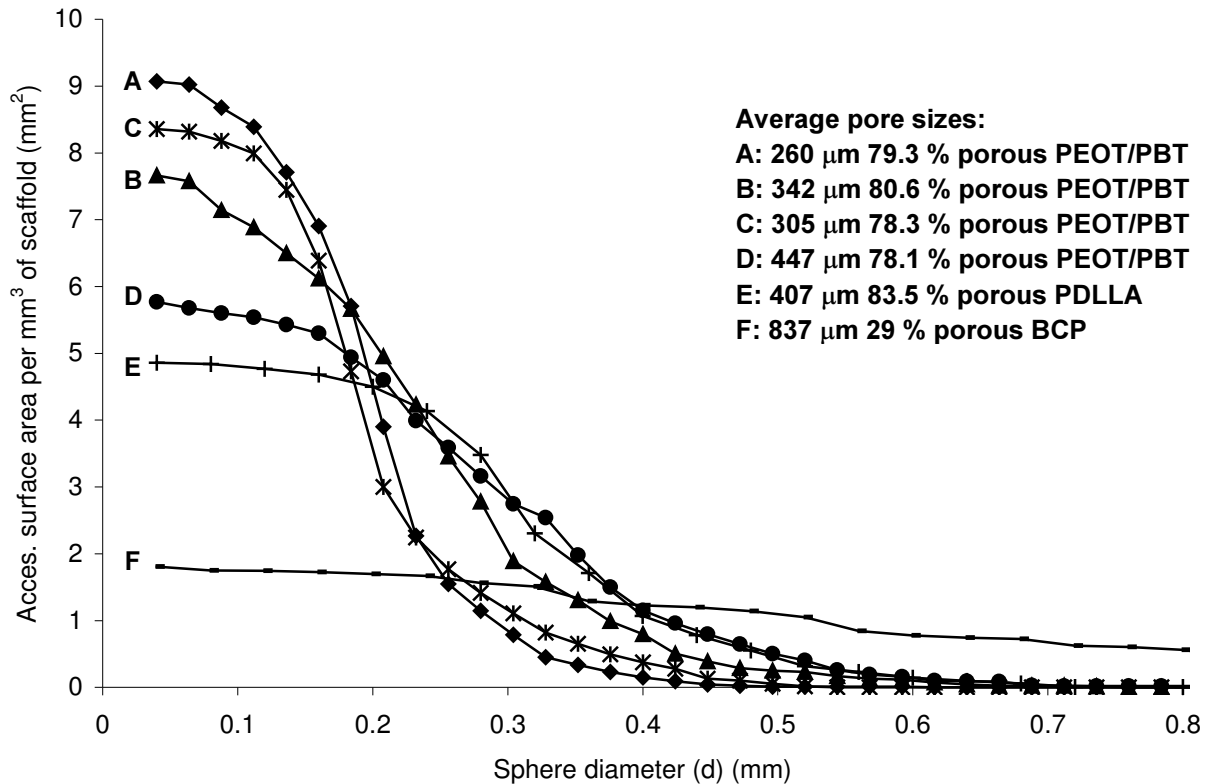


Figure 6.4 - Accessible surface area (normalized for the total volume) versus sphere diameter (d) for unseeded, dry scaffolds before gas plasma treatment.

For all sphere diameters (d) the accessible pore volume of PDLLA scaffold E is higher than (or equal to) the accessible pore volume of the 1000PEOT70PBT30 scaffolds. Although the BCP scaffold (F) has a low porosity, 20 % of the total volume is accessible for simulated spheres with a diameter (d) up to 750  $\mu\text{m}$ .

At sphere diameters (d) smaller than 100  $\mu\text{m}$ , the polymeric scaffolds A-E of comparable porosity, but with different average pore sizes show a comparable accessible pore volume.

The accessible surface area in the dry state differs considerably for the different scaffolds (Figure 6.4). For the 1000PEOT70PBT30 scaffolds with a porosity of approximately 80 %, an increase in the average pore size (as determined by  $\mu\text{-CT}$ ) results in a decrease in the accessible surface area, at simulated sphere diameters smaller than 100-150  $\mu\text{m}$ . For 1000PEOT70PBT30 scaffolds of 4 $\times$ 4 $\times$ 4 mm the obtained values would correspond to surface areas between 369 (scaffold D) and 580 (scaffold A)  $\text{mm}^2$ , values in the same order of magnitude as previously reported based on model calculations.<sup>[16]</sup>

Rat BMSCs (first passage), expanded in culture in the presence of osteogenic factors, were seeded into the scaffolds ( $2 \times 10^5$  cells/scaffold) and cultured for 7 d. Figure 6.5 shows SEM pictures of the rat BMSCs seeded porous structures after 7 d of culture. The outsides of all gas plasma treated and cell-seeded 1000PEOT70PBT30 scaffolds (A-D) as well as PDLLA (E) and BCP scaffolds (F) were fully covered with rat BMSCs, whereas unseeded 1000PEOT70PBT30 (G) did not contain cells.

At higher magnification scaffold A shows a fiber-like network, most likely collagen. This indicates that prior to implantation the constructs consisted of a scaffold with cultured tissue-like material, forming an extracellular matrix.<sup>[19]</sup> Scaffolds B and D (not shown in Figure 6.5) had a similar appearance as scaffolds A and C (Figure 6.5).

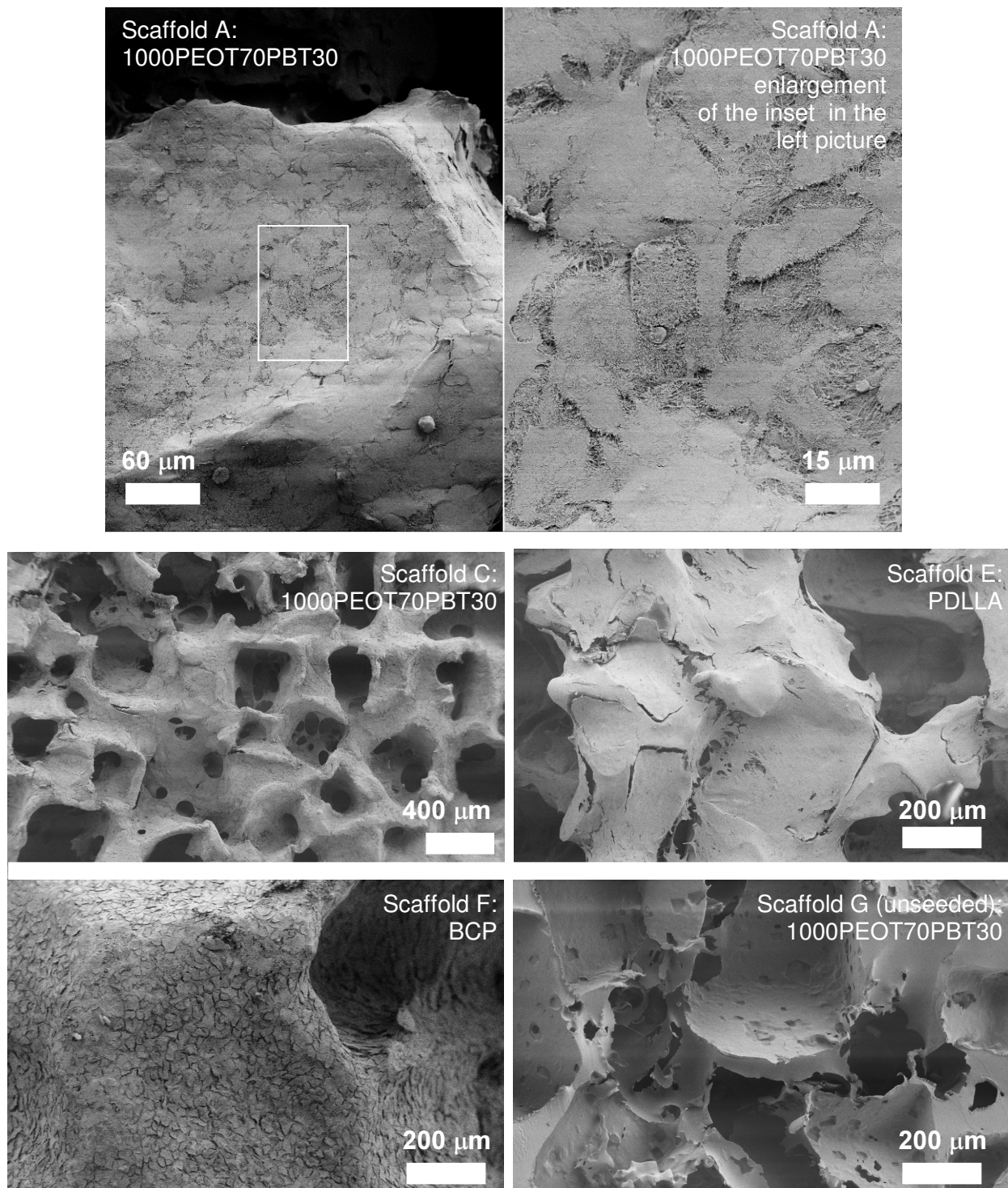


Figure 6.5 - SEM pictures of the external surface of selected cell-seeded scaffolds after 7 d of in vitro cell culture. Rat BMSCs are well attached and spread on scaffolds A, C, E and F. Bottom right: unseeded scaffold G.

Rat bone marrow cell differentiation into the osteogenic cell lineage, was verified by staining the cells for alkaline phosphatase (ALP) activity, an enzyme not present in undifferentiated BMSCs. One of the first signs of bone marrow cell differentiation is the presence of alkaline phosphatase.<sup>[21,28-30]</sup> When rat BMSCs are exposed to osteogenic supplements, immediately after collection, the alkaline phosphatase activity is known to increase rapidly during culture



from day 7 to 14.<sup>[29]</sup> Active cells stain dark blue/dark purple whereas inactive cells stain yellowish (color of the staining medium).

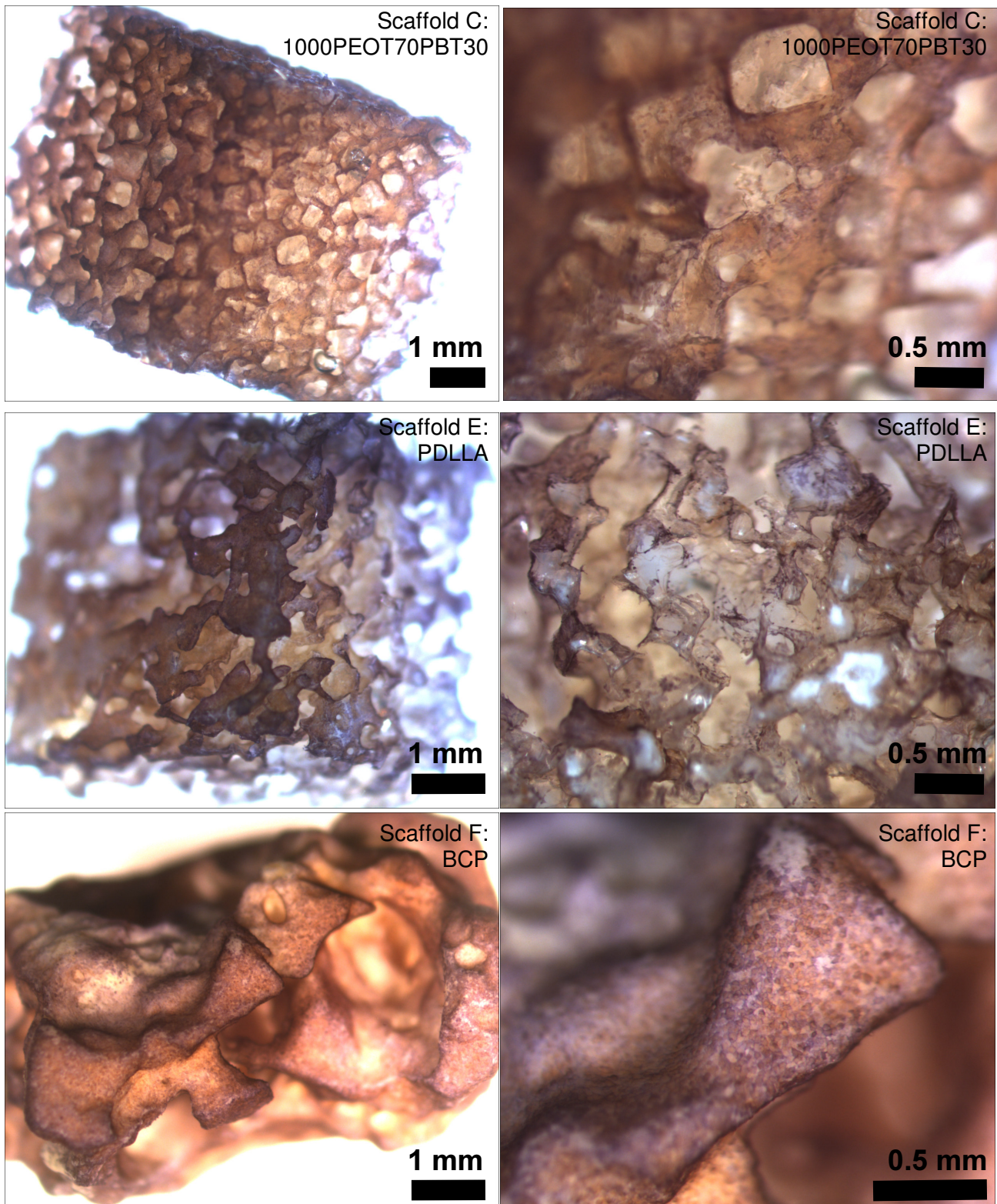


Figure 6.6 - Light micrographs of the surface of rat BMSC seeded scaffolds stained for ALP activity after 7 d of culture. Top: 1000PEOT70PBT30 (scaffold C), middle: PDLLA (D), bottom: BCP (E). [Color figure on p. 172]

Figure 6.6 shows ALP-active cells present on 1000PEOT70PBT30 (scaffold C, scaffolds A, B and D had a similar appearance), PDLLA (E) and BCP (F), indicating the ability of the rat BMSCs to differentiate into the osteogenic lineage on the various scaffolds. Although most ALP-active cells were present on the outsides of the scaffolds, micrographs of scaffold cross-sections also showed ALP-active cells in the center of the scaffolds. This shows that the plasma treatment is able to modify the pore surface even in the center of 4×4×4 mm 1000PEOT70PBT30 scaffolds.

The amount of DNA present in cells on the different scaffolds after 7 d of in vitro cell culture was fluorometrically quantified using CyQuant<sup>®</sup> dye. As shown in Figure 6.7, the 1000PEOT70PBT30 scaffolds A, B, C and D show a slight, although not statistically significant, decrease in the amounts of DNA detected in the scaffolds. For the negative control (scaffold G) no DNA was detected.

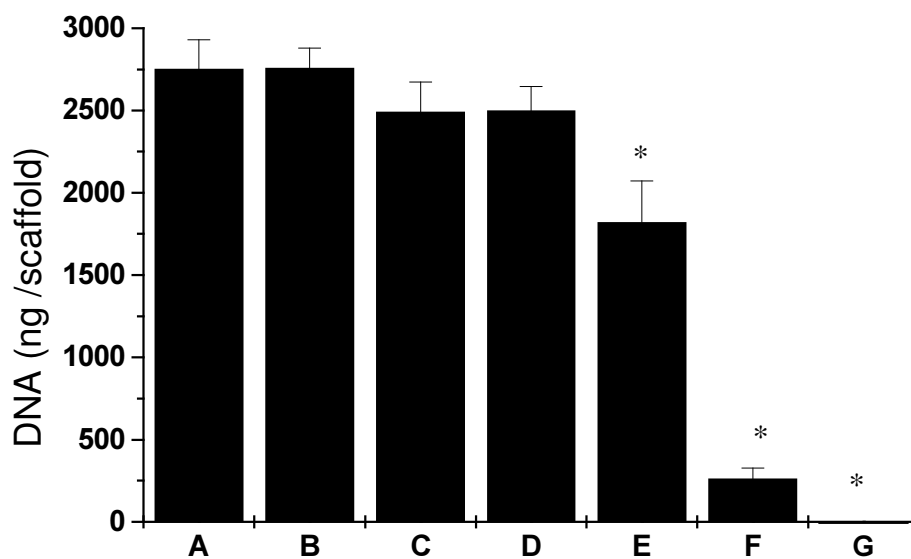


Figure 6.7 - Fluorometric quantification of DNA present on the different scaffolds after 7 d of in vitro rat BMSC culture. \*: Value significantly different from the other 6 scaffolds. Scaffold A, B, C and D: cell-seeded 1000PEOT70PBT30, E: cell-seeded PDLLA, F: cell-seeded BCP, G: 1000PEOT70PBT30, unseeded.

The in previous paragraphs presented SEM and ALP data clearly show that gas plasma treated 1000PEOT70PBT30, PDLLA and BCP are suitable substrate materials for the attachment of rat BMSCs. All three materials show many well spread BMSCs on their surfaces.

The significantly lower amount of DNA determined for the PDLLA and BCP scaffolds is most likely due to the lower accessible surface area of these scaffolds as compared to the 1000PEOT70PBT30 scaffolds (see Figure 6.4, at values of sphere diameter (d) smaller than 150  $\mu\text{m}$ ). Based on the differences in accessible surface area between the 1000PEOT70PBT30 scaffolds A-D, one also would expect differences in the amount of cells (and hence DNA) in these scaffolds after 7 days of in vitro cell culture. Although a slight decrease in the amount of DNA detected in the scaffolds was observed, these differences were not statistically significant. A previously conducted in vitro study with rat BMSCs seeded 1000PEOT70PBT30 scaffolds (porosity of approximately 85 %) also showed approximately equal amounts of DNA in scaffolds with different pore sizes.<sup>[16]</sup>

To correlate the amount of DNA present in the scaffolds to the number of rat BMSCs, the amount of DNA was determined as a function of cell number. Cells were lysed under the same conditions as the cell-seeded scaffolds (see Materials and methods). A value of  $1.32 \pm 0.03$  pg



DNA/cell was found. This corresponds to  $1.8\text{--}2.0 \times 10^6$  BMSCs per 1000PEOT70PBT30 scaffold after 7 d of cell culture. The obtained value of  $1.32 \pm 0.03$  pg DNA/cell is considerably lower than the value of 10.4 pg DNA/cell previously reported by Mikos *et al.*<sup>[31]</sup> A commonly accepted reference value is 6.90 pg DNA/cell<sup>[32]</sup>, therefore it appears that the lysis and RNase incubation conditions greatly influence the obtained results. Care has to be taken when comparing the amounts of DNA/cell obtained under different lysis conditions. After 7 d of in vitro cell culture in an osteogenic medium, the cell-seeded scaffolds were implanted subcutaneously in the back of immunodeficient mice for a time period of 4 wks.

To investigate bone formation the undecalcified explanted samples were embedded in PMMA and saw-microtomed. The sections were stained using methylene blue and basic fuchsin.<sup>[19]</sup> This staining allows for the differentiation between bone, bone marrow, cartilage and fibrous tissue. Basic fuchsin also stains the 1000PEOT70PBT30 scaffolds pink, whereas PDLLA does not adsorb the dye. Representative middle sections of the different scaffolds, which were implanted in one mouse, are shown in Figure 6.8.

The various cell-seeded 1000PEOT70PBT30 scaffolds show bone and bone marrow formation both at the periphery and in the center of the scaffolds. The formed tissue, however, is not homogeneously distributed. A better distribution of stromal cells and hence bone tissue is likely to be achieved by dynamic seeding<sup>[33]</sup> and culturing techniques.<sup>[31,34]</sup> The negative control scaffold G (unseeded, gas plasma treated 1000PEOT70PBT30) does not show formation of bone or bone marrow at all and is mainly filled with fibrous tissue and wound exudate. At higher magnifications the different tissue types can be identified, as shown in Figure 6.9. Scaffold F (BCP) confirms the ability of the BMSCs to induce ectopic bone formation as bone and bone marrow are present in and on the surface of the scaffold. BCP shows bone formation only in close contact to the material. The cell-seeded polymeric scaffolds (1000PEOT70PBT30 and PDLLA) typically show bone formation both in close contact to the material as well as in the center of the pores.

The different types of tissue were quantified using histomorphometry. The amounts of the different tissues were determined in middle cross-sections of the different scaffolds (implanted in 5 fold) and averaged. The porosity (area of the cross sections corresponding to the pores) and the amounts (relative areas) of the different tissues (normalized for porosity) as determined from histomorphometry are shown in Table 6.2.

The porosity in the 1000PEOT70PBT30 scaffolds is consistently lower than expected on the basis of the overall porosity obtained by density measurements and  $\mu$ -CT. A possible explanation for this is the swelling of 1000PEOT70PBT30 in MMA during embedding. As the volume of the scaffold is restricted by tissue, the porosity is decreased upon swelling.

The relative amounts of bone and bone marrow formed in the 1000PEOT70PBT30 scaffolds are in the range of 5 to 8 and 5 to 13 %, respectively. The relative amounts of ectopic bone determined in the 1000PEOT70PBT30 scaffolds, are considerably lower than the value of 36 % of bone previously reported by Mendes *et al.*<sup>[19]</sup> In that study smaller scaffolds were used ( $3 \times 3 \times 2$  mm, compared to  $4 \times 4 \times 4$  mm used here). As the same amount of cells ( $2 \times 10^5$  per scaffold) was seeded, this results in a lower cell seeding density in our case.

In the study of Mendes *et al.* the determined amount of DNA per scaffold at the time of implantation was also higher, approximately 20.000 ng per scaffold compared to the values of 2.400 to 2.700 ng per scaffold reported here. As discussed in a previous paragraph, the amounts of DNA determined per scaffold can be influenced by the lysis conditions employed in the DNA assay. Therefore, one should be careful in directly comparing the obtained values.

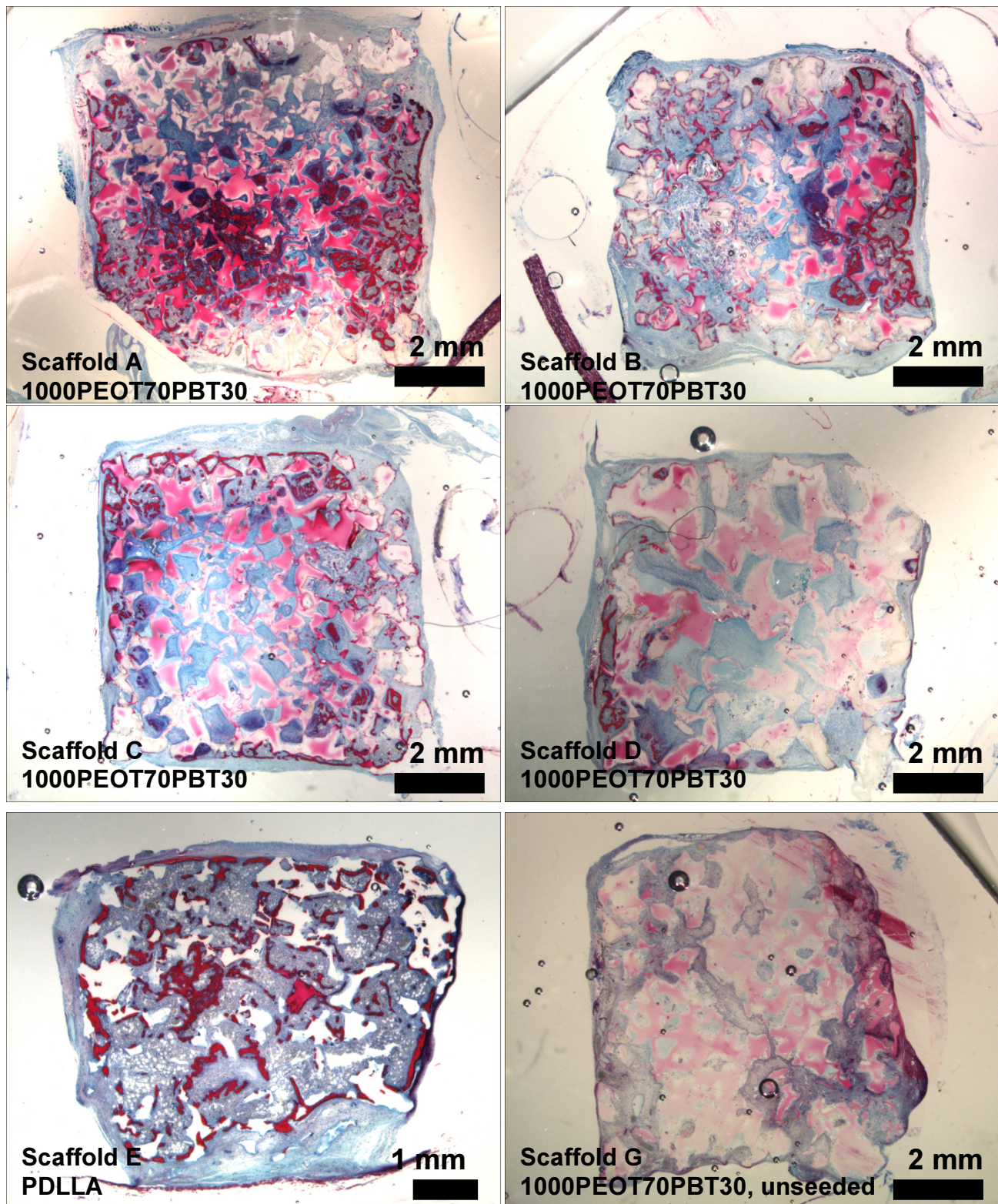


Figure 6.8 - Representative cross sections of scaffolds after 4 wks of subcutaneous implantation. The sections shown were taken from the middle of the scaffolds and stained using methylene blue and basic fuchsin. 1000PEOT70PBT30 stains pink, whereas PDLLA appears transparent. All scaffolds (except G) show bone (dark red) and bone marrow (blue/gray) formation. Fibrous tissue and wound exudate stain bright blue.  
[Color figure on p. 173]



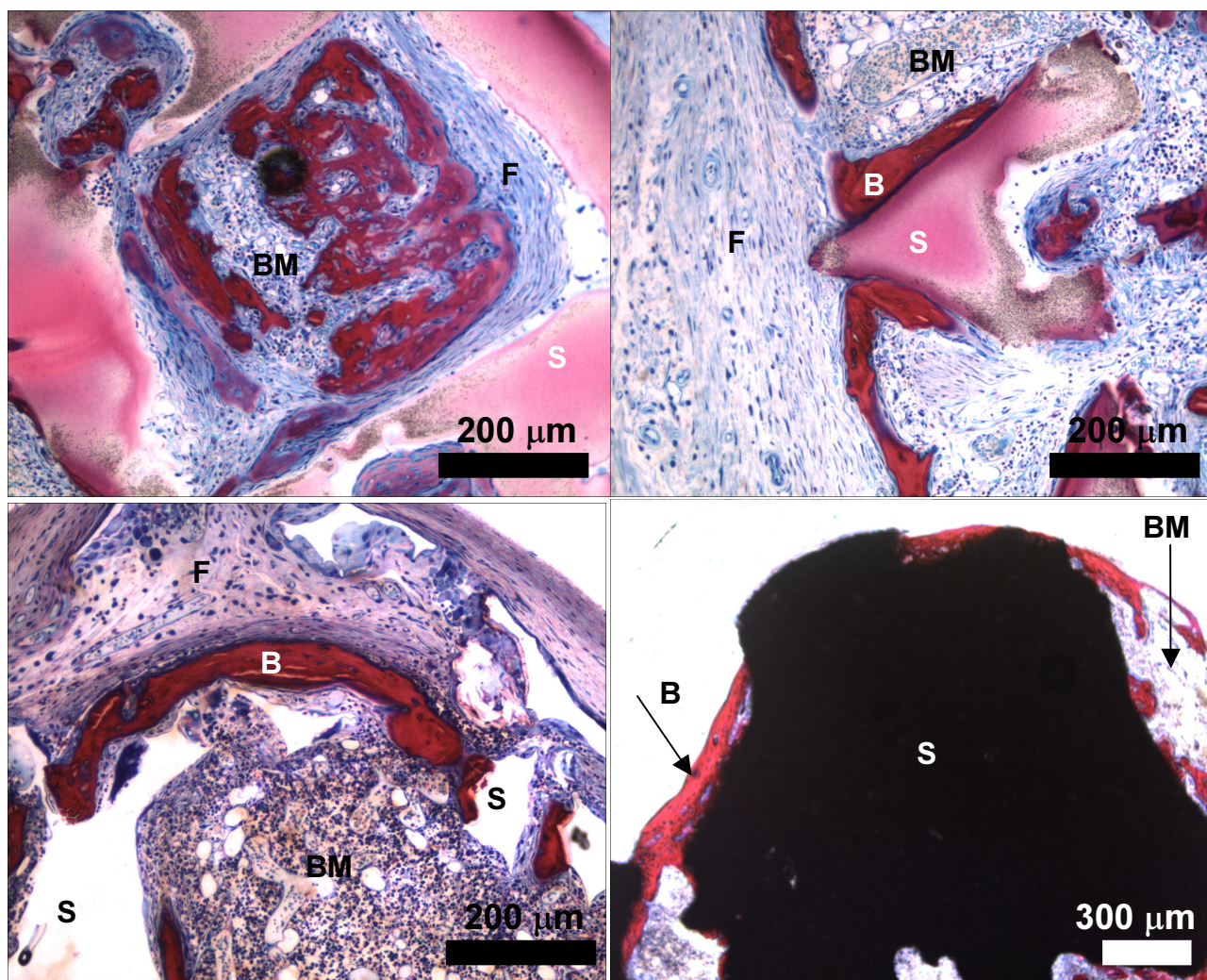


Figure 6.9 - Bone formation in the various scaffolds. Top left and right: 1000PEOT70PBT30 (scaffold C). Bottom left: PDLLA (E), bottom right: BCP (F). B: bone, BM: bone marrow, S: scaffold material and F: fibrous tissue. [Color figure on p. 174]

For scaffolds B, C, and D a trace amount of cartilage (less than 0.2 %) was observed in 1 out of 5 mice. Oxygen and nutrient supply ensured by thorough vascularization is important for bone formation.<sup>[35]</sup> Poorly accessible pores can lead to a lack of nutrient and oxygen supply, which results in the formation of cartilage instead of bone.<sup>[35,36]</sup> Besides bone and bone tissue, large amounts of fibrous tissue were observed in many of the 1000PEOT70PBT30 scaffolds. It has been reported that the ingrowth of fibrous tissue took place in subcutaneous implanted (in rats) poly(L-lactic acid) scaffolds with pore sizes comparable to the pore sizes of our scaffolds.<sup>[37,38]</sup>

No bone or bone marrow was observed in unseeded scaffold G, showing that the seeding and culturing of BMSCs in 1000PEOT70PBT30 scaffolds is essential for ectopic bone formation. The results obtained for PDLLA scaffold E clearly show that for this material an average pore size of 407  $\mu\text{m}$  and pore sizes up to approximately 760  $\mu\text{m}$  (determined by  $\mu\text{-CT}$ ) allow for abundant in vivo bone and bone marrow formation. 1000PEOT70PBT30 scaffold D with a somewhat higher average pore size of 447  $\mu\text{m}$  and pore sizes up to approximately 720  $\mu\text{m}$  (determined by  $\mu\text{-CT}$ ), shows considerably less bone and bone marrow formed than in the PDLLA scaffolds.

Table 6.2 - Amounts (%) of bone, bone marrow, cartilage, fibrous tissue and wound exudate (as determined from the relative areas), normalized for the porosity. The porosity is the area of the cross section corresponding to the pores, given as the percentage of the total surface area of the microtomed scaffold section. The results are the average of 5 scaffolds ( $\pm$  s.d.), unless mentioned otherwise. Middle cross-sections of the implanted scaffolds were analyzed.

	Pore surface area (%)	Bone (%)	Bone marrow (%)	Cartilage (%)	Fibrous tissue (%)	Wound exudate (%)
A 1000PEOT70PBT30 250-425 $\mu$ m salt size	56.4 $\pm$ 9.1	6.1 $\pm$ 2.7	4.9 $\pm$ 4.8	-	62.7 $\pm$ 8.4	3.8 $\pm$ 0.8
B 1000PEOT70PBT30 425-500 $\mu$ m salt size	66.7 $\pm$ 3.9	7.5 $\pm$ 3.4	8.2 $\pm$ 9.3	0.01 $\pm$ 0.03	59.5 $\pm$ 14.9	3.0 $\pm$ 1.8
C 1000PEOT70PBT30 500-710 $\mu$ m salt size	60.6 $\pm$ 8.5	7.7 $\pm$ 3.2	13.4 $\pm$ 15.3	0.04 $\pm$ 0.08	48.7 $\pm$ 16.7	5.8 $\pm$ 3.9
D 1000PEOT70PBT30 710-1000 $\mu$ m salt size	58.0 $\pm$ 7.0	5.0 $\pm$ 4.1	7.8 $\pm$ 6.6	0.03 $\pm$ 0.07	54.2 $\pm$ 10.3	15.2 $\pm$ 12.6
E <sup>§</sup> PDLLA 425-500 $\mu$ m salt size	80.3 $\pm$ 0.1	8.6 $\pm$ 2.0	75.4 $\pm$ 7.5	-	3.8 $\pm$ 2.7	0.4 $\pm$ 0.5
F <sup>†</sup> BCP 29 % porous	29.2 $\pm$ 4.2	10.8 $\pm$ 4.5	36.5 $\pm$ 4.0	-	35.8 $\pm$ 6.9	-
G <sup>¶</sup> 1000PEOT70PBT30 425-500 $\mu$ m salt size unseeded	57.0 $\pm$ 14.1	-	-	-	72.7 $\pm$ 9.7	9.9 $\pm$ 5.7

§: average of 2 implants

†: average of 3 implants

¶: scaffold G = scaffold B not seeded with cells

No significant differences in the amount of bone and bone marrow in the 1000PEOT70PBT30 scaffolds A-D were observed. As shown in Figure 6.3, for simulated sphere diameters (d) up to 100  $\mu$ m, no large differences in accessible pore volume (as a fraction of the total volume) are observed (values in between 0.7 and 0.8). Diameters up to 100  $\mu$ m should be sufficiently large to allow the passage of rat BMSCs, with an approximate diameter of 15-20  $\mu$ m (see Figure 6.5)

As shown in Figure 6.3 with increasing sphere diameter the accessible pore volume of PDLLA scaffold E is always higher than (or equal to) the accessible pore volume of the 1000PEOT70PBT30 scaffolds (A-D). In a following study the effect of scaffold porosity and accessible pore volume of 1000PEOT70PBT30 scaffolds on ectopic bone formation will be investigated.

The scaffold material can, however, also be of great influence. In a stiffer and less hydrophilic scaffold a more accessible pore structure is more likely to be preserved under physiological conditions than in the hydrophilic 1000PEOT70PBT30 scaffolds. Both PDLLA and BCP scaffolds contain more bone and bone marrow and much less fibrous tissue and wound exudate than the different 1000PEOT70PBT30 scaffolds.

As was found in previous degradation studies of this material<sup>[5,8]</sup>, 1000PEOT70PBT scaffolds started to fragment after 4 wks of implantation. Histological sections showed the presence of

small copolymer fragments as indicated in Figure 6.10. PDLA and BCP did not show signs of fragmentation.

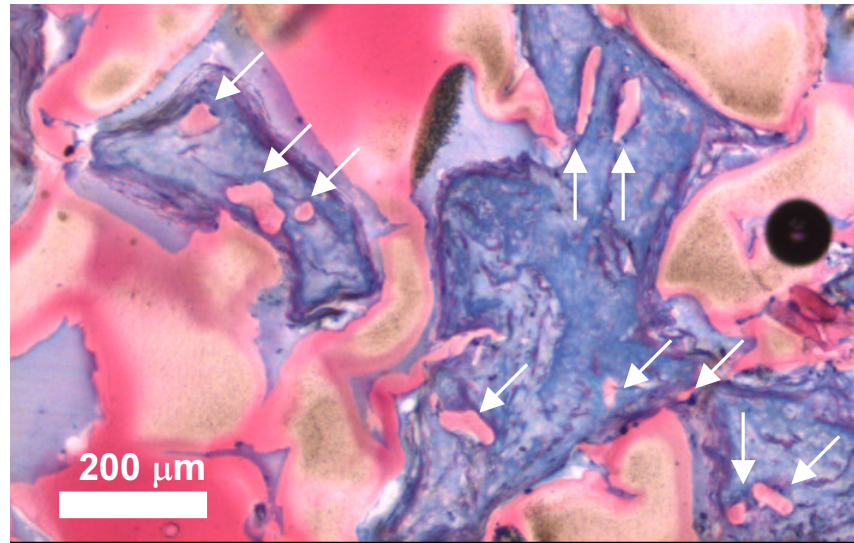


Figure 6.10 - Fragmentation of 1000PEOT70PBT30 scaffolds (scaffold B) after 4 wks of subcutaneous implantation in nude mice. Polymer fragments are indicated with arrows. [Color figure on p. 175]

## Conclusions

Rat BMSCs seeded 1000PEOT70PBT30 scaffolds that were pretreated with a CO<sub>2</sub> gas plasma and cultured for 7 d in vitro in an osteogenic medium, are able to form ectopic bone after subcutaneous implantation in immunodeficient mice. Porous 1000PEOT70PBT30 scaffolds were prepared by a salt-leaching process using salt crystals with sizes of 250-425, 425-500, 500-710 and 710-1000 μm. Calculations employing μ-CT data show different average pore sizes and pore size distributions for 1000PEOT70PBT30 scaffold D (prepared using leachable salt particles of 710-1000 μm) compared to 1000PEOT70PBT30 scaffolds A, B and C (prepared using leachable salt particles of 250-425, 425-500, 500-710 μm respectively). 1000PEOT70PBT30 scaffold D showed pore sizes up to approximately 720 μm and an average pore size of 447 μm, whereas scaffolds A, B and C had pore sizes up to 480, 648 and 528 μm and an average pore size of 260, 342 and 305 μm, respectively.

No significant differences in the amount of DNA (and hence cells) present in the 1000PEOT70PBT30 scaffolds A-D were observed, even though clear differences in accessible surface area, as derived from μ-CT data, were calculated.

The various cell-seeded 1000PEOT70PBT30 scaffolds show bone and bone marrow formation both at the periphery and in the center of the scaffolds. These tissues are not homogeneously distributed and a better distribution of stromal cells and hence of bone tissue and bone marrow is likely to be achieved by dynamic seeding and culturing techniques.

The relative amounts of bone (5 to 8 %) and bone marrow (5 to 13 %) detected in 1000PEOT70PBT30 scaffolds A, B, C and D with average pore sizes ranging from 260 to 447 μm and different pore size distributions (as determined by μ-CT), after explantation were not significantly different. For simulated sphere diameters (d) up to 100 μm, no large differences in accessible pore volume (as a fraction of the total volume) of the 1000PEOT70PBT30 scaffolds A-D were observed. PDLA scaffolds have a higher accessible pore volume than



1000PEOT70PBT30 scaffolds of comparable porosity. In a following study the effect of scaffold porosity and accessible pore volume of 1000PEOT70PBT30 scaffolds on ectopic bone formation will be investigated.

BMSC seeded PDLLA and BCP scaffolds (cultured for 7 d), which were used as controls, showed considerably more bone and bone marrow formation, less fibrous tissue ingrowth and wound exudate retention than the 1000PEOT70PBT30 scaffolds.

## Acknowledgements

The authors would like to thank Dr. L.M.H. Groenewoud for the gas plasma treatments (Ssens BV, Hengelo, The Netherlands), M.A. Smithers (University of Twente) for the scanning electron microscopy. This study was financially supported by the European Community (Brite-Euram project BE97-4612).

## References

1. A.I. Caplan, S.P. Bruder *Mesenchymal stem cells: building blocks for molecular medicine in the 21st century* Trends Mol. Med **2001**, 7, 259-264.
2. S.P. Bruder, N. Jaiswal, N.S. Ricalton, J.D. Mosca, K.H. Kraus, S. Kadiyala *Mesenchymal stem cells in osteobiology and applied bone regeneration* Clin. Orthop. Rel. Res. **1998**, S247-S256.
3. A.A. Deschamps, D.W. Grijpma, J. Feijen *Poly(ethylene oxide)/poly(butylene terephthalate) segmented block copolymers: the effect of copolymer composition on physical properties and degradation* Polymer **2001**, 42, 9335-9345.
4. R.J.B. Sakkars, J.R. de Wijn, R.A.J. Dalmeyer, R. Brand, C.A. van Blitterswijk *Evaluation of copolymers of polyethylene oxide and polybutylene terephthalate (polyactive): mechanical behaviour* J. Mater. Sci.-Mater. Med. **1998**, 9, 375-379.
5. C.A. van Blitterswijk, J. van der Brink, H. Leenders, D. Bakker *The effect of PEO ratio on degradation, calcification and bone bonding of PEO/PBT copolymer (Polyactive)* Cells and Materials **1993**, 3, 23-36.
6. C.A. van Blitterswijk, D. Bakker, S.C. Hesselting, H.K. Koerten *Reactions of cells at implant surfaces* Biomaterials **1991**, 12, 187-193.
7. A.M. Radder, H. Leenders, C.A. van Blitterswijk *Bone-bonding behavior of poly(ethylene oxide)-polybutylene terephthalate copolymer coatings and bulk implants - a comparative-study* Biomaterials **1995**, 16, 507-513.
8. A.M. Radder, H. Leenders, C.A. van Blitterswijk *Application of porous PEO/PBT copolymers for bone replacement* J. Biomed. Mater. Res. **1996**, 30, 341-351.
9. M.L.C. Anderson, W.J.A. Dhert, J.D. de Bruijn, R.A.J. Dalmeijer, H. Leenders, C.A. van Blitterswijk, A.J. Verbout *Critical size defect in the goat's os ilium - A model to evaluate bone grafts and substitutes* Clin. Orthop. Rel. Res. **1999**, 231-239.
10. M. Roessler, A. Wilke, P. Griss, H. Kienapfel *Missing osteoconductive effect of a resorbable PEO/PBT copolymer in human bone defects: A clinically relevant pilot study with contrary results to previous animal studies* J. Biomed. Mater. Res. **2000**, 53, 167-173.
11. R. Cancedda, B. Dozin, P. Giannoni, R. Quarto *Tissue engineering and cell therapy of cartilage and bone* Matrix Biol. **2003**, 22, 81-91.
12. J.D. de Bruijn, Y.P. Bovell, J. van den Brink, C.A. van Blitterswijk (to IsoTis) *Device for tissue engineering bone* U.S. Patent 6,228,117 **2001**.
13. J.D. de Bruijn, Y.P. Bovell, C.A. van Blitterswijk (to IsoTis) *Device for tissue engineering bone comprising biodegradable thermoplastic copolyester and cultured cells* Eur. Patent Appl. 0891783 A1 **1998**.
14. M.B. Claase, M.B. Olde Riekerink, J.D. de Bruijn, D.W. Grijpma, G.H.M. Engbers, J. Feijen *Enhanced bone marrow stromal cell adhesion and growth on segmented poly(ether ester)s based on poly(ethylene oxide) and poly(butylene terephthalate)* Biomacromolecules **2003**, 4, 57-63. Chapter 4 of this thesis.
15. M.B. Olde Riekerink, M.B. Claase, G.H.M. Engbers, D.W. Grijpma, J. Feijen *Gas plasma etching of PEO/PBT segmented block copolymer films* J. Biomed. Mater. Res **2003**, 65A, 417-428.

16. M.B. Claase, D.W. Grijpma, S.C. Mendes, J.D. de Bruijn, J. Feijen *Porous PEOT/PBT scaffolds for bone tissue engineering: preparation, characterization and in vitro bone marrow cell culturing* J. Biomed. Mater. Res **2003**, 64A, 291-300. Chapter 5 of this thesis.
17. T. Livingston, P. Ducheyne, J. Garino *In vivo evaluation of a bioactive scaffold for bone tissue engineering* J. Biomed. Mater. Res. **2002**, 62, 1-13.
18. S.L. Ishaug-Riley, G.M. Crane, A. Gurlek, M.J. Miller, A.W. Yasko, M.J. Yaszemski, A.G. Mikos *Ectopic bone formation by marrow stromal osteoblast transplantation using poly(DL-lactic-co-glycolic acid) foams implanted into the rat mesentery* J. Biomed. Mater. Res. **1997**, 36, 1-8.
19. S.C. Mendes, J. Bezemer, M.B. Claase, D.W. Grijpma, G. Bellia, F. Degli-Innocenti, R.L. Reis, K. de Groot, C.A. van Blitterswijk, J.D. de Bruijn *Evaluation of two biodegradable polymeric systems as substrates for bone tissue engineering* Tissue Eng. **2003**, 9, S91-S103.
20. Q. Hou, D.W. Grijpma, J. Feijen *Porous polymeric structures for tissue engineering prepared by a coagulation, compression moulding and salt leaching technique* Biomaterials **2003**, 24, 1937-1947.
21. C. Maniopoulos, J. Sodek, A.H. Melcher *Bone-formation in vitro by stromal cells obtained from bone marrow of young-adult rats* Cell Tissue Res. **1988**, 254, 317-330.
22. J.D. de Bruijn *Unpublished data* Isotis OrthoBiologics, Bilthoven, The Netherlands **2003**.
23. H.P. Yuan, M. van den Doel, S.H. Li, C.A. van Blitterswijk, K. de Groot, J.D. de Bruijn *A comparison of the osteoinductive potential of two calcium phosphate ceramics implanted intramuscularly in goats* J. Mater. Sci.-Mater. Med. **2002**, 13, 1271-1275.
24. T.L. Livingston, S. Gordon, M. Archambault, S. Kadiyala, K. McIntosh, A. Smith, S.J. Peter *Mesenchymal stem cells combined with biphasic calcium phosphate ceramics promote bone regeneration* J. Mater. Sci.-Mater. Med. **2003**, 14, 211-218.
25. T. Hildebrand, P. R  gegger *A new method for the model independent assessment of thickness in three-dimensional images* J. Microsc. **1997**, 185, 67-75.
26. W.E. Lorensen, H.E. Cline *Marching cubes: a high resolution 3D surface construction algorithm*. Comput. Graph. **1987**, 21, 163-169.
27. H.J. Wang, C.A. van Blitterswijk, J. Pieper, F. P  ters, E.N. Lamme *Synthetic scaffold morphology controls human connective tissue formation* Biomaterials **2003**, submitted for publication and H.J. Wang *Dermal tissue engineering*, Thesis, University of Twente, Enschede, The Netherlands **2003**.
28. H. Ohgushi, Y. Dohi, T. Katuda, S. Tamai, S. Tabata, Y. Suwa *In vitro bone formation by rat marrow cell culture* J. Biomed. Mater. Res. **1996**, 32, 333-340.
29. S.J. Peter, C.R. Liang, D.J. Kim, M.S. Widmer, A.G. Mikos *Osteoblastic phenotype of rat marrow stromal cells cultured in the presence of dexamethasone,  $\beta$ -glycerolphosphate, and L- ascorbic acid* J. Cell. Biochem. **1998**, 71, 55-62.
30. D.J. Rickard, T.A. Sullivan, B.J. Shenker, P.S. Leboy, I. Kazhdan *Induction of rapid osteoblast differentiation in rat bone-marrow stromal cell-cultures by dexamethasone and BMP-2* Dev. Biol. **1994**, 161, 218-228.
31. A.S. Goldstein, T.M. Juarez, C.D. Helmke, M.C. Gustin, A.G. Mikos *Effect of convection on osteoblastic cell growth and function in biodegradable polymer foam scaffolds* Biomaterials **2001**, 22, 1279-1288.
32. Handbook of biochemistry and molecular biology, Nucleic acids, volume II, 3 rd ed.; G.D. Fasman, Ed.; CRC Press: Cleveland, U.S.A., **1976**.
33. K.J.L. Burg, W.D. Holder, C.R. Culberson, R.J. Beiler, K.G. Greene, A.B. Loeb sack, W.D. Roland, P. Eiselt, D.J. Mooney, C.R. Halberstadt *Comparative study of seeding methods for three-dimensional polymeric scaffolds* J. Biomed. Mater. Res. **2000**, 51, 642-649.
34. V.I. Sikavitsas, G.N. Bancroft, A.G. Mikos *Formation of three-dimensional cell/polymer constructs for bone tissue engineering in a spinner flask and a rotating wall vessel bioreactor* J. Biomed. Mater. Res. **2002**, 62, 136-148.
35. J. Mahmood, H. Takita, Y. Ojima, M. Kobayashi, T. Kohgo, Y. Kuboki *Geometric effect of matrix upon cell differentiation: BMP- induced osteogenesis using a new bioglass with a feasible structure* J. Biochem. (Tokyo) **2001**, 129, 163-171.
36. C.A.L. Bassett, I. Hermann *Influence of oxygen concentration and mechanical factors on differentiation of connective tissues in vitro* Nature **1961**, 190, 460-461.
37. M.C. Wake, C.W. Patrick, A.G. Mikos *Pore morphology effects on the fibrovascular tissue-growth in porous polymer substrates* Cell Transplant. **1994**, 3, 339-343.
38. W.D. Holder, H.E. Gruber, A.L. Moore, C.R. Culberson, W. Anderson, K.J.L. Burg, D.J. Mooney *Cellular ingrowth and thickness changes in poly-L-lactide and polyglycolide matrices implanted subcutaneously in the rat* J. Biomed. Mater. Res. **1998**, 41, 412-421.





# Chapter 7

## Ectopic bone formation in cell-seeded poly(ethylene oxide)/poly(butylene terephthalate) copolymer scaffolds: II. Effects of porosity \*

*Biology is the search for the chemistry that works.*

R.P.J. Williams (1926- )

### Abstract

Scaffolds were prepared by methods involving compression molding and salt leaching of copolymers based on poly(ethylene oxide) and poly(butylene terephthalate), PEOT/PBT, with a PEO molecular weight of 1000 and a PEOT content of 70 weight % (1000PEOT70PBT30). Based on previous  $\mu$ -CT analyses, it was concluded that the accessible pore volume (expressed as a fraction of the total volume) is a factor that could influence the amount of in vivo formed bone and bone marrow in cell-seeded and cultured 1000PEOT70PBT30 scaffolds. To vary the fraction of accessible pore volume the scaffold porosity can be changed by adjusting the polymer to salt content ratio in the preparation of the scaffolds.

In this study gas plasma treated porous 1000PEOT70PBT30 structures seeded with rat bone marrow stromal cells (BMSCs, after in vitro culture for 7 d in an osteogenic medium) of 73.5, 80.6 and 85.0 % porosity were subcutaneously implanted for 4 wks in nude mice. All scaffolds were prepared using leachable salt crystals of 425-500  $\mu$ m to obtain scaffolds with a constant pore size. Poly(D,L-lactide) (PDLLA) and biphasic calcium phosphate (BCP) scaffolds were included in the study as references. After 4 wks implantation in nude mice all scaffolds showed ectopic formation of bone and bone marrow. The amounts of tissue were evaluated and quantified by histomorphometry. No significant differences were observed in the relative amounts of bone (7-9 %) and bone marrow (6-11 %) in the middle cross sections of the 1000PEOT70PBT30 scaffolds, even though  $\mu$ -CT data showed considerable differences

---

\*Menno B. Claase<sup>1</sup>, Sanne Both<sup>2</sup>, Mirella van den Doel<sup>2</sup>, Joost D. de Bruijn<sup>2</sup>, Dirk W. Grijpma<sup>1</sup>, Jan Feijen<sup>1</sup>

Submitted for publication in J. Biomed. Mater. Res. 2004

1) Institute for Biomedical Technology (BMTI) and Department of Polymer Chemistry and Biomaterials, Faculty of Science and Technology, University of Twente, P.O. Box 217, 7500 AE Enschede, The Netherlands

2) Isotis OrthoBiologics, P.O. Box 98, 3720 AB Bilthoven, The Netherlands

in accessible pore volume (as a fraction of the total volume) and accessible surface area. 1000PEOT70PBT30 scaffolds with a porosity of 85.0 % lacked sufficient rigidity and could not maintain their original shape *in vivo*. Surprisingly, 1000PEOT70PBT30 scaffolds with a porosity of 73.5 % showed cartilage formation. Although the effect of scaffold stiffness cannot be excluded, the observed cartilage formation is most likely due to poorly accessible pores in the scaffolds, as was observed in histological sections.  $\mu$ -CT data showed a considerably smaller accessible pore volume (as a fraction of the total volume) of 1000PEOT70PBT30 scaffolds of 73.5 % porosity, than of 1000PEOT70PBT30 scaffolds of 80.6 and 85.0 % porosity.

PDLLA scaffolds show considerably more bone marrow formation (38 %) and less wound exudate retention than the 1000PEOT70PBT30 scaffolds. BCP scaffolds also show considerably more bone and bone marrow formation (23 and 40 % respectively) and less fibrous tissue ingrowth and wound exudate retention than the 1000PEOT70PBT30 scaffolds.

## Introduction

When damaged, bone has a unique self-repairing capability that is in several ways similar to embryonic bone formation, and involves three stages: inflammation, followed by repair and remodeling.<sup>[1,2]</sup> Large defects, however, do not heal spontaneously and require surgical intervention for restoration. Besides established techniques like autografting and allografting, the rapidly developing field of tissue engineering offers advantageous approaches for defect repair.

Bone marrow contains a small population of stromal cells capable of differentiating into bone, cartilage, muscle, tendon and other connective tissues.<sup>[3]</sup> The *in vitro* culture of (rat) bone marrow stromal cells (BMSCs) in an osteogenic medium containing dexamethasone,  $\beta$ -glycerophosphate and L-ascorbic acid greatly increases the amount of cells with an osteoblastic phenotype.<sup>[4-7]</sup> In many systems, seeding of BMSCs (after expansion in culture) on a porous scaffold, followed by a period of *in vitro* cell culture in an osteogenic medium prior to implantation, resulted in enhanced ectopic bone formation compared to scaffolds that were seeded and implanted immediately.<sup>[8,9]</sup>

As scaffold materials, porous polymers have attracted much attention.<sup>[10]</sup> Due to the vast variety of preparation techniques, many different polymeric scaffold architectures can be obtained. The mechanical and physical properties of poly(ethylene oxide)/poly(butylene terephthalate) (PEOT/PBT) segmented block copolymers can be tuned by varying the PBT (hard segment) content and PEO (soft segment) content and molecular weight.<sup>[11,12]</sup> These properties make these copolymers interesting candidates for use as scaffold materials in (bone) tissue engineering. Several subcutaneous and intra-bone (tibia) implantations of dense and porous blocks and porous films in rats and goats showed bonding to bone, calcification and degradation for PEOT/PBT copolymers with high PEO content (60 and 70 weight % PEO containing soft segment, PEO molecular weight 1000).<sup>[13-17]</sup> Poor bone bonding, limited calcification and limited fragmentation were, however, observed after implantation of porous blocks of the composition with 70 weight % PEOT soft segment and PEO molecular weight 1000 (1000PEOT70PBT30) in goat<sup>[18]</sup> and human<sup>[19]</sup> ilia critical size defects. It is anticipated that seeding 1000PEOT70PBT30 scaffolds with BMSCs will result in structures with an osteoinductive effect<sup>[20]</sup>, that are better suited for bone tissue engineering than the scaffolds without BMSCs.<sup>[21,22]</sup> To enable *in vitro* BMSC attachment to the 1000PEOT70PBT30 copolymers a gas plasma surface treatment is necessary.<sup>[23-26]</sup> Subcutaneous implantation in nude mice of rat BMSC seeded porous 1000PEOT70PBT30 scaffolds (cultured for 7 d in an

osteogenic medium) of 75 % porosity, prepared with leachable salt particles of 400-600  $\mu\text{m}$ , showed bone formation to an extent that was comparable to the amounts found for hydroxyapatite particles, that were also seeded with rat BMSCs and cultured for 7 d in an osteogenic medium.<sup>[27]</sup>

In a previous study the effect of the pore structure of 1000PEOT70PBT30 scaffolds on ectopic bone formation was investigated by employing 1000PEOT70PBT30 scaffolds with a porosity of approximately 80 %, prepared with salt particles of different size ranges (250-425, 425-500, 500-710 and 710-1000  $\mu\text{m}$ ).<sup>[28]</sup> The obtained micro computed tomography data of these scaffolds was analyzed using an algorithm mimicking mercury intrusion porosimetry, where a simulated sphere of increasing diameter ( $d$ ) is moved through the structure. For simulated sphere diameters ( $d$ ) up to 100-150  $\mu\text{m}$ , no considerable differences in the accessible pore volume (as a fraction of the total pore volume) of the different 1000PEOT70PBT30 scaffolds was observed. A poly(D,L-lactide) (PDLLA) scaffold of higher porosity (83.5 %) had a larger accessible pore volume (for sphere diameters ( $d$ ) up to 100-150  $\mu\text{m}$ ) than the less porous 1000PEOT70PBT30 scaffolds. Although the influence of the stiffer PDLLA scaffold material could not be excluded, it appears that the accessible pore volume (as a fraction of the total volume) can be of influence on ectopic bone formation. The accessible pore volume can be influenced by changing the scaffold porosity.

So far, the porosity of these 1000PEOT70PBT30 scaffold materials has not been optimized for bone tissue engineering. Using a combined technique of polymer powder/salt crystal mixing followed by compression molding and salt leaching, porous 1000PEOT70PBT30 scaffolds can be prepared. By varying the polymer powder to salt ratio, it is possible to obtain stable porous structures with porosities ranging from 75 to 85 %, prepared with leachable salt crystals with sizes up to 1000  $\mu\text{m}$ .<sup>[25]</sup>

To study the effect of accessible pore volume (expressed as a fraction of the total volume) on ectopic bone formation and to optimize the porosity, gas plasma treated porous 1000PEOT70PBT30 structures seeded with rat BMSCs (and in vitro cultured for 7 d in an osteogenic medium) of 73.5, 80.6 and 85.0 % porosity were subcutaneously implanted in nude mice. The ectopic formation of bone and bone marrow, as well as other tissues, was evaluated and quantified by histomorphometry.

## Materials and methods

### Materials

*1000PEOT70PBT30 copolymer.* The copolymer was prepared by two-step polycondensation in the presence of titanium tetrabutoxide (Merck, Germany) as catalyst (0.1 wt %) as previously described<sup>[11]</sup>, with the exception that vitamin E (Sigma-Aldrich, Germany, approx. 95 % pure) was used as antioxidant. The composition is indicated as  $a\text{PEOT}b\text{PBT}c$ , where  $a$  is the starting poly(ethylene glycol) molecular weight,  $b$  the weight percentage of PEOT soft segments and  $c$ , the weight percentage of PBT hard segments.<sup>[11]</sup> The copolymer composition was determined by  $^1\text{H-NMR}$  (Varian Inova 300 MHz) and a soft to hard segment ratio of 71 to 29 was found. The copolymer was used as prepared.

*PDLLA.* PDLLA was obtained from Purac (Gorinchem, The Netherlands), inherent viscosity: 2.96 dL/g (chloroform, 25  $^{\circ}\text{C}$ , concentration 0.1 g/dL). The polymer was dissolved in chloroform and precipitated in a tenfold excess of technical grade ethanol to remove residual monomer. The precipitate was dried overnight under reduced nitrogen pressure in a vacuum oven and subsequently for 6 h at high vacuum.

*Porous structures prepared by compression molding of polymer/salt mixtures followed by salt leaching.* Both 1000PEOT70PBT30 copolymer granulate and PDLA copolymer precipitate were cryogenically ground using an IKA Labortechnik (Germany) A10 grinder. Polymer particles and sodium chloride crystals (Merck, Germany) were sieved using Endecotts (United Kingdom) test sieves of 250, 425, 500, 710, 1000 and 1180  $\mu\text{m}$  mesh size. The desired salt volume fractions (425-500  $\mu\text{m}$  particle size) were calculated using a salt density of 2.165  $\text{g}/\text{cm}^3$ . To obtain stable porous structures, the size of the polymer particles needs to be smaller than the size of the salt crystals used. The powders were mixed and subsequently compression molded in a laboratory hot press (THB 008, Fontijne Holland BV, The Netherlands) into 4 mm thick blocks. Mixed powders were heated at 180  $^{\circ}\text{C}$  for 3 min and subsequently pressed for 1 min at 2.9 MPa. Samples were leached with milliQ water for 48 h and dried under reduced nitrogen pressure in a vacuum oven. From the obtained blocks scaffolds of 4×4×4 mm were cut using a razor blade.

*Density determination of porous structures.* Density and porosity were determined by measurement of scaffold mass and dimensions (volume) in the dry state. The porosity was calculated using the following densities of the solid materials 1000PEOT70PBT30:  $\rho = 1.188 \text{ g}/\text{cm}^3$ , PDLA:  $\rho = 1.26 \text{ g}/\text{cm}^3$ .<sup>[29]</sup>

*CO<sub>2</sub> gas plasma treatment.* 1000PEOT70PBT30 porous structures were gas plasma treated for 30 min, according to a previously described procedure.<sup>[26]</sup> Discharge power was 50 W and the CO<sub>2</sub> gas-plasma pressure was 0.06 mbar. A gas flow of 10  $\text{cm}^3/\text{min}$  was used. Samples were treated with a pre-delay of 2 min and a post-delay of 2 min.

*OsSatura<sup>TM</sup> BCP granules.* Bicalcium phosphate granules were characterized by mercury intrusion porosimetry and provided by Isotis OrthoBiologics (Bilthoven, The Netherlands).

### Cell culturing and implantation

*Rat bone marrow stromal cell culturing.* Bone marrow stromal cells were isolated from 16 femora of 8 young male Wistar-rats (100-120 g). The osteogenic culture medium was minimal essential medium ( $\alpha$ -MEM, Life Technologies, The Netherlands) containing<sup>[4]</sup>: 15 % fetal bovine serum (Life Technologies, The Netherlands), 100 units/mL penicillin, 100  $\mu\text{g}/\text{mL}$  streptomycin (Life Technologies, The Netherlands), 2 mM L-glutamine (Life Technologies, The Netherlands), 0.2 mM ascorbic acid 2-phosphate (Life Technologies, The Netherlands), 10 mM  $\beta$ -glycerophosphate (Sigma, The Netherlands), 10<sup>-8</sup> M dexamethasone (Sigma, The Netherlands).

The femora were cut on both sides and the marrow was flushed out using 5 mL of medium per femur. The collected cells were re-suspended and cultured in T 75 standard tissue culture flasks (Nunc, Germany) at 37  $^{\circ}\text{C}$ , 5 % CO<sub>2</sub> for 6 d, with periodic medium changes every other day. After 6 d, the cells were confluent and were washed with PBS (Life Technologies, The Netherlands) and treated with 0.25 % trypsin/EDTA (Sigma, The Netherlands). The collected cell suspension contained 3.6×10<sup>7</sup> rat BMSCs. The suspension was centrifuged at 300×g for 10 min at room temperature and resuspended in medium to obtain a cell concentration of 6.7 × 10<sup>5</sup> cells/mL.

*Cell seeding and growth on porous scaffolds.* Scaffolds were placed in bacteriological well plates (Nunc, Germany) and washed with: distilled water, 100 % ethanol, distilled water, 70 % ethanol/water and 3x sterile PBS. Due to swelling in ethanol, PDLA scaffolds were washed with isopropanol. The scaffolds were put in culture medium overnight and seeded with 2×150  $\mu\text{L}$  of cell suspension (approximately 2×10<sup>5</sup> cells per scaffold). Cell suspensions were injected into the scaffolds with a pipette tip. Scaffolds were incubated at 37  $^{\circ}\text{C}$  for 3 h, after which 2 mL of cell culture medium was added. Cells were cultured at 37  $^{\circ}\text{C}$ , 5 % CO<sub>2</sub> for 7 d, with

periodic medium changes every other day. At day 7 the samples were either implanted or analyzed using SEM or a DNA assay.

*In vivo implantation.* Cell-seeded and cultured scaffolds were soaked in serum-free medium and washed with prewarmed PBS (37 °C) before implantation. Six immunodeficient mice (HsdCpb:NMRI-nu) were anaesthetized using a mixture of ketamine/xylazine and atropine, the surgical sites were cleaned with ethanol and subcutaneous pockets were created using blunt incisions. Six sites were created per mouse (3 on each side of the spine) and scaffolds were implanted according to a randomized scheme. After 4 wks the mice were sacrificed by asphyxiation with CO<sub>2</sub> gas. Scaffolds were removed and fixed with glutaraldehyde (Merck, Germany, 1.5 % solution in 0.14 M cacodylic acid buffer, pH = 7.35).

One mouse died prematurely and the implanted scaffolds were excluded from the experiment. For each of the 1000PEOT70PBT30 scaffolds 5 samples were analyzed, unless otherwise mentioned. BCP granules with an approximate diameter of 4-5 mm were used for implantation as positive controls.<sup>[30-32]</sup>

### Analyses

*Compression testing.* Compression moduli were determined at room temperature using a Zwick Z020 tensile tester. Moduli were measured at 10 % strain at a strain rate of 2 mm/min with a 0.1 N preload. The scaffolds had a diameter of 17 mm and a height of 8 mm. Results are averages of at least three measurements ( $\pm$  s.d.).

*Micro computed tomography.* Dry, unseeded scaffolds were scanned before gas plasma treatment without further sample preparation with a desktop Micro-CT ( $\mu$ CT-40, Scanco Medical, Bassersdorf, Switzerland) at a resolution of 12  $\mu$ m in all three spatial dimensions (X-Ray voltage 45 kVp), with the exception of the BCP and PDLLA scaffolds, which were scanned at a resolution of 20  $\mu$ m. Of every scaffold 300 slices were scanned with 1024x1024 pixels per slice, covering a depth of 3.6 mm. For evaluation, volumes of interest slightly smaller than the diameter of the sample (approximately 4x4x4 mm) were chosen to exclude crushed boundaries. The resulting gray-scale images were segmented using a low-pass filter to remove noise, and a fixed threshold to extract the polymer phase.

For the 3D evaluation of the structure of the scaffold, 'direct' three-dimensional techniques without model-assumptions for the appearance of the structure were used. Pore voxels can be defined as voxels corresponding to the void space and polymer voxels as voxels corresponding to the polymer phase.

Porosity and pore size. In  $\mu$ -CT data analysis, the porosity can be calculated from the number of polymer voxels and the total number of voxels. To determine the pore size, pores are completely filled with modelled spheres of different diameters. The pore diameter assigned to a pore voxel is then the diameter of the largest sphere (still containing that pore voxel) that fits inside the pore.<sup>[33]</sup> In the case of cubic pores, however, as is the case in this study, this underestimates the pore size assigned to pore voxels present in the corners of these pores. Therefore, the algorithm was modified to assign the diameter of the largest sphere fitting in the pore to all voxels within that pore.

The average pore size is calculated by averaging the product of the pore voxels with their assigned pore diameters over the total amount of pore voxels, according to the formula:<sup>[33]</sup>

$$\text{Average pore size} = \frac{\sum_i (\text{pore voxel}_i \times \text{pore size}_i)}{\sum_i \text{pore voxel}_i} \quad (7.1)$$

Accessible pore volume. An algorithm mimicking mercury intrusion porosimetry, by use of a simulated sphere with diameter ( $d$ ), was used to determine the accessible pore volume. Using a thresholding operation, all the pores not accessible for the sphere with diameter ( $d$ ) are suppressed. All pores of this thresholded structure not (inter)connected to the outside of the scaffold are discarded with a component labelling operation. The volume of the resulting pore structure is calculated, and plotted versus sphere diameter ( $d$ ), resulting in a graph of accessible pore volume (as a fraction of the total volume) versus sphere diameter ( $d$ ).

Accessible surface area. The surface area of the accessible pore volume as a function of sphere diameter ( $d$ ), was calculated using a triangularization algorithm.<sup>[34]</sup> The calculated surface consists of triangular surfaces contacting the scaffold and triangular surfaces not contacting the scaffold. Triangular surfaces not contacting the scaffold are suppressed, resulting in a surface area of the pore volume of the scaffold that is accessible for the simulated sphere of diameter ( $d$ ).

*Scanning Electron Microscopy (SEM).* Scaffolds containing rat BMSCs were fixed and dehydrated using an ethanol/water gradient (isopropanol for PDLLA). Dehydrated samples were dried using a Balzers CPD 030 critical point dryer before coating. The PDLLA scaffolds were air dried. Samples were coated with Au/Pd in a Polaron E5600 sputter coater. Pictures were taken with a Hitachi FE-SEM S-800 (6.0 kV).

*DNA-assay.* Scaffolds were washed with PBS at 37 °C and stored in a freezer (-80 °C) until further analysis. Scaffolds were cut in at least 4 pieces (except BCP granules) and incubated at 56 °C overnight in 0.5 mL of lysis-medium to lyse all cells. The lysis-medium consisted of proteinase K (Sigma, The Netherlands) in Tris/EDTA buffer (1 mg/mL, pH = 7.6).

The next day 250  $\mu$ L of these suspensions were mixed with 250  $\mu$ L RNase-solution. The RNase solution was prepared from 30  $\mu$ L RNase (Sigma, The Netherlands, 1.35 Kunitz units/ $\mu$ L) and 50  $\mu$ L heparin (Leopharma, The Netherlands, 5,000 IE/mL) in 12.5 mL PBS, and incubated at 37 °C for 60 min to remove single stranded RNA and DNA. Various dilutions were prepared with PBS. Dilutions were mixed with CyQUANT<sup>®</sup> dye. After 15 min, the fluorescence of the solutions in 96 well plates was measured using a Perkin Elmer Luminescence Spectrometer LS 50 B (excitation at 480 nm, slit width 2.5 nm, emission at 520 nm, slit width 4.5 nm). The measured fluorescence intensities were correlated to the amount of DNA using a calibration curve of DNA (Sigma) dilutions of known concentration. Data shown are the result of triplicate measurements ( $\pm$  s.d.).

*Histology/histomorphometry.* After 3 d in fixative, scaffolds were dehydrated using an ethanol/water gradient (isopropanol/water for PDLLA) and subsequently embedded in poly(methyl methacrylate) (PMMA). Sections were prepared using a histological diamond saw (Leica SP1600, Leica, Germany) and stained using 1 % methylene blue and 0.3 % basic fuchsin solutions. Samples were investigated using a Nikon SM2-10A stereomicroscope (0.75 and 1 $\times$  objective). For higher magnifications a Nikon Eclipse E600 with objectives 4-50 $\times$  was used. Digital photographs were taken using a Q Image Reticon 1000 camera.

To determine the relative amounts of tissue formed, the relative areas of the different tissues were calculated from the number of pixels as determined with Scion Image (version beta 4.02 for Windows, Scion Corporation, USA). Sections from the middle part of the scaffolds were analyzed at high magnifications and the relative amounts of the different tissues were calculated with respect to the porosity of the cross section (area of the cross sections corresponding to the pores). Data shown are the average of 5 scaffolds  $\pm$  s.d. unless otherwise mentioned.

*Statistical analysis.* Results were analyzed using one-way ANOVA, followed by a Games Howell post-hoc test. Results were considered statistically different when  $p < 0.05$ . ANOVA calculations were performed using SPSS software for Windows (version 11.0, SPSS, USA).

## Results and discussion

To study the effect of scaffold porosity on in vivo bone formation, 6 different scaffolds, seeded with rat BMSCs and cultured in vitro for 7 d in an osteogenic medium, were subcutaneously implanted in immunodeficient nude mice (4 wks) and evaluated for tissue formation. The used scaffolds and some of their main characteristics are summarized in Table 7.1. Three different 1000PEOT70PBT30 scaffolds differing in porosity (scaffolds A, B and C) were gas plasma treated using a CO<sub>2</sub> plasma. Gas plasma treatment of these 1000PEOT70PBT30 scaffolds has been shown to be an essential step to enable in vitro BMSC attachment to this specific material.<sup>[23-26]</sup> Untreated 1000PEOT70PBT30 (scaffold F) seeded with rat BMSCs and cultured for 7d in an osteogenic medium, was therefore used as a negative control for in vivo bone formation. For comparison scaffolds were also prepared from PDLA (scaffold D), a well-known biomaterial. Cell-seeded and cultured biphasic calcium phosphate (OsSatura<sup>TM</sup> BCP, scaffold E) was used as a positive control for in vivo bone formation to confirm the osteogenic potential of the cells used.<sup>[30-32]</sup>

As previously reported, the actual porosity of the prepared scaffolds is higher than could be expected on the basis of the used salt volume.<sup>[25]</sup> For the 1000PEOT70PBT30 scaffolds, a large decrease in compression modulus is observed with increasing porosity, in line with the exponential decrease observed in previous experiments.<sup>[25]</sup>

Table 7.1 - Main characteristics of scaffolds to be used for cell seeding and implantation. Dry, unseeded scaffolds were scanned before gas plasma treatment.

Scaffold description	Salt fraction used (μm)	Salt volume used (%)	Average pore size from μ-CT (μm)	Porosity* from μ-CT (%)	Compression modulus (dry) (N/mm <sup>2</sup> )
A: 1000PEOT70PBT30 gas plasma treated <sup>†</sup>	425-500	60	318	69.8 (73.5 ± 0.5)	0.33 ± 0.02
B: 1000PEOT70PBT30 gas plasma treated	425-500	70	342	78.2 (80.6 ± 0.6)	0.14 ± 0.03
C: 1000PEOT70PBT30 gas plasma treated	425-500	80	311	81.6 (85.0 ± 0.6)	0.03 ± 0.01
D: PDLA not treated	425-500	80	407	81.7 (83.5 ± 0.7)	2 <sup>¶</sup>
E: OsSatura <sup>TM</sup> BCP not treated	382 <sup>‡</sup>	-	837	36.2 (29 <sup>§</sup> )	n.d.

\*: porosity as obtained from density measurements is shown in parentheses

†: scaffold F = A without gas plasma treatment

¶: approximate value based on reference [29]

‡: average pore size, as determined by mercury intrusion porosimetry, pores < 100 μm were excluded

§: average porosity, as determined by mercury intrusion porosimetry, pores < 100 μm were excluded

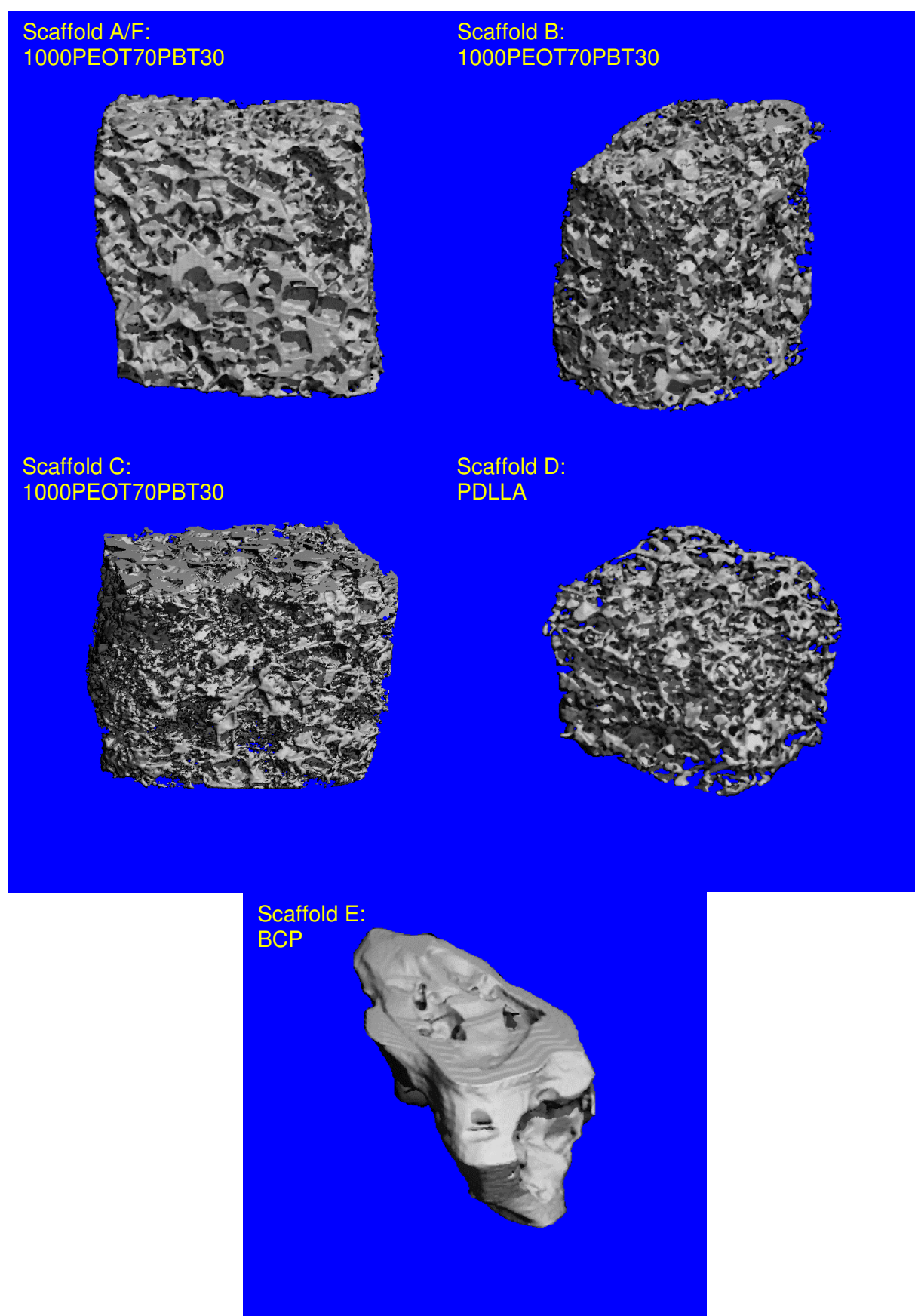


Figure 7.1 - 3D generated computer images constructed from  $\mu$ -CT scans of dry scaffolds, prior to gas plasma treatment and cell seeding. The images corresponding to scaffolds A, B, C, D, E and F (identical to A) as listed in Table 7.1 are shown. [Color figure on p. 176]



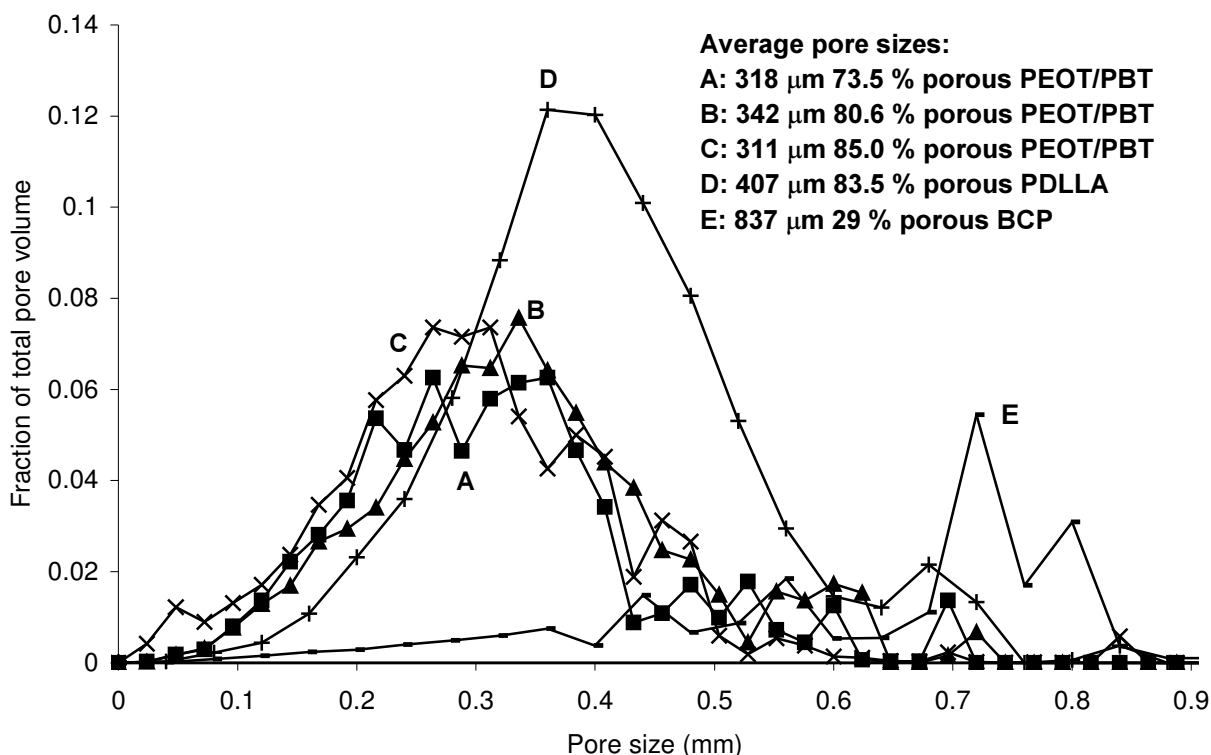


Figure 7.2 - Pore size distributions and average pore sizes derived from  $\mu$ -CT. Scaffolds A, B, C and D were prepared using salt crystals of 425-500  $\mu\text{m}$ . Scaffold F is identical to scaffold A.

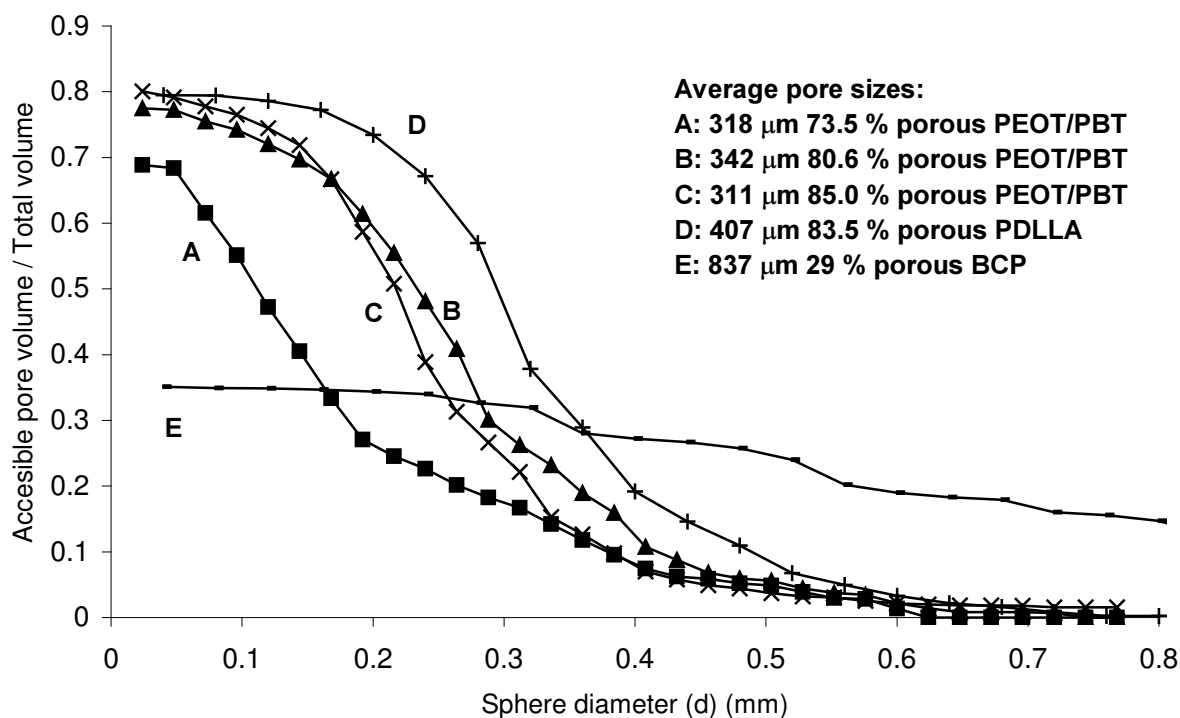


Figure 7.3 - Accessible pore volume (as a fraction of the total volume) versus sphere diameter ( $d$ ) for unseeded and dry scaffolds A-E. Notice the lower accessible pore volume of scaffold A.

The scaffolds (dry, prior to gas plasma treatment and cell seeding) were characterized using micro computed tomography ( $\mu$ -CT), resulting in computer generated 3D images, as shown in Figure 7.1. Besides 3D images, relevant parameters like scaffold porosity and pore size distribution were also calculated. As shown in Table 7.1, the porosity obtained from  $\mu$ -CT matches the values determined by density measurements quite well. Pore size distributions are plotted in Figure 7.2.

The pore size distributions of the 1000PEOT70PBT30 scaffolds A, B and C with pore sizes up to 648  $\mu\text{m}$  are very comparable, as could be expected for scaffolds prepared with salt of the same particle size. The pore size distributions of PDLLA (D) (pore sizes up to 760  $\mu\text{m}$ ) and BCP (E) (pore sizes up to 1000  $\mu\text{m}$ ) differ considerably from the distributions of the 1000PEOT70PBT30 scaffolds A, B and C.

The average pore sizes of the 1000PEOT70PBT30 scaffolds (318, 342 and 311  $\mu\text{m}$  for the scaffolds A, B, and C respectively) and the PDLLA scaffold (407  $\mu\text{m}$ ) are smaller than one would expect based on the size of the salt particles used (425–500  $\mu\text{m}$ ). In this study, however, the underestimation of the average pore size is less than in previous reports<sup>[35]</sup> due to an improved algorithm<sup>[28]</sup> more suitable for cubic pores, as is the case for scaffolds prepared by salt leaching.

The accessible pore volume of the scaffolds was determined using  $\mu$ -CT data, as described in the Materials and methods section. The resulting graphs of the accessible pore volume (given as a fraction of the total volume) versus the sphere diameter ( $d$ ) are shown in Figure 7.3. Even though the average pore sizes and pore size distributions are comparable, there are considerable differences in accessible pore volume (as a fraction of the total volume) of the 1000PEOT70PBT30 scaffolds.

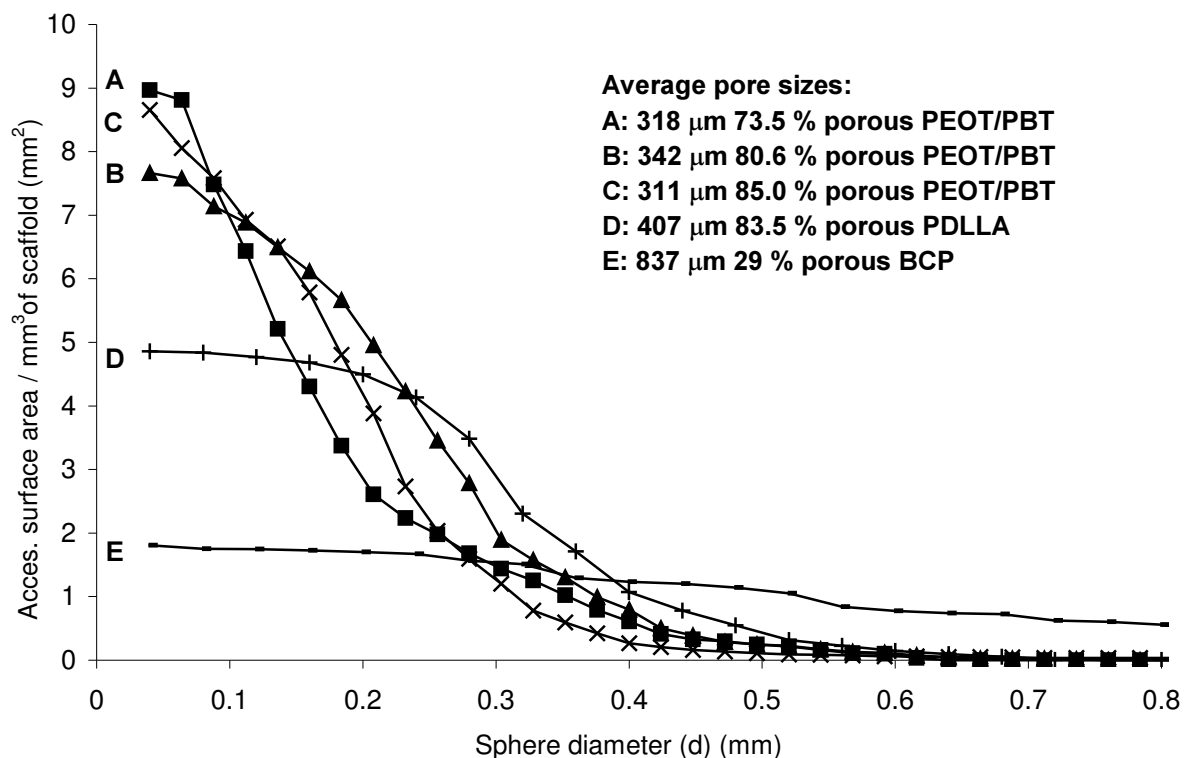


Figure 7.4 - Accessible surface area (normalized for the total volume) versus sphere diameter ( $d$ ) for unseeded and dry scaffolds A-E.

The curve for scaffold A shows that there is much less accessible pore volume at a sphere diameter ( $d$ ) smaller than 300  $\mu\text{m}$  than for the 1000PEOT70PBT30 scaffolds B and C and PDLLA scaffold D.

The accessible pore volume (as a fraction of the total volume) of the 1000PEOT70PBT30 scaffolds B and C is quite comparable, showing that the increase in scaffold porosity of 80.6 to 85.0 % does not result in a larger accessible pore volume. For all sphere diameters ( $d$ ) the accessible pore volume of PDLLA scaffold D is higher than (or equal to) the accessible pore volume of the 1000PEOT70PBT30 scaffolds.

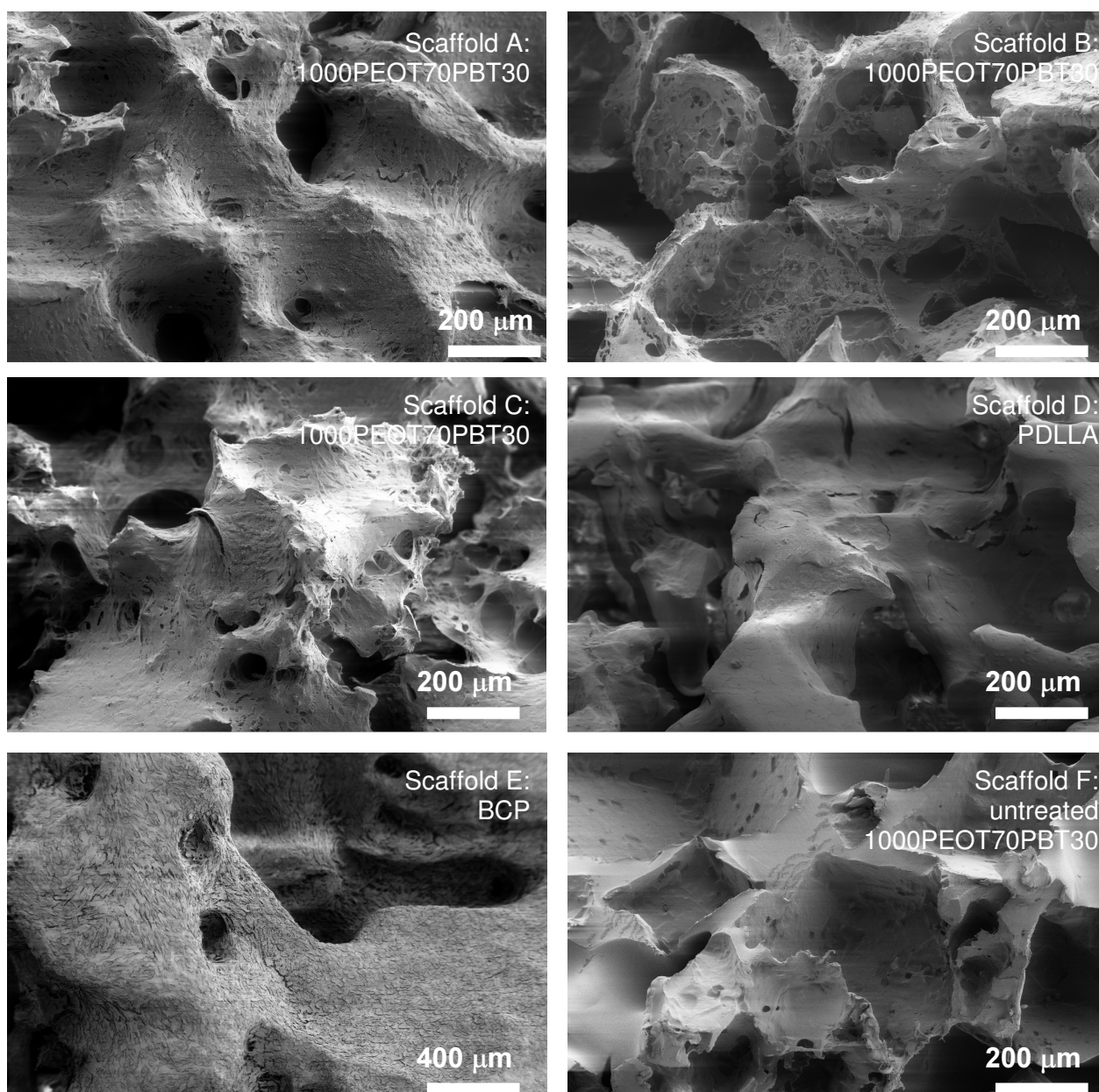


Figure 7.5 - SEM pictures of the rat BMSC seeded scaffolds after 7 d of in vitro cell culture. All scaffolds show well attached and spread rat BMSCs, except for the untreated 1000PEOT70PBT30 (scaffold F).

With increasing porosity one would expect a larger surface area available for the BMSCs to attach to and proliferate on. For simulated sphere diameters ( $d$ ) up to 100  $\mu\text{m}$

1000PEOT70PBT30 scaffold C of 85.0 % porosity indeed has a higher accessible surface area than scaffold B of 80.6 % porosity. Surprisingly scaffold A with the lowest porosity of 73.5 % shows the highest accessible surface area (for simulated spheres with a diameter (d) up to 100  $\mu\text{m}$ ) and PDLLA scaffold D of 83.5 % porosity shows the lowest accessible surface area of the polymeric scaffolds.

The average pore size is likely to be of influence here, resulting in larger surface areas for scaffolds (of comparable porosity) with smaller pore sizes, as previously observed in the accessible pore surface areas of 1000PEOT70PBT30 scaffolds with different pore sizes.<sup>[28]</sup>

Rat BMSCs were isolated from the femora of male Wistar rats and expanded in culture in an osteogenic medium containing dexamethasone.<sup>[4-7]</sup> First passage cells were seeded on the scaffolds (static seeding,  $2 \times 10^5$  cells/scaffold) and cultured for 7 d in an osteogenic medium. Figure 7.5 shows SEM pictures of the porous structures after 7 d of culture. The scaffolds show many well-attached BMSCs, except the untreated 1000PEOT70PBT30 scaffold F, on which almost no cells were observed. This is in line with our previous in vitro studies.<sup>[23-26]</sup>

At higher magnifications all scaffolds show a fiber-like network (not shown in Figure 7.5), most likely collagen. This indicates that prior to implantation the constructs consisted of a scaffold with cultured tissue-like material, forming an extracellular matrix.<sup>[27]</sup>

To obtain a quantitative insight in the amount of cells present on and in the different cell-seeded and cultured scaffolds, the amount of DNA in the scaffold was fluorometrically quantified using CyQuant<sup>®</sup> dye. The results are presented in Figure 7.6.

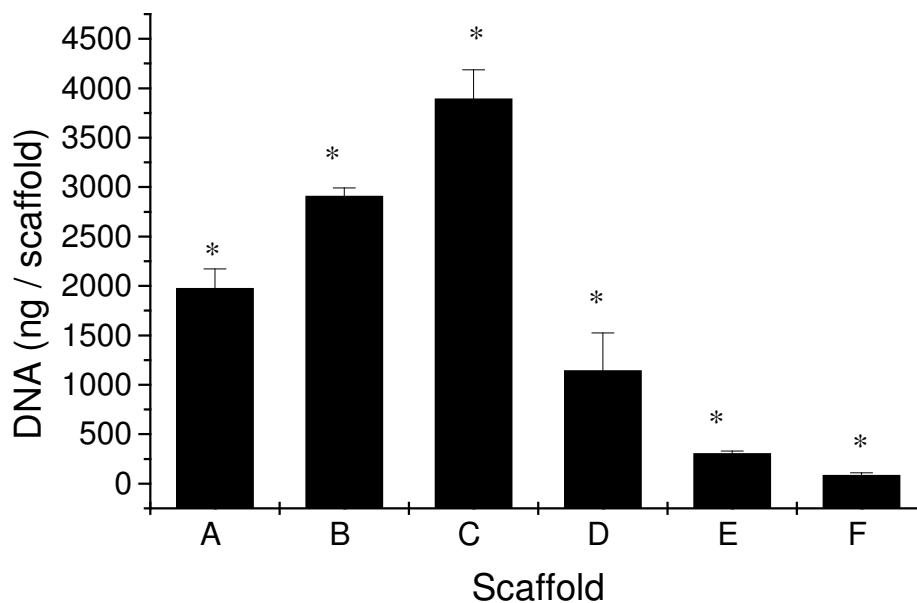


Figure 7.6 - Fluorometric quantification of DNA in the scaffolds after 7 d of in vitro rat BMSC culture (triplicate measurements). \*: Value significantly different from the other 5 scaffolds. A: 1000PEOT70PBT30, 73.5 % porous, average pore size 318  $\mu\text{m}$ , B: 1000PEOT70PBT30, 80.6 % porous, 342  $\mu\text{m}$ , C: 1000PEOT70PBT30, 85.0 % porous, 311  $\mu\text{m}$ , D: PDLLA, 83.5 % porous, 407  $\mu\text{m}$ , E: BCP, 29 % porous, average pore size: 837  $\mu\text{m}$ , F: 1000PEOT70PBT30, 73.5 % porous, untreated.



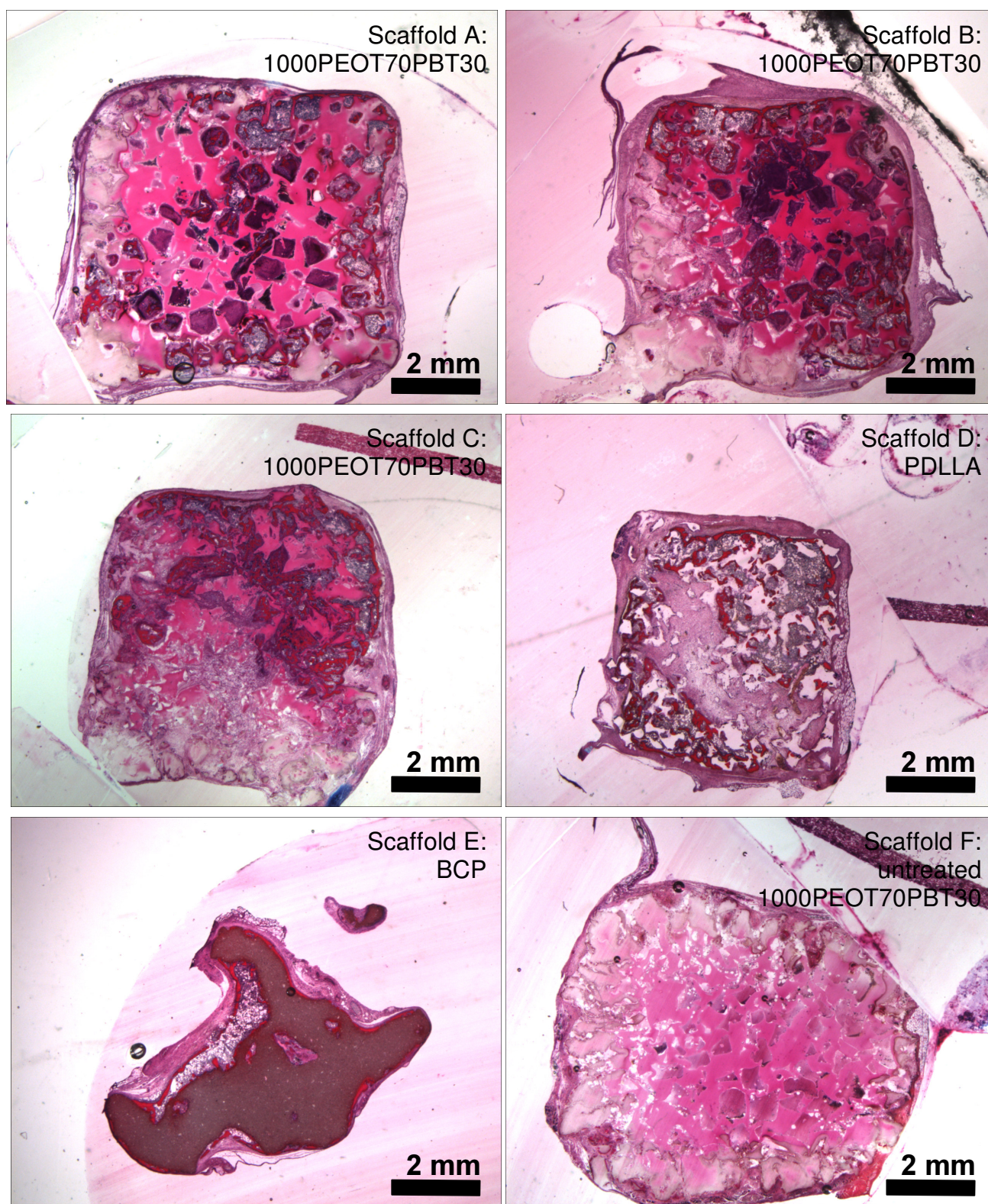


Figure 7.7 - Representative cross sections of scaffolds, seeded with rat BMSCs and cultured for 7d, after 4 wks of subcutaneous implantation. Sections shown were taken from the middle of the scaffolds and stained using methylene blue and basic fuchsin. 1000PEOT70PBT30 stains pink, whereas PDLLA appears transparent. All scaffolds (except F) show bone (dark red) and bone marrow (blue/gray) formation. Fibrous tissue and wound exudate stain pink. All scaffolds (except F) show bone and bone marrow formation. In addition scaffold A (1000PEOT70PBT30, porosity 73.5 %) shows the formation of cartilage (purple). [Color figure on p. 177]

The higher amounts of DNA present in scaffold C (85.0 % porosity), as compared to scaffold B (80.6 % porosity), reflect that with increasing porosity there is an increase in surface area for the cells to attach to and to proliferate on, in line with the previous  $\mu$ -CT observations concerning the accessible surface area. Interestingly enough scaffold A shows the smallest amount of DNA even though the  $\mu$ -CT data indicated that this scaffold has the largest accessible surface area (for sphere diameters (d) up to 100  $\mu$ m).

After 7 days of culture both the PDLLA and BCP scaffolds (D and E) contain a significantly lower amount of DNA (and hence cells) than the gas plasma treated 1000PEOT70PBT30 A, B and C scaffolds. The relatively low amount of DNA found in these experiments is likely due to the low accessible surface areas (as determined by  $\mu$ -CT) of these scaffolds. In line with the SEM observations in Figure 7.5 there is not much DNA (cells) present on untreated 1000PEOT70PBT30 scaffolds F.

To evaluate the bone induction potential of these rat BMSC seeded scaffolds (cultured in vitro for 7 d in an osteogenic medium) in vivo, they were implanted subcutaneously in the back of immunodeficient mice for a time period of 4 wks. At that time the samples (5 for each different scaffold) were removed, fixed, dehydrated and embedded in PMMA. After microtoming, the undecalcified sections were stained using methylene blue and basic fuchsin. This staining allows for the differentiation between bone, bone marrow, cartilage and fibrous tissue.<sup>[27]</sup>

Besides staining the different tissues present in the explants, basic fuchsin also stains the 1000PEOT70PBT30 scaffolds pink whereas PDLLA does not adsorb the dye. Representative middle sections of the different scaffolds, which were implanted in one mouse, are shown in Figure 7.7.

Although many histological sections showed concentrations of bone/bone marrow at one side of the scaffold, bone and bone marrow formation is not limited to the outside of the 1000PEOT70PBT30, PDLLA and BCP scaffolds, but was seen throughout the scaffolds. This was not the case in previous studies using porous PLGA scaffolds.<sup>[9]</sup> A more homogeneous distribution and/or better proliferation of stromal cells and hence bone tissue can be achieved by dynamic seeding<sup>[36]</sup> and culturing techniques.<sup>[37,38]</sup>

When comparing scaffold A, B and C not much difference is observed in terms of the amount of bone and bone marrow tissue formed (see Table 7.2). It was seen that several implants of scaffold C were severely distorted after explantation (data not shown). Porosity greatly affects the mechanical properties of a porous structure<sup>[25,29,39]</sup> and it seems that the rigidity of scaffold C (compression modulus of 0.03 N/mm<sup>2</sup>, Table 7.1) is insufficient for in vivo applications even in non-load bearing conditions. Depending on the stresses applied, it could still be a suitable scaffold for the in vitro culture of bone-like tissue in a bioreactor.

Scaffold E (BCP) clearly shows the ability of the used BMSCs to induce ectopic bone formation upon implantation, as bone and bone marrow are present at the surface of the scaffold. The negative control scaffold F (untreated 1000PEOT70PBT30, seeded with rat BMSCs and cultured for 7 d in an osteogenic medium) does not show any formation of bone or bone marrow. Typically these scaffolds were mainly filled with wound exudate and more or less infiltrated with fibrous tissue at the outside of the scaffold.

The different types of tissue were quantified using histomorphometry. The amounts of the different tissues were determined in middle cross sections of the different scaffolds (implanted in 5 fold) and averaged. The porosity (area of the cross sections corresponding to pores) and the amounts (relative areas) of the different formed tissues (normalized for the porosity) are shown in Table 7.2.

The histomorphometry data show a consistently lower porosity for the 1000PEOT70PBT30 scaffolds than one can expect based on the porosity values obtained by density measurements

or  $\mu$ -CT scans, while PDLLA and BCP scaffolds match those values fairly well. A possible explanation for this is the swelling of 1000PEOT70PBT30 in MMA during the embedding procedure for histological examination. As the volume of the scaffold is restricted by tissue, the area of the cross section corresponding to the pores (porosity) then decreases.

Table 7.2— Amounts (%) of bone, bone marrow, cartilage, fibrous tissue and wound exudate (as determined from the relative areas), normalized for the porosity. The porosity is the area of the cross section corresponding to the pores, given as the percentage of the total area of the microtomed scaffold section. The results are the average of 5 scaffolds ( $\pm$  s.d.), unless mentioned otherwise. Middle cross-sections of the explanted scaffolds were analyzed.

	Porosity <sup>†</sup> (%)	Bone (%)	Bone marrow (%)	Cartilage (%)	Fibrous tissue (%)	Wound exudate (%)
A 1000PEOT70PBT30 73.5 % porous	52.9 $\pm$ 10.3	7.2 $\pm$ 2.6	7.6 $\pm$ 4.5	4.7 $\pm$ 2.9	22.8 $\pm$ 6.8	35.5 $\pm$ 12.2 <sup>¶</sup>
B 1000PEOT70PBT30 80.6 % porous	65.8 $\pm$ 8.0	8.6 $\pm$ 5.0	6.4 $\pm$ 5.5	0.1 $\pm$ 0.2 <sup>§</sup>	58.0 $\pm$ 4.8	8.9 $\pm$ 5.9
C 1000PEOT70PBT30 85.0 % porous	68.6 $\pm$ 8.0	7.6 $\pm$ 3.8	11.3 $\pm$ 9.4	0	64.8 $\pm$ 10.7	0.2 $\pm$ 0.3
D <sup>‡</sup> PDLLA 83.5 % porous	79.7 $\pm$ 6.4	8.8 $\pm$ 2.1	38.3 $\pm$ 21.2	0	35.0 $\pm$ 14.0	0
E <sup>‡</sup> BCP 29 % porous	27.4 $\pm$ 7.1	23.4 $\pm$ 1.8 <sup>*</sup>	40.4 $\pm$ 8.9 <sup>#</sup>	0	8.4 $\pm$ 7.0	0.5 $\pm$ 0.6
F <sup>‡</sup> 1000PEOT70PBT30 73.5 % porous untreated	45.0 $\pm$ 6.3	0	0	0	28.9 $\pm$ 23.8	55.1 $\pm$ 25.3

†: determined by histomorphometry

¶: significantly higher than scaffolds B,C,D and E

§: cartilage only observed in 1 out of 5 samples

‡: average of 4 implants

\*: significantly higher than the other 5 scaffolds

#: significantly higher than scaffolds A,B,C and F

‡: average of 3 implants

The relative amounts of ectopic bone formed in the four different cell-seeded polymeric scaffolds are comparable and vary from 7 to 9 %. This is comparable to the relative amounts obtained from a study with 1000PEOT70PBT30 scaffolds of constant porosity (approximately 80 %) and prepared with salt crystals of 250-425, 425-500, 500-710 or 710-1000  $\mu$ m size range.<sup>[28]</sup> In addition, all 1000PEOT70PBT30, PDLLA and BCP scaffolds show bone marrow formation. The PDLLA scaffold contained considerably more bone marrow than the 1000PEOT70PBT30 scaffolds, even though at the time of implantation there was significantly less DNA (and hence cells) present in the PDLLA scaffold. Besides bone and bone marrow, fairly high amounts of fibrous tissue were observed in many of the scaffolds. It has been reported that the ingrowth of fibrous tissue took place in poly(L-lactic acid) scaffolds with pore sizes comparable to the pore sizes of our scaffolds.<sup>[40,41]</sup>

The observation of ectopic bone formation in the 1000PEOT70PBT30, PDLLA and BCP porous structures demonstrates their potential as scaffold materials for the tissue engineering of bone. The determined relative amounts of ectopic bone in the 1000PEOT70PBT30 scaffolds are considerably lower than the value of 36 % of bone previously reported by Mendes et al.<sup>[27]</sup> In that study, smaller scaffolds were used (3×3×2 mm, compared to 4×4×4



mm reported here) and with a same amount of cells ( $2 \times 10^5$  per scaffold) seeded, this results in a higher cell seeding density. At the time of implantation (after 7 d of in vitro culture) the amount of DNA from the cells present in/on the smaller scaffolds was also considerably higher, approximately 20.000 ng/scaffold compared to the 2.000 to 4.000 ng/scaffold reported here.

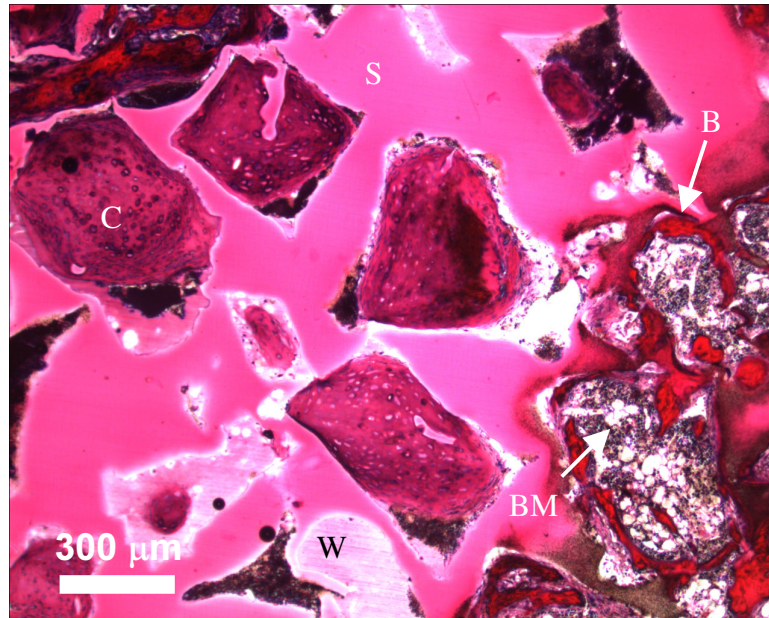


Figure 7.8 - Magnification of the cross-section shown in Figure 7.5 of scaffold A. Cartilage (C), bone (B), bone marrow (BM), wound exudate containing red blood cells (W) and scaffold material (S) are indicated. [Color figure on p. 178]

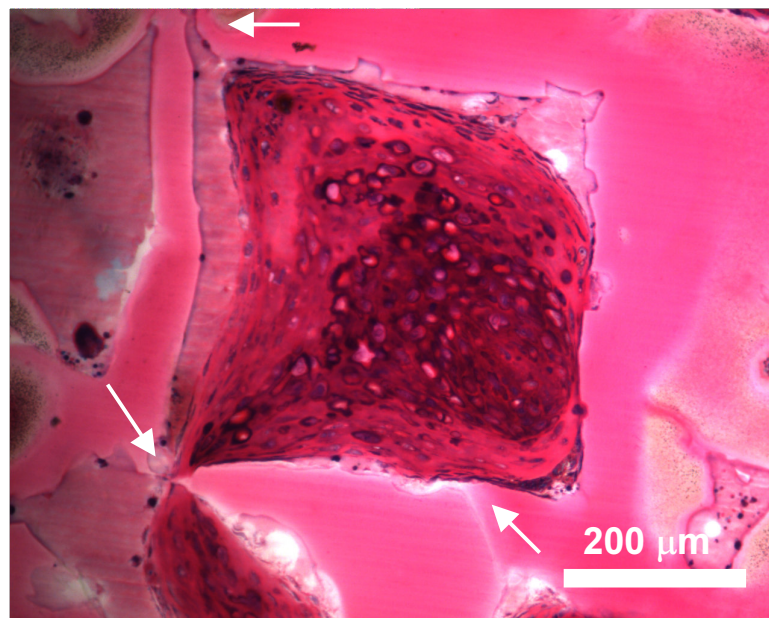


Figure 7.9 - Poorly interconnected pore containing cartilage. Interconnections to other pores are indicated with arrows. [Color figure on p. 179]



The amount of DNA determined can be influenced by the lysis conditions employed for the DNA assay.<sup>[28]</sup> Therefore one should be careful in directly comparing the obtained values.

The resulting amounts of bone and bone marrow in our 1000PEOT70PBT30 and PDLLA scaffolds are, however, higher than those for PLGA scaffolds reported by Ishaug-Riley et al.<sup>[9]</sup>, who observed  $3.8 \pm 2.4$  % of bone-like tissue in their scaffolds after 28 d of implantation. In that study the disc-like scaffolds (7 mm diameter, 1.9 mm height) were seeded with approximately  $2.6 \times 10^5$  rat BMSCs/scaffold and implanted after 7 d of in vitro cell culture. The scaffolds were 90 % porous with pore sizes ranging from either 150 to 300 or 500 to 710  $\mu\text{m}$ .

Surprisingly, scaffold A (porosity 73.5 %) also showed cartilage formation besides bone and bone marrow. At higher magnification, pores filled with cartilage, bone and bone marrow, can clearly be observed, as shown in Figure 7.8. The scaffold stiffness can greatly affect cartilage formation in vivo.<sup>[42,43]</sup> Although the effect of scaffold stiffness on cartilage formation cannot be excluded here, there is another more likely explanation for the observation of cartilage. From the histological sections it appears that the pores in which cartilage formation takes place are not well connected (Figure 7.9).

Cartilage formation is known to be favored by conditions in which the oxygen supply is limited.<sup>[44]</sup> Implantation of demineralized teeth resulted in cartilage formation when one side was left open and in bone formation when both sides were left open. A comparable observation was made after implantation of hydroxyapatite with channel-like pores, where cartilage was observed in the central zones of the pores.<sup>[45]</sup> Vascularization is needed for a good oxygen and nutrient supply and is therefore believed to be of great importance for bone formation.<sup>[46]</sup> Vascularization of tissue within a scaffold with large pores but with small pore interconnections may be difficult.<sup>[47]</sup>

The poor accessibility of the pore structure also follows from  $\mu\text{-CT}$  data. The 1000PEOT70PBT30 scaffold A with the lowest porosity (73.5 %) not only results in cartilage formation, it also shows considerably less ingrowth of fibrous tissue and contains much more wound exudate than the other scaffolds. The interconnecting pore network in this scaffold allows the passage of cell suspensions, both in cell seeding and in vivo, as it allows for passage of wound exudate containing red blood cells (Figure 7.8). The pore network does not allow for the ingrowth of fibrous tissue. The size of the interconnecting pore network appears to be too small to allow for fibrous tissue ingrowth. With the use of different fabrication techniques, for instance by use of fused salt particles<sup>[48,49]</sup> or 3D printing<sup>[50]</sup> it should be possible to obtain a more accessible pore network.

## Conclusions

The results presented show the suitability of BMSC seeded polymer scaffolds for bone tissue engineering. All implanted cell-seeded scaffolds show bone and bone marrow formation. By varying the scaffold porosity of 1000PEOT70PBT30 scaffolds it was possible to obtain scaffolds with a comparable pore size distribution (as determined by  $\mu\text{-CT}$ ), but with considerable differences in accessible pore volume (as a fraction of the total volume) and accessible surface area. However, no significant differences between the different 1000PEOT70PBT30 scaffolds were observed in terms of ectopically formed bone (7-9 %) and bone marrow (6-11 %).

Surprisingly, 1000PEOT70PBT30 scaffolds with a porosity of 73.5 % showed cartilage formation. Although the effect of scaffold stiffness cannot be excluded, cartilage formation is

most likely due to a poorly accessible pore network as shown by  $\mu$ -CT. Scaffolds of 85 % porosity lacked the required mechanical properties and were distorted after implantation. BMSC seeded PDLA and BCP scaffolds always showed considerably more bone and bone marrow formation and less fibrous tissue ingrowth than the 1000PEOT70PBT30 scaffolds, even though both scaffolds have a considerably lower accessible surface area (for sphere diameters (d) up to 100  $\mu$ m) and contain much less cells (as determined by a DNA assay) upon implantation.

The scaffold material can be of great influence. In a stiffer and less hydrophilic scaffold like PDLA, the accessible pore structure is more likely to be preserved under physiological conditions than in hydrophilic 1000PEOT70PBT30 scaffolds.

## Acknowledgements

The authors would like to thank Dr. L.M.H. Groenewoud for the gas plasma treatments (Ssens BV, Hengelo, The Netherlands), M.A. Smithers (University of Twente) for the scanning electron microscopy and Dr. A. Laib (Scanco Medical AG, Bassersdorf, Switzerland) for the  $\mu$ -CT scans. This study was financially supported by the European Community (Brite-Euram project BE97-4612).

## References

1. S.C. Marks Jr., D.C. Hermey *The structure and development of bone* in "Principles of bone biology", J.P. Bilezikian, L.G. Raisz, and G.A. Rodan Ed., Academic Press: San Diego, U.S.A. **1996**.
2. V.I. Sikavitsas, J.S. Temenoff, A.G. Mikos *Biomaterials and bone mechanotransduction* Biomaterials **2001**, 22, 2581-2593.
3. A.I. Caplan, S.P. Bruder *Mesenchymal stem cells: building blocks for molecular medicine in the 21st century* Trends Mol. Med **2001**, 7, 259-264.
4. C. Maniopoulos, J. Sodek, A.H. Melcher *Bone-formation in vitro by stromal cells obtained from bone marrow of young-adult rats* Cell Tissue Res. **1988**, 254, 317-330.
5. S.J. Peter, C.R. Liang, D.J. Kim, M.S. Widmer, A.G. Mikos *Osteoblastic phenotype of rat marrow stromal cells cultured in the presence of dexamethasone,  $\beta$ -glycerolphosphate, and L- ascorbic acid* J. Cell. Biochem. **1998**, 71, 55-62.
6. P.S. Leboy, J.N. Beresford, C. Devlin, M.E. Owen *Dexamethasone induction of osteoblast messenger-RNAs in rat marrow stromal cell-cultures* J. Cell. Physiol. **1991**, 146, 370-378.
7. D.J. Rickard, T.A. Sullivan, B.J. Shenker, P.S. Leboy, I. Kazhdan *Induction of rapid osteoblast differentiation in rat bone-marrow stromal cell-cultures by dexamethasone and BMP-2* Dev. Biol. **1994**, 161, 218-228.
8. S.C. Mendes, M. Sleijster, A. van den Muysenberg, J.D. de Bruijn, C.A. van Blitterswijk *A cultured living bone equivalent enhances bone formation when compared to a cell seeding approach* J. Mater. Sci.-Mater. Med. **2002**, 13, 575-581.
9. S.L. Ishaug-Riley, G.M. Crane, A. Gurlek, M.J. Miller, A.W. Yasko, M.J. Yaszemski, A.G. Mikos *Ectopic bone formation by marrow stromal osteoblast transplantation using poly(DL-lactic-co-glycolic acid) foams implanted into the rat mesentery* J. Biomed. Mater. Res. **1997**, 36, 1-8.
10. K.J.L. Burg, S. Porter, J.F. Kellam *Biomaterial developments for bone tissue engineering* Biomaterials **2000**, 21, 2347-2359.
11. A.A. Deschamps, D.W. Grijpma, J. Feijen *Poly(ethylene oxide)/poly(butylene terephthalate) segmented block copolymers: the effect of copolymer composition on physical properties and degradation* Polymer **2001**, 42, 9335-9345.
12. R.J.B. Sackers, J.R. de Wijn, R.A.J. Dalmeyer, R. Brand, C.A. van Blitterswijk *Evaluation of copolymers of polyethylene oxide and polybutylene terephthalate (polyactive): mechanical behaviour* J. Mater. Sci.-Mater. Med. **1998**, 9, 375-379.
13. C.A. van Blitterswijk, J. van der Brink, H. Leenders, D. Bakker *The effect of PEO ratio on degradation, calcification and bone bonding of PEO/PBT copolymer (Polyactive)* Cells and Materials **1993**, 3, 23-36.

14. C.A. van Blitterswijk, D. Bakker, S.C. Hesselting, H.K. Koerten *Reactions of cells at implant surfaces* Biomaterials **1991**, 12, 187-193.
15. A.M. Radder, H. Leenders, C.A. van Blitterswijk *Bone-bonding behavior of poly(ethylene oxide)-polybutylene terephthalate copolymer coatings and bulk implants - a comparative-study* Biomaterials **1995**, 16, 507-513.
16. A.M. Radder, H. Leenders, C.A. van Blitterswijk *Application of porous PEO/PBT copolymers for bone replacement* J. Biomed. Mater. Res. **1996**, 30, 341-351.
17. R. van Dijkhuizen-Radersma, S.C. Hesselting, P.E. Kaim, K. de Groot, J.M. Bezemer *Biocompatibility and degradation of poly(ether-ester) microspheres: in vitro and in vivo evaluation* Biomaterials **2002**, 23, 4719-4729.
18. M.L.C. Anderson, W.J.A. Dhert, J.D. de Bruijn, R.A.J. Dalmeijer, H. Leenders, C.A. van Blitterswijk, A.J. Verbout *Critical size defect in the goat's os ilium - A model to evaluate bone grafts and substitutes* Clin. Orthop. Rel. Res. **1999**, 231-239.
19. M. Roessler, A. Wilke, P. Griss, H. Kienapfel *Missing osteoconductive effect of a resorbable PEO/PBT copolymer in human bone defects: A clinically relevant pilot study with contrary results to previous animal studies* J. Biomed. Mater. Res. **2000**, 53, 167-173.
20. R. Cancedda, B. Dozin, P. Giannoni, R. Quarto *Tissue engineering and cell therapy of cartilage and bone* Matrix Biol. **2003**, 22, 81-91.
21. J.D. de Bruijn, Y.P. Bovell, J. van den Brink, C.A. van Blitterswijk (to Isotis) *Device for tissue engineering bone* U.S. Patent 6,228,117 **2001**.
22. J.D. de Bruijn, Y.P. Bovell, C.A. van Blitterswijk (to Isotis) *Device for tissue engineering bone comprising biodegradable thermoplastic copolyester and cultured cells* Eur. Patent Appl. 0891783 A1 **1998**.
23. M.B. Claase, M.B. Olde Riekerink, D.W. Grijpma, J. Feijen, S.C. Mendes, J.D. de Bruijn *Surface modifications of PEOT/PBT copolymers for the improvement of bone marrow stromal cell attachment* J. Control. Release **2003**, 87, 298-301.
24. M.B. Claase, M.B. Olde Riekerink, J.D. de Bruijn, D.W. Grijpma, G.H.M. Engbers, J. Feijen *Enhanced bone marrow stromal cell adhesion and growth on segmented poly(ether ester)s based on poly(ethylene oxide) and poly(butylene terephthalate)* Biomacromolecules **2003**, 4, 57-63. Chapter 4 of this thesis.
25. M.B. Claase, D.W. Grijpma, S.C. Mendes, J.D. de Bruijn, J. Feijen *Porous PEOT/PBT scaffolds for bone tissue engineering: preparation, characterization and in vitro bone marrow cell culturing* J. Biomed. Mater. Res **2003**, 64A, 291-300. Chapter 5 of this thesis.
26. M.B. Olde Riekerink, M.B. Claase, G.H.M. Engbers, D.W. Grijpma, J. Feijen *Gas plasma etching of PEO/PBT segmented block copolymer films* J. Biomed. Mater. Res **2003**, 65A, 417-428.
27. S.C. Mendes, J. Bezemer, M.B. Claase, D.W. Grijpma, G. Bellia, F. Degli-Innocenti, R.L. Reis, K. de Groot, C.A. van Blitterswijk, J.D. de Bruijn *Evaluation of two biodegradable polymeric systems as substrates for bone tissue engineering* Tissue Eng. **2003**, 9, S91-S103.
28. M.B. Claase, S. Both, J.D. de Bruijn, D.W. Grijpma, J. Feijen *The effect of scaffold pore size on ectopic bone formation in rat bone marrow stromal cell seeded porous scaffolds based on poly(ethylene oxide)/poly(butylene terephthalate) segmented block copolymers* Chapter 6 of this thesis **2003**.
29. Q.P. Hou, D.W. Grijpma, J. Feijen *Porous polymeric structures for tissue engineering prepared by a coagulation, compression moulding and salt leaching technique* Biomaterials **2003**, 24, 1937-1947.
30. J.D. de Bruijn *Unpublished data* Isotis OrthoBiologics Bilthoven, The Netherlands **2003**.
31. T.L. Livingston, S. Gordon, M. Archambault, S. Kadiyala, K. McIntosh, A. Smith, S.J. Peter *Mesenchymal stem cells combined with biphasic calcium phosphate ceramics promote bone regeneration* J. Mater. Sci.-Mater. Med. **2003**, 14, 211-218.
32. H.P. Yuan, M. van den Doel, S.H. Li, C.A. van Blitterswijk, K. de Groot, J.D. de Bruijn *A comparison of the osteoinductive potential of two calcium phosphate ceramics implanted intramuscularly in goats* J. Mater. Sci.-Mater. Med. **2002**, 13, 1271-1275.
33. T. Hildebrand, P. Rüeggsegger *A new method for the model independent assessment of thickness in three-dimensional images* J. Microsc. **1997**, 185, 67-75.
34. W.E. Lorensen, H.E. Cline *Marching cubes: a high resolution 3D surface construction algorithm* Comput. Graph. **1987**, 21, 163-169.
35. H.J. Wang, C.A. van Blitterswijk, J. Pieper, F. Péters, E.N. Lamme *Synthetic scaffold morphology controls human connective tissue formation* Biomaterials **2003**, submitted for publication and H.J. Wang *Dermal tissue engineering*, Thesis, University of Twente, Enschede, The Netherlands **2003**.
36. K.J.L. Burg, W.D. Holder, C.R. Culberson, R.J. Beiler, K.G. Greene, A.B. Loeb sack, W.D. Roland, P. Eiselt, D.J. Mooney, C.R. Halberstadt *Comparative study of seeding methods for three-dimensional polymeric scaffolds* J. Biomed. Mater. Res. **2000**, 51, 642-649.

37. A.S. Goldstein, T.M. Juarez, C.D. Helmke, M.C. Gustin, A.G. Mikos *Effect of convection on osteoblastic cell growth and function in biodegradable polymer foam scaffolds* Biomaterials **2001**, 22, 1279-1288.
38. V.I. Sikavitsas, G.N. Bancroft, A.G. Mikos *Formation of three-dimensional cell/polymer constructs for bone tissue engineering in a spinner flask and a rotating wall vessel bioreactor* J. Biomed. Mater. Res. **2002**, 62, 136-148.
39. R.C. Thomson, M.J. Yaszemski, J.M. Powers, A.G. Mikos *Fabrication of biodegradable polymer scaffolds to engineer trabecular bone* J. Biomater. Sci.-Polym. Ed. **1995**, 7, 23-38.
40. M.C. Wake, C.W. Patrick, A.G. Mikos *Pore morphology effects on the fibrovascular tissue-growth in porous polymer substrates* Cell Transplant. **1994**, 3, 339-343.
41. W.D. Holder, H.E. Gruber, A.L. Moore, C.R. Culberson, W. Anderson, K.J.L. Burg, D.J. Mooney *Cellular ingrowth and thickness changes in poly-L-lactide and polyglycolide matrices implanted subcutaneously in the rat* J. Biomed. Mater. Res. **1998**, 41, 412-421.
42. J.H. de Groot, F.M. Zijlstra, H.W. Kuipers, A.J. Pennings, J. Klompmaker, R.P.H. Veth, H.W.B. Jansen *Meniscal tissue regeneration in porous 50/50 copoly(L- lactide/epsilon-caprolactone) implants* Biomaterials **1997**, 18, 613-622.
43. T.G. van Tienen, R. Heijkants, P. Buma, J.H. de Groot, A.J. Pennings, R.P.H. Veth *Tissue ingrowth polymers and degradation of two biodegradable porous with different porosities and pore sizes* Biomaterials **2002**, 23, 1731-1738.
44. C.A.L. Bassett, I. Hermann *Influence of oxygen concentration and mechanical factors on differentiation of connective tissues in vitro* Nature **1961**, 190, 460-461.
45. Q.M. Jin, H. Takita, T. Kohgo, K. Atsumi, H. Itoh, Y. Kuboki *Effects of geometry of hydroxyapatite as a cell substratum in BMP-induced ectopic bone formation* J. Biomed. Mater. Res. **2000**, 51, 491-499.
46. J. Mahmood, H. Takita, Y. Ojima, M. Kobayashi, T. Kohgo, Y. Kuboki *Geometric effect of matrix upon cell differentiation: BMP- induced osteogenesis using a new bioglass with a feasible structure* J. Biochem. (Tokyo) **2001**, 129, 163-171.
47. J.T. Schantz, D.W. Hutmacher, H. Chim, K.W. Ng, T.C. Lim, S.H. Teoh *Induction of ectopic bone formation by using human periosteal cells in combination with a novel scaffold technology* Cell Transplant. **2002**, 11, 125-138.
48. W.L. Murphy, R.G. Dennis, J.L. Kileny, D.J. Mooney *Salt fusion: An approach to improve pore interconnectivity within tissue engineering scaffolds* Tissue Eng. **2002**, 8, 43-52.
49. Q. Hou, D.W. Grijpma, J. Feijen *Preparation of interconnected, highly porous polymeric structures by a replication and freeze-drying process* J. Control. Release **2003**, 87, 304-307.
50. T.B.F. Woodfield, J.M. Bezemer, J.S. Pieper, C.A. van Blitterswijk, J. Riesle *Scaffolds for tissue engineering of cartilage* Crit. Rev. Eukaryot. Gene Expr. **2002**, 12, 209-236.

# Chapter 8

## General discussion and conclusions

*What we call the beginning is often the end  
And to make an end is to make a beginning,  
The end is where we start from.*

T.S. Eliot (1888-1965)

### General discussion and conclusions

This thesis shows that surface modified porous 1000PEOT70PBT30 scaffolds seeded with bone marrow stromal cells (BMSCs, after expansion in an osteogenic medium) and cultured in vitro for 7 d are able to induce ectopic bone formation, when implanted subcutaneously in immunodeficient nude mice. BMSCs are, however, not able to attach to and grow on the unmodified 1000PEOT70PBT30 polymers. Surface modification by means of gas plasma treatment was shown to be an essential step in obtaining polymer-cell constructs that are able to induce ectopic bone formation. 1000PEOT70PBT30 scaffolds that were seeded with BMSCs and cultured for 7 d in an osteogenic medium, but that were not gas plasma treated or gas plasma treated 1000PEOT70PBT30 scaffolds without BMSCs (Chapter 6 and 7), did not show any formation of bone or bone marrow.

Gas plasma treated 1000PEOT70PBT30 scaffolds, seeded with BMSCs and cultured in vitro for 7 d in an osteogenic medium, showed ectopic bone formation, although the amount of bone (5-9 %) and bone marrow (5-13 %) was limited in comparison to scaffolds based on poly-D,L-lactide (PDLLA) and biphasic calcium phosphate (BCP).

#### *PEOT/PBT synthesis, characterization and properties*

The procedures for the synthesis of PEOT/PBT copolymers on a 1 kg scale described in Chapter 3 allow good control of copolymer composition and result in copolymers of high molecular weights. Although it has been suggested that tetrahydrofuran (THF)<sup>[1,2]</sup> or chloroform (CHCl<sub>3</sub>)<sup>[3-5]</sup> are suitable solvents for these copolymers, we found that these copolymers do not dissolve in THF and that CHCl<sub>3</sub> is not suited for GPC analysis of the copolymers.<sup>[6]</sup> 1,1,1,3,3,3-Hexafluoro-2-propanol (HFIP) containing 0.02 M sodium trifluoroacetate appears to be a solvent that is suitable for the whole PEOT/PBT family including the compositions with high PBT contents.<sup>[7]</sup> In our studies, the molecular weights of the copolymers were determined relative to PMMA using GPC with HFIP with 0.02 M sodium trifluoroacetate as eluent. Although HFIP is a potentially reactive solvent, no significant degradation of the copolymers dissolved in HFIP was observed up to a period of 11 d. Relative molecular weights of PEOT/PBT copolymers up to 150,000 g/mol were found.

Compression molding of the copolymers into films and porous structures decreases the molecular weight only slightly.

PEOT/PBT copolymers are flexible thermoplastic materials of which the physical and mechanical properties depend on the composition. A higher PEO content results in a lower modulus and a higher hydrophilicity. As described in Chapter 3, tensile properties like the E-modulus, elongation at break and tensile strength are significantly higher for 1000PEOT70PBT30 in the dry state than in the wet state (the E-modulus in the dry state is 27 N/mm<sup>2</sup> and in the wet state 17 N/mm<sup>2</sup>). Static creep experiments show much higher creep rates for 1000PEOT70PBT30 swollen in water as compared to the dry copolymer. The swollen samples broke within 4 h at loadings of 0.5-2.0 N/mm<sup>2</sup>, whereas dry samples were able to sustain loads of up to 4.0 N/mm<sup>2</sup> for 21 d. The introduction of porosity further decreases the stiffness and strength of this material; an exponential decrease in compression modulus is observed with increasing scaffold porosity (Chapter 5).

The limited mechanical properties of water-swollen PEOT/PBT copolymer scaffolds prohibit the exposure of these materials to large (tensile) forces during in vitro cell culture. It is expected that the formation of bone-like tissue in vitro will influence the mechanical properties of these cell-seeded and cultured scaffolds substantially. The changes of the mechanical properties of scaffolds of this material during cell culture need to be further investigated.

#### *Surface modifications*

We found (Chapter 4) that it was not possible to culture rat BMSCs on 1000PEOT70PBT30. Results from previous reports<sup>[8,9]</sup> on rat BMSC seeding on 1000PEOT70PBT30 and subsequent in vivo bone formation could not be substantiated. We found that rat and goat BMSCs only attach to the more hydrophobic PEOT/PBT copolymers. 1000PEOT70PBT30 scaffolds that were not gas plasma treated (Chapter 7) and that were seeded with BMSCs and cultured for 7 d in an osteogenic medium, did not show any formation of bone or bone marrow.

To ensure BMSC attachment to the more hydrophilic PEOT/PBT copolymers, surface modifications are necessary. Often used modifications are based on cell binding peptides or proteins adsorbed or covalently bound to the material surface (Appendix A of this thesis). For some polymers cell attachment can be improved by simple chemical or physical treatments. For example poly(glycolic acid) treated with a sodium hydroxide solution is a much better substrate for fibroblast attachment than the untreated material. As described in Chapter 4, chemical treatments were not very successful for PEOT/PBT copolymers. Etching with a 0.1 M sodium hydroxide solution in ethanol caused severe degradation of 1000PEOT70PBT30.

We have changed the surface characteristics of PEOT/PBT copolymers with CO<sub>2</sub> gas plasma treatments. Preliminary experiments using argon plasmas also appear to be effective in improving BMSC attachment to and growth on 1000PEOT70PBT30 copolymers.<sup>[10,11]</sup>

With the use of gas plasma treatments, only the top layer of the polymer substrates was modified and no degradation of the films was observed (Chapter 4). After rat BMSC seeding of gas plasma treated 4×4×4 mm 1000PEOT70PBT30 scaffolds, and in vitro culture for 7 d in an osteogenic medium, we observed the presence of osteogenic cells in the center of the scaffold (Chapter 5). This shows that plasma treatments are able to modify the pore surfaces even in the center of the 4×4×4 mm scaffolds.

It has to be noted that most cells are still present on the outside of the scaffold. This can be caused by a more effective surface treatment of the outside of the scaffold, enabling more cells to attach to the surface. Another factor can be diffusion limitation, resulting in slow exchange of nutrients and waste products in the center of the scaffolds during static seeding and culture.

Dynamic seeding and culture are expected to result in a more homogeneous cell distribution, when diffusion is the limiting factor.<sup>[12-14]</sup>

In later reports, oxygen plasmas have been used to improve palatal mesenchyme cell attachment to PDLLA<sup>[15]</sup> and osteoblast attachment to poly(3-hydroxybutyrate-co-3-hydroxyvalerate)<sup>[16]</sup>, showing the suitability of this technique to improve cell attachment onto different polymer surfaces. Gas plasmas have also been used for low-temperature sterilization<sup>[17]</sup>, providing the possibility of combining an essential surface modification step (to ensure BMSC attachment) and a sterilization step.

#### *Scaffold preparation and characterization*

Although the freeze-drying techniques, as applied in Chapter 5, offer good control over pore size and porosity, scanning electron micrographs of the resulting structures mostly show a poorly interconnected pore structure.

The process of cryogenic grinding, blending and compression molding followed by salt leaching to prepare porous structures, as described in Chapter 5, allows good control over pore size and porosity. The porosity is determined by the salt volume fraction, whereas the pore size can be controlled by the size of the salt crystals used. Stable PEOT/PBT scaffolds can be obtained in a porosity range of 73 to 85 %. Scanning electron micrographs of the salt leached scaffolds show a more interconnected pore structure than that of porous structures prepared by freeze-drying polymer solutions in 1,4-dioxane.

One of the most often employed techniques to characterize porous structures is mercury intrusion porosimetry. Unfortunately, the 1000PEOT70PBT30 scaffolds described in this thesis were unable to resist the pressures that need to be used in this technique, resulting in scaffold collapse (unpublished results). Other techniques are therefore necessary to characterize these porous structures.

From 3D images generated from micro-computed tomography scans, it was possible to determine relevant scaffold characteristics like porosity, pore size distribution, average pore size, accessible pore volume and accessible surface area. The obtained average pore sizes are considerably smaller than one might expect, when considering the size of the salt crystals used. For scaffolds of approximately 80 % porosity, salt sizes of 250-425, 425-500, 500-710, 710-1000  $\mu\text{m}$  resulted in average pore sizes of 260, 342, 305 and 447  $\mu\text{m}$  respectively. Although these values represent a considerable improvement (averages are approximately 100  $\mu\text{m}$  higher) compared to average values obtained from previously used algorithms<sup>[18]</sup>, it is worthwhile to further investigate algorithms, which can be adequately applied to such systems.

#### *Ectopic bone formation*

All scaffolds (1000PEOT70PBT30, PDLLA and BCP) that were seeded with BMSCs (after in vitro expansion and differentiation in an osteogenic culture medium) and cultured in vitro for 7 d in an osteogenic medium, showed the formation of bone and bone marrow upon subcutaneous implantation in nude mice for 4 wks. This shows the ability of the used BMSCs to induce ectopic bone formation. At constant pore size, a lower scaffold porosity resulted in a lower amount of detected DNA (and hence in a lower number of cells) after seeding and in vitro culture of rat BMSCs for 7 d. Even though the amount of DNA was significantly different, for 1000PEOT70PBT30 scaffolds of different porosity, all scaffolds showed more or less the same amount of bone and bone marrow formation after 4 wks of subcutaneous implantation.

PDLLA and BCP scaffolds contained considerably less BMSCs at the time of implantation (as determined by a DNA assay), but showed considerably more bone and bone marrow and much less fibrous tissue and wound exudate after 4 wks of subcutaneous implantation.

The 1000PEOT70PBT30 scaffolds of which the pore structure was less accessible led to cartilage formation in addition to bone formation. The lack of oxygen and the limited nutrient diffusion can result in cartilage formation instead of bone. Although an increase in porosity of the 4×4×4 mm 1000PEOT70PBT30 scaffolds resulted in higher accessible pore volumes, it did not result in more ectopic bone or bone marrow.

A further increase in the accessible pore volume of these 1000PEOT70PBT30 scaffolds could be achieved by reticulation techniques as well as by using fused salt particles<sup>[19,20]</sup> in the compression molding/leaching technique described in this thesis.

Previous implantation studies of similar cell-seeded and cultured 1000PEOT70PBT30 scaffolds by Mendes et al. showed considerably more bone formation.<sup>[21]</sup> The reported scaffold dimensions used were 3×3×2 mm compared to 4×4×4 mm in our studies, which suggests that the scaffold dimensions have a pronounced effect on ectopic bone formation. With the same amount of BMSCs seeded (approximately  $2 \times 10^5$  cells per scaffold) this also resulted in a lower cell seeding density for the larger scaffolds. The effects of scaffold dimensions and cell seeding density on the in vitro cell culture and in vivo bone formation need to be further addressed.

### *Degradation*

Many of the 1000PEOT70PBT30 scaffolds studied in Chapter 6 and 7, show the first signs of fragmentation after 4 wks of subcutaneous implantation in nude mice. Although many researchers have reported on the in vivo degradation of PEOT/PBT copolymers, it still remains unclear if these copolymers will be resorbed completely in time. The more hydrophobic copolymers that contain a high fraction of PBT, show a limited decrease in molecular weight upon implantation.<sup>[5,7]</sup> Implantation studies using hydrophilic copolymers, like 1000PEOT70PBT30, show clear fragmentation and a more rapid decrease in molecular weight than hydrophobic compositions.<sup>[5,7]</sup> Complete resorption, however, is not reported<sup>[22-24]</sup> and after 3 years implantation in goat ilia, 1000PEOT70PBT30 fragments could still be observed intracellularly.<sup>[25]</sup>

Detailed in vivo and in vitro studies have shown that during degradation of the 1000PEOT70PBT30 copolymer mainly PEO containing segments are leached out, thereby slowly changing the composition of the polymer to a low molecular weight, PBT rich copolymer.<sup>[6,7]</sup> During degradation an increase in the copolymer crystallinity was observed.<sup>[6,7]</sup> Previous studies on the degradation of PLLA show the presence of crystalline remnants after 4 years of implantation, resulting in inflammation at the site of implantation.<sup>[26]</sup> Whether the PBT remnants can be fully degraded and resorbed, remains an unanswered question and further research is required to study the effects in the long term of possible remnants on the surrounding tissue.

### *Further research*

The ectopic bone formation using rat BMSC-seeded and cultured (in an osteogenic medium) 1000PEOT70PBT30 scaffolds shows the ability of this system to generate bone tissue. In our approach rat BMSCs were statically seeded and cultured in vitro on the scaffolds for a period of 7 d before implantation. To optimize the tissue engineered constructs, a detailed analysis of the effect of variations in culture conditions (possibly dynamic) and culture times (up to several wks) is needed. The physical and mechanical properties of these engineered constructs are likely to change during the cell/tissue culture, as tissue is being formed and the polymer



matrix is (slowly) degraded. To study in vivo bone regeneration, these in vitro cultured tissue constructs, cultured under different culture conditions and culture times, need to be implanted in critical size bone defects, preferably in large animals like goats.

## Outlook

Scaffolds for bone tissue engineering should be prepared from a material that can easily be processed into any desired shape and size. The scaffold should allow for cell attachment and/or the controlled release of suitable bioactive molecules like BMP growth factors. Furthermore for the restoration of large defects angiogenesis has to take place.

With freeze-drying and salt leaching techniques it is possible to produce scaffolds of different porosities and pore sizes. Scaffolds with a complex shape or with a large size are, however, difficult to prepare with these techniques. Scaffolds with the required dimensions and pore morphology can be obtained by solid free form fabrication and 3D printing<sup>[27]</sup> using computer aided design. In this way, tissue engineered constructs can be prepared that exactly fit the shape of the defect with an optimal pore morphology for in vitro cell seeding and culturing. The thermoplastic PEOT/PBT copolymers can be processed using 3D printing techniques.<sup>[28]</sup> The implanted in vitro cultured cell/tissue construct should be able to release proteins like the osteoinductive BMPs and/or bioactive compounds that stimulate angiogenesis.<sup>[29]</sup> These proteins and bioactive compounds should be released from the cell/tissue construct in a controlled fashion to support the formation of bone-like tissue in vitro and/or the bone formation and angiogenesis in vivo. These proteins and compounds could be incorporated into the scaffold<sup>[30]</sup> (assuming the scaffold is still part of the implanted construct) and/or can be produced by (genetically modified) cells.<sup>[31-33]</sup> Great care, however, needs to be taken to ensure that these stimuli do not cause bone formation outside the defect after implantation of the in vitro cultured cell construct.<sup>[34]</sup> PEOT/PBT copolymers are well suited for the release of proteins.<sup>[35,36]</sup>

It should be kept in mind that other tissue engineering approaches can also result in successful bone healing. Injectable ceramics and hydrogels, containing cells or suitable proteins can/could also result in successful bone (re)generation.<sup>[37-39]</sup> The implantation of scaffolds (guided tissue regeneration), scaffolds with growth factors or scaffolds seeded with cells (not cultured in vitro before implantation) can result in successful healing of a bone defect (see Chapter 2 for an overview). The prepared BMSC-seeded and cultured PEOT/PBT scaffolds should, therefore, always be compared with other bone tissue engineering approaches and with other scaffold materials.

The in vivo implantation of BMSC-seeded and cultured BCP and PDLA resulted in abundant bone and bone marrow formation (Chapters 6 and 7). BCP, like many other ceramics, is difficult to process into the desired shape and size, but PDLA can easily be processed into a great variety of shapes and sizes (Chapters 5 and 6). Amorphous PDLA is completely resorbable<sup>[40-42]</sup> and is well tolerated by bone.<sup>[43]</sup> It has already been tested successfully as a scaffold for the controlled release of BMPs<sup>[44,45]</sup> and as a scaffold for the culture of human osteoblast-like cells<sup>[46]</sup> and human osteoprogenitor cells.<sup>[47]</sup>

The results presented in this thesis show that BCP and PDLA might have certain advantages over 1000PEOT70PBT30 and therefore should also be considered as scaffold materials in future bone tissue engineering approaches.

## References

1. N.N. (to Isotis) *Tissue engineering using mandibular cells* Eur. Patent Appl. 1113072 A1 **1999**.
2. N.N. (to Isotis) *Muscle tissue engineering* Eur. Patent Appl. 1038538 A1 **1999**.
3. J.M. Bezemer, J.R. de Wijn, J. Nieuwenhuis (to Isotis) *Molding of a polymer* US Patent Appl. 0128378 A1 **2002**.
4. J.M. Bezemer, J.R. de Wijn, R.E. Haan, M. Blom (to Isotis) *Biodegradable porous scaffold material* WO Patent Appl. 060508 A1 **2002**.
5. R. van Dijkhuizen-Radersma, S.C. Hesselting, P.E. Kaim, K. de Groot, J.M. Bezemer *Biocompatibility and degradation of poly(ether-ester) microspheres: in vitro and in vivo evaluation* *Biomaterials* **2002**, 23, 4719-4729.
6. M. Kellomaki, S. Paasimaa, D.W. Grijpma, K. Kolppo, P. Tormala *In vitro degradation of Polyactive (R) 1000PEOT70PBT30 devices* *Biomaterials* **2002**, 23, 283-295.
7. A.A. Deschamps, A.A. van Apeldoorn, H. Hayen, J.D. de Bruijn, U. Karst, D.W. Grijpma, J. Feijen *In vitro and in vivo degradation of poly(ether ester) block copolymers based on poly(ethylene glycol) and poly(butylene terephthalate)* *Biomaterials* **2004**, 25, 247-258.
8. J.D. de Bruijn, Y.P. Bovell, J. van den Brink, C.A. van Blitterswijk (to Isotis) *Device for tissue engineering bone* U.S. Patent 6,228,117 **2001**.
9. J.D. de Bruijn, Y.P. Bovell, C.A. van Blitterswijk (to Isotis) *Device for tissue engineering bone comprising biodegradable thermoplastic copolyester and cultured cells* Eur. Patent Appl. 0891783 A1 **1998**.
10. M.B. Olde Riekerink, M.B. Claase, G.H.M. Engbers, D.W. Grijpma, J. Feijen *Gas plasma etching of PEO/PBT segmented block copolymer films* *J. Biomed. Mater. Res* **2003**, 65A, 417-428.
11. A.A. Deschamps, M.B. Claase, W.J. Sleijster, J.D. de Bruijn, D.W. Grijpma, J. Feijen *Design of segmented poly(ether ester) materials and structures for the tissue engineering of bone* *J. Control. Release* **2002**, 78, 175-186.
12. K.J.L. Burg, W.D. Holder, C.R. Culberson, R.J. Beiler, K.G. Greene, A.B. Loeb sack, W.D. Roland, P. Eiselt, D.J. Mooney, C.R. Halberstadt *Comparative study of seeding methods for three-dimensional polymeric scaffolds* *J. Biomed. Mater. Res.* **2000**, 51, 642-649.
13. A.S. Goldstein, T.M. Juarez, C.D. Helmke, M.C. Gustin, A.G. Mikos *Effect of convection on osteoblastic cell growth and function in biodegradable polymer foam scaffolds* *Biomaterials* **2001**, 22, 1279-1288.
14. H. Terai, D. Hannouche, E. Ochoa, Y. Yamano, J.P. Vacanti *In vitro engineering of bone using a rotational oxygen- permeable bioreactor system* *Mater. Sci. Eng. C-Biomimetic Supramol. Syst.* **2002**, 20, 3-8.
15. H. Chim, J.L. Ong, J.-T. Schantz, D.W. Hutmacher, C.M. Agrawal *Efficacy of glow discharge gas plasma treatment as a surface modification process for three-dimensional poly (D,L-lactide) scaffolds* *J. Biomed. Mater. Res.* **2003**, 65A, 327-335.
16. G.T. Kose, H. Kenar, N. Hasirci, V. Hasirci *Macroporous poly(3-hydroxybutyrate-co-3-hydroxyvalerate) matrices for bone tissue engineering* *Biomaterials* **2003**, 24, 1949-1958.
17. M. Moisan, J. Barbeau, S. Moreau, J. Pelletier, M. Tabrizian, L.H. Yahia *Low-temperature sterilization using gas plasmas: a review of the experiments and an analysis of the inactivation mechanisms* *Int. J. Pharm.* **2001**, 226, 1-21.
18. H.J. Wang, C.A. van Blitterswijk, J. Pieper, F. Péters, E.N. Lamme *Synthetic scaffold morphology controls human connective tissue formation* *Biomaterials* **2003**, submitted for publication and H.J. Wang *Dermal tissue engineering*, Thesis, University of Twente, Enschede, The Netherlands **2003**.
19. Q. Hou, D.W. Grijpma, J. Feijen *Preparation of interconnected, highly porous polymeric structures by a replication and freeze-drying process* *J. Control. Release* **2003**, 87, 304-307.
20. W.L. Murphy, R.G. Dennis, J.L. Kileny, D.J. Mooney *Salt fusion: An approach to improve pore interconnectivity within tissue engineering scaffolds* *Tissue Eng.* **2002**, 8, 43-52.
21. S.C. Mendes, J. Bezemer, M.B. Claase, D.W. Grijpma, G. Bellia, F. Degli-Innocenti, R.L. Reis, K. de Groot, C.A. van Blitterswijk, J.D. de Bruijn *Evaluation of two biodegradable polymeric systems as substrates for bone tissue engineering* *Tissue Eng.* **2003**, 9, S91-S103.
22. A.M. Radder, H. Leenders, C.A. van Blitterswijk *Bone-bonding behavior of poly(ethylene oxide)-polybutylene terephthalate copolymer coatings and bulk implants - a comparative-study* *Biomaterials* **1995**, 16, 507-513.
23. C.A. van Blitterswijk, J. van der Brink, H. Leenders, D. Bakker *The effect of PEO ratio on degradation, calcification and bone bonding of PEO/PBT copolymer (Polyactive)* *Cells and Materials* **1993**, 3, 23-36.

24. M. Roessler, A. Wilke, P. Griss, H. Kienapfel *Missing osteoconductive effect of a resorbable PEO/PBT copolymer in human bone defects: A clinically relevant pilot study with contrary results to previous animal studies* J. Biomed. Mater. Res. **2000**, 53, 167-173.
25. A.A. van Apeldoorn, Y. Aksenov, J.D. de Bruijn, C.A. van Blitterswijk *The usage of confocal micro raman spectroscopy for the study of in vivo PEGT/PBT degradation* in 'Proceedings of the 8th Dutch Annual Conference on BioMedical Engineering'; W. M. G. F. Pontenagel and J. Feijen, Ed.; Research school 'Integrated BioMedical Engineering for restoration of human function' (iBME): Enschede, The Netherlands, **2001**.
26. J.E. Bergsma, W.C. de Bruijn, F.R. Rozema, R.R.M. Bos, G. Boering *Late Degradation Tissue-Response to Poly(L-Lactide) Bone Plates and Screws* Biomaterials **1995**, 16, 25-31.
27. D.W. Huttmacher *Scaffold design and fabrication technologies for engineering tissues - state of the art and future perspectives* J. Biomater. Sci.-Polym. Ed. **2001**, 12, 107-124.
28. T.B.F. Woodfield, J.M. Bezemer, J.S. Pieper, C.A. van Blitterswijk, J. Riesle *Scaffolds for tissue engineering of cartilage* Crit. Rev. Eukaryot. Gene Expr. **2002**, 12, 209-236.
29. B. Doll, C. Sfeir, S. Winn, J. Huard, J. Hollinger *Critical aspects of tissue-engineered therapy for bone regeneration* Crit. Rev. Eukaryot. Gene Expr. **2001**, 11, 173-198.
30. S.R. Winn, H. Uludag, J.O. Hollinger *Sustained release emphasizing recombinant human bone morphogenetic protein-2* Adv. Drug Deliv. Rev. **1998**, 31, 303-318.
31. K. Partridge, X.B. Yang, N.M.P. Clarke, Y. Okubo, K. Bessho, W. Sebald, S.M. Howdle, K.M. Shakesheff, R.O.C. Oreffo *Adenoviral BMP-2 gene transfer in mesenchymal stem cells: In vitro and in vivo bone formation on biodegradable polymer scaffolds* Biochem. Biophys. Res. Commun. **2002**, 292, 144-152.
32. R.O.C. Oreffo, J.T. Triffitt *Future potentials for using osteogenic stem cells and biomaterials in orthopedics* Bone **1999**, 25, 5S-9S.
33. P. Bianco, P.G. Robey *Stem cells in tissue engineering* Nature **2001**, 414, 118-121.
34. E. Vogelín, N.F. Jones, J.I. Huang, J.H. Brekke, J.M. Toth *Practical illustrations in tissue engineering: Surgical considerations relevant to the implantation of osteoinductive devices* Tissue Eng. **2000**, 6, 449-460.
35. J.M. Bezemer, D.W. Grijpma, P.J. Dijkstra, C.A. van Blitterswijk, J. Feijen *A controlled release system for proteins based on poly(ether ester) block-copolymers: polymer network characterization* J. Control. Release **1999**, 62, 393-405.
36. J. Sohler, R.E. Haan, K. de Groot, J.M. Bezemer *A novel method to obtain protein release from porous polymer scaffolds: emulsion coating* J. Control. Release **2003**, 87, 57-68.
37. J.L. Drury, D.J. Mooney *Hydrogels for tissue engineering: scaffold design variables and applications* Biomaterials **2003**, in press.
38. J.A. Burdick, D. Frankel, W.S. Dernell, K.S. Anseth *An initial investigation of photocurable three-dimensional lactic acid based scaffolds in a critical-sized cranial defect* Biomaterials **2003**, 24, 1613-1620.
39. J.A. Burdick, M.N. Mason, A.D. Hinman, K. Thorne, K.S. Anseth *Delivery of osteoinductive growth factors from degradable PEG hydrogels influences osteoblast differentiation and mineralization* J. Control. Release **2002**, 83, 53-63.
40. G.G. Henn, C. Birkinshaw, M. Buggy, E. Jones *A comparison of in-vitro and in-vivo degradation of poly(D,L-lactide) bio-absorbable intra-medullary plugs* Macromol. Biosci. **2001**, 1, 219-222.
41. W. Heidemann, S. Jeschkeit, K. Ruffieux, J.H. Fischer, M. Wagner, G. Kruger, E. Wintermantel, K.L. Gerlach *Degradation of poly(D,L)lactide implants with or without addition of calciumphosphates in vivo* Biomaterials **2001**, 22, 2371-2381.
42. R. Giardino, M. Fini, N.N. Aldini, G. Giavaresi, M. Rocca, L. Orienti, A. DeLollis, L. Fambri *Experimental evaluation of a resorbable intramedullary plug for cemented total hip replacement* Biomaterials **1997**, 18, 907-913.
43. A. Merolli, C. Gabbi, A. Cacchioli, L. Ragionieri, L. Caruso, L. Giannotta, P.T. Leali *Bone response to polymers based on poly-lactic acid and having different degradation times* J. Mater. Sci.-Mater. Med. **2001**, 12, 775-778.
44. D.I. Wheeler, D.I. Chamberland, J.M. Schmitt, D.C. Buck, J.H. Brekke, J.O. Hollinger, S.P. Joh, K.W. Suh *Radiomorphometry and biomechanical assessment of recombinant human bone morphogenetic protein 2 and polymer in rabbit radius osteotomy model* J. Biomed. Mater. Res. **1998**, 43, 365-373.
45. F. Kandziora, H. Bail, G. Schmidmaier, G. Schollmeier, M. Scholz, C. Knispel, T. Hiller, R. Pflugmacher, T. Mittlmeier, M. Raschke, N.P. Haas *Bone morphogenetic protein-2 application by a poly(D,L-lactide)-coated interbody cage: in vivo results of a new carrier for growth factors* J. Neurosurg. **2002**, 97, 40-48.

46. R. Malekzadeh, J.O. Hollinger, D. Buck, D.F. Adams, B.S. McAllister *Isolation of human osteoblast-like cells and in vitro amplification for tissue engineering* J. Periodont. **1998**, 69, 1256-1262.
47. X.B. Yang, H.I. Roach, N.M.P. Clarke, S.M. Howdle, R. Quirk, K.M. Shakesheff, R.O.C. Oreffo *Human osteoprogenitor growth and differentiation on synthetic biodegradable structures after surface modification* Bone **2001**, 29, 523-531.

# Appendix A

## Synthesis of PEG-RGD conjugates

*Problems worthy of attack  
Prove their worth by hitting back.*

Piet Hein (1905-1996)

### Abstract

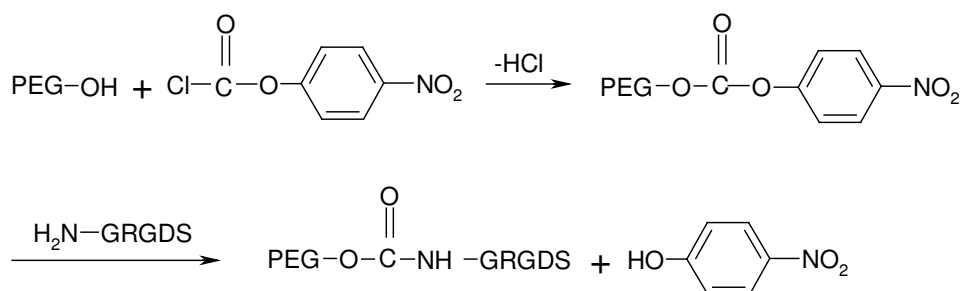
RGD-containing peptides sequences were coupled to poly(ethylene glycol)s of various molecular weights, that were activated with 4-nitrophenyl chloroformate. In cell culturing experiments, the incorporation of RGD-sequences into 1000PEOT70PBT30 by blending with PEG-RGD conjugates results in some clustered cells at the surface of films of the blends. The improvement in bone marrow stromal cell attachment as compared to unmodified 1000PEOT70PBT30 films, however, was not sufficient to justify the use of these materials in further studies. A likely explanation for the low cell attachment is the rapid washing out of a significant amount of blended PEG-RGD conjugates from the samples after contact with water.

### Introduction

To use the hydrophilic PEOT/PBT compositions in bone tissue engineering, the copolymer surface needs to be modified to improve in vitro cell attachment. Several approaches towards this end can be taken. Proteins like fibronectin and vitronectin play an important role in in vitro osteoblast adhesion.<sup>[1]</sup> These proteins contain the tripeptide RGD (Arg-Gly-Asp), which is the active-site sequence for cell adhesion.<sup>[2]</sup> By immobilizing proteins that contain this sequence or the peptide itself on the surface of a material, cell adhesion can be enhanced. Peptide grafting is quite easily controlled and stable in time, while protein adsorption is quite difficult to control and dynamic in nature. Therefore RGD-peptide grafting (usually employing an GRGDS sequence) may be advantageous over other approaches employed to improve long-term cell adhesion to biomaterials.<sup>[3]</sup>

A well-known way of enhancing cell attachment onto surfaces is the incorporation of peptides. After coupling of peptides to PEG, we investigated the possibility of improving bone marrow stromal cell (BMSC) attachment and growth, by blending PEG-RGD conjugates into PEOT/PBT copolymers. PEG-RGD conjugates have previously been reported to cluster cells in cell suspensions, showing the cell binding capacity of these types of molecules.<sup>[4,5]</sup> PEG-RGD conjugates are expected to entangle with the copolymer chains in the hydrophilic

PEO domains and remain within the material for relatively long times. PEG-RGD conjugates were synthesized using 4-nitrophenyl chloroformate as described by Jo *et al.* and shown in Scheme A.1.<sup>[6]</sup>



Scheme A.1 - Reaction scheme for the coupling of a GRGDS peptide sequence to the hydroxyl group of PEG by the use of 4-nitrophenyl chloroformate.

## Materials and methods

### Materials

All solvents used were analytical grade and all chemicals were at least 99 % pure, unless otherwise mentioned, and used as received. <sup>1</sup>H-NMR spectra were obtained using a Varian 300 MHz apparatus. <sup>13</sup>C-NMR spectra were obtained using a Varian 400 MHz apparatus. 1000PEOT70PBT30 and 300PEOT55PBT45 were synthesized as previously described, using vitamin E as an antioxidant.<sup>[7]</sup> Compositions according to <sup>1</sup>H-NMR were 945PEOT71PBT29 and 296PEOT53PBT47 respectively. PEOT/PBT copolymers were used without further purification.

*Films prepared by solution casting.* PEOT/PBT films (75-100 μm thick) were prepared by casting 20 % (w/v) polymer solutions in chloroform (1000PEOT70PBT30) or chloroform/1,1,1,3,3,3-hexafluoro-2-propanol (CHCl<sub>3</sub>/HFIP) mixtures (300PEOT55PBT45) on a glass plate using a casting knife. All films were placed in ethanol (overnight) to remove any residual HFIP and/or CHCl<sub>3</sub>. Films were dried in a vacuum oven under reduced nitrogen pressure for 5 d.

### PEG-RGD conjugate synthesis

*Determination of PEG molecular weight.* PEG (Fluka, Switzerland) molecular weights were determined by <sup>1</sup>H-NMR using trifluoroacetic anhydride (Sigma-Aldrich, Germany) to derivatize the PEG end groups. The following molecular weights were found: PEG 4000:  $\overline{M}_n = 4.5 \times 10^3$ , PEG 8000:  $\overline{M}_n = 8.4 \times 10^3$ , PEG 10000:  $\overline{M}_n = 11.1 \times 10^3$ . These experimentally determined molecular weights were used to calculate the yield of the coupling reaction with the RGD containing peptide, after pre-activation with 4-nitrophenyl chloroformate (NPC). Activation and coupling reactions were performed as previously described by Jo *et al.*<sup>[6]</sup>

*Activation of PEG 4000.* In a round-bottom flask PEG 4000 (10.090 g, 2.23 mmol) was dissolved in 150 mL anhydrous toluene (Biosolve, The Netherlands) at 40°C. To this solution 3.5 mL of triethyl amine (Merck, Germany) and subsequently 4-nitrophenyl chloroformate (4.214 g, 20.9 mmol, NPC, Acros, Belgium) were added. After addition of NPC, the solution colored slightly yellow. The reaction was continued for 4 h. The precipitated organic salt was removed by filtration. The activated PEG solution in toluene was precipitated in a tenfold

excess anhydrous diethyl ether, filtered and dried in vacuo for 36 h. Subsequently, the product was recrystallized from 100 mL ethyl acetate (Biosolve, The Netherlands) and dried in a vacuum oven. The product was a white wax, yield: 8.2g (76 %). According to  $^1\text{H-NMR}$  94 % of the PEG end groups had reacted.  $^1\text{H-NMR}$  ( $\text{D}_2\text{O}$ , 300 MHz):  $\delta$  3.4-3.7 (s, 408H,  $\{\text{CH}_2\text{CH}_2\text{O}\}_n$ ),  $\delta$  3.7 (m, 4H,  $\text{CH}_2\text{CH}_2\text{-}\{\text{CH}_2\text{CH}_2\text{O}\}_n\text{-CH}_2\text{CH}_2$ ),  $\delta$  4.4 (m, 4H,  $\text{CH}_2\text{CH}_2\text{-}\{\text{CH}_2\text{CH}_2\text{O}\}_n\text{-CH}_2\text{CH}_2$ ),  $\delta$  4.7 ( $\text{D}_2\text{O}$ ),  $\delta$  7.4 (d, 4H, Ar),  $\delta$  8.3 (d, 4H, Ar).

*Activation of PEG 8000.* Reaction conditions as in the activation of PEG 4000.

The product was a fluffy white powder, yield: 3.1g (55 %). According to  $^1\text{H-NMR}$  92 % of the PEG end groups had reacted.  $^1\text{H-NMR}$  ( $\text{D}_2\text{O}$ , 300 MHz):  $\delta$  3.4-3.7 (s, 756H,  $\{\text{CH}_2\text{CH}_2\text{O}\}_n$ ),  $\delta$  3.7 (m, 4H,  $\text{CH}_2\text{CH}_2\text{-}\{\text{CH}_2\text{CH}_2\text{O}\}_n\text{-CH}_2\text{CH}_2$ ),  $\delta$  4.4 (m, 4H,  $\text{CH}_2\text{CH}_2\text{-}\{\text{CH}_2\text{CH}_2\text{O}\}_n\text{-CH}_2\text{CH}_2$ ),  $\delta$  4.7 ( $\text{D}_2\text{O}$ ),  $\delta$  7.4 (d, 4H, Ar),  $\delta$  8.3 (d, 4H, Ar).

*Activation of PEG 10000.* Reaction conditions as in the activation of PEG 4000.

The product was a fine white powder, yield: 8.2 g (78 %). According to  $^1\text{H-NMR}$  91 % of the PEG end groups had reacted.  $^1\text{H-NMR}$  ( $\text{D}_2\text{O}$ , 300 MHz):  $\delta$  3.5-3.7 (s, 1004H,  $\{\text{CH}_2\text{CH}_2\text{O}\}_n$ ),  $\delta$  3.7 (m, 4H,  $\text{CH}_2\text{CH}_2\text{-}\{\text{CH}_2\text{CH}_2\text{O}\}_n\text{-CH}_2\text{CH}_2$ ),  $\delta$  4.4 (m, 4H,  $\text{CH}_2\text{CH}_2\text{-}\{\text{CH}_2\text{CH}_2\text{O}\}_n\text{-CH}_2\text{CH}_2$ ),  $\delta$  4.7 ( $\text{D}_2\text{O}$ ),  $\delta$  7.4 (d, 4H, Ar),  $\delta$  8.3 (d, 4H, Ar).

*Coupling GRGDS to activated PEG 4000.* In a round-bottom flask GRGDS (25.3 mg, 0.063 mmol, Bachem, Switzerland) was dissolved in 20 mL 0.1 M sodium phosphate buffer (pH=8.3). After 15 min PEG 4000(NPC) $_2$  (0.100 g, 0.020 mmol) was added. The clear solution colored slightly yellow. After 90 h of reaction, the product was dialyzed in milli-Q water for 24 h (molecular porous regenerated cellulose dialysis membrane (MWCO=2000) Spectra/Por 7, Spectrum Laboratories Inc., U.S.A.) with periodic media changes. Finally, the product was freeze-dried for 30 h. The product was obtained as a white powder, yield: 103 mg (94 %). According to  $^1\text{H-NMR}$ , 95 % of the PEG end groups were coupled to the RGD containing peptide. The spectrum showed no NPC peaks.  $^1\text{H-NMR}$  ( $\text{D}_2\text{O}$ , 300 MHz):  $\delta$  1.4-1.8 (m, 4H,  $\text{NHCH}_2\text{CH}_2\text{CH}_2$  Arg),  $\delta$  2.5-2.7 (m, 2H,  $\text{CH}_2$  Asp),  $\delta$  3.1 (t, 2H,  $\text{NHCH}_2\text{CH}_2\text{CH}_2$  Arg),  $\delta$  3.4-3.7 (s, 408H,  $\{\text{CH}_2\text{CH}_2\text{O}\}_n$ ),  $\delta$  3.7-3.8 (m, 4H,  $\text{CH}_2$  Ser and  $\text{CH}_2\text{-NH}_2$  Gly),  $\delta$  3.9 (s, 2H,  $\text{CH}_2$  Gly),  $\delta$  4.1 (m, 2H, CH Arg and CH Ser),  $\delta$  4.3 (q, 1H,  $\text{CH}_2\text{-CO-NH}$ ),  $\delta$  4.5-4.6 (m, 1H, CH Asp),  $\delta$  4.7 ( $\text{D}_2\text{O}$ ). A complete  $^1\text{H-NMR}$  spectrum with peak assignments is shown in Figure A.1

*Coupling GRGDS to activated PEG 8000.* Reaction conditions as in the coupling to activated PEG 4000. The product was obtained as a white powder, yield: 86 mg (84 %). According to  $^1\text{H-NMR}$ , 98 % of the PEG end groups were coupled to the RGD containing peptide. No NPC peaks were distinguished in the spectrum.  $^1\text{H-NMR}$  ( $\text{D}_2\text{O}$ , 300 MHz):  $\delta$  1.5-1.9 (m, 4H,  $\text{NHCH}_2\text{CH}_2\text{CH}_2$  Arg),  $\delta$  2.6-2.8 (m, 2H,  $\text{CH}_2$  Asp),  $\delta$  3.1 (t, 2H,  $\text{NHCH}_2\text{CH}_2\text{CH}_2$  Arg),  $\delta$  3.4-3.7 (s, 756H,  $\{\text{CH}_2\text{CH}_2\text{O}\}_n$ ),  $\delta$  3.7-3.8 (m, 4H,  $\text{CH}_2$  Ser and  $\text{CH}_2\text{-NH}_2$  Gly),  $\delta$  3.9 (s, 2H,  $\text{CH}_2$  Gly),  $\delta$  4.1-4.2 (m, 2H, CH Arg and CH Ser),  $\delta$  4.3 (q, 1H,  $\text{CH}_2\text{-CO-NH}$ ),  $\delta$  4.7 ( $\text{D}_2\text{O}$  and CH Asp).

*Coupling GRGDS to activated PEG 10000.* Reaction conditions as in the coupling to activated PEG 4000. The product was obtained as a white powder, yield: 139 mg (97 %). According to  $^1\text{H-NMR}$ , 94 % of the PEG end groups were coupled to the RGD containing peptide. No NPC peaks were observed.  $^1\text{H-NMR}$  ( $\text{D}_2\text{O}$ , 300 MHz):  $\delta$  1.5-1.9 (m, 4H,  $\text{NHCH}_2\text{CH}_2\text{CH}_2$  Arg),  $\delta$  2.6-2.8 (m, 2H,  $\text{CH}_2$  Asp),  $\delta$  3.1 (t, 2H,  $\text{NHCH}_2\text{CH}_2\text{CH}_2$  Arg),  $\delta$  3.4-3.7 (s, 1004H,  $\{\text{CH}_2\text{CH}_2\text{O}\}_n$ ),  $\delta$  3.7-3.8 (m, 4H,  $\text{CH}_2$  Ser and  $\text{CH}_2\text{-NH}_2$  Gly),  $\delta$  3.9 (s, 2H,  $\text{CH}_2$  Gly),  $\delta$  4.1-4.2 (m, 2H, CH Arg and CH Ser),  $\delta$  4.3 (q, 1H,  $\text{CH}_2\text{-CO-NH}$ )  $\delta$  4.5-4.6 (m, 1H, CH Asp),  $\delta$  4.7 ( $\text{D}_2\text{O}$ ).

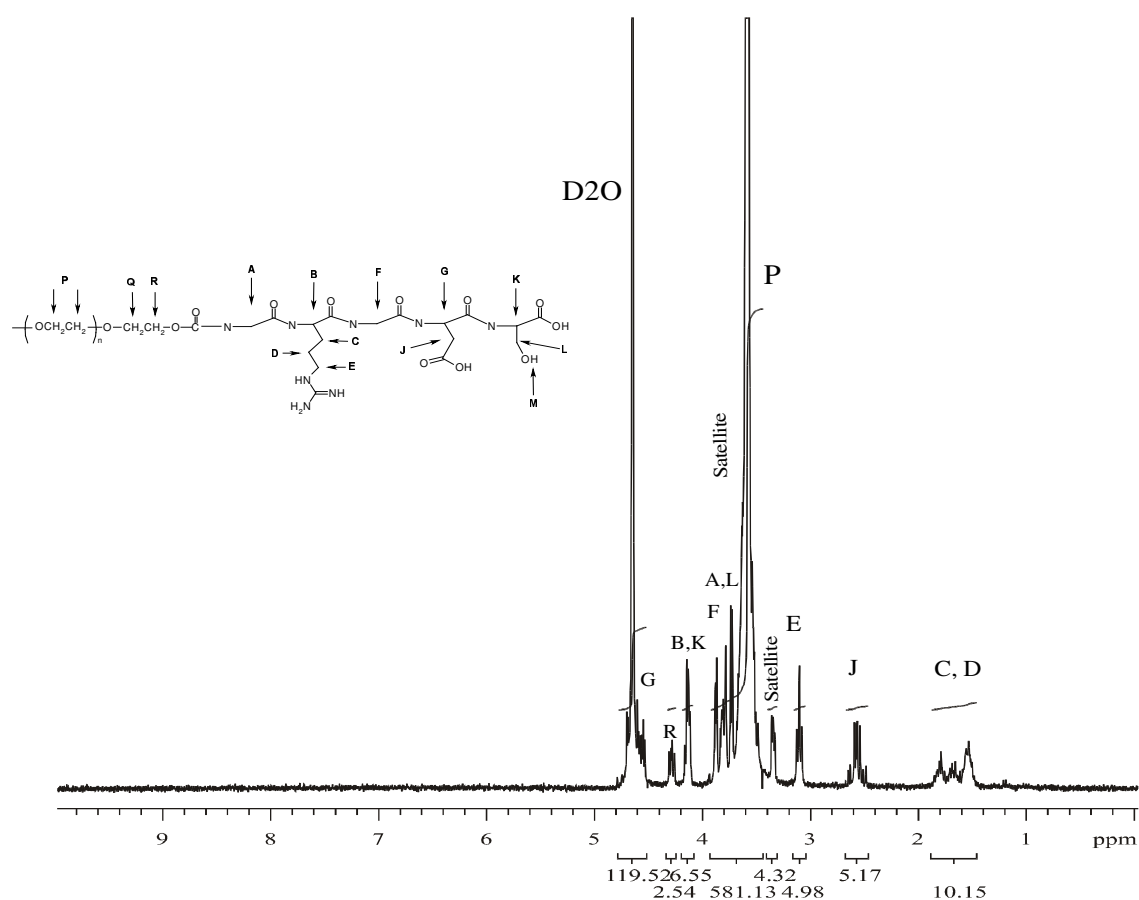


Figure A.1 -  $^1\text{H}$ -NMR of the PEG 4000-(GRGDS) $_2$  conjugate. No 4-nitrophenyl proton signals can be distinguished in the spectrum.

*Preparation of films.* Approximately 75  $\mu\text{m}$  thick films were prepared by casting mixtures of PEG-RGD conjugates or carboxylic acid terminated PEG (PEGDC, used as model compounds for PEG-RGD conjugates, Fluka, Switzerland) and 1000PEOT70PBT30 in  $\text{CHCl}_3$  and drying in a vacuum oven under reduced nitrogen pressure for 5 d. The following model compounds were used: O,O'-bis(carboxymethyl)polyethylene glycol 600, O,O'-bis(2-carboxyethyl)polyethylene glycol 2000, O,O'-bis(2-carboxyethyl)polyethylene glycol 6000.

*Release of PEGDC from films.* Circular samples of 28 mm in diameter were cut from the films described above. The samples were weighed and placed in glass containers with milliQ water at 37°C. After set times the samples were removed, dried and weighed again. From the mass loss, the loss of carboxylic acid terminated PEG (PEGDC) was determined.

#### Bone marrow stromal cell culture and analysis

*Goat bone marrow stromal cell culturing on copolymer films.* Samples with a diameter of 10 mm were cut from the copolymer films blended with PEG-RGD conjugates (solution cast). Before culturing, samples were washed with demineralized water (2x), 70 % ethanol/water and sterile PBS (3x). For preliminary screening experiments goat BMSCs, passage 3 were used. The cells were seeded with a density of 10,000 cells/ $\text{cm}^2$ , in the presence of 3 mL minimal essential medium ( $\alpha$ -MEM, Life Technologies, The Netherlands) containing<sup>[8]</sup>: 15 % (v/v) fetal bovine serum (Life Technologies, The Netherlands), 100 units/mL penicillin, 100  $\mu\text{g/mL}$  streptomycin (Life Technologies, The Netherlands), 2 mM L-glutamine (Life Technologies, The Netherlands), 0.2 mM ascorbic acid 2-phosphate (Life Technologies, The



Netherlands), 10 mM  $\beta$ -glycerophosphate (Sigma, The Netherlands),  $10^{-8}$  M dexamethasone (Sigma, The Netherlands).

**Methylene blue staining.** Samples were analyzed at day 1, 3 and 7. Films were washed with warm PBS containing 100 units/mL penicillin and 100  $\mu$ g/mL streptomycin and subsequently fixed with glutaraldehyde (Merck, Germany, 1.5 % solution in 0.14 M cacodylic acid (Fluka, Germany, buffer pH = 7.35). Then the samples were washed with water and stained for 30 s using a 1 % methylene blue solution in 0.1 M borax buffer (Sigma/Aldrich, Germany, pH = 8.5). Scaffolds were subsequently washed with demineralized water, until the water was clear. Samples were stored in a refrigerator until further analysis. Samples were evaluated using a Nikon SM2-10A stereomicroscope (1x objective). Digital photographs were taken using a Sony progressive 3 CCD camera.

## Results and discussion

The degree of activation with 4-nitrophenyl chloroformate (after product precipitation in ether) and the degree of coupling (after product dialysis in water) were determined by  $^1\text{H}$ -NMR. For the activation reaction 4 h were sufficient to reach conversions of 93 to 96 %. Subsequent reaction with GRGDS-sequences for at least 70 h lead to degrees of coupling of 94 % and higher. Shorter reaction times significantly reduced the degree of coupling of GRGDS to PEG; after 4 and 24 h only 8 and 40 %, respectively, were coupled. Besides  $^1\text{H}$ -NMR data, further evidence for the coupling of PEG with GRGDS was given by  $^{13}\text{C}$ -NMR, clearly showing a peak at  $\delta=161$  ppm, which could be assigned to the urethane linkage in the PEG-RGD conjugate. Other synthesis routes, like the activation of carboxylic acid functionalized PEGs with NHS, did not result in the desired compounds.

PEG-RGD conjugates were prepared using PEGs with molecular weights 4000, 8000 and 10000. The PEG-RGD conjugates based on PEG molecular weights of 4000, 8000 and 10000 were blended with the 1000PEOT70PBT30 copolymer (2.5 or 10 wt % conjugate). Solution cast films were produced on which goat BMSCs were cultured. After 3 d of cell culture the samples were stained with methylene blue and studied by microscopy (Figure A.2).

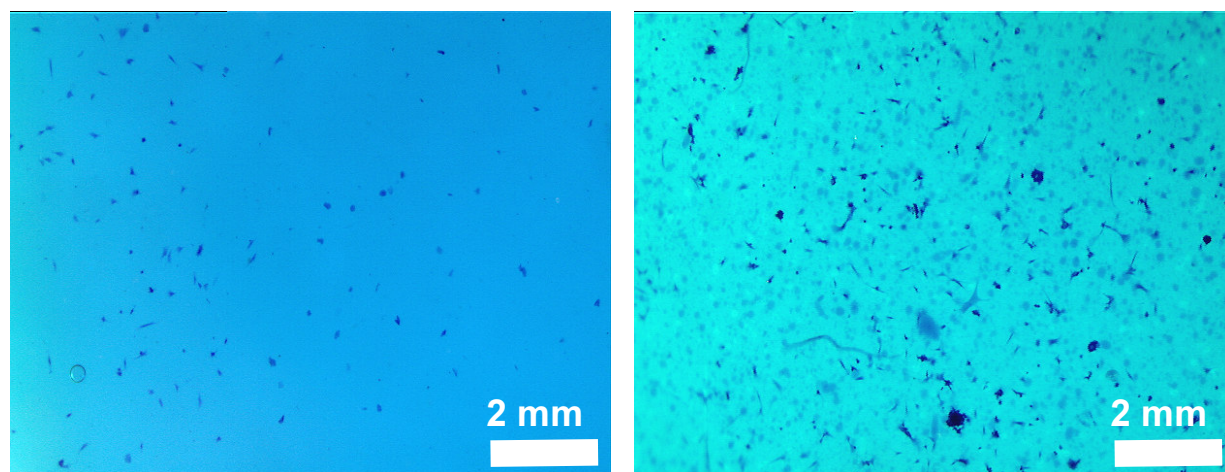


Figure A.2 - Microscopic images of 1000PEOT70PBT30 copolymer films with goat BMSCs after 3 d of culturing. The samples were stained with methylene blue: copolymer (light blue) and goat BMSCs (dark blue spots). Left: 1000PEOT70PBT30. Right: 1000PEOT70PBT30 blended with 10 wt % PEG-RGD conjugate based on PEG with a molecular weight of 8000. [Color figure on p. 180]

The films with 2.5 and 10 wt % blended PEG-RGD conjugate, of molecular weight 4000, 8000 and 10000 showed comparable results: clustered cells were observed on the surface. At larger amounts and higher molecular weights of the blended PEG-RGD conjugate more cells appeared to be present at the surface. A significant improvement of BMSC attachment compared to 1000PEOT70PBT30 controls was, however, not observed.

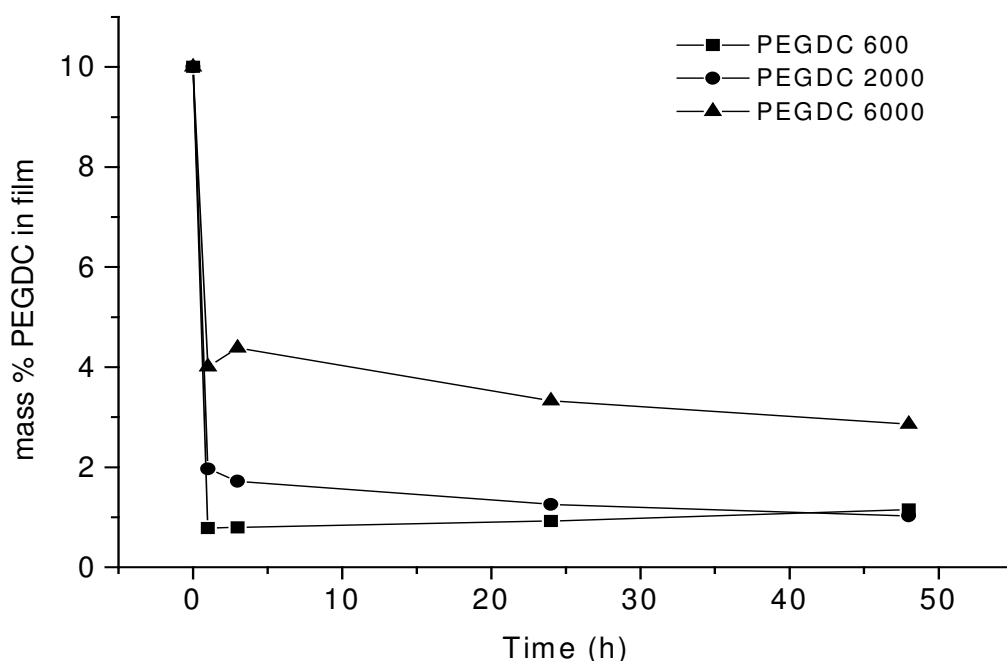


Figure A.3 - Mass loss of PEGDC containing 1000PEOT70PBT30 films.

To verify if the PEG-RGD conjugates indeed remained in the material, release profiles are required. Due to the relatively large amount of material needed, the release of PEG model compounds containing carboxylic acid end groups (PEGDC) was studied. These compounds were blended with the 1000PEOT70PBT30 copolymer and the mass loss of films was determined after extraction with water. As shown in Figure A.3 all films show rapid mass loss. This release is most likely caused by the fast and extensive swelling of 1000PEOT70PBT30 (approximately 69 mass % within two h, the equilibrium water uptake is 74 mass %) allowing the release of the incorporated PEGs.

PEGDC with a higher molecular weight was retained longer in the film than the lower molecular weight products. However, even in the case of PEGDC 6000 only 4 mass % from the original 10 mass % remained present after extraction in water. The rapid release of the PEGDC model compounds from the PEOT/PBT films suggests that PEG-RGD conjugates will also be rapidly released and that their surface concentration will be rather low in time.

Although the PEG-RGD conjugates present at the surface appear to be able to bind cells, the amount of the RGD containing peptide sequences<sup>[9-11]</sup>, is not sufficient to obtain a significant improvement in BMSC attachment.

Chemical modification of the surface of the material with gas plasma treatments, followed by RGD modification of the introduced functional groups, is likely to improve cell attachment, due to higher concentrations of RGD sequences at the surface, which will be maintained for a longer period of time.

## Conclusions

The incorporation of RGD-sequences into 1000PEOT70PBT30 by blending with PEG-RGD conjugates results in some clustered cells at the surface of films of the blends. The improvement in bone marrow stromal cell attachment as compared to 1000PEOT70PBT30 films, however, was not sufficient to justify the use of these materials in further studies. A likely explanation for the low cell attachment is the rapid washing out of a significant amount of blended PEG-RGD conjugates from the samples after contact with water. Therefore the available concentration of PEG-RGD at the surface is low and/or the RGD sequences at the surface are not available for cell attachment.

## Acknowledgements

M.C. Huijgen (University of Twente) is gratefully acknowledged for the synthesis and characterization of the PEG-RGD conjugates and W.J. Sleijster for the cell culture experiments (Isotis OrthoBiologics, Bilthoven, The Netherlands).

## References

1. K. Anselme *Osteoblast adhesion on biomaterials* Biomaterials **2000**, 21, 667-681.
2. M.D. Piersbacher *Cell attachment activity of fibronectin can be duplicated by small synthetic fragments of the molecule* Nature **1984**, 309, 30-33.
3. K.M. Shakesheff, S.M. Cannizzaro, R. Langer *Creating biomimetic micro-environments with synthetic polymer-peptide hybrid molecules* J. Biomater. Sci.-Polym. Ed. **1998**, 9, 507-518.
4. W.G. Dai, J. Belt, W.M. Saltzman *Cell-binding peptides conjugated to poly(ethylene glycol) promote neural cell-aggregation* Bio-Technology **1994**, 12, 797-801.
5. W.G. Dai, W.M. Saltzman *Fibroblast aggregation by suspension with conjugates of poly(ethylene glycol) and RGD* Biotechnol. Bioeng. **1996**, 50, 349-356.
6. S. Jo, H. Shin, A.G. Mikos *Modification of oligo(poly(ethylene glycol) fumarate) macromer with a GRGD peptide for the preparation of functionalized polymer networks* Biomacromolecules **2001**, 2, 255-261.
7. A.A. Deschamps, D.W. Grijpma, J. Feijen *Poly(ethylene oxide)/poly(butylene terephthalate) segmented block copolymers: the effect of copolymer composition on physical properties and degradation* Polymer **2001**, 42, 9335-9345.
8. C. Maniopoulos, J. Sodek, A.H. Melcher *Bone-formation in vitro by stromal cells obtained from bone marrow of young-adult rats* Cell Tissue Res. **1988**, 254, 317-330.
9. D.J. Irvine, A.M. Mayes, L.G. Griffith *Nanoscale clustering of RGD peptides at surfaces using comb polymers. 1. Synthesis and characterization of comb thin films* Biomacromolecules **2001**, 2, 85-94.
10. D.J. Irvine, A.G. Ruzette, A.M. Mayes, L.G. Griffith *Nanoscale clustering of RGD peptides at surfaces using comb polymers. 2. Surface segregation of comb polymers in polylactide* Biomacromolecules **2001**, 2, 545-556.
11. G. Maheshwari, G. Brown, D.A. Lauffenburger, A. Wells, L.G. Griffith *Cell adhesion and motility depend on nanoscale RGD clustering* J. Cell Sci. **2000**, 113, 1677-1686.



# Appendix B

## Grafting of poly(ethylene oxide)/poly(butylene terephthalate) block copolymers onto hydroxyapatite particles

*And now for something completely different.*

Monty Python's Flying Circus

### Abstract

Composite materials based on hydroxyapatite (HA) particles and poly(ethylene oxide)/poly(butylene terephthalate) copolymers, PEOT/PBT, were prepared by blending methods and by grafting. Composites based on PEOT/PBT copolymers with a PEO molecular weight of 1000 and a PEOT content of 70 weight % (1000PEOT70PBT30) were studied. The formation of 1000PEOT70PBT30 grafts onto HA filler particles (38-53  $\mu\text{m}$ ) by directly adding HA particles to the polycondensation reaction mixture is described. After extraction of the soluble components, TGA and IR analyses showed considerably more 1000PEOT70PBT30 on the HA particles of the composites prepared by grafting than of those prepared by blending.

In the dry state, an increase in HA content from 0 to 25 vol % in HA-composites prepared by grafting and by blending leads to an increase in Shore A hardness from 83 to 92. At 17.5 and 25 vol % HA a significant improvement in the elongation at break and the energy up to break, both in the dry and water-swollen state, was observed for the composites prepared by grafting. HA-composites containing 17.5 vol % HA, prepared by grafting, showed an elongation at break of 271 % in the dry state and 58 % in the water-swollen state. HA-composites with 17.5 vol % HA, prepared by blending, showed an elongation at break of 62 % in the dry state and 6.5 % in the water-swollen state. In the water-swollen state, the incorporation of HA (either by grafting or by blending) does not result in composite materials with improved mechanical properties, like tensile modulus and strength, compared to the original 1000PEOT70PBT30 copolymer.

For the composites prepared by grafting, the combined IR, TGA and tensile data indicate that the copolymer is chemically bound to the HA, most likely by the formation of copolymer grafts onto the surface of HA particles. To our knowledge this would be the first example of the direct formation of polymer grafts onto HA, prepared by a polycondensation reaction in the presence of HA particles. By employing freeze-drying techniques or compression molding

of polymer powder/salt mixtures followed by salt leaching, the HA-composites can be converted into porous structures.

## Introduction

In the search for the optimal bone substitute material many researchers have incorporated bioactive filler particles in their (co)polymer systems in order to obtain materials with improved biological and mechanical properties. One of the first successful systems was polyethylene reinforced with hydroxyapatite (HAPEX™) as developed by Bonfield and coworkers.<sup>[1-5]</sup> These materials need to function as permanent implants, since polyethylene is non-biodegradable.

A similar approach has also been used in designing biodegradable implants and scaffolds for bone tissue engineering. Biodegradable HA composite systems based on collagen<sup>[6]</sup>, gelatin<sup>[7-9]</sup>, chitosan<sup>[10-12]</sup> and chitin<sup>[13]</sup> have been described in literature. The most extensively studied group of biodegradable composites is based on HA and polyesters, mainly PLLA<sup>[14-22]</sup>, PDLA<sup>[23]</sup>, PGA<sup>[24]</sup>, PCL<sup>[25]</sup> and their copolymers.<sup>[26-28]</sup> PEOT/PBT<sup>[29-31]</sup> and poly(hydroxy butyrate)<sup>[32]</sup> based composites with HA have also attracted much attention.

The physical and mechanical properties and the degradation behavior of PEOT/PBT copolymers, a family of segmented block copolymers consisting of poly(ethylene oxide) (soft segment) and poly(butylene terephthalate) (hard segment), can be tuned by varying the soft to hard segment ratio.<sup>[33,34]</sup> The composition is indicated as  $a$ PEOT $b$ PBT $c$ , where  $a$  is the starting poly (ethylene glycol) molecular weight,  $b$  the weight percentage of PEOT soft segments and  $c$ , the weight percentage of PBT hard segments. Subcutaneous and intra-bone (tibia) implantations of dense and porous blocks and porous films in rats and goats showed bone bonding, calcification and degradation for copolymers with a high PEO content (1000PEOT60PBT40 and 1000PEOT70PBT30).<sup>[35-38]</sup>

To obtain composite materials with a higher stiffness than the copolymer itself, HA particles can be incorporated in a 1000PEOT70PBT30 matrix. Previous research in the dental field showed that PEOT/PBT-HA composite films are biocompatible and biodegradable (as shown by in vivo fragmentation) and have been suggested for use in guided tissue regeneration.<sup>[39]</sup> Therefore, composite materials based on 1000PEOT70PBT30 and HA are interesting candidates as scaffold materials in bone tissue engineering applications.

We intend to prepare porous PEOT/PBT scaffolds for bone tissue engineering, that can be seeded and cultured with bone marrow stromal cells before implantation in the bone defect. The incorporation of HA into the copolymer may result in composite materials with improved biological and mechanical properties compared to the copolymer itself.

A good interaction between the HA filler and the polymer matrix is essential to provide the composite with good mechanical properties (i.e. strength and toughness). In tensile testing a poor interaction between the polymer matrix and the inorganic filler (poor interfacial bonding) often leads to filler particle debonding and pull-out, resulting in void formation and crack propagation.<sup>[1,4,15,40,41]</sup> Several approaches have been used to improve the interaction between filler and matrix. The use of silane<sup>[42-44]</sup>, zirconate-based<sup>[45]</sup> coupling agents or diisocyanates<sup>[46,47]</sup> to obtain chemical bonds between the filler and the polymer matrix have proven to be efficient. It has to be noted that in many cases these compounds are cytotoxic.<sup>[48]</sup> Hydroxyl groups present on the HA particle surface are known to be reactive towards diisocyanates<sup>[46]</sup> and can act as initiator in ring-opening polymerizations.<sup>[49]</sup> Making use of the reactivity of hydroxyl groups present on the surface of HA, acrylate<sup>[30,31,42,43]</sup> and PEOT/PBT<sup>[46]</sup> (co)polymers have been grafted onto the HA particle surface resulting in

improved mechanical properties of the corresponding composites. In the latter case the PEOT/PBT copolymer was grafted onto HA by use of a diisocyanate coupling agent.

In this study we set out to covalently bind 1000PEOT70PBT30 to HA by direct surface grafting via polycondensation, avoiding the use of potentially harmful coupling agents or surface modifications. The mechanical properties of composites based on grafted HA particles are discussed and compared to HA-composites prepared by blending.

## Materials and methods

### Materials

All solvents were of analytical grade and all chemicals were at least 99 % pure, unless otherwise mentioned, and all were used as received.  $^1\text{H}$ -NMR spectra were obtained using a Varian 300 MHz apparatus. Sintered HA with a particle size of 38-53  $\mu\text{m}$  was provided by professor F.J. Monteiro (INEB, Porto, Portugal) and was used as received.

### Composite preparation

*Copolymer synthesis.* A 1000PEOT70PBT30 multiblock copolymer was prepared by two-step polycondensation in the presence of titanium tetrabutoxide (Merck, Germany) as catalyst (0.2 wt %) as previously described<sup>[33]</sup>, with the exception that vitamin E (Sigma-Aldrich, Germany, approx. 95 % pure) was used as antioxidant. The composition was varied by adjusting the poly(ethylene glycol) (Fluka, Switzerland) to dimethyl terephthalate (Merck, Germany)/1,4-butanediol (Acros, Belgium) ratio. The resulting copolymer composition according to  $^1\text{H}$ -NMR was 917PEOT70PBT30.

*HA-composites prepared by blending.* 1000PEOT70PBT30 was dissolved in chloroform (Biosolve Ltd., The Netherlands) overnight. To these polymer solutions of approximately 20 % (w/v) sintered HA was added. The suspension was stirred for 3 h and precipitated into a tenfold excess of technical grade ethanol (Fisher, The Netherlands). The obtained composites were dried in a vacuum oven at reduced nitrogen pressure for at least 6 d. For calculation of the HA volume percentage the following densities were used: 1.188  $\text{g}/\text{cm}^3$ <sup>[50]</sup> for 1000PEOT70PBT30 and 3.156  $\text{g}/\text{cm}^3$  for HA.<sup>[51]</sup>

*HA-composites prepared by grafting.* The desired amount of HA was immediately added to the polymerization reaction mixture. The synthetic procedure was the same as for the copolymer described above. After 7 to 8 h, when the mixture could not be stirred efficiently, the reaction was stopped by quenching with liquid nitrogen. The composites were discharged from the reaction vessel.

### Composite processing

*Films prepared by compression molding.* Films of HA-composites prepared by blending were prepared by compression molding at 140  $^{\circ}\text{C}$ , the precipitates were heated for 3 min and subsequently molded for 1 min at 2.9 MPa using a laboratory hot press (THB 008, Fontijne Holland BV, The Netherlands). HA-composites prepared by grafting were compression molded at 180  $^{\circ}\text{C}$ , since compression molding at 140  $^{\circ}\text{C}$  did not result in homogeneous films. The film thickness for both the composites prepared by blending and by grafting was approximately 500  $\mu\text{m}$ .

*Porous structures prepared by freeze-drying.* A solution (10 % w/v) of 1000PEOT70PBT30 in 1,4-dioxane (Merck, Germany) was obtained after heating to 60  $^{\circ}\text{C}$ . Approximately 10 % (v/v, relative to the copolymer) sintered HA was added and vigorously stirred. Suspensions were poured into polyethylene vials and frozen at two different temperatures for 12 h: -28  $^{\circ}\text{C}$

(freezer) and +7 °C (refrigerator). Subsequent freeze-drying (5 d, 20 mbar) yielded grayish foams.

*Porous structures prepared by compression molding of polymer/salt mixtures followed by salt leaching.* Granulates of HA-composites prepared by grafting were cryogenically ground using an IKA Labortechnik (Germany) A10 grinder. The obtained composite powder (particle size < 425 µm) and sodium chloride (Merck, Germany, 425-500 µm) were obtained using Endecotts (England) test sieves of 425 and 500 µm mesh size. The powders were mechanically mixed overnight and subsequently compression molded into the desired shapes using a laboratory hot press. Powders were heated at 220 °C for 3 min and subsequently molded for 1 min at 2.9 MPa in a pre-heated mold. Samples were leached with milliQ water (Millipore, USA) for 60 h, after which the water was replaced by ethanol (Merck, Germany). The obtained structures were air-dried.

### Analyses

*Water uptake.* Composite films were swollen in milliQ water at 37 °C for 48 h. The water uptake (single measurements) was determined as the mass gain of the polymer specimens after 48 h, according to equation B.1:

$$\text{water uptake} = \frac{m - m_0}{m_0} \times 100 \quad (\text{mass}\%) \quad (\text{B.1})$$

where  $m_0$  is the initial sample mass and  $m$  the mass of the sample after water uptake.

*Tensile testing.* Strips of 50 x 500 mm (HA-composites prepared by grafting) or 50 x 1000 mm (HA-composites prepared by blending) were cut from compression molded films and subjected to tensile testing. A Zwick Z020 universal tensile testing machine was equipped with a 500 N load cell and the strips were clamped in pneumatic clamps with sandpaper (to prevent slippage). A grip-to-grip separation of 30 mm (HA-composites prepared by grafting) or 50 mm (HA-composites prepared by blending), a pre-load of 0.1 N and a crosshead speed of 50 mm/min were used. The tensile modulus was determined from the initial part (0.1- 0.3 % elongation) of the stress-strain curve. The sample deformation was derived from the grip-to-grip separation, therefore the presented values of the E-modulus give only an indication of the stiffness of the different composites. Samples were measured both in the dry and in the water-swollen state (after 48 h equilibration in milliQ water).

*Hardness measurements.* Shore A hardness was determined using a Zwick hardness meter (ISO R868). Pieces of film (4) were stacked and the hardness was determined in six fold at different places on the top film with a measuring time of 20 s.

*Extraction of the soluble fraction of HA-composites.* Compression molded HA-composite films were extracted using a Soxhlet setup with boiling chloroform over calcium chloride (Merck, Germany). Samples were extracted for 48 h and subsequently air-dried for 4 d.

*Thermogravimetric analysis (TGA).* TGA measurements were performed using a Perkin Elmer TGA 7 Thermogravimetric analyser. Samples of 10-15 mg were heated from 50 to 700 °C at a heating rate of 10 °C/min under a nitrogen flow. The residual weights were used to determine the volume and mass percentages of HA in the HA-composites.

*Infrared spectroscopy (IR).* IR spectra were recorded using a Biorad FTS-60. Spectra were obtained using 256 scans at a resolution of 4 cm<sup>-1</sup> over the range of 4000-800 cm<sup>-1</sup>. Extracted HA-composites and pure HA were ground and mixed with KBr and pressed into a pellet (approximately 10 mg of sample/100 mg KBr). Samples that could not be ground at room temperature (1000PEOT70PBT30 and the residues of the 10 and 17.5 % HA-composites prepared by grafting) were dissolved/suspended in chloroform and the equivalent of 10 mg of



sample was allowed to evaporate on a KBr (Merck, Germany) pellet of approximately 100 mg. Cryogenic grinding of the samples was avoided to limit the exposure to moisture.

*Scanning Electron Microscopy.* Freeze-dried scaffolds were cut with a razor blade and coated with Au/Pd in a Polaron E5600 sputter coater. Micrographs were taken using a Hitachi FE-SEM S-800 at 6 kV. HA-composite films were freeze-fractured in liquid nitrogen. Porous structures of the HA-composites were cut with a razor blade. Micrographs of both were taken using a LEO Gemini 1550 FEG-SEM, fitted with a field emission gun. Samples were not coated and pictures were typically taken at a low voltage of 0.5–1.0 kV.

### Statistical analysis

The properties of dry and wet samples were compared using a two tailed, two sample Student's t-test assuming unequal variance. Differences were considered statistically significant when  $p < 0.05$ .

## Results and discussion

PEOT/PBT copolymers were prepared using a polycondensation reaction of dimethyl terephthalate, poly(ethylene glycol) and an excess of 1,4-butanediol. The hydroxyl groups of the alcohols react with the terephthalate ester groups by transesterification. By distilling of the excess of 1,4-butanediol a polymer is eventually formed. Hydroxyl groups present on the HA surface are known to be reactive.<sup>[46,49]</sup> Making use of the reactivity of the hydroxyl groups present on the surface of HA, we investigated the formation of grafts of 1000PEOT70PBT30 onto HA filler particles (38-53  $\mu\text{m}$ ) by polycondensation, by directly adding HA to the polycondensation reaction mixture. For comparison, a series of composite blends was prepared by mixing HA with a solution of the copolymer in chloroform and precipitating the resulting suspension in ethanol. The prepared composites are listed in Table B.1. TGA measurements show that the actual volume percentages of HA are close to the intended ones, both for HA-composites prepared by blending as for the composites prepared by grafting. 1000PEOT70PBT30 is a hydrophilic polymer with a high water uptake. Addition of HA decreases the water uptake, but composites with 25 vol % of HA, still take up a high amount of water (52-56 mass %).

Table B.1 - Composites of 1000PEOT70PBT30 with HA prepared by blending and grafting.

Intended composition	vol % HA by TGA <sup>§</sup>	Water uptake (mass %) <sup>‡</sup>
1000/70/30	- <sup>*</sup>	79
10 vol % HA blended	9.6	69
17.5 vol % HA blended	17.0	62
25 vol % HA blended	24.3	52
10 vol % HA grafted	9.6	60
17.5 vol % HA grafted	16.4	61
25 vol % HA grafted	24.9	56

§: single measurements, unprocessed material, onset of mass loss 400-404 °C

‡: single measurements, compression molded film

\*: a residue of 4.7 mass % was found, this value was used to correct the vol % of HA found for the composites

To study whether the copolymer was chemically bound to the HA particles, HA-composite films were extracted with dry chloroform for 48 h using a Soxhlet setup. This time period was

long enough to completely dissolve a 1000PEOT70PBT30 film. The residues of the extracted HA-composite films were analyzed using TGA. The results are summarized in Table B.2.

Table B.2 - TGA data of extracted composites films, prepared by compression molding.

Composite	vol % HA	Onset of mass loss	mass % 1000/70/30 remaining after extraction
Pure HA	98.9	No onset	-
10 vol % HA blended <sup>§</sup>	95.6	385 °C	1.7
17.5 vol % HA blended <sup>§</sup>	96.8	378 °C	1.2
25 vol % HA blended <sup>§</sup>	97.2	378 °C	1.1
10 vol % HA grafted <sup>‡</sup>	11.7 ± 0.1	411 ± 2 °C	73.9 ± 0.2
17.5 vol % HA grafted <sup>‡</sup>	71.5 ± 3.0	401 ± 1 °C	13.1 ± 1.7
25 vol % HA grafted <sup>‡</sup>	95.5 ± 0.1	397 ± 1 °C	1.7 ± 0.1

§: single measurement

‡: average result of a duplicate measurement

Clear differences are observed between the residues of extracted HA-composites prepared by blending and those prepared by grafting. The residues of the extracted composites prepared by blending all show small amounts of copolymer (up to 1.7 mass %), most likely due to physical adsorption of the copolymer onto the HA. After extraction the residues of the composites prepared by grafting with 10 and 17.5 vol % HA show a considerable mass loss at about 400 °C (this is in the same temperature range (390-410 °C) as for the unextracted composites and the copolymer without HA).

Table B.2 shows that especially the residues of the extracted composites with 10 and 17.5 vol % HA, prepared by grafting, contain quite high amounts of copolymer. To get an indication of the maximal amount of copolymer that can be present on a HA particle, a model calculation was performed. Assuming spherical and non-porous HA particles with a diameter of 38-53 µm, covered with polymer chains with a cross-sectional area of 0.13 nm<sup>2</sup> (minimal area that a single ethylene oxide unit occupies)<sup>[52]</sup> and a molecular weight of 150,000 g/mol (which is the maximum chain length obtained during polymerization in the absence of HA (Chapter 3)), one can calculate that a maximum value of 6.4-8.7 mass % of copolymer can be expected on the surface of HA particles.

The higher amounts of copolymer observed in the extracted residues of HA-composites prepared by grafting with 10 and 17.5 vol % HA, could be the result of a subsequent cross-linking reaction of bound (to HA) and unbound copolymer chains during the polycondensation reaction. To verify if the HA-composites showed signs of cross-linking, possibly resulting in network formation, they were placed in chloroform (CHCl<sub>3</sub>) and in 1,1,1,3,3,3-hexafluoro-2-propanol (HFIP). The HA-composite with 10 vol % HA prepared by grafting showed gel formation in CHCl<sub>3</sub> and in HFIP, indicative of network formation. Gel formation was not observed for the HA-composites prepared by grafting containing 17.5 and 25 vol % HA, although the presence of cross-linked copolymer chains in these composites cannot be excluded.

A possible cause for cross-linking during the synthesis of the HA-composites prepared by grafting is the removal of the vitamin E antioxidant from the reaction mixture during the polycondensation reaction (b.p. of vitamin E at 0.1 bar: 200-220 °C)<sup>[53]</sup>, it is known that the PEO segments in PEOT/PBT copolymers cross-link under oxidizing conditions.<sup>[54-56]</sup>

IR-spectra of the residues after extraction of the HA-composites prepared by blending and grafting were compared to the spectra of 1000PEOT70PBT30 and HA. An example (residues from HA-composites prepared with approximately 17.5 vol % HA) is shown in Figure B.1. The spectra clearly show the difference between the HA-composites prepared by blending and by grafting. After extraction, the residue of the HA-composite prepared by blending shows minimal amounts of 1000PEOT70PBT30 on HA. After extraction, the residue of the HA-composite prepared by grafting clearly shows characteristics of the absorption spectrum of the copolymer, indicating a strong bond (most likely chemical) between the copolymer and the HA.

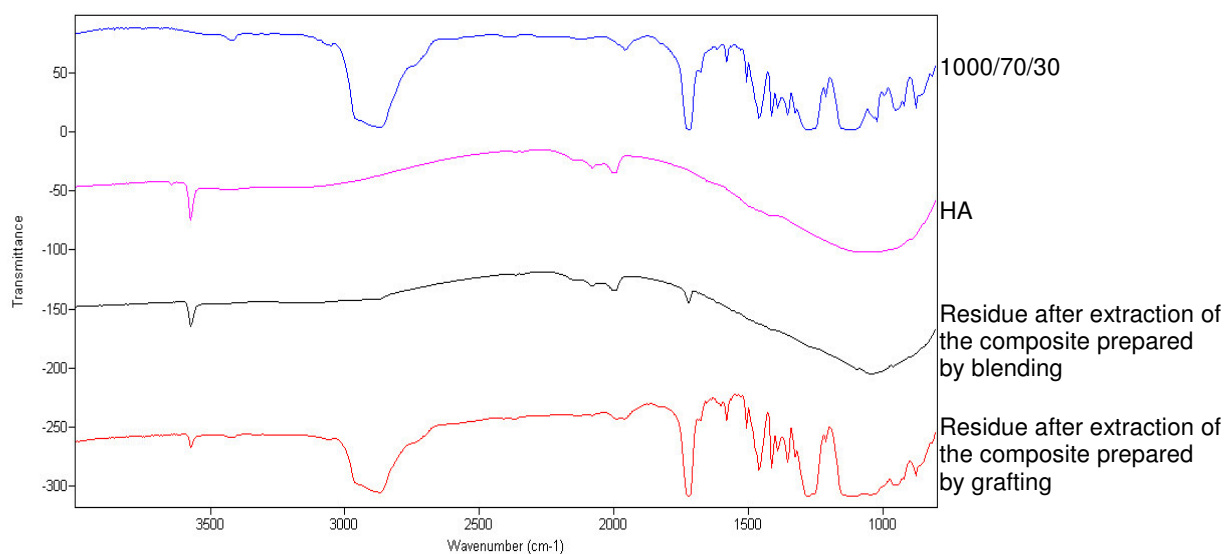


Figure B.1 - IR-spectra of 1000PEOT70PBT30, HA and the extracted residues of HA-composites prepared by blending and grafting (17.5 vol % HA). The copolymer is present in the residue of the extracted HA-composite prepared by grafting, but the composite prepared by blending only shows minimal amounts of copolymer.

Composite films of 500  $\mu\text{m}$  thickness were prepared by compression molding and cross-sections of freeze-fractured films are shown in Figure B.2. As can be seen, HA-composites prepared by grafting and HA-composites prepared by blending show well-dispersed HA particles in the polymer matrix. A poor dispersion of filler particles would lead to a lower elongation at break and lower tensile strength compared to films with well-dispersed fillers.

The interface between the copolymer and HA in the two types of HA-composites was investigated using SEM (Figure B.3). High magnifications show that there is close contact between the HA and the 1000PEOT70PBT30 polymer matrix for both HA-composites prepared by blending and grafting.

The effect of the grafting procedure on the mechanical properties was investigated as well. Figure B.4 shows the effect of increasing HA content of the composites on the Shore A hardness (in the dry state). As expected there is an increase in hardness with increasing hard filler content. HA-composites prepared by blending and by grafting appear to follow the same trend.

Differences in terms of mechanical properties between HA-composites prepared by blending and grafting, however, should become more evident in tensile testing. This will directly reflect the effect of the interaction between filler and polymer matrix.<sup>[30,42,43,47]</sup> Composite films were subjected to tensile testing, both in the dry and water-swollen state. Data are presented in Table B.3.

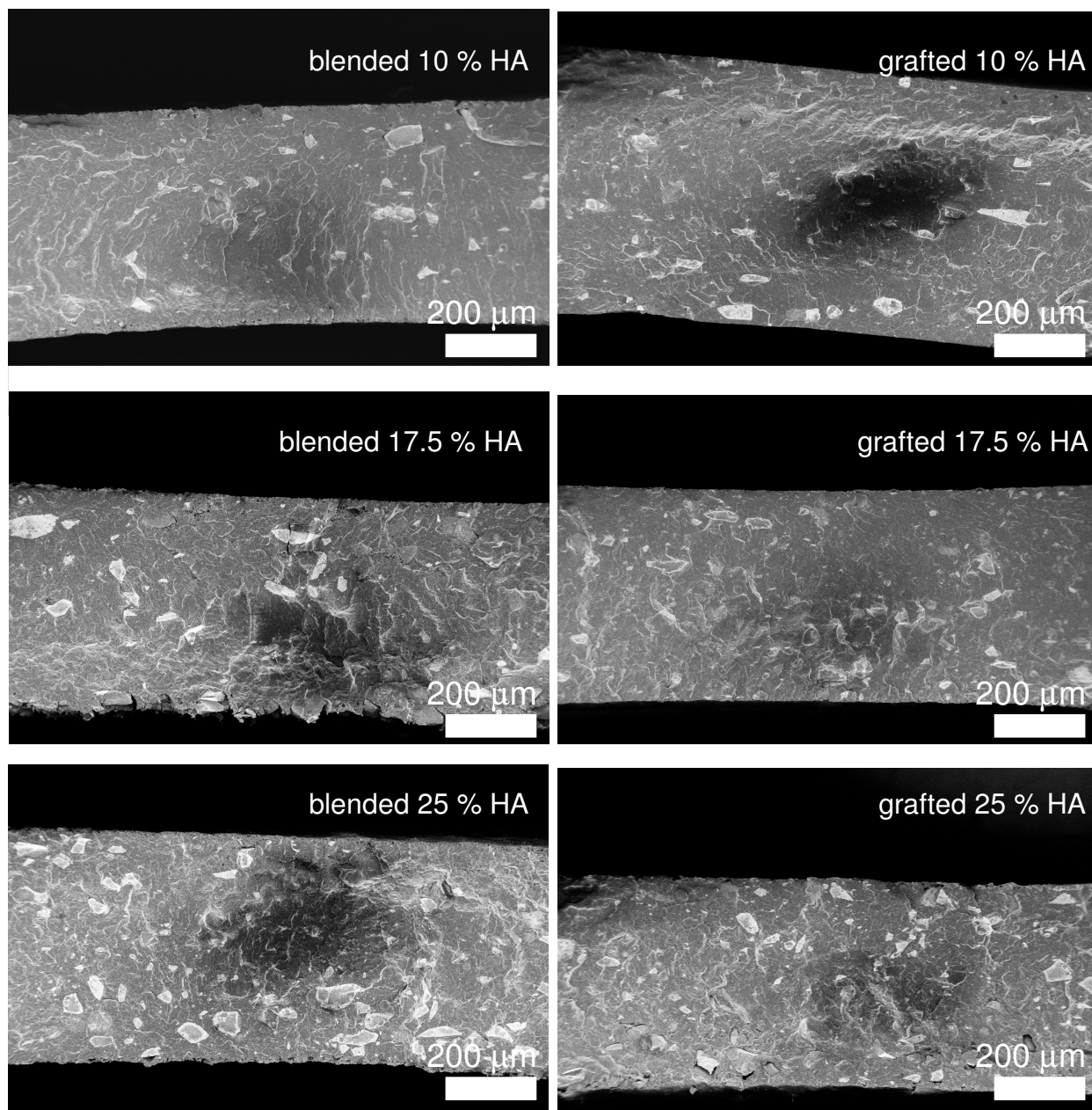


Figure B.2 - Scanning electron micrographs of cross-sections of freeze-fractured 1000PEO70PBT30-HA composite films (blended and grafted), showing well-dispersed HA particles.

In correspondence with other HA filled (bio)materials, an increase in filler volume, results in an increase in tensile modulus (in the dry state)<sup>[3]</sup>, but this is accompanied with a decrease in elongation at break<sup>[1,2,8]</sup> and/or tensile strength<sup>[15,18,40,41]</sup> (Table B.3). The HA particles are most likely acting as initiation sites for crack formation, decreasing the elongation at break and the maximal tensile strength of the composite.

In the water-swollen state these hydrophilic composites show a substantial decrease in the mechanical properties, as does the unmodified copolymer. With an increasing amount of blended HA a decrease in E-modulus is observed. Swelling causes loose embedding of the filler particles, resulting in a lower modulus and tensile strength at a higher volume percentage of HA.<sup>[46]</sup>

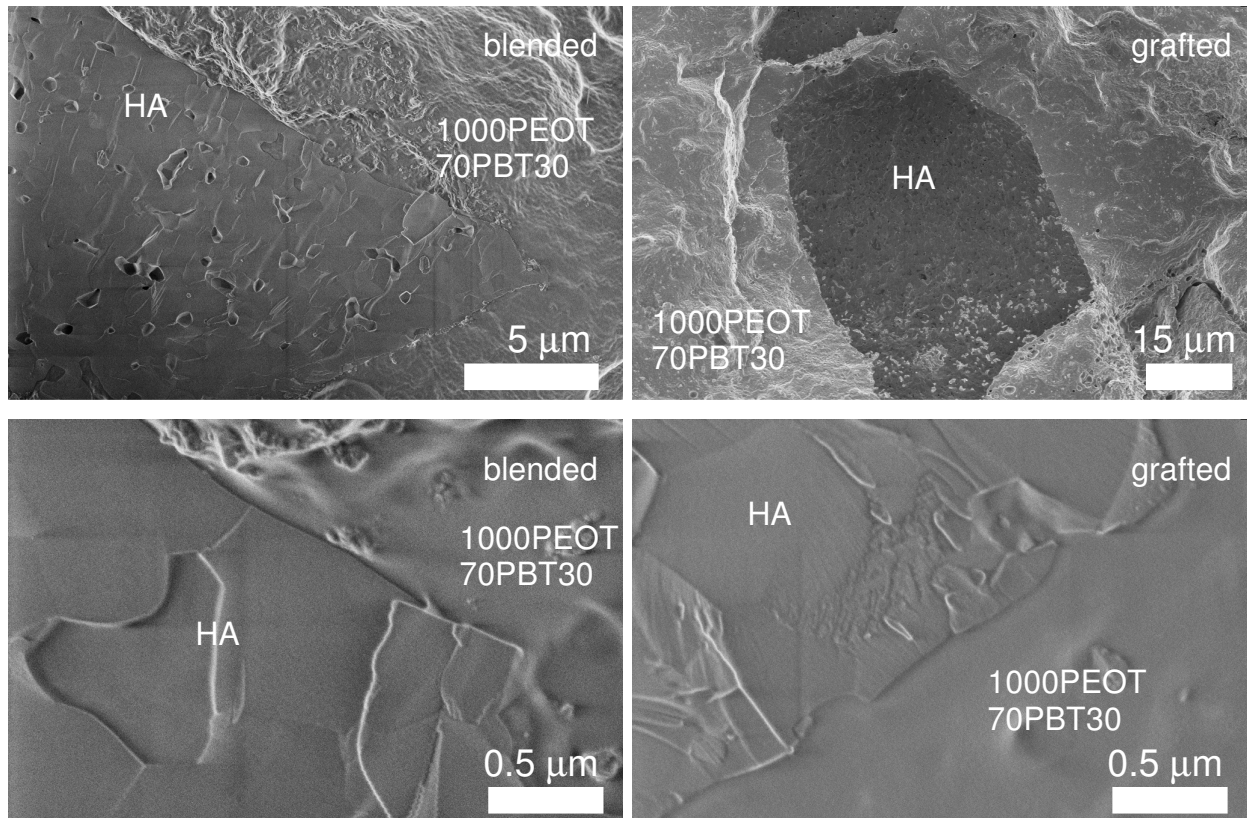


Figure B.3 – Scanning electron micrographs of HA-polymer interface in freeze-fractured 1000PEO70PBT30-HA composite films. Both HA-composites show the polymer matrix in close contact with HA particles. Left: composite prepared by blending with 25 vol % HA. Right: composite prepared by grafting (25 vol % HA).

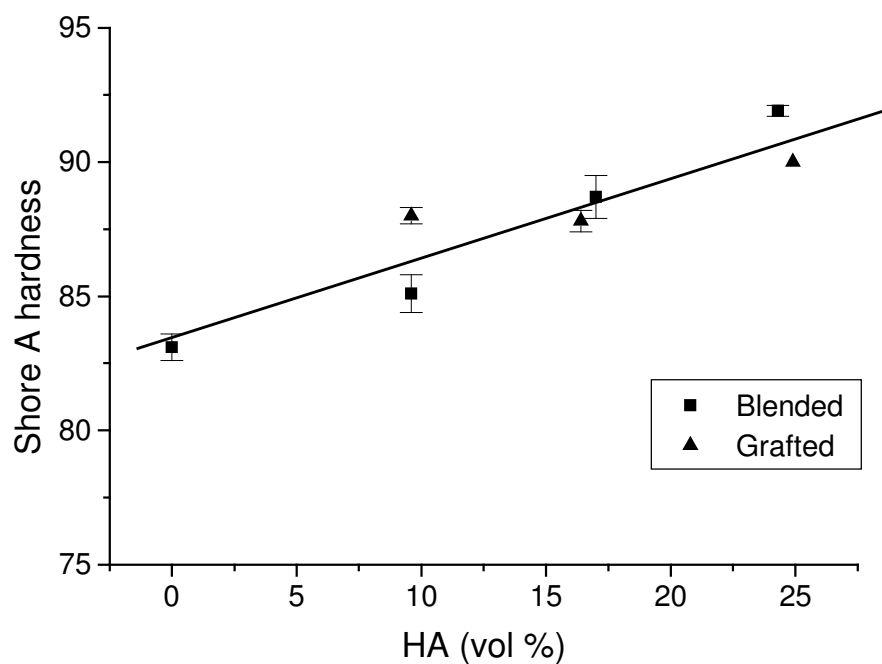


Figure B.4 - Shore A hardness of composites in the dry state, as a function of the HA volume content.

Table B.3 - Tensile properties of 1000PEOT70PBT30- HA composites. Results after 48 h of water uptake are shown in parentheses. All results are averages of four measurements ( $\pm$  s.d.).

Composite	E-modulus <sup>†</sup> (N/mm <sup>2</sup> )	$\sigma_{\max}$ (N/mm <sup>2</sup> )	$\epsilon_{\text{break}}$ (%)	$\sigma_{\text{break}}$ (N/mm <sup>2</sup> )	Energy up to break (Nmm)
1000/70/30	27 $\pm$ 3 (23 $\pm$ 1)	11.1 $\pm$ 0.5 (6.5 $\pm$ 0.2)	981 $\pm$ 153 (144 $\pm$ 33)	10.9 $\pm$ 0.7 (6.3 $\pm$ 0.2)	6380 $\pm$ 1237 (1084 $\pm$ 334)
10 vol % HA blended	45 $\pm$ 4 (20 $\pm$ 2)	7.0 $\pm$ 0.2 (3.1 $\pm$ 0.3)	214 $\pm$ 32 (32 $\pm$ 4)	6.9 $\pm$ 0.2 (3.0 $\pm$ 0.3)	960 $\pm$ 188 (96 $\pm$ 22)
17.5 vol % HA blended	54 $\pm$ 5 (15 $\pm$ 1)	6.2 $\pm$ 0.4 (1.2 $\pm$ 0.3)	62 $\pm$ 15 (11 $\pm$ 3)	5.9 $\pm$ 0.3 (1.1 $\pm$ 0.3)	264 $\pm$ 79 (13.4 $\pm$ 6.4)
25 vol % HA blended	78 $\pm$ 1 (12 $\pm$ 2)	6.8 $\pm$ 0.1 (0.67 $\pm$ 0.08)	34 $\pm$ 2 (6.5 $\pm$ 0.7)	6.7 $\pm$ 0.1 (0.66 $\pm$ 0.09)	133 $\pm$ 10 (3.8 $\pm$ 0.7)
10 vol % HA grafted	37 $\pm$ 2 (16 $\pm$ 1)	6.9 $\pm$ 1.5 (3.7 $\pm$ 0.7)	87 $\pm$ 39 (29 $\pm$ 6)	6.9 $\pm$ 1.4 (3.4 $\pm$ 0.9)	396 $\pm$ 258 (113 $\pm$ 48)
17.5 vol % HA grafted	47 $\pm$ 2 (10 $\pm$ 1)	7.2 $\pm$ 0.6 <sup>§</sup> (3.3 $\pm$ 0.2) <sup>‡</sup>	271 $\pm$ 93 <sup>§</sup> (58 $\pm$ 11) <sup>‡</sup>	7.1 $\pm$ 0.6 <sup>§</sup> (3.2 $\pm$ 0.3) <sup>‡</sup>	1467 $\pm$ 587 <sup>§</sup> (205 $\pm$ 56) <sup>‡</sup>
25 vol % HA grafted	61 $\pm$ 3 (12 $\pm$ 1)	6.1 $\pm$ 0.2 <sup>§</sup> (2.0 $\pm$ 0.2) <sup>‡</sup>	179 $\pm$ 20 <sup>§</sup> (28 $\pm$ 5) <sup>‡</sup>	5.8 $\pm$ 0.1 <sup>§</sup> (1.9 $\pm$ 0.2) <sup>‡</sup>	813 $\pm$ 104 <sup>§</sup> (57 $\pm$ 17) <sup>‡</sup>

†: The sample deformation was derived from the grip-to-grip separation, therefore the presented values of the E-modulus give only an indication of the stiffness of the different composite

§: significantly different from the corresponding values of the blended composite in the dry state

‡: significantly different from the corresponding values of the blended composite in the water-swollen state

Significant differences are observed between the HA-composites prepared by grafting and the HA-composites prepared by blending. The HA-composites with 17.5 and 25 vol % HA, prepared by grafting, show a higher elongation at break and a higher energy up to break both in the dry and the water-swollen state than the corresponding HA-composites prepared by blending.

The mechanical properties of the HA-composites prepared by grafting compare well with previously reported composites where 1000PEOT70PBT30 was covalently bound to HA by diisocyanate coupling agents.<sup>[46]</sup> The tensile strength and elongation at break values of the composites in the water-swollen state correspond well with data presented here for HA-composites prepared by grafting. In contrast to our expectations HA-composites prepared by blending and those prepared by grafting show a decrease in E-modulus in the water-swollen state with an increase in HA vol %. It should be realized that the presented E-moduli are only an indication of the stiffness of the different composites. For correct determinations, tests should be repeated using standard test methods like ISO R527.

With tissue engineering applications in mind, the HA-composites were used to prepare porous scaffolds. Many approaches employ a freeze-drying technique to prepare composite

scaffolds.<sup>[57-59]</sup> In analogy to PEOT/PBT scaffolds prepared by freeze-drying<sup>[50]</sup>, porous composite structures were prepared. Suspensions of HA in a PEOT/PBT-1,4-dioxane solution were frozen at different temperatures and subsequently freeze-dried, resulting in stable porous structures as shown in Figure B.6. In line with previous reports, larger pore sizes are obtained when freezing the polymer solution at higher temperatures.<sup>[50]</sup>

In another processing technique the polymer is cryogenically ground, sieved and the resulting polymer powder mixed with the desired amount of salt (sodium chloride). This mixture is then compression molded and leached, resulting in stable porous structures.<sup>[50]</sup> This technique was applied to the HA-composites (10 and 25 vol % HA) prepared by grafting, resulting in stable porous composite structures. Figure B.7 shows scanning electron micrographs of the porous structure obtained from the 1000PEOT70PBT30-HA composite (10 vol % HA) prepared by grafting. Higher magnifications clearly show the apatite particles in the polymer matrix.

## Conclusions

By directly adding HA particles to the polycondensation reaction mixture, it was possible to obtain composite materials with improved mechanical properties compared to composites prepared by blending.

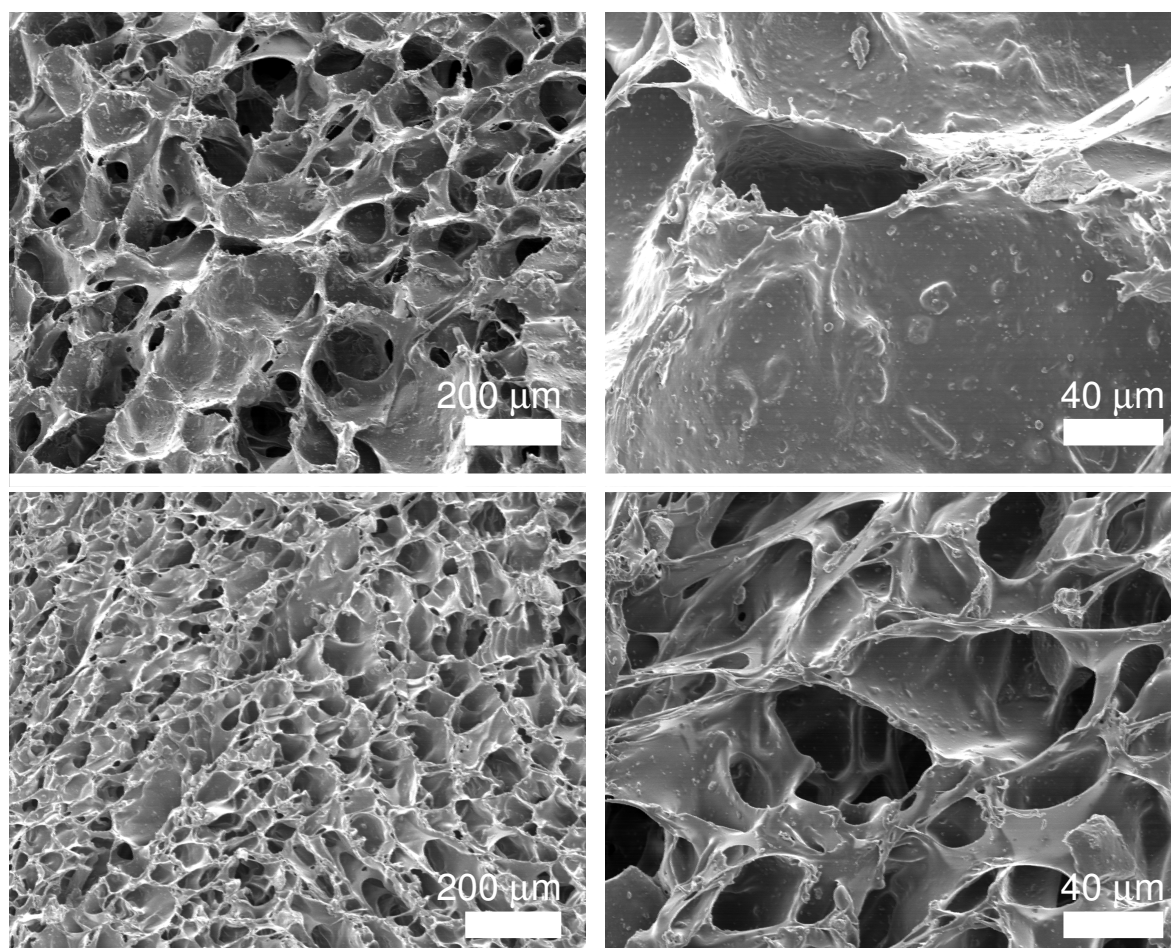


Figure B.6 - Scanning electron micrographs of porous composites prepared by blending and freeze-drying (11.3 vol % HA, porosity: 91.3 %) Top: prepared at +7 °C, bottom: prepared at -28 °C. Left: overview, right: close-up, clearly showing the HA particles. Composites scaffolds were cut at room temperature using a razor blade.



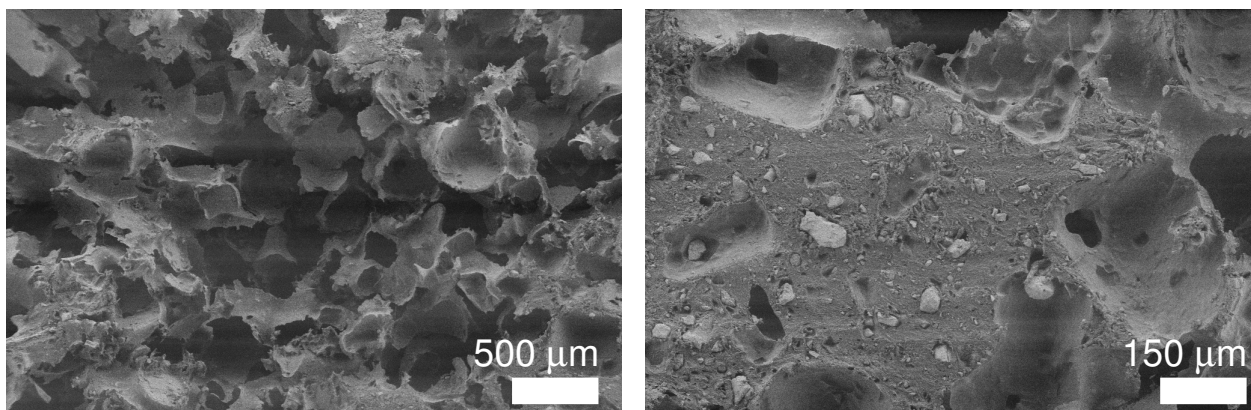


Figure B.7 - Scanning electron micrographs of a porous structure based on a 1000PEOT70PBT30-HA composite prepared by grafting with 10 vol % HA. Scaffolds were prepared by compression molding /salt leaching. Porosity  $75.7 \pm 1.5$  %, salt size: 425-500  $\mu\text{m}$ . Left: overview, right: higher magnification showing the HA particles. Composites scaffolds were cut at room temperature using a razor blade.

TGA and IR-data of extracted composites prepared by grafting show the presence of relatively high amounts of copolymer compared to the extracted composites prepared by blending. The composite with 10 vol % prepared by grafting showed gel formation, most likely due to cross-linking of the copolymer chains.

In terms of mechanical properties significant differences were found. The presented tensile data show a large increase in the elongation at break and energy up to break for the HA-composites prepared by grafting (with 17.5 and 25 vol % HA) compared to those prepared by blending. Both in the dry and water-swollen state the composites prepared by grafting (with 17.5 and 25 vol % HA) were significantly stronger and tougher than those prepared by blending. The combined IR, TGA and tensile data suggest that the copolymer is grafted onto the surface of HA particles. HA has previously been used as an initiator in ring-opening polymerization, but to our knowledge this would be the first example of the direct formation of polymer grafts onto HA, prepared by a polycondensation reaction in the presence of HA particles. Except for an increase in Shore A hardness, the incorporation of HA (either by grafting or by blending) does not result in composite materials, however, with improved mechanical properties compared to the original 1000PEOT70PBT30 copolymer.

By employing freeze-drying techniques or compression molding of polymer powder/salt mixtures followed by salt leaching, the HA-composites can be converted into porous structures.

## Acknowledgements

The authors would like to thank M.A. Smithers (Mesa+, University of Twente) for the scanning electron microscopy and professor F.J. Monteiro (INEB, Porto, Portugal) for the sintered HA. This study was financially supported by the European Community (Brite-Euram project BE97-4612).

## References

1. M. Wang, R. Joseph, W. Bonfield *Hydroxyapatite-polyethylene composites for bone substitution: effects of ceramic particle size and morphology* *Biomaterials* **1998**, 19, 2357-2366.
2. M. Wang, D. Porter, W. Bonfield *Processing, characterisation, and evaluation of hydroxyapatite reinforced polyethylene composites* *Brit. Ceram. Trans.* **1994**, 93, 91-95.



3. M. Wang, C. Berry, M. Braden, W. Bonfield *Young's and shear moduli of ceramic particle filled polyethylene* J. Mater. Sci.-Mater. Med. **1998**, 9, 621-624.
4. Y. Zhang, K.E. Tanner *Impact behavior of hydroxyapatite reinforced polyethylene composites* J. Mater. Sci.-Mater. Med. **2003**, 14, 63-68.
5. S.N. Nazhat, R. Joseph, M. Wang, R. Smith, K.E. Tanner, W. Bonfield *Dynamic mechanical characterization of hydroxyapatite reinforced polyethylene: effect of particle size* J. Mater. Sci.-Mater. Med. **2000**, 11, 621-628.
6. C. Du, F.Z. Cui, Q.L. Feng, X.D. Zhu, K. de Groot *Tissue response to nano-hydroxyapatite/collagen composite implants in marrow cavity* J. Biomed. Mater. Res. **1998**, 42, 540-548.
7. K.S. Tenhuisen, P.W. Brown *The formation of hydroxyapatite-gelatin composites at 38- Degrees-C* J. Biomed. Mater. Res. **1994**, 28, 27-33.
8. A. Bigi, S. Panzavolta, N. Roveri *Hydroxyapatite-gelatin films: a structural and mechanical characterization* Biomaterials **1998**, 19, 739-744.
9. N. Sasaki, H. Umeda, S. Okada, R. Kojima, A. Fukuda *Mechanical-properties of hydroxyapatite-reinforced gelatin as a model system of bone* Biomaterials **1989**, 10, 129-132.
10. T. Kawakami, M. Antoh, H. Hasegawa, T. Yamagishi, M. Ito, S. Eda *Experimental-study on osteoconductive properties of a chitosan-bonded hydroxyapatite self-hardening paste* Biomaterials **1992**, 13, 759-763.
11. M. Ito *In vitro properties of a chitosan-bonded hydroxyapatite bone- filling paste* Biomaterials **1991**, 12, 41-45.
12. Y.J. Yin, F. Zhao, X.F. Song, K.D. Yao, W.W. Lu, J.C. Leong *Preparation and characterization of hydroxyapatite/chitosan- gelatin network composite* J. Appl. Polym. Sci. **2000**, 77, 2929-2938.
13. A.C.A. Wan, E. Khor, G.W. Hastings *Hydroxyapatite modified chitin as potential hard tissue substitute material* J. Biomed. Mater. Res. **1997**, 38, 235-241.
14. S. Higashi, T. Yamamuro, T. Nakamura, Y. Ikada, S.-H. Hyon, K. Jamshidi *Polymer-hydroxyapatite composites for biodegradable bone fillers* Biomaterials **1986**, 7, 183-187.
15. C.C.P.M. Verheyen, J.R. de Wijn, C.A. van Blitterswijk, K. de Groot *Evaluation of hydroxylapatite poly(L-lactide) composites - mechanical-behavior* J. Biomed. Mater. Res. **1992**, 26, 1277-1296.
16. C.C.P.M. Verheyen, J.R. de Wijn, C.A. van Blitterswijk, K. de Groot, P.M. Rozing *Hydroxylapatite poly(L-lactide) composites - an animal study on push-out strengths and interface histology* J. Biomed. Mater. Res. **1993**, 27, 433-444.
17. C.C.P.M. Verheyen, C.P.A.T. Klein, J.M.A. de Bleeck-Hogervorst, J.G.C. Wolke, C.A. van Blitterswijk, K. de Groot *Evaluation of hydroxylapatite poly(L-lactide) composites - physicochemical properties* J. Mater. Sci.-Mater. Med. **1993**, 4, 58-65.
18. Y. Shikunami, M. Okuno *Bioresorbable devices made of forged composites of hydroxyapatite (HA) particles and poly-L-lactide (PLLA): Part I. Basic characteristics* Biomaterials **1999**, 20, 859-877.
19. Y. Shikunami, M. Okuno *Bioresorbable devices made of forged composites of hydroxyapatite (HA) particles and poly L-lactide (PLLA). Part II: practical properties of miniscrews and miniplates* Biomaterials **2001**, 22, 3197-3211.
20. N.C. Bleach, K.E. Tanner, M. Kellomaki, P. Tormala *Effect of filler type on the mechanical properties of self- reinforced polylactide-calcium phosphate composites* J. Mater. Sci.-Mater. Med. **2001**, 12, 911-915.
21. N. Ignjatovic, S. Tomic, M. Dakic, M. Miljkovic, M. Plavsic, D. Uskokovic *Synthesis and properties of hydroxyapatite/poly-L-lactide composite biomaterials* Biomaterials **1999**, 20, 809-816.
22. M. Matsumoto, E. Chosa, K. Nabeshima, Y. Shikunami, N. Tajima *Influence of bioresorbable, unsintered hydroxyapatite/poly-L- lactide composite films on spinal cord, nerve roots, and epidural space* J. Biomed. Mater. Res. **2002**, 60, 101-109.
23. S.A.T. van der Meer, J.R. de Wijn, J.G.C. Wolke *The influence of basic filler materials on the degradation of amorphous D- and L-lactide copolymer* J. Mater. Sci.-Mater. Med. **1996**, 7, 359-361.
24. W. Linhart, F. Peters, W. Lehmann, K. Schwarz, A.F. Schilling, M. AmLing, J.M. Rueger, M. Epple *Biologically and chemically optimized composites of carbonated apatite and polyglycolide as bone substitution materials* J. Biomed. Mater. Res. **2001**, 54, 162-171.
25. S.C. Rizzi, D.T. Heath, A.G.A. Coombes, N. Bock, M. Textor, S. Downes *Biodegradable polymer/hydroxyapatite composites: Surface analysis and initial attachment of human osteoblasts* J. Biomed. Mater. Res. **2001**, 55, 475-486.
26. C. Durucan, P.W. Brown *Low temperature formation of calcium-deficient hydroxyapatite-PLA/PLGA composites* J. Biomed. Mater. Res. **2000**, 51, 717-725.
27. E. Ural, K. Kesenci, L. Fambri, C. Migliaresi, E. Piskin *Poly(D,L-lactide/epsilon-caprolactone)/hydroxyapatite composites* Biomaterials **2000**, 21, 2147-2154.

28. A. Senkoylu, E. Ural, K. Kesenci, A. Simsek, S. Ruacan, L. Fambri, C. Migliaresi, E. Piskin *Poly(D,L-lactide/epsilon-caprolactone)/hydroxyapatite composites as bone filler: An in vivo study in rats* Int. J. Artif. Organs **2002**, 25, 1174-1179.
29. Q. Liu, J.R. de Wijn, C.A. van Blitterswijk *Nano-apatite/polymer composites: mechanical and physicochemical characteristics* Biomaterials **1997**, 18, 1263-1270.
30. Q. Liu, J.R. de Wijn, D. Bakker, C.A. van Blitterswijk *Surface modification of hydroxyapatite to introduce interfacial bonding with polyactive 70/30 in a biodegradable composite* J. Mater. Sci.-Mater. Med. **1996**, 7, 551-557.
31. Q. Liu, J.R. de Wijn, D. Bakker, M. van Toledo, C.A. van Blitterswijk *Polyacids as bonding agents in hydroxyapatite polyester-ether (Polyactive (TM) 30/70) composites* J. Mater. Sci.-Mater. Med. **1998**, 9, 23-30.
32. C. Doyle, E.T. Tanner, W. Bonfield *In vitro and in vivo evaluation of polyhydroxybutyrate and of polyhydroxybutyrate reinforced with hydroxyapatite* Biomaterials **1991**, 12, 841-847.
33. A.A. Deschamps, D.W. Grijpma, J. Feijen *Poly(ethylene oxide)/poly(butylene terephthalate) segmented block copolymers: the effect of copolymer composition on physical properties and degradation* Polymer **2001**, 42, 9335-9345.
34. R.J.B. Sakkers, J.R. de Wijn, R.A.J. Dalmeyer, R. Brand, C.A. van Blitterswijk *Evaluation of copolymers of polyethylene oxide and polybutylene terephthalate (polyactive): mechanical behaviour* J. Mater. Sci.-Mater. Med. **1998**, 9, 375-379.
35. C.A. van Blitterswijk, J. van der Brink, H. Leenders, D. Bakker *The effect of PEO ratio on degradation, calcification and bone bonding of PEO/PBT copolymer (Polyactive)* Cells and Materials **1993**, 3, 23-36.
36. C.A. van Blitterswijk, D. Bakker, S.C. Hesselting, H.K. Koerten *Reactions of cells at implant surfaces* Biomaterials **1991**, 12, 187-193.
37. A.M. Radder, H. Leenders, C.A. van Blitterswijk *Bone-bonding behavior of poly(ethylene oxide)-polybutylene terephthalate copolymer coatings and bulk implants - a comparative-study* Biomaterials **1995**, 16, 507-513.
38. A.M. Radder, H. Leenders, C.A. van Blitterswijk *Application of porous PEO/PBT copolymers for bone replacement* J. Biomed. Mater. Res. **1996**, 30, 341-351.
39. J.A. Jansen, J.E. de Ruijter, P.T.M. Janssen, Y. Paquay *Histological-evaluation of a biodegradable Polyactive(R)/hydroxyapatite membrane* Biomaterials **1995**, 16, 819-827.
40. P. Cheang, K.A. Khor *Effect of particulate morphology on the tensile behaviour of polymer-hydroxyapatite composites* Mater. Sci. Eng. A-Struct. Mater. Prop. Microstruct. Process. **2003**, 345, 47-54.
41. M.S. Abu Bakar, P. Cheang, K.A. Khor *Mechanical properties of injection molded hydroxyapatite-polyetheretherketone biocomposites* Compos. Sci. Technol. **2003**, 63, 421-425.
42. S. Deb, M. Wang, K.E. Tanner, W. Bonfield *Hydroxyapatite-polyethylene composites: effect of grafting and surface treatment of hydroxyapatite* J. Mater. Sci.-Mater. Med. **1996**, 7, 191-193.
43. M. Wang, W. Bonfield *Chemically coupled hydroxyapatite-polyethylene composites: structure and properties* Biomaterials **2001**, 22, 1311-1320.
44. D.W. Jones, A.S. Rizkalla *Characterization of experimental composite biomaterials* J. Biomed. Mater. Res., Appl. Biomater. **1996**, 33, 89-100.
45. C.M. Vaz, R.L. Reis, A.M. Cunha *Use of coupling agents to enhance the interfacial interactions in starch-EVOH/hydroxylapatite composites* Biomaterials **2002**, 23, 629-635.
46. Q. Liu, J.R. de Wijn, C.A. van Blitterswijk *Composite biomaterials with chemical bonding between hydroxyapatite filler particles and PEG/PBT copolymer matrix* J. Biomed. Mater. Res. **1998**, 40, 490-497.
47. M. Bos, G.W. van Dam, T. Jongsma, P. Bruin, A.J. Pennings *The effect of filler surface modification on the mechanical properties of hydroxyapatite-reinforced polyurethane composites* Composite Interfaces **1995**, 3, 169-176.
48. A.M.P. Dupraz, S.A.T. van der Meer, J.R. de Wijn, J.H. Goedemoed *Biocompatibility screening of silane-treated hydroxyapatite powders, for use as filler in resorbable composites.* J. Mater. Sci.-Mater. Med. **1996**, 7, 731-738.
49. E. Helwig, B. Sandner, U. Gopp, F. Vogt, S. Wartewig, S. Henning *Ring-opening polymerization of lactones in the presence of hydroxyapatite* Biomaterials **2001**, 22, 2695-2702.
50. M.B. Claase, D.W. Grijpma, S.C. Mendes, J.D. de Bruijn, J. Feijen *Porous PEOT/PBT scaffolds for bone tissue engineering: preparation, characterization and in vitro bone marrow cell culturing* J. Biomed. Mater. Res **2003**, 64A, 291-300. Chapter 5 of this thesis.
51. S.H. Li, J.R. de Wijn, P. Pierre Layrolle, K. de Groot *Novel method to manufacture porous hydroxyapatite by dual-phase mixing* J. Am. Ceram. Soc. **2003**, 86, 65-72.

52. R. Myrvold, F.K. Hansen, B. Balinour *Monolayers of some ABA block-copolymers at the air-water interface* Colloid Surf. A-Physicochem. Eng. Asp. **1996**, *117*, 27-36.
53. *Merck Index*; 11th ed.; S. Budavari, M.J. O'Neil and A. Smith, Ed.; Merck & Co. Inc.: Rahway, U.S.A. **1989**.
54. A.A. Deschamps *The PEO-containing phase in poly(ether ester) block copolymers (Chapter 3)* in "Segmented Poly(ether ester)s and Poly(ether ester amide)s for Use in Tissue Engineering", Thesis, University of Twente, Enschede, The Netherlands, **2002**.
55. A.A. Deschamps, D.W. Grijpma, J. Feijen *Biomaterials based on PEOT/PBT block copolymers: mechanical properties and degradation behavior*; Bante, I. and Feijen, J., Ed.; Research school 'Integrated BioMedical Engineering for restoration of human function' (iBME): Enschede, The Netherlands, **2000**.
56. M. Kellomaki, S. Paasimaa, D.W. Grijpma, K. Kolppo, P. Tormala *In vitro degradation of Polyactive (R) 1000PEOT70PBT30 devices* Biomaterials **2002**, *23*, 283-295.
57. R. Zhang, P.X. Ma *Poly( $\alpha$ -hydroxyl acids)/hydroxyapatite porous composites for bone-tissue engineering. I. Preparation and morphology* J. Biomed. Mat. Res. **1999**, *44*, 446-455.
58. J.A. Roether, J.E. Gough, A.R. Boccaccini, L.L. Hench, V. Maquet, R. Jerome *Novel bioresorbable and bioactive composites based on bioactive glass and polylactide foams for bone tissue engineering* J. Mater. Sci.-Mater. Med. **2002**, *13*, 1207-1214.
59. H. Lo, M.S. Ponticiello, B.S. Leong, K.W. Leong *Fabrication of controlled release biodegradable foams by phase separation* Tissue Eng. **1995**, *1*, 15-28.



# Summary

This thesis describes the development of polymeric scaffolds containing bone marrow stromal cells (BMSCs) that are cultured in an osteogenic medium and can be used for the formation of functional bone tissue upon implantation. The proposed polymer/cell constructs comprise *bone marrow stromal cells* that are *seeded* and *cultured* in three-dimensional porous biodegradable polymer scaffolds, based on PEOT/PBT (polyethylene oxide/polybutylene terephthalate) copolymers. The composition of these copolymers is indicated as  $a\text{PEOT}b\text{PBT}c$ , where  $a$  is the starting poly(ethylene glycol) molecular weight,  $b$  the weight percentage of PEOT soft segments and  $c$ , the weight percentage of PBT hard segments. Available literature suggests that the more hydrophilic PEOT/PBT (1000PEOT70PBT30) copolymers are suitable as scaffolding materials for bone tissue engineering because of their *in vivo* calcification, bone bonding and degradation. In this thesis the synthesis of PEOT/PBT copolymers, the preparation of porous structures and the *in vitro* and *in vivo* evaluation of rat BMSC-seeded and cultured scaffolds are described. To study the osteogenic potential of the cultured polymer/cell constructs, rat BMSCs were seeded and cultured in an osteogenic medium on 1000PEOT70PBT30 scaffolds and subsequently subcutaneously implanted in immunodeficient nude mice for a period of 4 wks.

Several bone tissue engineering approaches are discussed in **Chapters 1 and 2**. The main components in bone tissue engineering are: a) osteoinductive agents, b) osteogenic cells and c) scaffolds. Biomaterials seeded with the appropriate cells and/or releasing suitable bioactive molecules can be osteoinductive, where the material by itself is at best only osteoconductive. BMSCs are responsible for the maintenance of bone turnover throughout life and can be regarded as a mesenchymal progenitor/precursor cell population derived from adult stem cells. Cultured BMSCs can be stimulated to differentiate into bone, cartilage, muscle, marrow stroma, tendon, fat and a variety of other connective tissues. The *in vitro* culture of rat BMSCs in an osteogenic medium containing dexamethasone,  $\beta$ -glycerophosphate and L-ascorbic acid greatly increases the amount of cells with an osteoblastic phenotype. In many systems seeding followed by a period of *in vitro* cell culture in an osteogenic medium of stromal cells on a porous scaffold, resulted in improved bone formation *in vivo* compared to scaffolds that were seeded and implanted immediately. The (mechanical) properties of the scaffold need to allow for cell proliferation, cell differentiation and tissue formation *in vitro* and *in vivo*.

From all the different techniques available for the preparation of porous structures those that are based on particulate leaching and liquid-solid phase separation (freeze-drying) appear to be the most versatile ones. With both techniques it is possible to prepare scaffolds with a wide range of porosities and pore sizes, without the need for special equipment.

PEOT/PBT block copolymers have been prepared by two-step polycondensation on scales up to 1 kg (**Chapter 3**). Gel permeation chromatography using 1,1,1,3,3,3-hexafluoro-2-propanol (with 0.02 M sodium trifluoroacetate) as a solvent was used to determine the copolymer molecular weights. Weight average molecular weights (relative to poly(methyl methacrylate) standards) of 110,000 to 150,000 g/mol have been obtained. The thermal process conditions used for the preparation of films and porous structures by compression molding resulted in only a small decrease in the relative molecular weights of the PEOT/PBT copolymers.

Due to the uptake of water, 1000PEOT70PBT30 copolymers in the wet state have significantly decreased tensile and creep properties as compared to those in the dry state. The

mechanical requirements for in vitro cell culture (for instance in bioreactors) and the changes in these properties upon culture need to be further investigated.

BMSC attachment onto hydrophilic PEOT/PBT copolymers was poor. Two ways of surface modifying these materials to improve in vitro BMSC attachment and growth are discussed in **Chapter 4**: 1) Blending of hydroxyapatite (HA) followed by CO<sub>2</sub> gas plasma etching. 2) Surface modification using CO<sub>2</sub> gas plasma treatments. It was observed that not only HA, but also the CO<sub>2</sub> plasma treatment by itself had a positive effect on BMSC attachment and growth. Gas plasma treatment resulted in a large increase in the amount of BMSCs present on the surface (as determined by a DNA assay). The amount of DNA present on the gas plasma treated 1000PEOT70PBT30 copolymer films, was comparable to the amount present on poly(D,L-lactide) (PDLLA) films and significantly higher than the amount present on poly( $\epsilon$ -caprolactone) films after 7 d of cell culturing. The fact that after gas plasma treatment BMSCs do attach to 1000PEOT70PBT30 copolymers, enables in vitro BMSC culturing on these scaffolds, making bone tissue engineering with these materials possible.

An attempt to improve cell attachment by use of PEG-RGD conjugates is described in **Appendix A**. The incorporation of RGD-sequences into 1000PEOT70PBT30 by blending with PEG-RGD conjugates results in some clustered BMSCs at the surface. The improvement in cell attachment and growth, however, was not sufficient to justify the use of these materials in tissue engineering applications. A likely explanation for the low cell attachment is that a significant amount of the blended PEG-RGD molecules is rapidly washed out of the samples after contact with water.

To improve the mechanical properties of the composites we investigated the formation of grafts of 1000PEOT70PBT30 onto HA filler particles (38-53  $\mu$ m) by polycondensation, without the use of potentially harmful coupling agents (**Appendix B**). After extraction of the soluble components, TGA and IR analyses showed the presence of 1000PEOT70PBT30 on the HA particles. At 17.5 and 25 vol % HA a significant improvement in the elongation at break and the energy to break, both in the dry and wet state, was observed for the composites prepared by grafting, compared to those prepared by blending. The combined IR, TGA and tensile data suggest that the copolymer is grafted onto the surface of HA particles. To our knowledge this would be the first example of the direct formation of grafts of a polycondensate onto HA, made by a polycondensation reaction in the presence of HA. By employing freeze-drying techniques or compression molding of polymer powder/salt mixtures followed by salt leaching, the HA-composites can be converted into porous structures.

In **Chapter 5** the preparation, characterization and in vitro BMSC culturing on porous 1000PEOT70PBT30 copolymer scaffolds is described. Porous structures were prepared using a freeze-drying and a cryogenic grinding/compression molding/leaching technique, the latter one resulting in highly porous interconnected structures with large pores. This technique enables good control over scaffold pore size and porosity. The porosity is determined by the salt volume fraction, whereas the pore size can be controlled by variation of the size of the salt crystals used. Stable 1000PEOT70PBT30 scaffolds can be obtained in a porosity range of 73 to 85 %.

Gas plasma treatment of porous 1000PEOT70PBT30 scaffolds with CO<sub>2</sub> generated an appropriate surface throughout the entire structure, enabling BMSCs to attach. The amount of DNA was determined as a measure for the amount of cells present on the scaffolds. No significant effect of pore size on the amount of DNA present, was seen for scaffolds prepared with salt crystals with sizes between 250-1000  $\mu$ m. Light microscopy data showed cells in the center of the scaffolds and more cells were observed in scaffolds prepared with salt crystals of 425-500  $\mu$ m and 500-710  $\mu$ m size compared to the ones prepared with 250-425  $\mu$ m and 710-

1000  $\mu\text{m}$  salt crystal size. Our studies show that gas plasma treatments are able to modify the pore surfaces even in the center of 4×4×4 mm scaffolds.

The ectopic bone formation in cell-seeded and cultured porous 1000PEOT70PBT30 structures after subcutaneous implantation in nude mice is investigated in **Chapters 6 and 7**.

**Chapter 6** describes the preparation of scaffolds with different pore sizes at a constant porosity of approximately 80 %. Porous 1000PEOT70PBT30 and PDLLA structures were prepared by a compression molding and salt leaching technique, using salt crystals with sizes of 250-425, 425-500, 500-710 and 710-1000  $\mu\text{m}$  respectively. A detailed analysis of the pore structure of the different scaffolds by  $\mu$ -CT showed differences in pore size distribution, average pore size, accessible pore volume and accessible surface area. The average pore sizes of these scaffolds determined by  $\mu$ -CT are smaller than expected (260, 342, 305 and 477  $\mu\text{m}$ ) based on the salt sizes used (250-425, 425-500, 500-710, 710-1000  $\mu\text{m}$  respectively) in the porosification method.

In literature methods to calculate the pore size distribution and average pore size from the  $\mu$ -CT data were used, that underestimate the pore size. In this study the underestimation of the average pore size is less than in previous reports due to the use of an algorithm (averages are approximately 100  $\mu\text{m}$  higher) more suitable for cubic pores, as is the case in this study for the scaffolds prepared by salt leaching.

No significant differences in the amount of DNA (and hence in cells) present in the 1000PEOT70PBT30 scaffolds were observed, even though clear differences in accessible pore volume and accessible surface area, as derived from  $\mu$ -CT data, were seen.

Gas plasma treated 1000PEOT70PBT30 scaffolds were seeded with rat BMSCs, cultured in vitro for 7 d in an osteogenic medium, and subcutaneously implanted in nude mice for 4 wks. Seeded and cultured PDLLA (porosity 83.5 %, average pore size from  $\mu$ -CT: 407  $\mu\text{m}$ ) and biphasic calcium phosphate (BCP, porosity 29 %, average pore size from  $\mu$ -CT: 837  $\mu\text{m}$ ) scaffolds were included in the study as references. The presence of different tissue types, including bone and bone marrow, was studied and quantified using histomorphometry. All 1000PEOT70PBT30, PDLLA and BCP scaffolds showed the formation of bone and bone marrow. No significant differences were observed in the amounts (normalized for the porosity) of bone (5-8 %) and bone marrow (5-13 %) in the middle cross sections of 1000PEOT70PBT30 scaffolds with different pore sizes. Although the PDLLA and BCP scaffolds contained less BMSCs at the time of implantation (as determined by a DNA assay), they showed considerably more bone and bone marrow formation and less fibrous tissue ingrowth and wound exudate retention than the 1000PEOT70PBT30 scaffolds after 4 wks of subcutaneous implantation in nude mice.

To study the effect of scaffold porosity on tissue formation, gas plasma treated porous 1000PEOT70PBT30 structures seeded with rat BMSCs (after in vitro culture for 7 d in an osteogenic medium) of 73.5, 80.6 and 85.0 % porosity were subcutaneously implanted for 4 wks in nude mice (**Chapter 7**). All scaffolds were prepared using salt crystals of 425-500  $\mu\text{m}$  to obtain scaffolds with equal sized pores. The average pore sizes of the 1000PEOT70PBT30 scaffolds were in the range of 311-342  $\mu\text{m}$ , as determined by  $\mu$ -CT. PDLLA and BCP scaffolds were again included as references. After implantation the 1000PEOT70PBT30, PDLLA and BCP scaffolds showed the formation of bone and bone marrow. The 1000PEOT70PBT30 scaffolds with a porosity of 85.0 % lacked sufficient stiffness and could not maintain their shape in vivo. Surprisingly, 1000PEOT70PBT30 scaffolds with a porosity of 73.5 % showed notable cartilage formation. Although the effects of scaffold stiffness cannot be excluded, the cartilage formation is most likely due to poorly accessible pores (as observed in histological sections) leading to an oxygen-poor environment that favors cartilage

formation. Scaffolds of 73.5 % porosity containing cartilage, also showed a considerably lower accessible pore volume (as a function of the total volume) than 1000PEOT70PBT30 scaffolds of 80.6 and 85.0 % porosity. Gas plasma treated 1000PEOT70PBT30 scaffolds not seeded with BMSCs or 1000PEOT70PBT30 scaffolds that were seeded with BMSCs and cultured for 7 d, but that were not gas plasma treated (**Chapters 6 and 7**), did not show any formation of bone or bone marrow. In line with the studies described in **Chapter 6**, BMSC-seeded and cultured PDLA and BCP scaffolds always showed considerably more bone and bone marrow formation than the 1000PEOT70PBT30 scaffolds.

Previous implantations of BMSC-seeded and cultured 1000PEOT70PBT30 scaffolds by Mendes et al. resulted in considerably more in vivo bone formation (the amount of bone that filled the pores was 36 %). The reported scaffold dimensions were 3×3×2 mm compared to 4×4×4 mm in our studies, with the same amount of BMSCs seeded ( $2 \times 10^5$  per scaffold). This suggests that the scaffold dimensions and/or the cell seeding density have a pronounced effect on bone formation. The effects of scaffold dimensions and cell seeding density on the in vitro cell culture and in vivo bone formation need to be further addressed.

To optimize the tissue engineering constructs, a detailed analysis of the effects of culture conditions (possibly dynamic) and culture times (up to several weeks) is needed. The physical and mechanical properties of these constructs are likely to change during the tissue culture, when new tissue is formed and the polymer matrix is (slowly) degraded. To study the effect on in vivo bone (re)generation, these in vitro cultured tissue constructs, cultured under different culturing conditions and culture times, need to be implanted in critical size bone defects, preferably in large animals like goats.

The prepared BMSC-seeded and cultured 1000PEOT70PBT30 scaffolds should always be compared with other bone tissue engineering approaches and with other scaffold materials. The in vitro and in vivo results presented in this thesis (**Chapters 6 and 7**) show that BCP and PDLA might have certain advantages over 1000PEOT70PBT30 and therefore should be considered as scaffold materials in future bone tissue engineering approaches.



# Samenvatting

In dit proefschrift staat de ontwikkeling beschreven van polymere dragermaterialen voor de vorming van functioneel botweefsel. Deze poreuze dragers bevatten beenmerg-stromacellen (BMSC's) die voor implantatie gekweekt zijn in een osteogeen medium. De voorgestelde polymeer-celconstructen bestaan uit BMSC's, die *gezaaid* en *gekweekt* zijn in drie dimensionale poreuze, bioafbreekbare, polymere dragers op basis van PEOT/PBT (polyethyleen oxide/polybutyleen tereftalaat) copolymeren. De samenstelling van deze copolymeren is aangegeven als  $a\text{PEOT}b\text{PBT}c$ , met  $a$  het molgewicht van de uitgangsstof poly(ethyleen glycol) (PEG),  $b$  het gewichtspercentage PEOT zacht segment en  $c$  het gewichtspercentage PBT hard segment. Beschikbare literatuur suggereert dat de meer hydrofiele PEOT/PBT (1000PEOT70PBT30) copolymeren geschikt zijn als dragermaterialen voor de tissue engineering van bot, vanwege hun in vivo calcificatie, botbinding en degradatie. In dit proefschrift staan de synthese van PEOT/PBT copolymeren, de vervaardiging van poreuze structuren en de in vitro en in vivo evaluatie van poreuze dragers, bezaaid en gekweekt met BMSC's van ratten, beschreven. Om het osteogene potentieel van de gekweekte polymeer-celconstructen te bestuderen zijn BMSC's van ratten gezaaid op poreuze 1000PEOT70PBT30 dragers en gekweekt in een osteogeen medium. Vervolgens zijn deze constructen gedurende 4 weken subcutaan geïmplanteerd in immunodeficiënte naakte muizen. Verscheidene benaderingswijzen voor de tissue engineering van bot worden besproken in **Hoofdstuk 1 en 2**. De belangrijkste componenten in de tissue engineering van bot zijn: a) osteoinductieve middelen, b) osteogene cellen en c) (poreuze) dragermaterialen. Biomaterialen die bezaaid zijn met geschikte cellen en/of geschikte bioactieve moleculen afgeven, kunnen osteoinductief zijn, terwijl het materiaal zelf op zijn best osteoconductief is. BMSC's zijn gedurende het leven verantwoordelijk voor het onderhouden van de opbouw en afbraak van bot en kunnen gezien worden als voorlopercellen afkomstig van volwassen stamcellen. Gekweekte BMSC's kunnen gestimuleerd worden tot differentiatie in bot, kraakbeen, spierweefsel, mergstroma, pezen, vet en een grote verscheidenheid aan ander bindweefsel. De in vitro kweek van BMSC's van ratten in een osteogeen medium, dat dexamethason,  $\beta$ -glycerofosfaat en L-ascorbinezuur bevat, zorgt voor een sterke toename in het aantal cellen met een osteoblastisch fenotype. In veel systemen leidt het zaaien van stromacellen in een poreuze drager, gevolgd door een periode van in vitro celkweek in een osteogeen medium, tot een verbeterde botvorming in vivo in vergelijking met poreuze dragers die met cellen bezaaid en direct geïmplanteerd zijn. De (mechanische) eigenschappen van de poreuze drager moeten, zowel in vitro als in vivo, celproliferatie, -differentiatie en weefselvorming toelaten. Van de verschillende technieken die beschikbaar zijn voor de vervaardiging van poreuze structuren lijken degenen gebaseerd op het uitwassen van deeltjes en vloeibaar-vaste fasenscheiding (vriesdrogen) het meest bruikbaar. Zonder gebruik te maken van speciale apparatuur is het met beide technieken mogelijk poreuze structuren te maken van verschillende porositeiten en poriegroottes. PEOT/PBT blokcopolymeren zijn gesynthetiseerd d.m.v. een tweestaps polycondensatie op een schaal tot 1 kg (**Hoofdstuk 3**). Gelpermeatiechromatografie met 1,1,1,3,3,3-hexafluor-2-propanol (met 0.02 M natriumtrifluoracetaat) als oplosmiddel is gebruikt ter bepaling van de molgewichten van de copolymeren. Gewichtsgemiddelde molgewichten (relatief t.o.v. poly(methylmethacrylaat) standaarden) van 110.000 tot 150.000 g/mol zijn verkregen. De omstandigheden voor thermische verwerking d.m.v. persen, gebruikt in de vervaardiging van

films en poreuze structuren, resulteren slechts in een kleine afname in het relatieve molgewicht van de PEOT/PBT copolymeren.

Door de opname van water bezitten 1000PEOT70PBT30 copolymeren in de natte toestand aanzienlijk slechtere rek- en kruipeigenschappen dan copolymeren in de droge toestand. De mechanische eisen voor in vitro celkweek (bij voorbeeld in bioreactoren) en de veranderingen in deze eigenschappen gedurende de kweek vereisen verder onderzoek.

De hechting van BMSC's aan de hydrofiele PEOT/PBT copolymeren was slecht. Twee manieren van oppervlaktemodificatie van deze materialen om de in vitro BMSC hechting en groei te verbeteren staan beschreven in **Hoofdstuk 4**: 1) Het blenden van hydroxyapatiet (HA) gevolgd door etsen met een CO<sub>2</sub>-gasplasma. 2) Oppervlakte modificatie d.m.v. CO<sub>2</sub>-gasplasmabehandelingen. Het is aangetoond dat niet alleen de HA, maar ook de CO<sub>2</sub>-gasplasmabehandeling een positieve invloed heeft op BMSC hechting en groei. Gasplasmabehandeling resulteerde in een grote toename van het aantal BMSC's aanwezig op het oppervlak (bepaald m.b.v. een DNA-analyse). De hoeveelheid DNA aanwezig op gasplasma behandelde 1000PEOT70PBT30 copolymeer films was vergelijkbaar met de hoeveelheid DNA aanwezig op poly(D,L-lactide) (PDLLA) films en significant groter dan de hoeveelheid DNA aanwezig op poly(ε-caprolacton) films na 7 dagen celkweek. Het feit dat na gasplasmabehandeling BMSC's wel hechten aan 1000PEOT70PBT30 copolymeren staat in vitro BMSC kweek op deze dragermaterialen toe, waardoor tissue engineering van bot met deze materialen mogelijk wordt.

Een poging om de celhechting d.m.v. PEG-RGD conjugaten te verbeteren staat beschreven in **Appendix A**. Het incorporeren van RGD-sequenties in 1000PEOT70PBT30 door het blenden van PEG-RGD conjugaten resulteerde in enkele geclusterde BMSC's op het oppervlak. De verbetering in celhechting en -groei is echter niet voldoende om het gebruik van deze materialen in tissue engineering toepassingen te rechtvaardigen. Een mogelijke verklaring voor de matige celhechting is, dat een aanzienlijk deel van de geblende PEG-RGD moleculen snel uit de monsters gewassen wordt, nadat de monsters in contact zijn gekomen met water.

Om de mechanische eigenschappen van de composieten te verbeteren, is de vorming van 1000PEOT70PBT30 'grafts' op HA vullerdeeltjes (38-53 μm) via polycondensatie onderzocht (**Appendix B**). Op deze manier zijn geen (mogelijk) schadelijke 'coupling agents' nodig. Na extractie van de oplosbare componenten toonden TGA en IR analyses de aanwezigheid van 1000PEOT70PBT30 op de HA deeltjes aan. Bij 17.5 en 25 vol % HA is een significante verbetering in de rek bij breuk en de energie tot breuk, zowel in de droge als in de natte toestand, waargenomen voor de composieten gemaakt d.m.v. 'graften' t.o.v. composieten gemaakt d.m.v. blenden. De gecombineerde data van IR, TGA en trek-rek testen suggereert dat het copolymeer op het oppervlak van de HA deeltjes 'gegraft' is. Voor zover bekend, is dit het eerste voorbeeld van de directe vorming van 'grafts' van een polycondensaat op HA, gemaakt d.m.v. een polycondensatiereactie in de aanwezigheid van HA. Door gebruik te maken van vriesdroogtechnieken of het persen van polymeerpoeder/zout mengsels gevolgd door het uitwassen van de zoutdeeltjes, kunnen deze HA-composieten in poreuze structuren veranderd worden.

In **Hoofdstuk 5** staan de vervaardiging en karakterisering van de in vitro BMSC kweek op poreuze 1000PEOT70PBT30 dragers beschreven. Poreuze structuren zijn vervaardigd d.m.v. vriesdrogen en een techniek waar het polymeer eerst cryogeen gemalen wordt, vermengd wordt met zoutdeeltjes, geperst en vervolgens de zoutdeeltjes uitgewassen worden. Deze laatste techniek resulteert in zeer poreuze structuren met grote en met elkaar verbonden poriën. Met deze techniek is een goede controle over de poriegrootte en porositeit van de structuur mogelijk. De porositeit wordt bepaald door de zoutvolumefractie en de poriegrootte wordt gecontroleerd m.b.v. de grootte van de gebruikte zoutkristallen. Stabiele

1000PEOT70PBT30 poreuze dragers kunnen verkregen worden in een porositeitsbereik van 73 tot 85 %.

Gasplasmabehandeling van poreuze 1000PEOT70PBT30 dragers met CO<sub>2</sub> resulteert in de hele structuur in een oppervlak dat geschikt is voor de hechting van BMSC's. De hoeveelheid DNA is bepaald als een maat voor de hoeveelheid cellen aanwezig op de poreuze dragers.

Er zijn geen significante effecten van de poriegrootte op de aanwezige hoeveelheid DNA waargenomen in dragers vervaardigd met zoutkristallen met groottes tussen de 250 en 1000 µm. Lichtmicroscopiefoto's tonen cellen in het midden van de dragers en meer cellen in het midden van de dragers gemaakt met zoutkristallen van 425-500 en 500-710 µm in vergelijking met dragers gemaakt met zoutkristallen van 250-425 en 710-1000 µm. De hier beschreven studies tonen aan dat gasplasmabehandelingen zelfs in staat zijn het porie-oppervlak in het midden van 4×4×4 mm dragers te modificeren.

De ectopische botvorming in BMSC bezaaide en daarna gekweekte poreuze 1000PEOT70PBT30 structuren na subcutane implantatie in naakte muizen is onderzocht in **Hoofdstuk 6 en 7**. In **Hoofdstuk 6** is de vervaardiging van dragers beschreven met verschillende poriegroottes en een porositeit van ongeveer 80 %. Poreuze 1000PEOT70PBT30 en PDLA structuren zijn vervaardigd d.m.v. persen en het uitwassen van zoutdeeltjes, waarbij gebruik gemaakt is van zoutdeeltjes met respectievelijk een grootte van 250-425, 425-500, 500-710 en 710-1000 µm. Een gedetailleerde analyse van de poriestructuur van de verschillende poreuze dragers m.b.v. micro computed tomography (µ-CT) toonde verschillen in poriegroottedistributie, gemiddelde poriegrootte, toegankelijk porievolumen en toegankelijk oppervlak. De gemiddelde poriegroottes van deze poreuze dragers zoals bepaald m.b.v. µ-CT zijn kleiner dan verwacht (260, 342, 305 en 477 µm) op basis van de grootte van de zoutdeeltjes (respectievelijk 250-425, 425-500, 500-710 en 710-1000 µm) gebruikt voor de vervaardiging van de poreuze structuren. In de literatuur zijn methoden gebruikt voor de berekening van de poriegroottedistributie en gemiddelde poriegrootte op basis van µ-CT data, die de poriegrootte onderschatten. In de hier beschreven studie is de onderschatting van de gemiddelde poriegrootte minder groot dan in vorige berichten. Dit komt door het gebruik van een algoritme dat meer geschikt is voor kubische poriën, zoals het geval is in deze studie, waar de poreuze dragers gemaakt zijn door het uitwassen van zoutkristallen. Hierdoor liggen de gemiddelde waarden ongeveer 100 µm hoger. Voor de hoeveelheid DNA (en dus het aantal cellen) aanwezig in de poreuze 1000PEOT70PBT30 dragers zijn geen significante verschillen waargenomen, hoewel er duidelijke verschillen in toegankelijk porievolumen en toegankelijk oppervlak zijn, zoals afgeleid is uit µ-CT data.

Gasplasma behandelde poreuze 1000PEOT70PBT30 dragers, bezaaid met BMSC's van ratten en gekweekt in vitro gedurende 7 dagen in een osteogeen medium, zijn 4 weken subcutaan geïmplantéerd in naakte muizen. Bezaaid en gekweekt PDLA (porositeit 83.5 %, gemiddelde poriegrootte volgens µ-CT: 407 µm) en bifasisch calciumfosfaat (BCP, porositeit 29 %, gemiddelde poriegrootte volgens µ-CT: 837 µm) dragers zijn in deze studie gebruikt ter controle. De aanwezigheid van verschillende types weefsel, waaronder bot en beenmerg, zijn bestudeerd en gekwantificeerd m.b.v. histomorfometrie. Alle poreuze 1000PEOT70PBT30, PDLA en BCP dragers vertonen de vorming van bot en beenmerg. Er zijn geen significante verschillen waargenomen in de hoeveelheden (genormaliseerd voor de porositeit) bot (5-8 %) en beenmerg (5-13 %) in de middelste dwarsdoorsneden van poreuze 1000PEOT70PBT30 dragers met verschillende poriegroottes. Hoewel de poreuze PDLA en BCP dragers minder BMSC's bevatten op het moment van implantatie (bepaald m.b.v. een DNA-analyse), vertoonden ze aanzienlijk meer bot- en beenmergvorming en minder ingroei van fibreus

weefsel en retentie van wondvocht dan de poreuze 1000PEOT70PBT30 dragers na 4 weken subcutane implantatie in naakte muizen.

Om de invloed van de porositeit van de poreuze drager op de weefselvorming te onderzoeken, zijn gasplasma behandelde poreuze 1000PEOT70PBT30 structuren (73.5, 80.6 en 85.0 % poreus) bezaaid met BMSC's van ratten, 7 dagen in vitro gekweekt in een osteogeen medium, subcutaan geïmplantéerd in naakte muizen en na 4 weken verwijderd (**Hoofdstuk 7**). Alle dragers zijn vervaardigd met zoutkristallen van 425-500 µm om poreuze dragers te krijgen met poriën van gelijke grootte. De gemiddelde poriegroottes van de poreuze 1000PEOT70PBT30 dragers waren tussen de 311 en 342 µm, zoals bepaald m.b.v. µ-CT. Poreuze PDLA en BCP dragers zijn wederom gebruikt ter controle. Na implantatie vertoonden de poreuze 1000PEOT70PBT30, PDLA en BCP dragers bot- en beenmergvorming. De poreuze 1000PEOT70PBT30 drager met een porositeit van 85.0 % bezat niet voldoende stijfheid en kon in vivo zijn vorm niet behouden. Verrassenderwijs vertoonden de poreuze 1000PEOT70PBT30 dragers met een porositeit van 73.5 % duidelijk waarneembare kraakbeenvorming. Hoewel effecten van de stijfheid van de poreuze drager niet uitgesloten kunnen worden, wordt de kraakbeenvorming waarschijnlijk veroorzaakt door de slecht toegankelijke poriën (zoals waargenomen in histologiesecties) resulterend in een zuurstof-arme omgeving die kraakbeenvorming bevordert. Poreuze dragers van 73.5 % porositeit, die kraakbeen bevatten, hadden ook een aanzienlijk lager toegankelijk porievolume (als een functie van het totale volume) dan de poreuze 1000PEOT70PBT30 dragers van 80.6 en 85.0 % porositeit. Gasplasma behandelde poreuze 1000PEOT70PBT30 dragers niet bezaaid met BMSC's of poreuze 1000PEOT70PBT30 dragers, bezaaid met BMSC's, gekweekt voor 7 dagen in vitro, maar niet gasplasma behandeld (**Hoofdstuk 6 en 7**) vertoonden geen enkele bot- of beenmergvorming. Overeenkomstig met de studies beschreven in **Hoofdstuk 6**, vertonen BMSC bezaaide en gekweekte poreuze PDLA en BCP dragers altijd aanzienlijk meer bot- en beenmergvorming dan de poreuze 1000PEOT70PBT30 dragers. Eerdere implantatiestudies met BMSC bezaaide en gekweekte poreuze 1000PEOT70PBT30 dragers uitgevoerd door Mendes et al. resulteerden in aanzienlijk meer in vivo botvorming (de hoeveelheid bot die de poriën vulde was 36 %). De gerapporteerde afmetingen van de poreuze dragers waren 3×3×2 mm, in vergelijking met 4×4×4 mm in de hier beschreven studie. In beide gevallen zijn dezelfde hoeveelheid BMSC's gezaaid ( $2 \times 10^5$  per poreuze drager). Dit suggereert dat de afmetingen van de poreuze drager en/of de zaaidichtheid van de cellen een sterke invloed hebben op botvorming. De effecten van de afmetingen van de drager en de zaaidichtheid van cellen op de in vitro celkweek en in vivo botvorming dienen verder onderzocht te worden.

Om de tissue engineering constructen verder te optimaliseren, is een gedetailleerde studie nodig naar de effecten van kweekcondities (mogelijk dynamisch) en kweektijden (tot meerdere weken). De fysische en mechanische eigenschappen van deze constructen veranderen hoogstwaarschijnlijk tijdens de weefselkweek, wanneer nieuw weefsel gevormd wordt en de polymere matrix (langzaam) afbreekt. Om het effect op in vivo bot (re)generatie te bestuderen, moeten deze in vitro gekweekte weefselconstructen, gekweekt onder verschillende kweekcondities en gedurende verschillende kweektijden, geïmplantéerd worden in botdefecten van een kritische grootte, bij voorkeur in grote proefdieren zoals geiten.

De BMSC bezaaide en gekweekte poreuze 1000PEOT70PBT30 dragers zouden altijd vergeleken moeten worden met andere geschikte benaderingen voor de tissue engineering van bot en met andere dragermaterialen. De in vitro en in vivo resultaten beschreven in dit proefschrift (**Hoofdstuk 6 en 7**) tonen dat BCP en PDLA mogelijke voordelen kunnen hebben t.o.v. 1000PEOT70PBT30. BCP en PDLA dienen dan ook in overweging genomen te worden als dragermaterialen in toekomstige benaderingen in de tissue engineering van bot.

# Curriculum vitae

*Life is what happens to you while you are busy making other plans.*

John Lennon (1940-1980)

De auteur van dit proefschrift werd op 17 januari 1973 geboren te Nijmegen. Na het behalen van zijn gymnasium  $\beta$  diploma in 1991 aan het Geert Groote College te Deventer, begon hij zijn studie Scheikunde aan de Katholieke Universiteit Nijmegen. Tijdens deze studie is een uitgebreide hoofdrichting in de Organische Chemie gevolgd onder begeleiding van prof. dr. R.J.M. Nolte. Het onderzoek was getiteld: 'Porphyrin functionalized clip molecules: synthesis, structure and binding properties'. Daarna is een uitgebreide nevenrichting gevolgd in de vakgroep Polymeerchemie en Biomaterialen aan de Universiteit Twente onder begeleiding van prof. dr. J. Feijen en dr. D.W. Grijpma. Dit onderzoek was getiteld: 'Synthesis and properties of PEO/PBT block copolymers'. Na het cum laude voltooien van de studie Scheikunde begon hij in dezelfde groep als assistent in opleiding. Onder begeleiding van prof. dr. J. Feijen en dr. D.W. Grijpma heeft hij zijn promotieonderzoek uitgevoerd, waarvan de resultaten beschreven staan in dit proefschrift. Het onderzoek is uitgevoerd in het kader van een Europees Brite-Euram project getiteld: 'IsoBone: a tissue-engineered living bone equivalent'. Tevens is hij in 2001 geregistreerd als polymeerkundige in het Register Polymeerkunde.



# List of publications

*Ectopic bone formation in cell-seeded poly(ethylene oxide)/poly(butylene terephthalate) copolymer scaffolds: Effects of pore structure*

M.B. Claase, A. Laib, S. Both, J.D. de Bruijn, D.W. Grijpma, J. Feijen  
Biomaterials **2004**, submitted for publication

*Ectopic bone formation in cell-seeded poly(ethylene oxide)/poly(butylene terephthalate) copolymer scaffolds: Effects of porosity*

M.B. Claase, S. Both, M. van den Doel, J.D. de Bruijn, D.W. Grijpma, J. Feijen  
Journal of Biomedical Materials Research **2004**, submitted for publication

*Evaluation of two biodegradable polymeric systems as substrates for bone tissue engineering*

S.C. Mendes, J. Bezemer, M.B. Claase, D.W. Grijpma, G. Bellia, F.D. Innocenti, R.L. Reis, C.A. van Blitterswijk, J.D. de Bruijn  
Tissue Engineering **2003**, 9, S91-S103

*Gas plasma etching of PEO/PBT segmented block copolymer films*

M.B. Olde Riekerink, M.B. Claase, G.H.M. Engbers, D.W. Grijpma, J. Feijen  
Journal of Biomedical Materials Research **2003**, 65A, 417-428

*Surface modifications of PEOT/PBT copolymers for the improvement of bone marrow stromal cell attachment*

M.B. Claase, M.B. Olde Riekerink, S.C. Mendes, D.W. Grijpma, J.D. de Bruijn, J. Feijen  
Journal of Controlled Release **2003**, 87(1-3), 298-301

*Development and properties of polycaprolactone/hydroxyapatite composite biomaterials*

M.C. Azevedo, R.L. Reis, M.B. Claase, D.W. Grijpma, J. Feijen  
Journal of Materials Science, Materials in Medicine **2003**, 14(2), 103-107

*Enhanced bone marrow stromal cell adhesion and growth on segmented poly(ether ester)s based on poly(ethylene oxide) and poly(butylene terephthalate)*

M.B. Claase, M.B. Olde Riekerink, J.D. de Bruijn, D.W. Grijpma, G.H.M. Engbers, J. Feijen  
Biomacromolecules **2003**, 4(1), 57-63

*Porous PEOT/PBT scaffolds for bone tissue engineering: Preparation, characterization, and in vitro bone marrow cell culturing*

M.B. Claase, D.W. Grijpma, S.C. Mendes, J.D. de Bruijn, J. Feijen  
Journal of Biomedical Materials Research **2003**, 64A, 291-300

*Design of segmented poly(ether ester) materials and structures for tissue engineering of bone*

A.A. Deschamps, M.B. Claase, W.J. Sleijster, J.D. de Bruijn, D.W. Grijpma, S.C. Mendes, J.D. de Bruijn, J. Feijen  
Journal of Controlled Release **2002**, 78(1-3), 175-186

*The different behaviors of skeletal muscle cells and chondrocytes on PEGT/PBT block copolymers are related to the surface properties of the substrate*

M. Papadaki, T. Mahmood, P. Gupta, M.B. Claase, D.W. Grijpma, J. Riesle, C.A. van Blitterswijk, R. Langer

Journal of Biomedical Materials Research **2001**, 54(1), 47-58

*Porphyrin clips derived from diphenylglycoluril. Synthesis, conformational analysis, and binding properties*

J.A.A.W. Elemans, M.B. Claase, P.P.M. Aarts, A.E. Rowan, A.P.H.J. Schenning, R.J.M. Nolte

Journal of Organic Chemistry **1999**, 64(19), 7009-7016



# **Color figures**

**Color micrographs of relevant figures in  
Chapters 3, 4, 5, 6, 7 and appendix A**



Figure 3.4 - 1 Kg scale synthesis unit. Left: overview. Top right: helical shaped stirrer. Bottom right: Cover plate of the reaction vessel, showing inlet valves and various sensors and the stirrer equipped with a 800 Ncm magnetic coupling fitted with a sensor for registering the torque. Next to the manometer is the connection for the condensor and cold trap (not shown). [Black and white figure on p. 41].

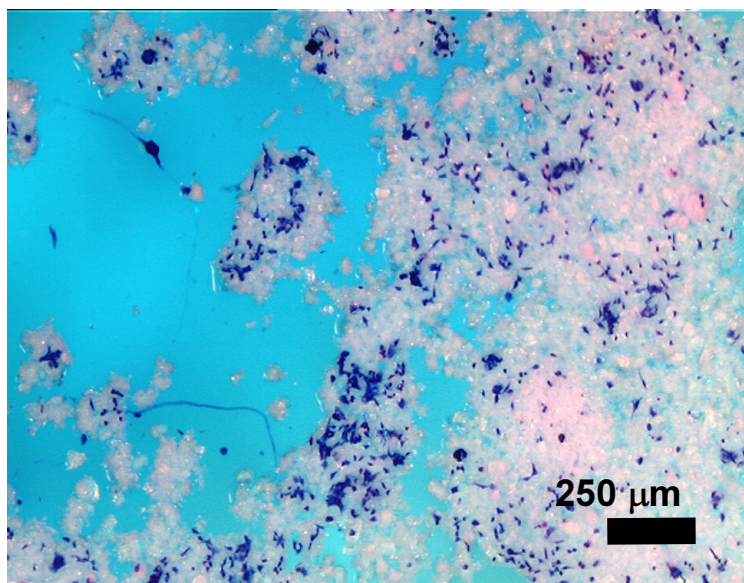


Figure 4.1 - Stereomicroscopic image of a 1000PEOT70PBT30 copolymer film of which the surface is partially covered with hydroxyapatite after 3 d of goat BMSC culturing. The methylene blue stained (dark blue) cells are only present on the white hydroxyapatite. [Black and white figure on p. 59]

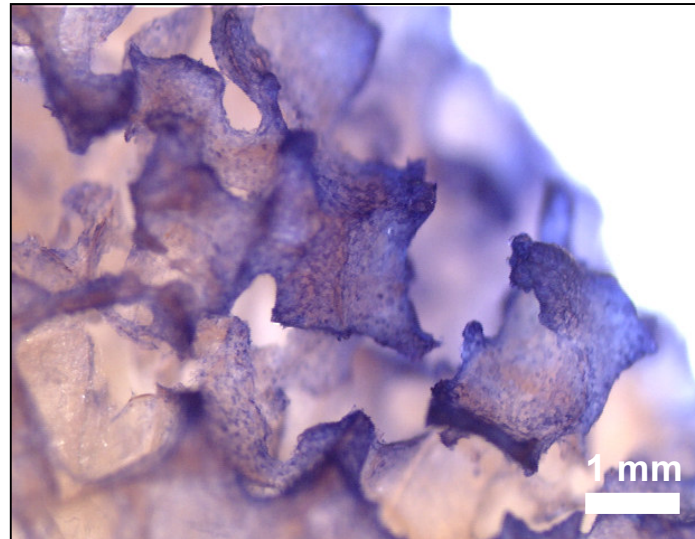


Figure 5.9 - Alkaline phosphatase stained 1000PEOT70PBT30 scaffold of 710-1000  $\mu\text{m}$  after 10 d of rat BMSC culturing. Cells containing alkaline phosphatase (differentiated) color purple. [Black and white figure on p. 77]



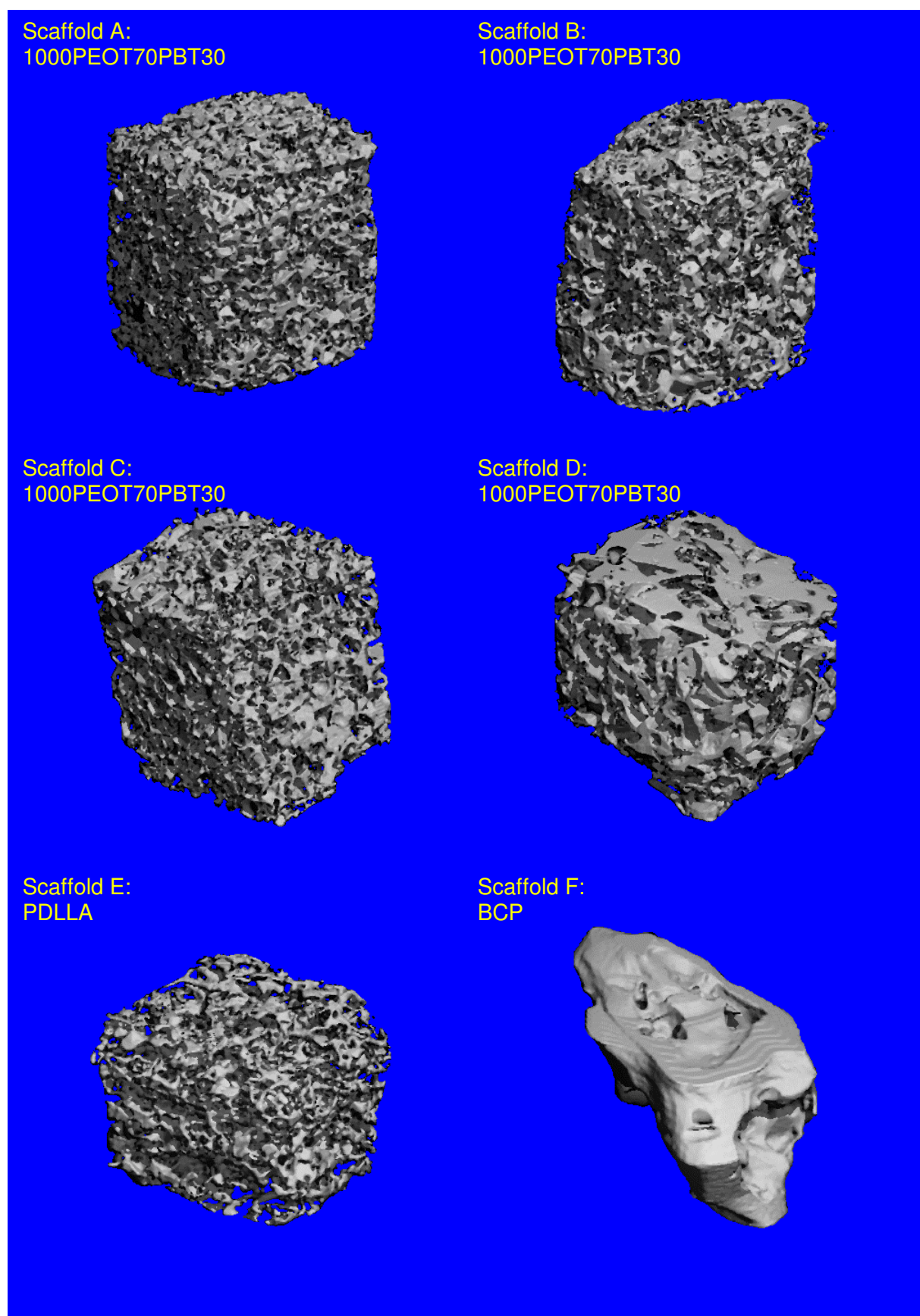


Figure 6.1 - 3D generated computer images of scaffolds constructed from  $\mu$ -CT scans. Dry, unseeded scaffolds before gas plasma treatment, corresponding to scaffolds A, B, C, D, E, F and G (identical to B) as listed in Table 6.1 are shown. [Black and white figure on p. 89]

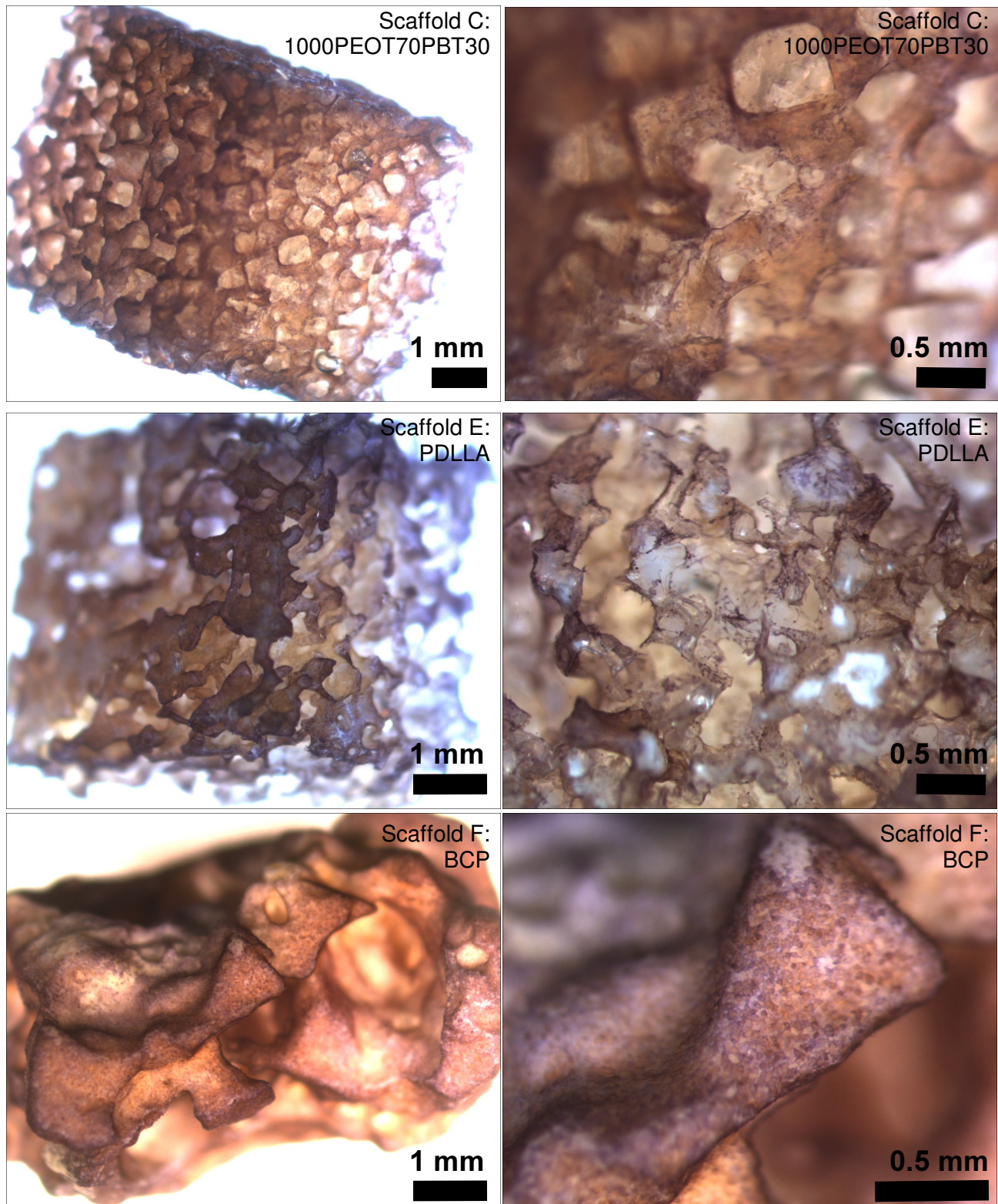


Figure 6.6 - Light micrographs of the surface of rat BMSC seeded scaffolds stained for ALP activity after 7 d of culture. Top: 1000PEOT70PBT30 (scaffold C), middle: PDLLA (D), bottom: BCP (E).  
[Black and white figure on p. 93]



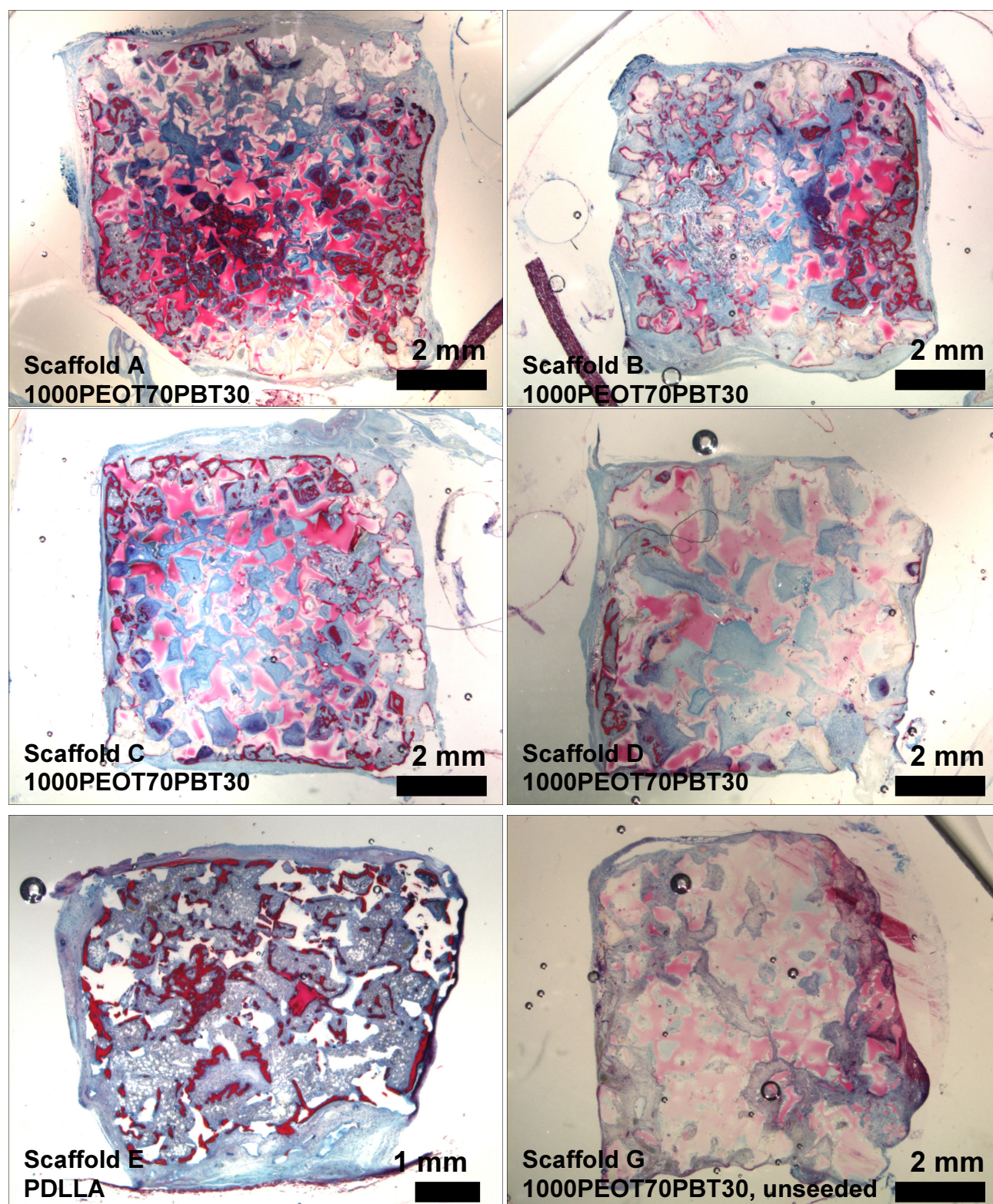


Figure 6.8 - Representative cross sections of scaffolds after 4 wks of subcutaneous implantation. The sections shown were taken from the middle of the scaffolds and stained using methylene blue and basic fuchsin. 1000PEOT70PBT30 stains pink, whereas PDLLA appears transparent. All scaffolds (except G) show bone (dark red) and bone marrow (blue/gray) formation. Fibrous tissue and wound exudate stain bright blue.

[Black and white figure on p. 96]



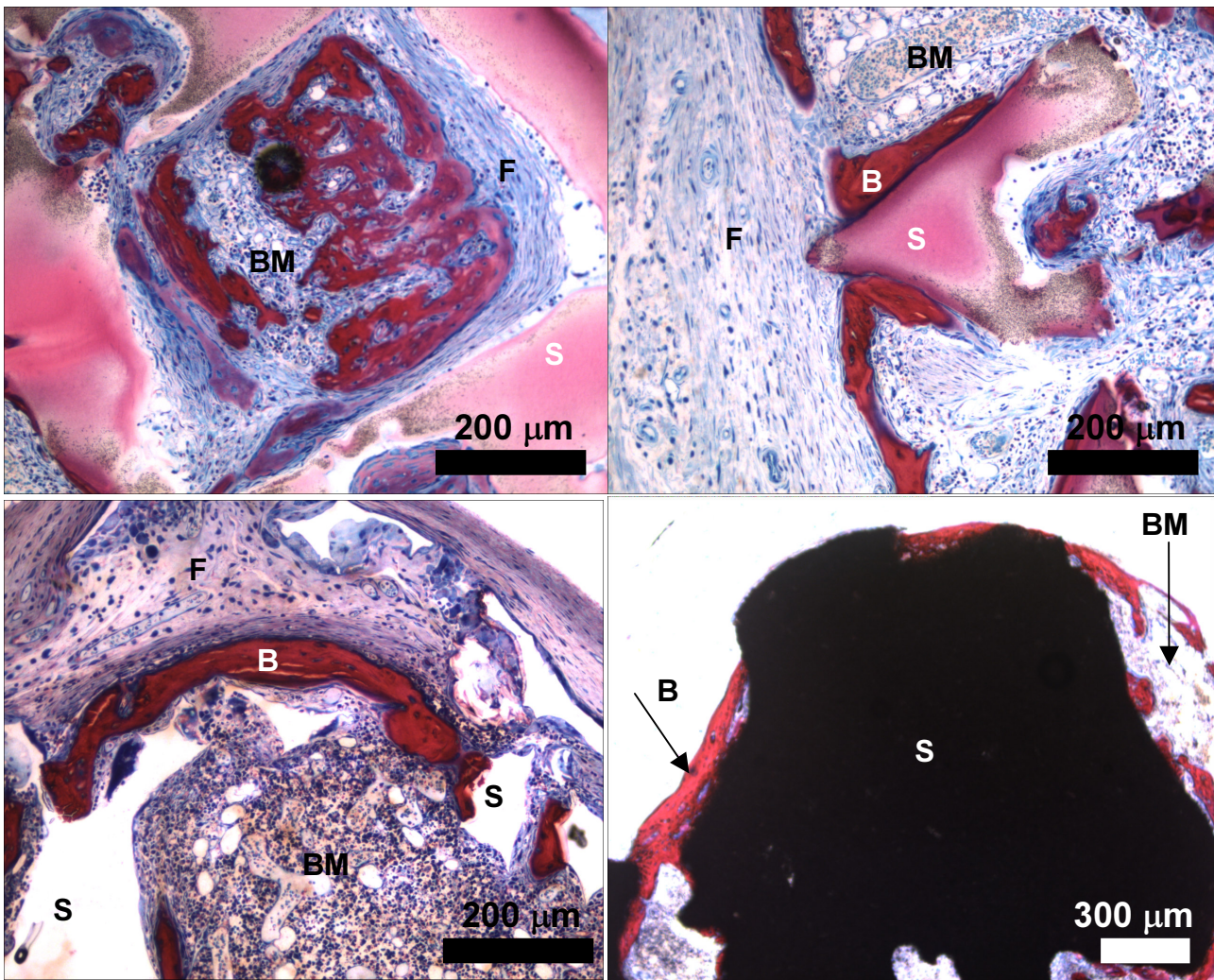


Figure 6.9 - Bone formation in the various scaffolds. Top left and right: 1000PEOT70PBT30 (scaffold C). Bottom left: PDLLA (E), bottom right: BCP (F). B: bone, BM: bone marrow, S: scaffold material and F: fibrous tissue. [Black and white figure on p. 97]



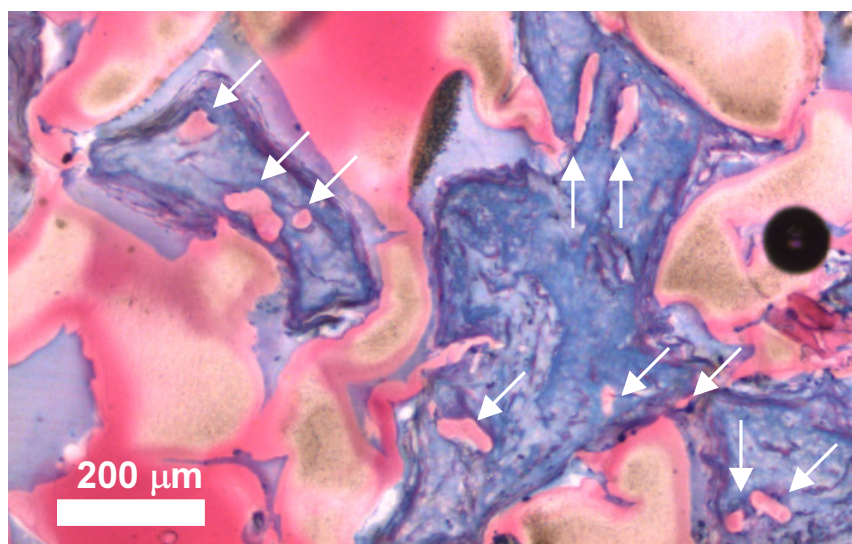


Figure 6.10 - Fragmentation of 1000PEOT70PBT30 scaffolds (scaffold B) after 4 wks of subcutaneous implantation in nude mice. Polymer fragments are indicated with arrows. [Black and white figure on p. 99]

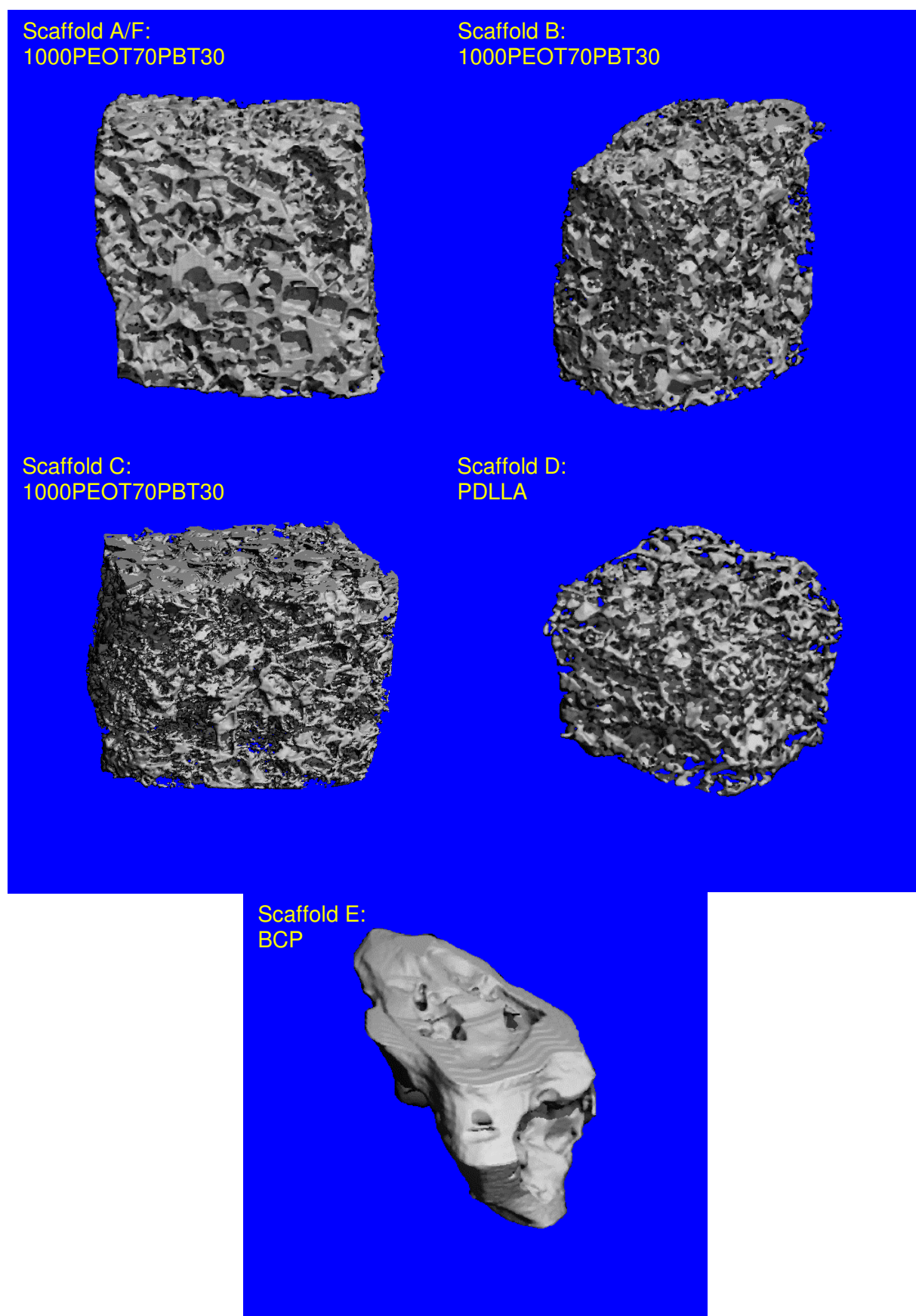


Figure 7.1 - 3D generated computer images constructed from  $\mu$ -CT scans of dry scaffolds, prior to gas plasma treatment and cell seeding. The images corresponding to scaffolds A, B, C, D, E and F (identical to A) as listed in Table 7.1 are shown. [Black and white figure on p. 110]



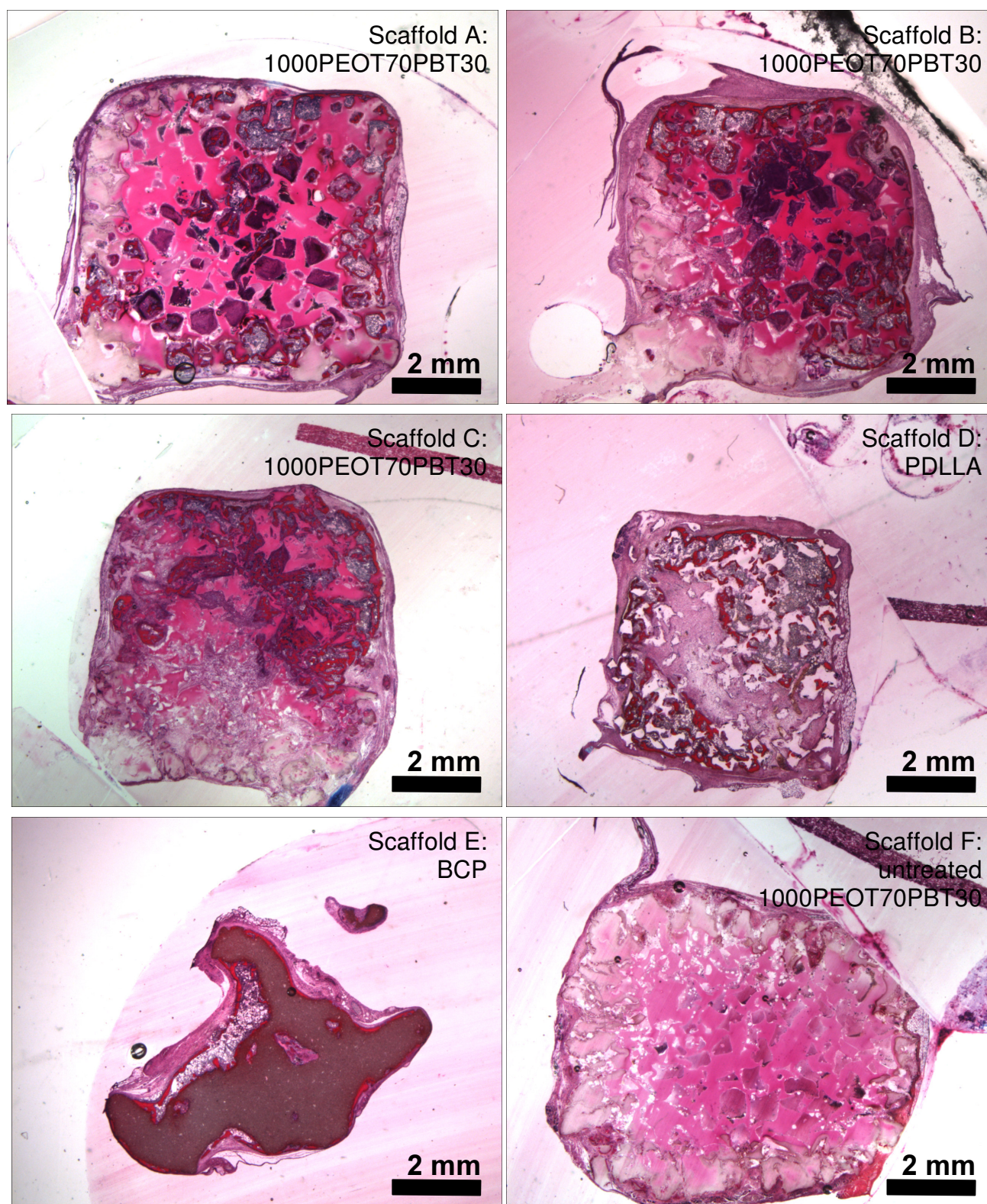


Figure 7.7 - Representative cross sections of scaffolds, seeded with rat BMSCs and cultured for 7d, after 4 wks of subcutaneous implantation. Sections shown were taken from the middle of the scaffolds and stained using methylene blue and basic fuchsin. 1000PEOT70PBT30 stains pink, whereas PDLLA appears transparent. All scaffolds (except F) show bone (dark red) and bone marrow (blue/gray) formation. Fibrous tissue and wound exudate stain pink. All scaffolds (except F) show bone and bone marrow formation. In addition scaffold A (1000PEOT70PBT30, porosity 73.5 %) shows the formation of cartilage (purple).

[Black and white figure on p. 115]



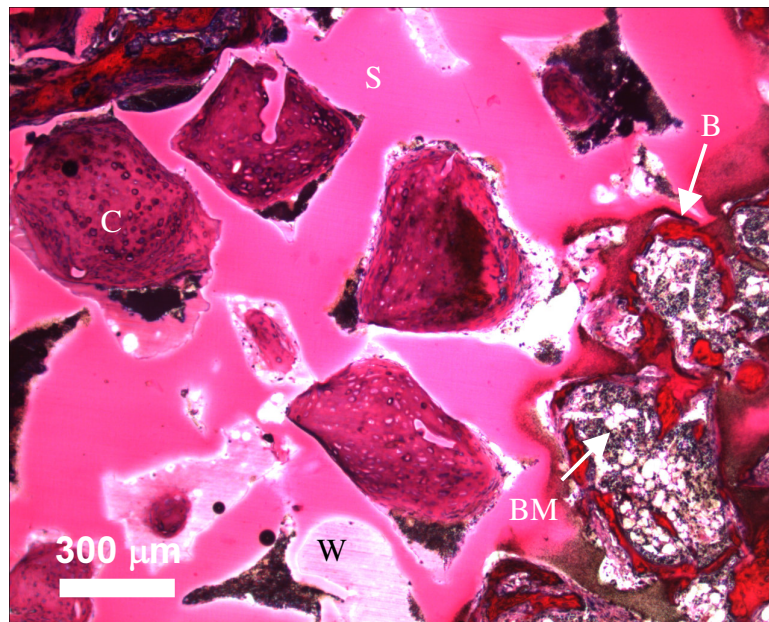


Figure 7.8 - Magnification of the cross-section shown in Figure 7.5 of scaffold A. Cartilage (C), bone (B), bone marrow (BM), wound exudate containing red blood cells (W) and scaffold material (S) are indicated.  
[Black and white figure on p. 118]

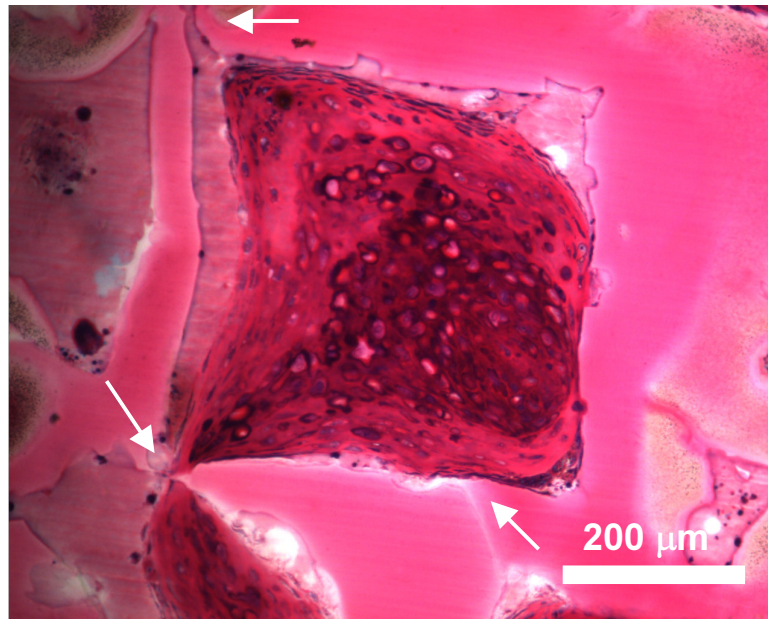


Figure 7.9 - Poorly interconnected pore containing cartilage. Interconnections to other pores are indicated with arrows. [Black and white figure on p. 118]

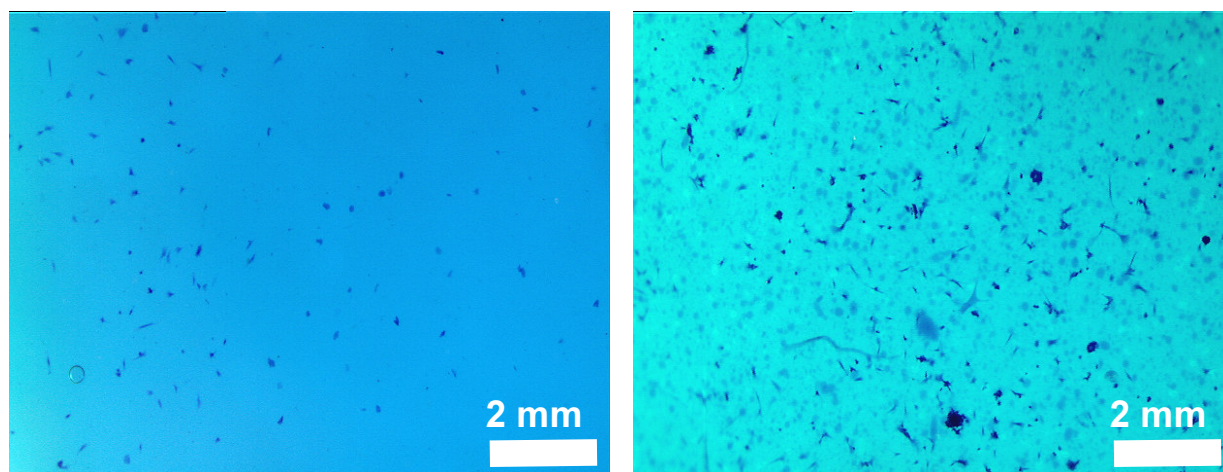


Figure A.2 - Microscopic images of 1000PEOT70PBT30 copolymer films with goat BMSCs after 3 d of culturing. The samples were stained with methylene blue: copolymer (light blue) and goat BMSCs (dark blue spots). Left: 1000PEOT70PBT30. Right: 1000PEOT70PBT30 blended with 10 wt % PEG-RGD conjugate based on PEG with a molecular weight of 8000. [Black and white figure on p. 135]